INTERACTION MECHANISM OF HEPATITIS C VIRUS AND BLOOD CELLS TREATED WITH CONVENTIONAL ANTIVIRAL DRUGS AND PLANTS EXTRACT

BY

IWERIOLOR, SUNDAY

2014247001F

A DISSERTATION SUBMITTED TO THE DEPARTMENT OF MECHANICAL ENGINEERING, FACULTY OF ENGINEERING, NNAMDI AZIKIWE UNIVERSITY, AWKA

IN PARTIAL FULFILMENT OF THE REQUIREMENTS FOR THE AWARD OF DOCTOR OF PHILOSOPHY (Ph.D) IN MECHANICAL ENGINEERING

FEBUARY, 2021

CERTIFICATION

This research work on interaction mechanism of hepatitis c virus and blood cells treated with conventional antiviral drugs and plants extract was originally carried out by me under the supervision of Prof. C.H Achebe.

Iweriolor Sunday

Department of Mechanical Engineering,

School of Postgraduate Studies,

Nnamdi Azikiwe University.

…….

APPROVAL

This research work on *Interaction Mechanism of Hepatitis C Virus and Blood Cells Treated with Conventional Antiviral Drugs and Plants Extract* has been read and approved as having satisfied the requirements for the award of Doctor of Philosophy (Ph.D) degree in Mechanical Engineering, Faculty of Engineering, Nnamdi Azikiwe University, Awka.

_____ _____

Engr. Prof. C.H. Achebe Date
(Supervisor)

_____ _____

Engr. Dr. J. L. Chukwuneke Date
(Head of Department)

_____ _____

Prof. Nnamdi V. Ogueke Date
(External Examiner)

_____ _____

Engr. Prof. Harold Godwin Date
(Dean, Faculty of Engineering)

_____ _____

Engr. Prof. P.K. Igbokwe Date
(Dean, SPGS)

DEDICATION

This work is dedicated to the Awesome God, who through his divine wisdom, direction and inspiration made this dissertation a great success.

ACKNOWLEDGEMENTS

I wish to acknowledge the following persons for their immense contributions towards making this work a reality. First among them is my supervisor, Professor C.H. Achebe for his guidance, encouragement and whose constructive criticism ensured that this research work is successfully done.

Not left out are the relentless contributions of the amiable staff of Mechanical Engineering Department; Professor Sam Omenyi, Engr. Dr. Ugochukwu Okonkwo, Engr. Dr. Chukwuneke Jeremiah for their undiluted assistance in the course of this research.

Special thanks to the management of Model laboratory in Agbor and Anambra State University Teaching Hospital in Amaku for the provision of necessary equipment needed for this research.

The significant efforts of Mrs Iweriolor Sandra and Miss Sunday Daniella cannot be forgotten. I will forever be indebted to you.

ABSTRACT

The interaction of Hepatitis C virus in the presence of conventional antiviral drugs and bio-extract was investigated in this study. A total of twenty blood samples were used for the study. The conventional antiviral drugs used are *interferon alfa (IFN), Ribavirin (RBV), Atazanavir/ritonavir (ATR) and Efavirenz/lamivudine/tenofovir* (ELT) while the scientifically prepared herbal extracts are the leaves of *Bryophyllum pinnatum(BP), Anona muricata(AM), vernonia amygdalina(VA)* and *phyllantus amarus.* Phytochemical screening and Fourier transform infrared spectroscopy were done on the plant extracts to identify the bioactive ingredients and functional group. Inoculation of blood and smearing of slides were done to allow for contact angle experiment. These were done at room temperature and allowed to dry. Glycerin was dropped on the surface of the smeared slide while the spreading process captured immediately with a Nikkon digital camera. The angle formed at the solid-serum interface was measured. The experimented data was used for the Matlab computation of surface energy, the energy of adhesion and Hamaker coefficient. The average contact angles obtained for infected white blood cells were observed to be the highest $63.4^0 \pm 3.20$. The surface energy of $44.35 \pm 1.90 mJ/m^2$ for uninfected blood sample was reduced to 33.54 ± 2.31 mJ/m^2 due to the virus. Mathematical models were generated using Response surface methodology to establish the actual relationship between the variables and the predicted response. The concept of combined negative Hamaker coefficient employed served as a useful determinant in the prediction of attraction or repulsion between the interacting viral particles and blood cells in the presence of the various drugs. The combined negative Hamaker coefficient gave a value of -0.150×10^{-25}J which signifies that repulsion of the interacting particles is attainable. The combined negative Hamaker coefficient obtained using various conventional drugs in mJ/m^2 are IFN 0.462×10^{-19}, RBV -0.132×10^{-19}, 1.291×10^{-19} for ATR and ELT -0.138×10^{-19}. Similarly those of the herbal extracts are as follows; AM 1.045×10^{-19}, VA -0.592×10^{-20}, BP -0.672×10^{-19} and DH -0.210×10^{-18}. The results of the study have shown the possible effectiveness of natural compounds in managing human diseases. The thermodynamic model and the implication of the negative Hamaker Coefficient obtained are a good indicator and as such should be considered by the pharmaceutical industries in the process of drug design and production.

TABLE OF CONTENTS

LIST OF TABLES

APPENDIX

*Appendix B for Surface Energy of Adhesion

*Appendix E for Hamaker Coefficient

LIST OF FIGURES

LIST OF PLATES

CHAPTER ONE

INTRODUCTION

1.1 Background of the Study

Hepatitis C virus (HCV) infection is a global health burden to both industrialized and developing countries infecting an estimated 3% of the world population. It represents a viral pandemic that is 4-5 times more prevalent than HIV infection, therefore the reduction of global mortality and morbidity related to hepatitis C is of great concern to public health (Lavanchy, 2009). It is an infectious disease affecting the liver with no symptoms at the initial stage of the infection and at the chronic stage of the infection causes permanent liver damage, cirhhosis, hepatocellular carcinoma and even death (WHO, 2013).

An estimated 130-200 million people worldwide are infected with hepatitis C virus. In 2013, almost 11million new cases occurred mostly in Africa and Asia with about seven million developing to hepatocellular carcinoma and liver cirrhosis (Hajarizadeh et al, 2013). Despite infecting a great number of people worldwide, the global burden of HCV infection remains at large a silent epidemic because acute infection is generally asymptomatic while morbidity and mortality arise after years of infection (Ray and Thomas, 2010). HCV infection has however continued to receive attention asit has surpassed HIV as a cause of death in many parts of the world(Rice and Saeed, 2014).

The spread of the hepatitis C virus (HCV) is primarily by blood- to- blood contact associated with intravenous drug users, poorly sterilized medical equipment, and needlestick injuries in health care, unprotected sex with infected person and blood transfusion. It can also be transfer from an infected mother to her offspring during childbirth. With the recent technology of blood screening before transfusion, the risk from transfusion is less than one per two million (Maheshwari and Thuluvath, 2010).

As at 2018, no approved vaccine protects against hepatitis C virus (Abdelwahab and Ahmed, 2018).Enormous advances have been made in the treatment of hepatitis C

virus infection. Currently the combination of pegylated interferon–alpha and ribavirin (RBV) is the standard treatment for the infection and it has so far achieved less than 50% success(Shiffman et al, 2007). Prevention includes testing of donated blood, harm reduction efforts among people who use intravenous drugs.

This combination therapy has numerous shortcomings that make it difficult for the patients to endure. The side effects are fever, anemia, flue, uncontrolled depression, viral resistance to drugs, psychosis and above all it is expensive, thus making it inaccessible for patients of low income (Calland et al, 2012).The chronic stage is the leading reason for liver transplant, though the virus usually reoccurs after the transplant. Inflammation occurs to the liver of those infected before cirrhosis develops. This transformation occurs at the rate of 1-3% per year and being co-infected increases this risk further (Fattovich et al, 2004).

Before now treatment successes recorded from the use of antiviral drugs has been achieved from various markers such as CD4 cell counts, virological and immunological responses. Sustained virological response is achieved when the continuous administration of the antiviral drugs reduces the viral load of HCV to clinically undetectable levels within the first 12-24 weeks. Within this period, the immunological response by virtue of the steady administration of the drugs on the HCV infected blood is established by increase in CD4 cell count. Clinically, the symptoms of the infection as believed will subside within this period. But these antiviral drugs do not eliminate totally the virus from the blood stream and only provides a functional cure with side effects.This study has looked beyond the current practice owing to the failure and challenges of the treatments and is anchored on the thermodynamic response. This is intended to be achieved by determining the net repulsive van der Waal forces between the HCV and the drug coated lymphocytes which will result in a change of the surface free energy. A negative value of the van der Waalforces of interaction (Hamaker Coefficient) suggests total separation of the virus and the blood cell.

The numerous unsatisfactory issues such as viral resistance to drugs, high cost of treatment, low virological response rate that surrounds the use of conventional

antiviral drugs have triggered a search for a new, safe, and inexpensive therapy. This new therapy is also expected to have less side effects. It ought tobe an efficient and effective bioactive antiviral substance capable of curbing mortality and morbidity associated with hepatitis C infection.Medicinal plants have been found to play a major role in managing human diseases. Historically, lots of modern drugs have been developed from molecules originally isolated from natural sources (Balanus and Kinghorn, 2006). The search for new bioactive molecules in key therapeutic areas such as infectious viral disease, cancer, immunosupression and metabolic disorder is still an active part of pharmaceutical research (Newman and Cragg, 2012).

Persons who may have been infected with hepatitis C may appear to clear the virus but remain infected. The virus is not detected with conventional testing but can be found with ultra–sensitive test (Carreno, 2006). The original detection technique was by demonstrating the viral genome within liver biopsies but newer methods include the antibody test for the virus core protein and detection of the viral genome after first concentrating the viral particles by ultracentrifugation.Diagnosis is by blood testing to look for either antibodies to the virus or its ribonucleic acid (RNA). The diagnosis of acute and chronic HCV is based on the detection of HCV-RNA by sensitive molecular methods. Anti–HCV antibodies are detectable by enzymes immunoassays (EIA) but may be negative for newly infected patients as well immunosuppressed patients.

1.2 **Statement of Problem**

A major challenge to mankind is the fight against hepatitis C which affects more than 150 million people in the world and eventually leads to death in most cases. People are unable to afford the treatment with antiviral drugs as they either lack the resources or the insurance coverage that can foot the bills.Currently, there is no authenticated vaccine available for the cure of the disease and the current approved treatment (Standard of Care) is a combination pegylated interferon alpha (PegIFN-α) and antiviral nucleoside analogue ribavirin (RBV) which its use and duration of treatment is dependent of the patients genotype. All genotypes of hepatitis C virus show different sustained virological responses(Dienstagand and McHutchison, 2006). This

combination therapy has severe side effects resulting in highly variable outcome and it is very expensive thus making it very unbearable for the patients.

Moreover, the high diversity of the viral isolates of this pandemic disease makes it difficult to develop a vaccine since treatment response is dependent on infecting genotype. The structure of the viral particle is still unknown and the circulating HCV particles are associated with apolipoproteins having highly variable buoyant densities, the lighter ones being the most infectious (Bartenschlager et al, 2011). This genetic variation has made it possible for the virus to defile clinical solutions.Subsequently, another barrier to breakthrough against the fight with hepatitis C virus is the lack of cultured system supporting primary virus replication which has made the interpretation of experiments assessing HCV replication hematopoietic cells difficult.

Aspects concerning the mechanism of actions, surface interaction dynamics of the particles (blood cell and HCV) and surface tensiometry of biological fluids characteristics are not well established in the field of medicine.From the foregoing, these problems need to be solved to enhance the sustained response rate in infected patients. This necessitated the use of surface thermodynamic approach to investigate both conventional and natural compounds in view of evolving better treatment options.

1.3 Aim and Objectives

The aim of this study is toinvestigate the interaction mechanism of hepatitis C virus-blood cells treated with bio-extracts and conventional antiviral drugs.

To achieve this aim, the research has its objectives as follows:

- To study the efficacy of the currently used drugs for the treatment of hepatitis c virus.
- To investigate a natural compound that will target the viral protein not the host cell.

- To investigate the ethnomedical uses of the selected plants by practitioners of complementary and alternative medicine.
- To ascertain the degree of wetting made by the bio-extract and conventional drugs(*pegylated interferon alfa,ribavirin, atazanavir/ritonavir and efavirenz/lamivudine/tenofovir)*in the interacting medium.
- To determine and compare the interfacial energies of interactionsof the infected, uninfected and the treated samples obtained in using both the conventional drugs and the bio-extracts.
- To determine the possibility of total repulsion of the virus from the blood cells.employing the concept of negative Hamaker Coefficient.

1.4 Significance of the Study

The adverse effects encountered by the use of conventional antiviral treatment have informed this study to investigate natural compounds that can suppress or eliminate the hepatitis C infection. This has to be achieved without the problem of toxicity and other side effects. The therapy should be easily accessed and above all cheap.The energies of interactions obtained using this approach is a veritable tool used in determining the interaction process occurring at the HCV and drug coated interface. Several thermodynamic models were used to characterize the interaction of the HCV and the drug coated lymphocytes to predict their nature and the van der Waal forces of attraction on solid–liquid(serum) interface.The thermodynamic prediction will allow pharmaceutical experts to ascertain the drugs that will offer functional cure or eradication cure. It is intended that this study presents an alternative measure of combined negative Hamaker which will serve the pharmaceutical industries as an added parameter to clinical approach in the course ofdrug design and production.

1.5 Scope and Limitations of the Study

The virus and its general signs and symptom as well as its channels of transmission will be assessed. The virology and serology of the virus and the progression from acute to chronic stages is within the content of this research. The *in vitro* experimental

procedures of the infected blood samples subjected to the therapeutic treatments of the conventional and natural compounds under study is also part of this research.The analyses of sustained response on infected samples under the treatment of conventional drugs and finding new therapeutic approach formulations with bio-extracts will equally be done. The molecular mechanism of HCV viral entry and attachment into the host cells will also be studied. This research also embodies the determination of contact angle and wetting properties of the conventional drugs and the selected natural compoundsunder study. The determination of the interfacial free energy and the Hamaker coefficient of the therapeutic measures under study will also be done.MATLAB computational software will be used as a tool for modeling the interactions of HCV-RNA and drugs using the data obtained from the experimental contact angle measurement.

This research also includes the phytochemical screening/test analysis of the bio-extracts used for this study and literatures on the plants under study has helped in the knowledge of the phytochemical compositions of the extracts and their anti-microbial capabilities. Also included in the phytochemical analysis is the Fourier transform infrared spectroscopy carried out on the methanolic extract of the various leaves of the plants under study for the determination of present functional group. The blood samples used for this study are only HCV monoinfected and are yet to commenced treatment.

Lastly, response surface methodology will also be employed as a statistical tool to investigate the interactions between the variables in the process to build a mathematical model and generate three-dimensional and contour-response surface plots that will clearly demonstrate the impact of virus on the blood cells on both the infected and the treated blood components.

This study did not predict the pharmokinetics of the drug interaction with the human body chemistry, the microbiological pathways needed for viral clearance to occur and also the genetic characterization for determing the hepatitis c viral strains as these aspects are left for professional in the field to ascertain.

CHAPTER TWO

LITERATURE REVIEW

2.1 Discovery of Hepatitis C Virus and its Economic Impact

In the mid 1970, a team of researchers headed by the chief of infectious disease section in the department of transfusion medicine at the National Institute of Health, Harvey .J.Alter demonstrated how most post- transfusion hepatitis cases were not due to hepatitis A or B virus. Despite this discovery, International research efforts failed to identify the virus regarded as not due to hepatitis A or B virus.In 1987, Michael Houghton and his team in conjunction with David Bradley at the center for disease control and prevention used a molecular cloning approach to identify the unknown organism and developed diagnostic test (Boyer, 2001).

The discovery of hepatitis C virus (HCV) was first published in 1987 in the article of journal science which led to the significant improvement in its diagnosis and antiviral treatment (Kuo et al,1989). The economic implication of hepatitis C is a great burden both to individual and the society at large, the United States estimated the life cost of the disease in 2003 to be 33,407 USD (Wong, 2006) and the cost of liver transplant as at 2011 to be approximately 200,000 USD (El Khoury et al, 2011).The availability and potency of the antiviraldrugs is a major concern which researchers have attributed cause to lack of suitable animal models. Despite moderate success in the development of treatments, researchers over time have advocated the need for pre-clinical testing in mammalian systems such as mouse, particularly for the developments of vaccines for the poorer communities. Reducing this cost by looking beyond conventional treatments to propose a natural compound having a better efficiency and can be easily accessed is the knowledge gap that this research hopes to amend.The image of HCV virus is shown in fig. 2.1.

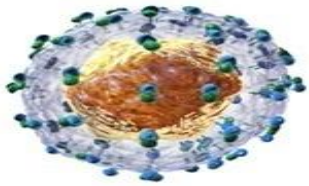

Fig 2.1: Image of HCV (Wong, 2006)

Currently, HCV affects humans and chimpanzees only, though scientist have made use of human cell culture such as hepatocytes but issues have been raised about their accuracy in reflecting the body response to infection and the use of chimpanzees has ethical and regulatory restrictions. Xenotransplantation (a strategy of introducing the liver tissue from human to mice) is an aspect of hepatitis C research that will generate chimeric mice and expose the mice-HCV infection thereby creating a humanized mice which allows to study hepatitis C within 3D architectural design of the liver and evaluating the potency of these antiviral compounds (Sandmann and Ploss, 2013).

Hepatitis C virus is a spherical, enveloped single- stranded virus of 9.6kb classified as the type member of genus Hepacivirus within the virus family of Flaviviridae and Flavivirus genus (Simmonds et al,2005).It has at least six distinct but related genotypesand more than 50 subtypes which shows substantial genetic diversity from each other.(Simmonds et al, 2011).

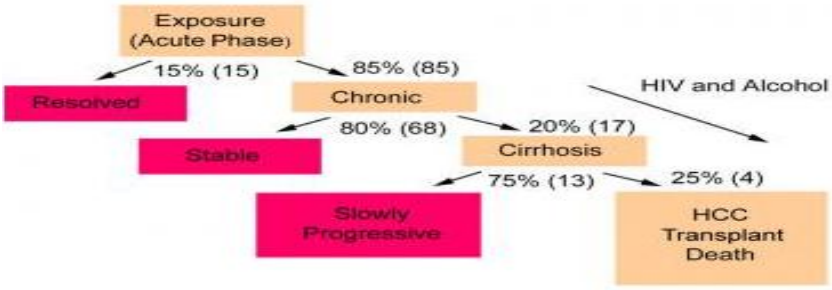

Figure2.2: Schematic representation of HCV infection (Bellentani et al, 1999)

Most infected of the virus has little or no symptoms during the acute stage of the infection but fatigue, liver cancer, liver failure characterize the chronic stage. About 85% of those exposed to the virus develop a chronic infection which is the presence of detectable viral replication for at least six months of infection. The progression from the acute to the chronic stage is rapid in people who are aged, human immunodeficiency virus (HIV) co-infected, immunosuppressed, consumers of more than 50g of alcohol daily as shown in figure 2.2.

The genome of HCV has five untranslated region (UTR) that works as an internal ribosomal entry site (IRES) which is considered important for the independent translation of viral RNA (Nomoto et al,1992). This entry site (IRES) located in the 5"UTR leads to the translation of an open reading frame (ORF) that encodes the amino acid polyprotein precursor which is ultimately cleaved by host and viral protease.

The N- terminal of the viral polyprotein contains the structural proteins which are the core protein and two enveloped glycoprotein E1 and E2. The C- terminal part of the viral polyprotein contains the non structural proteins required for RNA replication which are: NS2, p7 (viroporin) enhancing autoprotease activities during the maturity of the polyprotein precursor, NS3, NS4A, NS4B, NS5A, NS5B (Yi and Lemon, 2003) as seen in figure 2.3.

Researchers have shown that the structural and non structural proteins are the best targets to develop molecular inhibitors.NS3 along side with NS4A has overtime been given undue attention because of its protease and helicase domains that are important viral replication enzymes(Foy et al,2003). It should be noted that this single-stranded genomic RNA virus contains a single frame surrounded by only two untranslated region (2'UTR) out of the 5'UTR that are necessary for translation and replication of the viral genome .

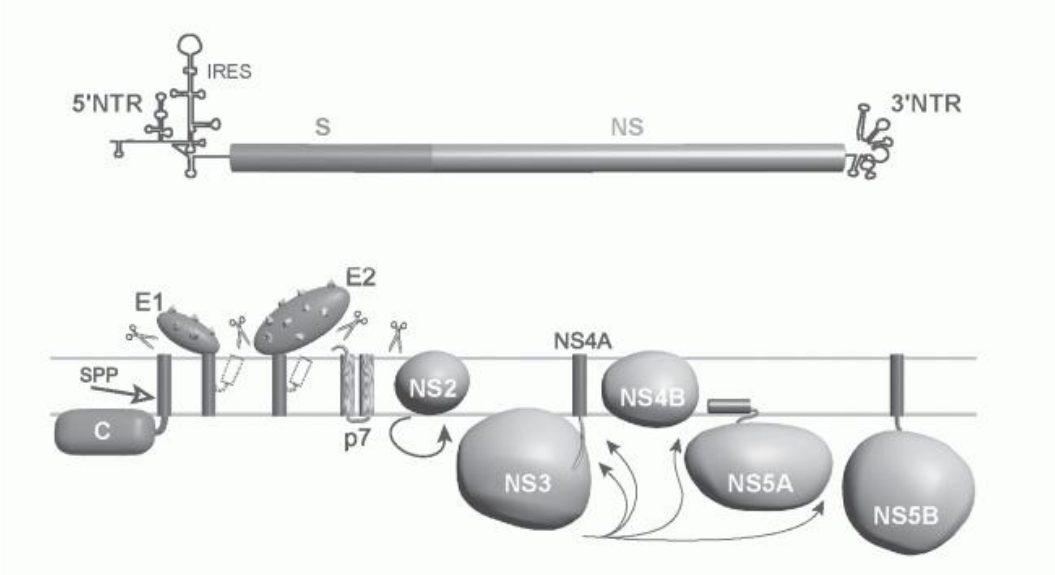

Figure 2.3: Structure of Hepatitis C virus RNA (Hepatitis C Resource Network, 2004)

Molecular differences between genotypes are relatively large having at least 30% difference at the nucleoside level. The major genotype worldwide is genotype 1 which accounts for 40-80% of all the isolates. It also can be associated with more severe liver disease and a higher risk of carcinoma.Genotypes details and prevalence is as follows:

- Genotype 1a occurs in 50-60% of patients in the United States
- Genotype 1b occursin 15-20% of patients in the United States
- Genotype 1c occurs in less than 1% of patients in the United States
- Genotype 2a, 2b and 2c is most distributed and occurs in 10-15% of patients in the United States, it is also most responsive to medication.
- Genotype 3a and 3b occurs in 4-6% of patients in the United States. This type is most prevalent in India, Pakistan, Thailand, Australia and Scotland.
- Genotype 4 occurs in less than 5% of patients in the United States, it is most prevalent in Egypt.
- Genotype 5 occurs in less than 5% of patients in the United States, it is most prevalent in South Africa
- Genotype 6 occurs in less than 5% patients in the US, it is more prevalent in Hong Kong and Macao

Within a region,a specific genotype may also be associated with a specific mode of transmission such as genotype 3 among person in Scotland who abuses intravenous drugsand also genotype 1 in the United States where street drug injections are high(Page et al,2013).

Persistent infection of hepatitis C virus involves not only the liver but also various extrahepatic organs. It can infect hepatocytes, lymphoid cells and probably other cells through the CD81 and other receptor candidates (Kondo et al, 2011).As earlier stated, most patients with chronic hepatitis C infection are asymptomatic or may have non-specific symptoms such as fatigue or malaise in the absence of hepatic synthetic dysfunction. These symptoms first develop as clinical findings in extrahepatic organs manifesting in the joints, muscles and skin. At a large scale study 74% of medical workers with hepatitis C infection demonstrated extrahepatic manifestation.The commonly occurring extrahepatic manifestations are myalgias, parenthesias, pruritus, arthralgias, sensory neuropathy, dryness, palmer erythemia and yellowing of the eyes and skin as shown in figure in 2.4

Figure 2.4: Patient with Palmer Erythemia(Dervis and Serez, 2005)

Most patients with hepatitis C infection do not have abnormal physical examination findings until they develop decompensated liver disease. Signs with decompensated liver disease include small testes, scanty body hair, ankle edemia and skin signs. Fukuhara et al,(2012) reported that the lymphotropic reservoirs contribute to the occurrence of hepatitis C virus infection.Hence a clear understanding of the direct

effect of HCV on lymphoid cells is needed to clarify the immunopathogenesis of HCV persistent infection

2.2 Interaction Mechanism of Hepatitis C Virus

The knowledge of HCV life cycle has greatly improved in recent years followingits mechanism of interactionexposed in the finding of a viral strain (JFH-1) able to replicate in cell culture(Wakita et al,2005).Prior to the establishment of HCV cell culture model (HCVcc), the life cycle of HCV has been on investigation using other experimental model systems recapitulating RNA viral entry and replication.The life cycle of the virus can be divided into three major steps;viral cell entry into its target cells by receptor mediated endocytosis, cytoplasm and membrane associated replication of the RNA genome and assembly and release of the progeny virions (Belouzardet al, 2011)

The absence of appropriate animal models and an efficient cell cultured systems interpreting the complete life cycle of HCV has for a long time hindered the true understanding of the mechanism of HCV entry and interactions with the host cell. Several surrogate models were used in the study of HCV before the development of an *in vitro* cell cultured systems allowing the reproduction of all the steps of HCV cell entry and replication cycle(Wakita et al,2005).

- Plasma-Derived HCV Model

The inoculation of human hepatocytes was the first approach in the study of infection related to hepatitis C virus. However, this model was not without limitations such as low level production of infectious virus particles, low level of HCV replication which requires the use of RT-PCR to detect viral RNA in infected cells, difficulties in discriminating between the newly synthesized and the input HCV-RNA.

- Recombinant E2 Glycoprotein Model

This model utilizes the soluble form of E2 glycoprotein to search for candidate receptors involved in the HCV entry. Only two major receptors can be captured with this model which is the scavenger receptor class B type 1(SR-B1) and tetraspanin

CD81. This is evident for the interaction of E2 with the heparan sulphate proteoglycans (Barth et al, 2003). The differences in the behavior of E2 and E1 in the viral isolates, the sE2 binds to various lines of cells in the human system, the above reasons serves as the limitations to this model.

- HCV-like Particles Model

The HCV-like particles produced in baculovirus expression systems binds and enter into the hepatoma cells and human primary hepatocytes in a receptor- mediated manner. Although E1 and E2 form a heterodimeric complex in this system, glycosylation in insects do not properly mimic the situation in human cells. Moreover the particles are not secreted but retained in intracellular vesicles thereby making their preparations difficult. Finally it is still not clear how this particle reflects the earliest stage of infection by the human version of HCV(Barth et al,2006).

- HCV Pseudoparticles Model (HCVpp)

An important breakthrough in getting access to a system that most closely mimics the entry of HCV particles was the development of HCVpp. Viral particles producedincorporated unmodified HCV glycoprotein into the lipids envelops. This breakthrough was achieved by trans co-infection of 293T- Cells with a plasmids encoding three components; full length glycoprotein, retroviral core and polymerase protein, proviral genome carrying a marker gene such as green fluorescent protein or luciferase. These particles are infectious and showed a tropism for human liver cells.

Moreover, cell entry of HCVpp is neutralized by antibodies directed against E2 protein (Keck et al, 2008), the main disadvantages of this model is that it only mimic the very early steps from particle binding to liberation of the capsid. Unlike the natural virus, HCVpp does not possess lipoproteins since they are produced in 293T kidney cells that do not synthesize lipoproteins.

- Cell Cultured HCV Model (HCVcc)

This is an authentic breakthrough that actually mimics the human viral activities, itis the development of the first in vitro model representing the complete viral replication cycle and supporting the authentic virus particles that are infectious. This model developed belongs to genotype 2 virus strain and was name JFH-1, it was cloned from a Japanese HCV infected serum, subclones of the human hepatoma cell line Huh-7 (Huh 7.5 and Huh7-innet) transferred with JFH-1 genome efficiently replicated the virus and secret infectious particles(Wakita et al,2005).

This in vitro replication model mimics a natural HCV infection accurately but it is limited to two particular cell lines (Huh-7 and LH 86) which has abnormal lipoprotein metabolism and essentially to JFH-1 strain. Another limitation of this model is that despite its production of infectious virus in Huh-7 cells, viral titres are very low and not robust enough to allow detailed studies of the virus entry. Moreover, the specific infectivity of the virus produced in infected human cells is higher than the infectivity achieved with the JFH-1(Lindenbach et al, 2006).

This observation most likely reflects the defective lipoproteins in Huh-7 cells, hence the difference in the structure of virus particle produced *in vivo* and *in vitro*. Animal derived virus has a lower density but a higher infectivity than the cell cultured produced virus(Purcelland Bukh,2006). But for reasons still unknown till date, other viral isolates do not replicate efficiently in cell cultured systems.

With this recent introduction of various assays based on the HCVcc model, the search for the direct acting antiviral can be highly stimulated with substantial increase reports on natural compounds possessing anti-HCV properties.

The structure of HCV particles remains poorly characterized despite substantial progress in cell cultured systems enabling the production, biochemical and morphology of the viral particle studies.HCV particles are about 50-80cm in diameter and contain a single stranded RNA genome, core and glycoprotein (Vieyres et al, 2014). The E1 and E2 are type 1 transmembrane proteins with a large N-terminal ectodomain and a short C- terminal transmenbrane domain which forms a non

covalent heterodimer within infected cells. But they assemble as large covalent complex stabilized by disulfide bonds on a viral particle.

Theglycoproteins are major viral determinants of HCV entry into host cells, playing a role in receptor binding and ultimately initiate the fusion process between the viral envelop and the host membrane. The hypervariable region(HVR) in E2 glycoprotein is involved in the virus interaction with human SR-B1 receptor, due to the high variability, the region may contribute to virus escape from host immune response(Von Hahn and Rice,2008).Antibodies produced by the host are directed to block the interaction with HCV glycoprotein so as to neutralize response, therefore reducing the virus particles infectivity. Although, sub-saturated levels of antibodies enhances viral infectivity.This explains the poor detection or availability of HCV glycoprotein at the virion surface(Dao Thi et al,2012)

Furthermore, the study ofHCVcc produced particles, depicts the lipid composition resemblance of very low density proteins (VLDP) and low density lipoproteins (LDL) with cholesterol esters accounting for almost half of the total HCV lipids(Merz et al,2010).It has been reported that glycosaminoglycans (GAGs) chains on the surface of the cell(proteoglycans) provides a primary docking sites for the binding of various virus and other micro-organisms. It provides the platform for HCV attachment before the virus is transferred to high affinity entry receptors. In fact the incubation of HCV-like particles with the highly sulfated heparin sulfate results in a decreased internalization of these particles (Barth, 2003).

Due to the virion association with lipoproteins, apolipoproteins such as apo-E, apo-B,apo-A1, apo-C1, apo-C2, apo-C3 can also be seen in association with hepatitis C virus particles.It can be stated here that lipoproteins and apolipoproteins are required for HCV infectivity and production. They are not HCV- specific based on the fact that they interact with other viruses, thus apo-I interact with dengue and hepatitis B virus. HDL and LDL interact with rotavirus and herpes simplex virus(Faustino et al,2014).

2.3 Host Cells Response Determinants

HCV attachment and entry into host cells is a complex and multistep process, using various experimental cell models as earlier discussed, several cell surface molecules have been identified to interact with HCV.These cell surface molecules considered essential are CD81,SR-B1,Claudin-1(CLDN-1) and Occludin(Evans et al,2007).In addition,glycosaminoglycans such as heparin sulfate, lectins (Dentric Cells Specific Intercellular adhesion molecules -3-grabbing Non-integrin (DC-SIGN) and liver-specific(L-SIGN),low density lipoprotein receptors(LDL-R) has been implicated in HCV attachment and entry.

2.3.1 Tetraspanin CD81

CD81 is a member of tetraspanin family containing a small extracellular and a large cellular loop.It is the first molecule identified with a soluble truncated form of HCV-E2 glycoprotein and to be a critical host cell for viral entry. A major feature of CD81 is the formation of an extended network at the cell surface which organizes the membrane for interactions with the glycoprotein.In their functional form, they have distinct role of cellular signaling, migration,adhesion,fusion,cytosceletal,re-organizing and proliferation (Brazzoli et al,2008).

CD81 is part of the B and T cellsreceptors complex involved in the fusion of vesicles. It is required for normal CD 19 expression and plays multiple roles in the processing, intracellular trafficking and membrane functions of CD19 (Shoham, 2008).CD81 has been proposed as an HCV receptor molecule based on its large extracellular loop(LEL) binding to sE2.The binding is specific to only HCV in humans as the sE2 does not bind mice or rat(Flint et al,2006).

In addition, it has been demonstrated that CD81 expression levels on hepatoma cells correlates with HCV infectivity (Koutsoudakis et al,2006).These results suggests that susceptibility to HCV infection may be link to CD81 density on the cell surface. The study elucidated the cellular pathway triggered by HCV binding to CD81 and engagement to CD81 plays a fundamental role in HCV infectivity.

Infection of primary human hepatocytes or hepatoma cell lines(Huh-7) was inhibited by anti CD81 antibodies and after down regulation of CD81 using the siRNA approach, the hepatoma cell lines which do not express CD81 becomes permissive to HCVcc(Molina et al,2007).This findings suggest that either the primary role of CD81 is not to mediate binding the virus to the cell surface or that its role extends beyond. Interestingly, a protein found to interact with CD81 inhibited HCV-CD81 interactions and blocked the viral cell entry in a dominant negative-fashion.Furthermore, HCV has been shown to spread via cell to cell transmission, a process that occurs independently of CD81(Witteveldt et al,2009)

2.3.2 **Scavenger Receptor- Class B member 1(SR-B1)**

SR-B1 has 509 amino glycoprotein with a large extracellular loop anchored to the plasma membrane at both the N- and C- termini by transmembrane domain with short extension of cytoplasm.Besides its association with apoptosis, SR-B1 serves as a lipoprotein receptor responsible for the selective uptake and binding of the cholesterol ester from high density and low density lipoproteins. It is clear that the two step mechanism of the SR-B1 is its involvement in binding of lipoproteins to its extracellular domains followed by lipid uptake (Connely and Williams,2003).

During the process, the core of the cholesteryl esters from the high density lipoproteins (HDL) particle is delivered into the cell without degradation of the protein moiety. SR-B1 Mediated cholesterol efflux to HDL plays an important role in reverse cholesterol transport and atherogenesis.Similar to CD81, SR-B1 has also been reported as a receptor mediated sE2 binding to human hepatic cells(Rhainds and Brissette,2004).

In addition to its established function in HDL, SR-B1 also plays an important physiological role in the catabolism of VLDL and in the selective cholesterol uptake from VLDL as was currently revealed in the study of mouse models and human primaryhepatocytes (Van Eck et al,2008).SR-B1 has been proposed to act as a putative HCV entry molecule on the basis of its reactivity with sE2. Its binding with sE2 appears to be specie-specific as mouse does not bind to sE2.The hypervariable

region of E2 is responsible for binding SR-B1, since the deletion of HVR impairs the attraction between SR-B1 and sE2 and reduces infectivity.Antibodies against SR-B1 also significantly reduce HCVpp infectivity. Similar to CD81, SR-B1 act as post binding receptor and antibodies against both receptors inhibited infection when added 60minutes after the virus binding (Zeisel et al,2007).

HDL, the main SR-B1 ligand facilitates HCVpp and HCVcc cell entry with no evidence for a direct interaction between HDL and virus particle(Dreux et al,2006). It has been postulated that the enhancing effects of HDL on HCVcc and HCVpp cell entry could be mediated through either an interaction between HDL and lipid membrane or the activation of SR-B1 by HDL. The efficiency of HCV neutralizing antibodies can also be reduced by HDL mechanism of cell entry stimulation.

Several studies suggested that SR-B1 cooperatively interacts with CD81 in HCV cell entry. Zeisel et al, (2007) revealed that HDL enhances HCVcc infectivity only when CD81 was expressed.Furthermore,the depletion of cholesterol from cholesterol-enriched plasma membrane micro- domain by treatment with methyl-β-cyclodextrin significantly reduces the expression of CD81 but not SR-B1 on the plasma membrane, thereby decreasing the levels of cells infection with HCVpp and HCVcc(Kapadia et al, 2007).

The role of SR-B1 was confirmed by finding that high avidity directed against SR-B1 efficiently infects hepatoma cells in vitro and that the expression levels of SR-B1 modulated HCVcc infectivity (Grove et al,2007).Recently there are advances in the development of therapeutic measures targeting a decrease in the expression levels of SR-B1 on cell surface thereby restricting virus attachment and entry into hepatocytes (Murao et al, 2008)

2.3.3 **Tight Junction Proteins: Claudin-1(CLDN-1) and Occludin(OCLN)**

Tight junctions are major components of cell to cell entry adhesion complex that separates apical from basolateral membrane domain. Itmaintains cell polarity by forming intermembrane.This permits the diffusion of certain molecules and limits others(Shin et al, 2006). The tight junction multiprotein complex consists of four

transmembrane proteins; claudins, occludins, junction associated molecules(JAMs) and the Coxsackie virus receptors(Greber and Gastaldelli,2007).

Claudin-1 is a new protein belonging to claudin gene family associated with HCV entry. The hepatocytes tight junction plays a major role in several liver functions including bile formation and secretion. They also regulate paracellular transport of solutes, water and ions. With the discovery of tight junction proteins as entry factors, the role of cell differentiation and polarization in the HCV cell entry process has become important.The dependence of HCV assembly on an active VLDL assembly suggests indirectly that cell differentiation is important for HCV production because VLDL assembly is a metabolic function that characterized differentiated hepatocytes.HCV infection has been shown to provoke downregulation of claudin-1 and occludins expression and to induce the polarization of infected hepatocytes with potential pathological consequences(Liu et al, 2009)

The actual role of CLDN-1 and OCLN in HCV entry remains unclear but interestingly direct interactions between HCV envelop glycoprotein and OCLN has been shown in the work of Benedicto et al, (2008).Furthermore, the knock down of OCLN in a cell to cell fusion assay where fusion activity depends on cell surface expression of the HCV glycoprotein complex diminishes fusion activity, suggesting that OCLN may be implied in the HCV fusion process(Cukierman et al,2009).

Two other members of claudin family, CLDN 6 and CLDN9 also mediate HCV entry(Meertens et al,2008), these molecules are expressed in the liver and also present in peripheral blood monocellular cells, hence providing another replication site in addition to the human hepatocytes (Zheng et al, 2007).

2.3.4 Glycosaminoglycans (GAGs)

GAGs are linear polysaccharides expressed on the cell surface that acts as binding sites for many viruses. They may primarily show low affinity but are abundant receptors involved in the initial interaction of the virus with the cell surface prior to binding with high affinity receptors. (Morikawa et al, 2007)

Glycosaminoglycans exist in different forms but only highly sulphated GAGS in particular appears to be involved in the interaction process with several virus triggering their subsequent uptake and docking between HCV and GAGs.A high sulphated GAG,heparin and heparinase inhibits attachments to cells and treating cell with glycosidases reduces HCV infectivity (Basu et al, 2007).

However,the high sulphate GAGs binds sE2 with high affinity but studies with HCVpp which carries E1-E2 heterodimer on their surface fails to confirm these findings. These observations suggests that either the heparin binding site is not accessible on the functional E1-E2 heterodimer or the attachment of authentic HCV particle to cellular GAGs is mediated by lipoproteins associated with virus particle. HCV can bind and enter the cells by GAGs dependent pathway due to the interaction of the virus lipoproteins with its lipase mediating cell entry(Andreo et al,2007).

2.3.5 **Lectins: (DC-SIGN and L-SIGN)**

Lectins are another class of molecules involves in cell binding and entry of several viruses.DC-SIGN and L-SIGN are homotetrameric type II proteins from the C-typelectin family. They are involved in the binding, internalization and elimination of a variety of pathogens(Cambi et al, 2005).

2.3.6 **Mechanism of Viral Cell Entry**

From recent studies, it is clear that the interaction between virus and the host cell during the first step of virus-host encounter is not just limited to the hospitality of the host cells to the virus resulting in cellular binding and entry. Virus-host interaction is a two way dialogue in which the virus takes advantage of the host cells owned signal transduction system to transmit signals to the cells (Smit and Helenius, 2004).These signals usually generated at the cell surface induces change to facilitate entry, prepares the cells for invasion and neutralizes the host defense mechanism.

HCV entry is first engage by the initial capture of the viral particles by attachment factors and receptors on the cell surface in a spatiotemporally regulated manner (Lefevre et al,2014). The initial attachment is mediated by heparin sulfate

proteoglycans(HSPG) syndecan-1 or SR-B1 depending on the virion density. It was initially thought that HCV glycoprotein are responsible for the virion binding to HSPG or SR-B1,however more recent research data suggest that apoE could be involve in this contact(Dao Thi et al,2012 and Jiang et al,2013).

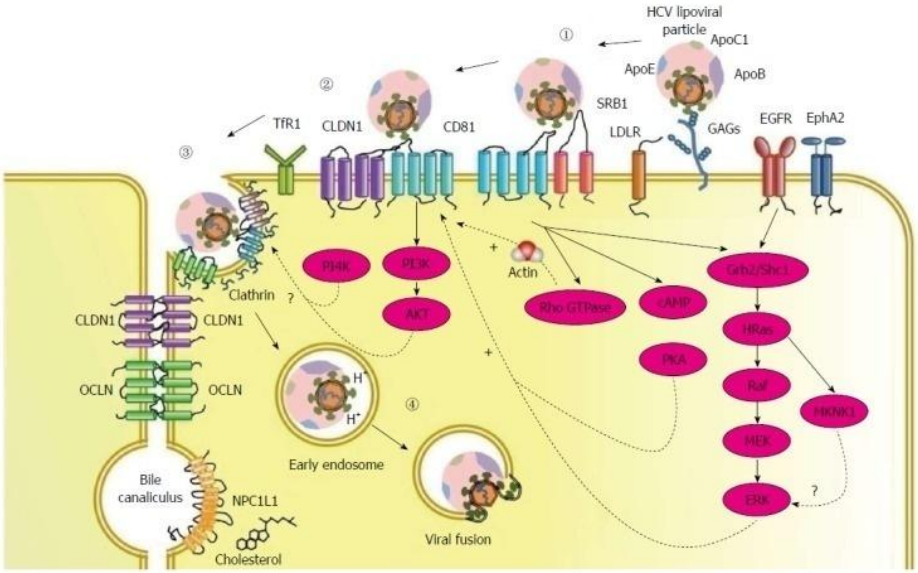

Figure 2.5: Hepatitis C virus entry into hepatocytes (Mirjam et al, 2011)

To infect a target cell, the viral particles needs to proceed through multistep entry process during which each step is tightly regulated in time and space as illustrated in figure 2.5. The steps involved in entry are viral attachment to cells, internalization and fusion of the viral particles with cellular membranes, the release of the viral genome into the host cell cytosol and the initiation of viral replication.

Upon infection, the HCV particles are transported via the blood stream and enter in contact with the hepatocytes after crossing the fenestrated endothelium of the liver sinusoids. Once present in the space where basolateral membranes of hepatocytes are exposed, it becomes significant.

As earlier discussed, the HCV entry is initiated by anchoring of the envelop glycoprotein to the cell surface thereby offering multiple novel targets for antiviral therapy. Multiple strategies evolved by the virus in order to escape from the host

immune system have to be taken into account for the design of efficient novel antiviral strategies. Current approaches for HCV antiviral drugsdesigns should target viral enzyme interfering with HCV entry process. Also as the understanding of molecular mechanism underlying HCV interaction with the host cell is growing, it holds promise for future drug design.

Viral entry may be inhibited by blocking interaction between the virus and the target cell, interfering with post binding events, interfering with viral fusion. Viral proteins are recognized as foreign particles by the host immune system and induced the production of antibodies, small proportion of this antibodies exhibits antiviral potentials in vitro and are referred to as virus-neutralizing antibodies. These antibodies render thevirion non infectious by interfering with receptor binding and entry.Many successful vaccines are based on the induction of neutralizing antibodies.

Isolation and characterization of antibodies targeting distinct steps of HCV entry is an important strategy for protection against this virus and provides a rationale basis for the development of HCV vaccines.Antibody mediated neutralization occurs during HCV infection in vivo but the role of antibody in the control of HCV infection is not clear (Walker, 1999).Antibodies with HCV neutralizing properties was first described in experimental infection of chimpanzee, these antibodies were directed against epitome in the Hypervariable region (HVR) of the HCV glycoprotein E2.The presence of antibodies directed against HVR has also been associated with viral clearance in HCV infected humans(Zibert et al,1997).

Chapel et al,(2001) with his colleague carried out a study on HCV infected patients with primary antibody deficiency, the result showed that the antibody deficient patients have an accelerated rate of disease progression, establishing HCV infection despite the induction of the humoral immune response that targets various epitomes of the envelop glycoprotein.

Recently, a functional study analyzing the neutralizing antibody response during acute to chronic infection using HCV model system demonstrated a lack of neutralizing antibody in the majority of the patients with acute HCV infection.Other studies using

HCVpp models systems demonstrated that neutralizing antibodies are induced in the early phase of infection by patients who subsequently clears the virus or controlled viral infection (Lavillette et al,2005), the result suggested that a strong early neutralizing antibody response may play a role in the outcome. HCV infected patients who do not clear the virus develop high viral titre and even cross neutralization antibodies during the chronic phase of the infection(Pestka et al,2007).

2.3.7 Internalization and Fusion of HCV Particle

Viral particle interaction with receptors, co- receptors and cofactors leads to a major molecular rearrangement at the plasma membrane resulting in internalization of the viral particle-receptor complexes through clathrin- dependent endocytosis. The binding of envelop virus to cell surface is followed by the fusion of the lipids enveloped with a cellular membrane. The process is tightly coordinated in time and space requiring drastic conformational changes in the fusion proteins which are triggered by cellular factors(Blanchard et al,2006). It has been shown that the HCV particle entry into the target cells is clathrin-mediated and fusion occurred in early endosomes as depicted in figure 2.5. Furthermore the acidic pH of the endosomes triggers the fusion by inducing conformational changes in the envelop proteins (Meertens et al,2006).

After the fusion between the viral envelope and an endosomemembrane, the viral genome is release to the cytosol.It should be noted that the exposure to cell surface bound virion to acidic pH followed by a return to neutral pH does not affect HCV infectivity. A recent study by Sharma et al, (2011) revealed that the use of bafilomycin A1 that affects endosomal acidic environment by preventing re-acidification has been shown to block HCV infection. The degree of acidification required for fusion is for now not completely characterized.

Finally ,the possibility of HCV cell to cell contact transmission has also been noticed, suggesting it as an alternative route for virus spreading, the mechanism of cell to cell transmission has not been characterized and the importance of this cell to cell transmission within the liver has not been determined till date (Timpe et al, 2007)

Importantly,HCV entry process may even be more complicated with the discovery of Ewi-2wint, a new partner of CD81 which block E2-CD81 interactions and provides additional evidence for the complexity of HCV entry process(Rocha-Perugini et al, unpublished data)

2.3.8 Entry Inhibitors of Viral Attachment

The lectin,cyanovirin-N(CV-N) is an active antiviral compound against HIV and the likes of other enveloped virus. It has been shown that the glycans in the envelop glycoprotein of the HCV cells interacts with CV-N resulting in HCV antiviral activity by blocking the HCV entry target cell(Helle et al,2006).As most of the HCV glycosylation are highly conserved, drugs targeting glycans on HCV glycoprotein may not lead so rapidly viral escape/resistance as it is the case for HIV.

Antiviral compounds targeting viral entry may either act on conserved mechanism or target specific cell surface molecules. Insight on molecular mechanism of HCV fusion are just about to rise and molecules that may likely interfere with HCV penetration has not yet been described(Blanchard et al,2006). As HCV enters the host cell through endocytosis and requires low pH for delivery of its genome (Tscherne et al, 2006)

As earlier stated, the development of HCV model has helped gaining a thorough insight into the complicated mode of HCV cell entry thereby providing new therapeutic advances and knowledge to prevent the virus from reaching its replication site. The host factors and viral components may serve as targets for the development of HCV entry inhibitors. The optimal entry inhibitor will block viral binding sites on receptors without affecting the functional physiological binding ligands.

It is preferable to target the viral protein than the host component because of the adverse effects resulting from interference with normal cell functions .This concept consist of developing more efficient and better tolerated therapies that need shorter treatment periods without toxicity of the individual compound and emergence of resistant virus. One major objective of this research was born out of this desire.

2.4 Host Neutralizing Response

The replication of HCV virus starts upon infection of the host hepatocytes and HCV-RNA becomes detectable in serums within the first three weeks. The type and strength of the host immune response during the acute phase of HCV infection determines the outcome. The role of antibodies for a long time has been contentious among researchers.

Majority of the antibodies produced during infection by HCV have no antiviral activity, they may be generated intracellular, degraded, incompletely processed proteins release from dying cells or directed against epitopes that do not play any role in the virus entry process(Hangartner et al, 2006).

Antibodies directed against the viral enveloped protein may prevent or control viral infection if they are directed against epitopes implicated in viral entry. This neutralizing antibodies exhibits antiviral activities in neutralizing assay in vitro. They have in their functional form the ability to block the virus attachment to the host and thus inhibit dissemination of infection. Neutralizing antibodies may act as opsomins in enhancing phagocytosis of the virus particles thereby decreasing the viral load. They could be classified as isolate-specific or cross neutralizing, depending on their ability to neutralize viral strain. In addition, antibodies may also interfere with post binding steps such as entry and transcription of the viral genome. These roles of antibodies were pointed out as control for hepatitis C virus infection (Reading and Dimmock, 2007).

HCV infected patient with primary antibody deficiencies has been reported to have accelerated rate of disease progression , although alteration in T-cell function mayhave also contributed to the rapid progression of disease in the infected patient.In another scenario, passive protection of HCV has been demonstrated in patients undergoing liver transplantation for HCV and HBV related liver cirrhosis and receiving infusion of anti-HBV hyper immune globulin containing anti HCV antibodies (Feray,1998).

Despite these evidences, there has been controversial view in the role of antibodies in HCV clearance. A recent study showing complete HCV resolution in the absence of detectable anti-HCV antibodies instandard diagnostic testing and anti-HCV antibody present after the initial HCV infection did not prevent re-infection in polytransfussed thalassaemic children(Lai et al, 1994).

Other studies involving health care worker and young intravenous users failed to show any clearances evidence associated with the presence of a neutralizing antibodies in the acute phase of infection and viral clearance(Meunier et al,2005), this study suggest that viral clearance can occur in the absence of neutralizing antibodies. This fact is still under investigation.

Hepatitis C virus specific T-lymphocytes appears 5-9 weeks after infection and important role in both viral control and liver injury.$CD4^+$T-cells have a major regulatory function as they help $CD8^+$ T-cell to eliminate infected cells and B-cells to generate antibodies.Similarly, Pestka et al, (2007) demonstrated that patients who spontaneously clear HCV infection mount vigorous multiple epitope -specific $CD4^+$ and $CD8^+$ T- cell responses.

Following this procedure, a study stating the prominentrole of $CD4^+$ T-cells in the control of human HCV infection showed that a cellular immune response persisted for years after the elimination of the virus, whereas, the neutralizing antibody response became weak or is lost after the viral clearance.

These studies suggest that clearance of HCV may be mediated by interplay of cellular and neutralizing immune response. This is in line with the recent study demonstrating that immune control of other poorly cytopathic virus such as lymphocytic choriomeningitis virus or HIV requires a collaboration of both the neutralizing antibodies and antiviral cellular response (Ciurea et al,2006).

2.4.1 Viral Escape from Host Neutralizing Response

Upon contamination of HCV, majority of infected persons after six months persist to chronic stage, this is as a result of the inability of the immune system to eliminate the

virus. HCV replication estimated by HCV-RNA peripheral blood level seems to remain relatively stable in these individuals.Persistent infections is characterized by the induction of HCV-specific antibody directed against the structural and non structural proteins and are able to cross-neutralize heterologous viruses or quasi species that arise in the course of infection.(Von Hahn et al,2007).

Pestka et al, (2007) in his kinetic study of neutralizing antibody response against the viral inoculums in a single course outbreak of HCV, showed that isolate-specific as well as cross-neutralizing antibodies emerge at the chronic stage of infection. Another alternative kinetic study of acute mono-infected patients revealed that high density lipoproteins(HDL) is a serum factor that impairs the efficiency of cross neutralizing antibodies that are present during the acute phase of the disease.(Lavillette et al, 2005).

Conclusively, this results indicates that HCV has evolved a mechanism that counteracts the impact of humoral response during both the acute and chronic phase of the disease and that the host neutralizing response are not able to control the circulating pool of viruses during the chronic infection.

Viral escape from antibody neutralization has been shown to occur at several levels, these include:

-The high variability of the HCV genome and the limited induction of cross neutralization antibodies

-The induction of antibodies interfering with neutralizing antibodies from the host cell

-Association of HCV with serum factors like LDL and VLDL, which shield the virus from neutralizing antibodies.

-The interplay of HCV glycoprotein with HDL

-The shedding of neutralizing epitopes by glycosylation of defined amino acid of envelope glycoprotein.

-Direct cell to cell transfer of virus.

Thus, a combination of different mechanism such as masking of neutralizing epitopes or receptor binding sites by mutational variation or glycosylation is also applicable to HCV.As HCV replicates through an error-prone viral replicase, the virus exist as a pool of constantly changing, distinct but related genomic variants in infected individuals. The immune system exerts constant pressure on these viral variants favoring the emergence of B-cell and T-cell escape mutants. It is most certainly internalized in a clathrin –dependent manner and the genome delivery into the host cell is pH sensitive (Tscherne et al, 2006)

Most recently, it has been shown that anti-HCV antibody containing immunoglobulin preparation comprises of interfering antibodies and neutralizing antibodies(Zhang et al, 2007), thorough analysis of the epitopes targeted by this immunoglobulin revealed two distinct HCV enveloped glycoprotein epitopes but only one is involve in HCV neutralization. This data suggest that HCV induces both the neutralizing and non-neutralizing antibodies but the non-neutralizing antibodies are able to interfere with the functions of the neutralizing antibodies, thereby allowing escape from the host humoral response.

Finally, HCV may also escape sensing from neutralizing antibodies by infecting surrounding cells by direct cell to cell passage. It infects the surrounding cells after the formation of viral particles that are release from the infected cells and enter naive cells by a receptor dependent mechanism. Alternatively, the virus may use cell to cell transfer to infect neighboring cells thereby escaping potential interaction with neutralizing antibodies (Marsh and Hellenius,2006)

2.5 Interactions between HCV and HIV

In the United States, 13-43% of HIV infected persons are also living with HCV with up to 85% being chronologically infected (Den et al, 2000). The co-infection route recognized is by parenteral exposure to blood such as blood transfusion andintravenous drug users, though a reduction of infection through blood transmission is on the decline by virtue of blood screening.

Although HCV and HIV share the same route of transmission, variation in the relative efficiency of transmission do exist. HCV is approximately 10times more infectious than HIV by percutaneous blood exposure to small volume of blood being transmitted by 15-30 of every 1000 needlestick injury (Shiao et al,2000) compared with 3 per 1000 for HIV but among heterosexual partners and mother-infant transmission, HIV is more transmissible. HCV co-infection in an individual with HIV is likely to increase of HCV transmission in sexual partners.

2.5.1 Impact of HIV on HCV

Infections with HCV can be self-limiting, asymptomatic but co-infection with HIV could be disastrous. Torriani and Soriano,(2000) in their study on HCV and HIV dynamics in co-infected subjects, they estimated HCV virion half- life was longer with HIV co-infection, which clearly suggest that co-infection may contribute to slower clearance of HCV. Hepatitis C viraemia levels are higher in HIV co-infected patients than in those infected with HCV only.

When HAARTs is initiated in co-infected patients with HIV and HCV, it could be hypothesized that HCV levels would immediately decline due to improved immune response. However the effects of HAARTs on HCV serum remains controversial as most study findings show no change in HCV-RNA titres on HAARTs administration. Some studies have shown transient or sustained increase in HCV load (Puoti et al, 2000) while other showed a decrease in HCV-RNA levels and even a sustained clearance in some cases(Perez-Olmeda et al, 2000).These controversial ideologies emanating from the studies was traceable to other factors such as severity of liver dysfunction, natural fluctuations over time , HIV plasma viraemia level,CD4 T-lymphocyte count, HCV genotype and the level of alcohol consumable by the patient.

Soto et al, (1997) in their work titled ‘Human immunodeficiency virus infection modifies the natural history of chronic parenterally-acquired hepatitis C” reported that infection with HIV worsen the histological course of HCV infection by increasing and accelerating the risk of cirrhosis. Also in the cross sectional study, after 10 years HCV infection, 15% of HIV positive patients developed cirrhosis compared with only 3% in

the HIV negative group and the mean time of estimated onset of HCV infection to cirrhosis was significantly longer in HIV negative (23years) than HIV positive patients(7years). For HCV mono-infected, the major factor known to be associated with an increase risk of progression to cirrhosis are male gender, older age at HCV infection and excess alcohol consumption.

In the year 2000, one-fourth of death registered among intravenous drug users in the Aquitaine cohorts and in the French National Survey wasHCV related.Morbidity and mortality were compared among 263 patients with HIV alone and 166 patients with HCV co-infection, liver decompensation developed in 100% of patients with co-infection whereas no liver related death or decompensation occurred in patients with HIV alone(Monga et al, 2001).

Also, HCV seroreversion is observed more frequently in HIV co-infected patient than in the HCV mono-infected. Mechanism that could explain the accelerated progression of HCV in HIV positive patients are for now not fully understood. The decline in the humoral immunity mediated by the cell associated with HIV enhances HCV viral replication of the genome.

2.5.2 Impact of Alcohol on Hepatitis C

Alcohol consumption by infected patients enhances the risk of disease progression and life threatening consequences(Powell et al,2010). Researchers first became aware of the major effects of alcoholism on HCV when they noted that alcoholism was associated with HCV not (HBV) even in people who do not show classic risk factors such as intravenous drug abuse and blood transfusion.

In addition to promoting the acquisition or persistence of HCV,alcohol was shown to affect two major processes that are harbingers of rapid and severe progression of liver disease and of patient's deterioration namely inflammation and fibrosis.Other studies suggested that heavy consumption of alcohol enhances the ability of the virus to enter and persist in the body,concluding that the presence of inflammation in the liver is associated with presences of antibodies to HCV in alcoholic patients who have no other known risk factor for the infection(Rosman et al, 1993).

Furthermore, moderation of alcohol consumption was shown to result in a decreased number of viral particles in the blood.Though till date, researchers do not yet fully understand the mechanism through which alcohol affects the viral titre. It is well know that alcohol impairs the functions of certain compound in the body immune system(Ince and Wands,1999).An impaired immune function in turn may influence the ability of the virus to persist in the body rather than be eliminated by the immune cells.

Another mechanism through which alcohol consumption favors the progression of HCV infection is the oxidation stress. It refers to the presences of excessive loads of highly reactive molecules called free radicals in the cell or lack of oxidants that can eliminate free radicals.HCV itself can leads to oxidation stress.The virus induced-oxidation stress may be exacerbated by breakdown of alcohol in which the liver can generate free radicals that contributes to oxidation and are a major cause of alcohol related hepatic injury (Liber, 2001).

Several studies have shown that the rate at which HCV-induced hepatic scarring progresses is significantly correlated with alcohol consumption. Pessione et al, (1998) found that even moderate alcohol intake of approximately one or two standard drink per day increased not only the virus level in the blood but also the extent of hepatic fibrosis. Wiley et al,(1998) examined the effect of long-term heavy drinking on the progression of tissue damage and clinical symptoms associated with HCV infection, the study included women who consumed more than 40g of alcohol daily and men who consumed more than 60g daily for more than 5years, it was concluded that alcohol is an independent risk factor for the progression of HCV infection , specifically heavy drinkers have a two-three fold greater risk of cirrhosis and decompensated liver than the control subjects.

These findings that alcohol can accelerate liver damage associated with HCV infection are particularly important because HCV infected patients generally do not become sick or die because of the presence of virus in the blood but because of the complication to cirrhosis.HCV infection and alcohol enhances the risk of cirrhosis,

their combination results in a marked increased in the risk and consequently in accelerated development of hepatocellular carcinoma.

Owing to these influences of alcohol on HCV infected patients,the National Institute of Health consensus conference stated that ‘more than one drink per day is strongly discouraged in patients with hepatitis C andabstinence from alcohol is recommended (NIH, 1997). In fact continued alcohol intake for various reasons isconsidered a major contra-indication to interferon or ribavirin therapy(McHutschison,2006). Even in an HCV-infected alcoholic who stopsdrinking, the response rate to IFN-α which is a function of the level of alcohol consumption before the initiation of the therapy will be less compared to non alcoholics.However the actual level of alcohol intake that significantly promotes hepatic fibrosis in HCV infected patients are still unknown, based on this a greater number of clinical studies is needed to settle this uncertainty.Conclusively in any event, complete cessation of alcohol intake or at least reduction to moderate levelis crucial in HCV infected patients and should receive the highest priority when treating these patients.

2.6Therapeutic Development and Challenges of Conventional Treatments

In the early 2000, the combination of pegylated interferon(pegIFN) and ribavirin(RBV) became the standard anti- HCV treatment(Garg and Kar,2009). However, the therapy has some sort of shortcomings because it is associated with fatigue, epilepsy, flu-like symptoms and requires weekly injections. The numerous systematic side effects encountered from the use of this combination therapy for the treatment of hepatitis C virus have however led to thesearch for and development of numerous, well tolerated , new oral direct acting antiviral(DAAs) as a result of advances in the understanding of the HCV life cycle (Pawlotsky,2014).In principle, every step of HCV life cycle including receptor attachment, endocytosis, uncoating, polyprotein processing, replication,virion,assembly, maturity and release can be a target for new antiviral(Sheel and Rice,2013).

In 2011, the United States FDA approved the first DAAs, boceprevir with trade name victrelis and telaprevir having a trade name of incivek for the treatment of chronic

HCV genotype 1 infection (Poordad et al, 2011). In 2013, simprevir, sofosbuvir was approved. They are both protease inhibitors,non- structural RNA based with a potential advantage of shorter therapy duration of 12-24weeks for the treatment of genotype 1, 2 and 4 and 24 weeks for the treatment of genotype 3 compared to the long awaiting period of 48weeks for standard interferon and ribavirin treatment.

In December 2013, the licensed treatment for HCV infection includes ribavirin, pegylated interferon alpha(pegIFN-α), the NS3/4A protease inhibitors (boceprevir, telaprevir and simprevir) and NS5B nucleotide polymerase inhibitor,sofosbuvir. By 2014, the FDA approved harvoni, a combination of ledispavir and sofosbuvir to treat chronic HCV genotype 1(AASLD,2014).

EASL,(2015) reported that this new DAAs(simprevir,daclatasvir,sofosbuvir) was licensed in the European union with a clause that each of them be used as a combination regime with pegIFN-α and ribavirin, though their side effects profile and management remains challenging.

2.6.1 Ribavirin (Ribetol)

The introduction of ribavirin has no doubt reduced the relapse rate after interferon alpha monotherapy and significantly improved the sustained virological response rate. Ribavirin inhibits viral RNA polymerase, thereby inhibiting protein synthesis. Brok et al,(2010) in the study of randomized control trial involving 12,707 patients found that ribavirin combination with interferon therapy improved the likelihood of SVR in the treatment of naive HCV patients as compared with interferon alone.Despite this finding, the United States Food and Drug Administration issued a box warning for ribavirin usagebecause of the risk of hemolytic anemia, the medication may also worsen cardiac disease leading to myocardial infarction. This complication may result in ribavirin dose reduction or even discontinuation which may significantly affects the overall sustained virological response rate.

Therefore, it is a main task to reduce anemia, treatment with erythropoietin can effectively reverse ribavirin associated anemia and allow full adherence to therapy but the treatment is expensive and will not beaffordable in many countries.This problem

emphasizes the needs for alternative drugs with less toxicity and higher efficacy in attacking the virus.

2.6.2 Pegylated Interferon

Pegylated interferon inhibits viral replication by antiviral, antiproliferative and immunomodulatory effects. The two approved formulation are pegInterferon alfa-2a(pegasy as trade name) and pegInterferon alfa-2b(Peg-Intron as trade name). Two meta-analysis studies revealed that SVR was significantly higher for pegasys than for pegintron for all genotypes(Flori et al,2013).

The side effects associated with the use of interferon based therapy are life-threatening neuropsychiatric, autoimmune, ischemic and infectious disorders Neuropsychiatric side effects such as irritability,fatigue and apathy are frequent.Severe depression can occur and even suicide has been reported((Sulkowski et al, 2011).

The treatment with pegIFN-α induces autoimmune thyroiditis which starts with hyperthyroidism that later becomes hypothyroidism.Autoimmune thyroiditis has been reported in up to 20% of patients under and after IFN-α based therapy. This may not be reversible after stopping the therapy. Other autoimmune diseases can be aggravated by IFN-α therapy e.g. diabetes. Patients with documented hepatitis infection may deteriorate during IFN treatment.

2.6.3 NS3/4A inhibitors

Telaprevir(incivek) and boceprevir (victrelis) approved by FDA for the treatment of chronic HCV infection when use in combination with ribavirin or pegylatedinterferon. They are necessary for the proteolytic cleavage of the HCV encoded polyprotein into matured form of NS4A, NS4B, NS5A and NS5B proteins by inhibiting viral replications.The combination of ribavirin and victrelis should not be initiated until a report of negative pregnancy test has been obtained before starting the therapy. Patients under this drug must be advised of its embryocidal risk and must practice effective contraception during therapy. The two methods of contraception is

intranterine device and barrier method. Other side effects of this therapy include anaemia and neutropenia. Regimes including telaprevir and boceprevir are less effective and are associated with higher rate of serious adverse effects(AASLD,2015).Simprevir(olysio) is effective for genotype 1, 4, 5 and 6. The most common adverse effects includeanemia, flu-like symptoms, pruritus, headache and nausea. Boceprevir will be discontinued in the United States (Miller et al, 2015).

2.6.4 NS5B Inhibitors

Sofosbuvir (sovaldi) inhibits HCV viral assembly and RNA polymerase, thus inhibiting viral replication and it is effective for all HCV genotype (Miller et al, 2015).Sofosbuvir with ribavirin and interferon appears to be 80% effective in those with genotype 1,4,5 and 6 infections (Declerq, 2013). Ribavirin with sofosbuvir appears to be 60-80% effective in type 2 and 3 infection but has a high rate of adverse effect. The treatment that combines sofosbuvir and ritonavir for genotype 1 has a high success rate but it is expensive(Liang and Ghany,2013). In clinical studies,fatigue and headache were more common in patients treated with sofosbuvir and ritonavir (Jacobson et al,2013)

2.6.5 Treatment Regimes for HCV Infections

The American society for the study of liver disease in 2015 releases the recommendation for the treatment of infected patients and the cost estimate associated with each treatment regime as can be seen in table 2.1

Table2.1: Treatment Regimes and Cost Estimates (ASSLD, 2015)

Genotypes	AASLD Recommendations	Cost Estimate
1a	Ledispasvir/sofosbuvir (Harvoni) for 12 weeks	$93,000
	Ombistasvir/paritaprevir/ritonavir plus dasabuvir(viekira) and weight based ribavirin for 12 weeks(no cirrhosis) or 24 weeks(cirrhosis)	$94,000 $94,400(if RBV is used)
	Sofosbuvir(sovaldi) plus simprevir (olysio) with or without weight based ribavirin for 12weeks (no cirrhosis) or 24 weeks(cirrhosis)	$156,000 $156,400(if RBV is used)
1b	Ledispasvir/sofosbuvir for 12 weeks	$93,000
	Ombistasvir/paritaprevir/ritonavir plus dasabuvir for 12 weeks(no cirrhosis) or with addition of weight based ribavirin for 24 weeks(cirrhosis)	$94,000 $90,400(if RBV used)
	Sofosbuvir(sovaldi) plus simprevir (olysio) for 12 weeks(no cirrhosis) or 24 weeks (cirrhosis)	$152,000
2	Sofosbuvir(sovaldi) plus weight based ribavirin for 12weeks(no cirrhosis) or 16 weeks(cirrhosis)	$86,000 $86,400(if RBV used)
3	Sofosbuvir (sovaldi) plus weight based ribavirin for 24weeks	$86,000 $86,400(if RBV used)
4	Ledispasvir/sofosbuvir(Harvoni) for 12 weeks. Ombistasvir/paritaprevir/ritonavir plus dasabuvir(viekira)plus weight based ribavirin for 12weeks. Sofosbuvir(sovaldi) plus weight based ribavirin for 24weeks	$93,000 $94,000 $94,400(if RBV used) $188,00 $180,800(if RBV used)
5	Sofosbuvir(sovaldi) plus pegylated interferon plus weight based ribavirin for 12weeks	$97,000 $93,400
6	Ledispasvir/sofosbuvir(Harvoni) for 12weeks	$93,000

2.6.7 Treatment Indication Priorities for Hepatitis C Patients

Infected persons who do not take their medications on a regular basis exhibits less sustained response to full "adherence to therapy". It is an obvious case for all medical therapy, the context of adherence to therapy as used here is the 80/80 rule, patients who receive more than 80% of medication and were treated for more than 80% of the planned duration of the treatment are considered adherent (McHutchison et al,2002)

All treatment of patients with chronic liver disease related to HCV, who are willing to be treated and have no contra-indications to treatment should be considered for therapy, the following are the basis for treatment priorities;

- fibrous stage
- Risk of progression towards more advance disease
- Decompensated liver cirrhosis
- Patients who have contra-indication to interferon alpha(IFN-α) can be safely treated with IFN free regimes
- Presence of extrahepatic manifestations of HCV infections
- Risk of HCV transmission.
- High group priorities which includes patients with debilitating fatigues, patients with pre or post liver transplant settings, patients with hepatitis B virus(HBV) or human immunodeficiency virus(HIV) co-infection

For patients with moderate fibrosis, no severe extrahepatic manifestation, informed deferral can be considered. This category of patients with informed deferral can be assessed on a regular basis for evidence of progression and to discuss new therapies as they emerge.

2.6.8 Potency of Conventional Antiviral Drugs Using Medical Approach

Medically**,** sustained virological response is achieved when the antiviral on continued administration reduces the viral load of HCV to clinically undetectable levels within the first 12-24 weeks. Within this period, the immunological response by virtue of the steady administration of the drugs on the HCV infected blood is the increased of CD4 cell count. Clinically, the symptoms of the infection as believed will subside within this period. But these antiviral drugs do not eliminate totally the virus from the blood stream and only provides a functional cure with side effects.

Ani, (2015) verified the efficacy of five conventional antiretroviral drugs against the HIV particles suspended in the blood stream using the Hamaker concepts of surface energetics. He reported that the reaction of the administered antiretroviral drugs with the virus facilitated the repulsion between the virus and the lymphocytes. The positive values of the absolute combined Hamaker coefficients for uninfected blood-drug interactions imply attraction or coating of lymphocyte particles by the drug particles. Therefore, the power of effecting functional cure is the potency of the antiretroviral drugs that have been quantitatively and qualitatively verified.He equally reported that the surface energy is being lowered by the presence of the virus but upon the administration of the antiretroviral drugs, the surface energy of the blood cells increases.

Chukwuneke, (2015) investigated the nature of interaction between mycobacterium Tuberculosis (M-TB), macrophage and HIV particles. He confirmed that the positive value of the absolute combined Hamaker coefficient which entails net positive van der Waals forces demonstrates attraction between M-TB and the macrophage. But in the presence of HIV, the interaction energy is reduced and the negative value of the absolute combined Hamaker coefficient indicates that the repulsion of M-TB is attainable.

2.6.9 Drug Administration Standard

Appropriate mediation for hepatitis C infected patient influences adherence, concordance, symptoms control and further management of the infection since total

eradication of the virus is unattainable. Medication administration is not without problems, drugs can be dangerous and poisonous to the body if there is an error in the process of prescribing, dispensing, preparing and administering drugs for the treatment of viral diseases. To this effect, the National Patient Safety Agency (NPSA) was set up to monitor drug administration errors and relates to all health professionals involved in medication management.

Most serious medication incidents reported are caused by errors in administration (41%), Prescribing (32%).Over half of all drug errors relates to dosage, strength, frequency or a failure to administer, poor labeling and storage, expired drugs etc. The NPSA (2007) reported that 71% of fatal and serious harm from medication incidents are due to;

1. The wrong dose being written
2. Unclear prescription
3. Wrong frequency being prescribed.
4. The drug being omitted.
5. The medicine being delayed.
6. Wrong quantity being described.

The Nation Prescription centre NPC, (2012) made it clear that the responsibility for managing the environment in which drug administration takes place and reducing the possibility of drug error is a multi-disciplinary concern. Therefore, there is a requirement for all health professional to employ a broader, holistic understanding of medication management.

NMC, (2015) tasked all drug prescribing and non prescribing professionals to ultimately aimed at pro vision of safe medication administration which is based on the evidence of the purpose of the prescribed drug(s).NPC (2012) came up with a frame work of the Ten ‘R’ approach to safe drug administration for nurses and other health professional to consider then roles in medication management. These approaches are are depicted in table 2.2.

Table 2.2: Drug Administration Criteria(National Prescription Center, 2012)

Ten R	Considering the following	Tine
Right Patent	• Has this patent been prescribed the drug • Has the patent name band been checked • Does this patent been receiving the drugs and why	Before Administration
Right Drug	• Do you know where to obtained the drug • Are all the drugs prescribed in one location • Does this prescribed drugs has a similar name	Drug preparation
Right dosage	• Is the dose appropriate for the drug prescribed? • If appropriate, has the drug been checked by another professional.	
Right time	• Has the time gap between end drug administration been adequate, sufficient, too long or short	
Right routes	• Is the route appropriate for the drug prescribed	
Right to refuse (patient or nurse)	• Know what action to take of a patient refuses the prescribed medication.	
Right questions or challenges	• Is this the right prescription • Is this the appropriate drug for the patient condition • Can the writing be read easily	
Right knowledge	• Knowledge of the drug side effects, possible, intraction, overdosing the drug possible occurance of advisable effects.	
Right Advice	• Can you give patient advice, details, information about medication.	
Right response or outcome.	• Do you know the expected outcome of the drug, allergic reactions of the drug interactions.	

.

2.7 Medicinal Plants and its Components

To date, many medicinal plants have been tested against HCV and have proved beneficial as antiviral mediators. The use of complementary and alternative medicine is widespread with approximately 40% of Americans using some form of this therapy.Some have substituted alternative medicine for scientifically accepted treatment modalities, some utilize this therapy as a supplement to conventional medicine. Thereasons for this preference are as follows:

- A desire to have more autonomy in choosing their treatment
- A perception that alternative therapies are safer and more natural
- A concern over the cost and side effects of the conventional medicine
- A sense that that they will be able to have more person relation and time with the practitioners than in a conventional settings.
- A sense of their multiple target activities.

The phytochemicals of these medicinal plants such as flavonoids,limonoids,alkaloids,lignama, organosulfur, terpernoids, phenolics, chlorophyllins,conmaris,furyl, saponins and so on are considered important due to their efficiency at hampering viral entry, blocking and limiting the RNA genome replication and their anti-oxidant activities (Naithani et al, 2008).Natural compounds extracts can serve as a source of potential new antiviral drugs against hepatitis C infection, its use can be extended to either as prophylactic or therapeutic treatment administered as teas, powders and other herbal formulations.Phenolic compounds are often responsible for the bioactivities of the plant crude extracts (Samuelsson and Bohlin, 2004).

The identification of precisely the active molecules in the plant extracts has led to a systematic screening of natural molecules present in the plant extracts and test the activities of this phytochemicals using appropriate assays depending on the pathology studied. Some natural compounds have been shown to possess antiviral activities against herpes simplex virus (HSV), influenza virus, human immunodeficiency virus(HIV) and hepatitis B and C virus(Cavallaro et al,1995). Medicinal plants have

various effects on living systems such as antioxidants, hepato-protective,cardio protective, sedatives, analgesic, antispasmodics and immunomodulatory functions (Okwu and Ezenagu,2008).

Recently, medicinal plants from Indonesia have been tested for their antiviral activities against HCV, ethanolic extracts from Indonesia plants were analyzed in the Huh 7.5 cell line and HCV strain of different genotype. Among the tested plants, toona sureni leaves(TSL) showed IC_{50} value of 13.9, melocope latifolia leaves (MLL) showed IC_{50} value of 3.5, melanolepis multigalandulosa stem(MMS) showed IC_{50} value of 17.1 and fiscusfistulosa leaves (FFL) showed IC_{50} of 15. Among these plants, MLL,TSL,FFL and MMS exhibited antiviral activities against all genotypes and thus suggest that these plants may prove good candidate to develop inhibitory drugs against HCV(Wahyuni, 2013)

Jacob et al,(2004) investigated a Korean medicinal plant, milk thistle aqueous extract for antiviral activity. It was found that the plant showed effective antiviral capability at the concentration of 100μg/ml. Some of the plants implicated for their potency towards HCV are milk thistle, solanum migrum, Q.inferia and lamina album but these extracts awaits clinical trials and some have its uses from literature background.

- **Flavonoids**

These are class of plant secondary metabolites that are naturally present in plants. More than 4500 flavonoids have so far been characterized and it is been classified according to their chemical structure within different subgroups.

- **Ladanein**

Haid et al,(2012) isolated a molecule with anti-HCV activity in a screen of a library of natural phenolic compounds from plant extracts. From the most active plant extracts, the characterized and re-synthesized components exhibitedthe highest antiviral activity. Ladannein is a molecule belonging to a sub group of flavonoids family and was identified as an active anti-HCV component.

- **Luteolin and Apigenim**

These are two other natural flavones molecules identified as anti –HCV agents in plants via a pharmacophore search. Liu et al,(2012)in their study established a designed pharmacophore from NS5B inhibitors selected from a literature according to different criteria. It was shown that luteolin exhibited a good inhibition of NS5B polymerase enzymatic function. Although a number of natural compounds with anti-HCV were identified in recent years, many aspects concerning their mechanism of action remain unknown, more often the replication was the only step of the virus life cycle that was investigated and conclusion was only based on in vitro models. Yet, ladanein proved to be a potent entry inhibitor.

2.7.1 Review of Selected Plants used for the Study

The following medicinal plants were selected for the study based on the claimed by the local practitioners of complementary and alternative medicine for its ability to control hepatitis C virus infection. This information was gotten on my attendance to the Delta State Traditional Medicine Board during their Scientific Herbal Exhibition held at Agbor in Ika south local government area of Delta state on September 2016.

- **Vernonia Amygdalina**

Vernonia amygdalina is a small shrub that belongs to the family of Asteraceac. It grows to a height of about6.6-16.4feet.Its leaves are elliptical and 20cm long. It is called bitter leaf in English name and has a rough bark. The leaves are used for human consumption and are washed before eating to get rid of the bitter taste. It is use as vegetables and stimulates the digestive systems as well as reduction of fever, chimpanzees eats it if they have attack by parasites (Ijeh and Ejike, 2011).

Vernonia amygdalina is now been used in place of hops to make beer drinks.The bitter taste is due to anti-nutritional factors such as alkanoids,saponins,tannins and glycosides. It is a medicinal herb popular among alternative medicine practitioners due to its functions as a blood purifier,anti-laxative and anti-helminths. It is also used by scientist in the cure of joint pains associated with diabetics, AIDS, persistent

headache, while its root applied in the treatment of gastrointestinal dysfunction, toothache and fertility problems(Momoh et al,2010).The decoction from the leaves have been reported for its medicinal powers against bacteria and viruses.

A lot of research has been done in the past to ascertain the medicinal power of vernonia amygdalina using streptozotocin-induced diabetic laboratory animalsand was found that its administration decreased blood glucose by 50% compared to untreated diabetic animals(Nwanjo,2007). Vernonia amygdalina has also been fed to broilers where it was able to replaced 300kg/kg of maize-based diets without affecting the feed intake, body weight gain and feed efficiency.Sweeney et al,(2008) reported that V.amygdalina extracts may strengthened the immune systems through many cytokinesmolecules. In other studies, vernonia amygdalina was found to reducethe blood estrogen level in the etiology of estrogen receptor.

- **Bryophyllum Pinnatun**

Bryophyllum pinnatum also known as resurrection plant, miracle leaf, life plant and cathedral bell is a succulent plant native to Madagascar, Central America and South Africa.It is a popular house plant and has become naturalized in tropical and sub-tropical areas. It has tall hollow stem, freshly dark green leaves that reproduces through the leave bulbis and the seed.

B.pinnatum is used in ethnomedicine for the treatment of earache, burns,abscesses,ulcer, insect bites,whitlow, diarrhea and cithiaris (Agoha,1974).It is use to cut the umbilical cord in new born babies, induce vomiting of blood,cure acute and chronic bronchitis, expelling of worms from the stomach, pneumoniaand other respiratory tract infections(Mudi and Ibrahim,2008).It is also medicinally used in tropical Africa, South America, India, China, and Australia where it grows as weeds. Theleaves stem, root and bark are used both internally and externally as an analgesic, its roots and leaves can also be soaked in cold water to drink (Almeida et al, 2006).

Several biological activities include hepato-protective immunosuppressive effects, acetylcholinesterase inhibition, rheumatism and inflammatory process inhibition (Almaida et al, 2006).

B. pinnatum has been reported in Trinidad and Tobago as being used for the traditional treatment of hypertension (Lans, 2006).It has also been reported to contain wide range of bioactive compounds that has strong inherent ability to modify the body reaction to allergies, viruses, and carcinogens(Okwu,2008), suggestive of its anti-allergic, anti-inflammatory, anti-microbial and anti-cancer potentialities.

Furthermore, β- and α- amyrin acetate has also been isolated from the leaves of B. pinnatum and other important phytochemicals.Hydrocarbons have also been reported as isolates from B.pinanatum.

- **Phyllantus Amarus**

Phyllantus genus family was first identified in Central and Southern India in 18th century,it is commonly called carry me go, stone-breaker, gala of wind.Phyllantus amarus is an erect annual herb of about 1.5ft tall having small leaves and yellow flowers.In folk medicine, phyllantus amarus have been reportedly used in the treatment of jaundice,diabetics,skin ulcer, diarrhea, gastrointestinal disturbances. It blocks DNA polymerase of viruses duringproduction (Oluwafemi and Debiri,2008).Several compounds including alkanoids,flavonoids,lignan,phenols and terpenes were isolated from this plant and some of them interact with mostly key enzymes (Joseph and Raj,2010).

In traditional medicine, it is use for its hepatoprotective, anti-diabetic, anti-hypertensive,anti-inflammatory, analgesic and antimicrobial properties(Adeneye et al,2006).Its antiviral activities, antimutagenic activities and anti-carcinogenic activities have been established.The phytochemical compounds contained in phyllantus amarus are lignin,geramin , quercertin,astralgin,rutin and isoquercitrin(Thyagarajan et al, 1998).

Alcoholic,hexane,chloroform, butanol and water extracts of phyllantus amarus were tested for in vitro effects on HbsAg, HbcAg and HBV-DNA in serum samples positive for HBV antigens followed byscreening of the respective antigens by Elisa. The extracts were effective against HBV antigens, the butanol extract being the most effective (Mehrotra et al, 1999).

Another antiviral activity of phyllantus amarus was demonstrated on mice infected with woodchuck hepatitis virus, when administered with extracts was effective in three animals in reducing the virus within 3-6 weeks eliminating both the surface antigen titre and DNA polymerase activities in serum(Venkateswaran et al,1987).

- **Anona Muricata**

Anona muricata popularly known as soursop in English is a broad leaf belonging to the family of Anonaceace and has its native in Central America. The fruits are dark green, ovoid with a moderate firm texture, their flesh is juicy, whitish and aromatic (Pier, 2008). A flesh of the fruit consist of an edible white pulp and a core of indigestible black seeds, it is use to make fruit nectar,smoothies, fruit juice drinks ,candies, ice cream flavoring and other beverage products in many parts of the world.

Intensive chemical investigations of the leaves and seed have resulted in the isolation of great number of acetogenins which displayed interesting biological and pharmacological activities such as anti-tumoral, cytotoxicity and antiviral. Leaf extracts of anona muricata is use in the treatment of various infectious disease such as pneumonia, diarrhea, urinary tract infection and even some skin disease. It contains wide spectrum of activities ranging from food source to medicinal in the life of human (Pathak et al, 2010). It is also medicinally used in tropical Africa, South America, India, China, and Australia where it grows as weeds. Theleaves stem, root and bark are used both internally and externally as an analgesic, its roots and leaves can also be soaked in cold water to drink. (Duraipandiyan et al, 2006).

2.8 Thermodynamic Approach to Hepatitis C virus and Blood Cells Interaction

The mechanism and treatment of hepatitis C virus is a developing area that demands an interdisciplinary approach. This method as adopted by this research will help investigate how well the treatments with both the conventional and the bio-extracts coats the virus which indicates the degree of wetting when the HCV-RNA is inoculated in the experiment *in vitro*. The interaction between the HCV-RNA and the treatments can be likened to particle – particle interactions (Achebe et al,2012).

Mechanism of interactions can be achieved with an in-depth knowledge of the surface properties determination of the interacting particles. A common area of contact is established as soon as two particles meet each other. Therefore, a certain portion of each particle gets displaced through work. Work responsible for the displacement of a unit area is known as surface free energy. The consecutive impact on the surface is known as surface thermodynamic effects. In this particular study similar occurrence can be envisaged to characterize the HCV-RNA particles (Chukwuneke et al, 2015).

2.8.1 The Concept of Contact Angle

Precise characterization of solid material surfaces plays a vital role in research and product development in many industrial and academic areas. Wettability of the surface is important in processes like painting and printing, and has been utilized in the study of cell - biomaterial interactions

The contact angle less than 90^0($\theta<90^0$) indicates that the wetting of the surface is favorable and the fluid spread over a large area of the surface while the angle greater than 90^0($\theta>90^0$) generally means that the wetting of the surface under consideration is not favorable and as such the fluid will minimize its contact with the surface to form a compact liquid droplets. More specifically, contact angle of zero($\theta=0$) characterize complete wetting as the droplets turns into a flat puddle (Yuan and Lee, 2013).

Young equation defines contact angle as:

$$\gamma_{lv}\cos\theta = \gamma_{sv} - \gamma_{sl} \qquad (2.1)$$

γ_{lv}represent the liquid-vapor interfacial tension,γ_{sv} represent the solid-vapor interfacial tension,γ_{sl}represent the solid-liquid interfacial tension andθ is the contact angle.

With the application of young's equation to the HCV-RNA particles, there exist three thermodynamic parameters as earlier statedγ_{lv},γ_{sv}, γ_{sl}which determined the unique contact angle θ. If the three contact line is in actual motion as in the case of blood stream with HCV particles, the contact angle produce is a dynamic contact angle.

It should be emphasized that to obtain finite, measurable contact angle, γ_l must be greater than $\gamma_{s.}$ When γ_l<γ_s, the liquid forms no contact angle on the solid but spreads and wet it completely. The extent of partial wetting of the soild by the liquid is quantified by the value of θ. The lower value of θ signifies a better wetting ability and conversely, higher value of θ indicates a poorly wet surface.

Examples of poorly wetting systems are mercury on glass and water on hydrophobic surfaces where little liquid drops can be seen rolling over the surface. Complete wetting occurs when liquid fully covers the solid and spread spontaneously over the surface and no contact angle can be defined.

At this point, the spreading coefficient S becomes necessary, which is a measure of the difference in surface energy between the bare dry solid and the moist solid covered by the macroscopic film of liquid.

$$S=\gamma_s - (\gamma_{sl}+\gamma_l) \qquad (2.2)$$

If $S \geq 0$, spreading occurs (complete wetting), then the work of adhesion is higher than the work of cohesion. When S is negative, the surface prefers to remain dry which is the case of partial wetting. The liquid will only spread to cover part of the solid and in equilibrium will assume a finite contact angle. It is worth stating here that the water contact angle can be taken as a measure of the relative hydrophilicity or hydrophobicity of a given solid. That is the higher the contact angle is, the more

hydrophobic the solid surface becomes. In principle, solids having lower surface free energies ($\gamma_{sv)}$ exhibits higher values of contact angles.(Rullison, 2008)

Contact angle hysteresis is the difference in the angle formed as a result of either expanding (advancing) or contracting (receding) of the liquid. The advancing angle approaches a maximum value while receding approaches a minimum value(Krumpfer et al,2010).

$$H = \theta_a - \theta_r \qquad (2.2a)$$

Where θ_a is the advancing angle while θ_r is the recedingangle and H isthe contact angle hysteresis

The significance of contact angle hysteresis is that it arises from the surface roughness and heterogeneity. In cases where surface roughness plays the role of generating the hysteresis, the actual microscopic variation of the slope on the surface creates barriers that slow the motion of the contact line and as such altering the contact angle. Therefore, interpreting such angles based on young's equation could be prone to error as the equation does not put the surface topography into consideration.From young's equation, only two measurable quantities can be obtained, the contact angle θ and the surface tension of the liquid $\gamma_{lv,.}$ In determining γ_{sv} and γ_{sl}, an additional relation between these quantities must be established.

Zisman et al (1964) carried out several studies on contact angle using high energy liquids on low energy solid surfaces, they found that for a given solid, the measured contact angle do not vary randomly upon change of the test liquid, instead the change of cosθ versus liquid surface tension γ_{lv}falls into a trend for a homologous series of liquids. The critical surface tension γ_c where cosθ=1 established the theoretical fact that for any liquid with surface tension equal to or less than $\gamma_{c\,,}$ will completely wet the solid surface(θ=1).

Neumann et al, (1974) measured the contact angle of a large number of liquids on solid surfaces, from which a curve of γ_{lv}plotted against γ_{lv} Cosθ was obtained and it

agrees with the equation of state. The equation of state can be used to determine the value of γ_{sv} from a single contact angle and the surface tension of the liquid.

$$\gamma_{lv}\text{Cos}\theta = f(\gamma_{lv},\gamma_{sv}) \qquad (2.3)$$

Combining (2.1) and (2.3) yields

$$\gamma_{sl}=\gamma_{sv}-f(\gamma_{lv},\gamma_{sv})=f(\gamma_{lv},\gamma_{sv}) \qquad (2.4)$$

The experimental procedure for measuring contact angle and its interpretation in terms of young's equation was analyze in the works of Kwok and Neumann,(2003), stressing the need of how efficiently contact angle can be measured with strict adherence to the following assumptions;

-All approaches rely on the validity and applicability of young's equation for surface energetic from the experimental contact angles.

-The values of γ_{lv}, γ_{sv}, γ_{sl} are assumed to be constant during the experiment i.e. no reaction is expected between the liquid and the solid.

- The surface tension of the test liquid should be higher than the anticipated solid surface tension

-The values of γ_{sv} in going from liquid to liquid are also assumed to be constant.

-Advancing angles instead of receding angles should be used as this minimizes the possible swelling, chemical and physical effects.

There is now a lot of spectroscopic and other analytical techniques for probing surface properties of solid materials and their liquid interactions, however only contact angle analysis is capable of yielding the actual surface or interfacial properties(Van Oss and Giese,2002).

2.8.2 Sessile Drop Techniques

Several techniques are available for the measurement of contact angle such as wilhelmy balance method, capillary rise method, dunoy ring method and sessile drop

method but the use of sessile drop method as a means of characterizing surfaces is increasingly on the lead. The advantages of this method are easy handling and rapid data collection, high reproducibility through automatic dosing and positioning of test liquids and user-independent measurement through software controlled contact angle determination. It can be stated here that contact angle are not limited to liquid vapor interface on solids, they are also applicable to liquid-liquid interface on a solid.

The sessile drop technique is a method used for the characterization of surface energies of both solids and liquids. Parameters like contact angle, known surface energy of the liquid can be used to calculate the surface energies of the solid and the liquids used for such experiments are called the probe liquids. The measured angle θ is the contact angle as shown in figure 2.7.

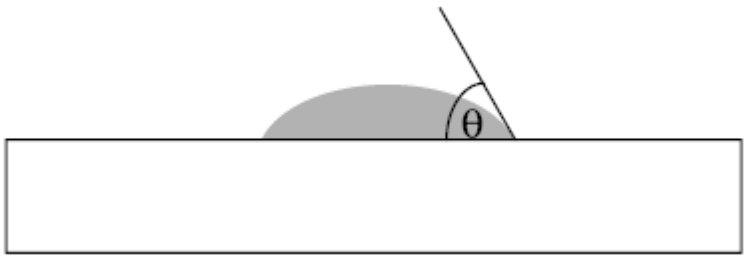

Figure 2:7 Contact angle diagram (Rullison,2008)

The surface tension of liquids is measured in Newton per meter (Nm^{-1}) and can be obtained through various methods. The interfacial tension can be viewed as being products of different intermolecular forces. The values obtained through sessile drop depend not only on the solid samples in contact but also as a result of the properties of the probe liquids used.

The Zisman plot used for the determination of surface energy of the liquid is limited to single parameter rather than accounting for the fact polar interactions may be encountered which greatly may alter the calculations.

2.8.3 **Free Energy of Cohesion andAdhesion**

Dupreintroduced the work of adhesion w_a and cohesion w_c after the works of young. The equations given by Dupre can be use to derive other parameters from the experimental contact angle and surface tension result.

Considering the reversible process of bringing together two cylinders of a condensed-phase material initially in vacuum, to form a continuous body, the free energy change per unit area is the free energy of cohesion or the negative work of cohesion.

$$. -w_c = -2\gamma = \Delta G \qquad (2.5)$$

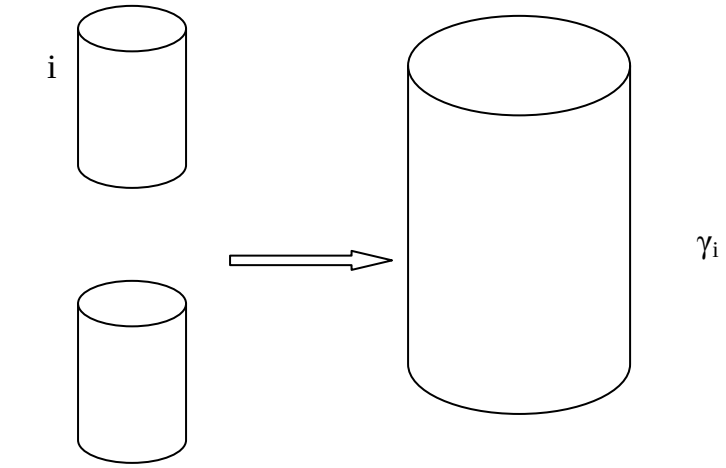

Figure 2.8a: Conceptual illustration of Cohesion Process

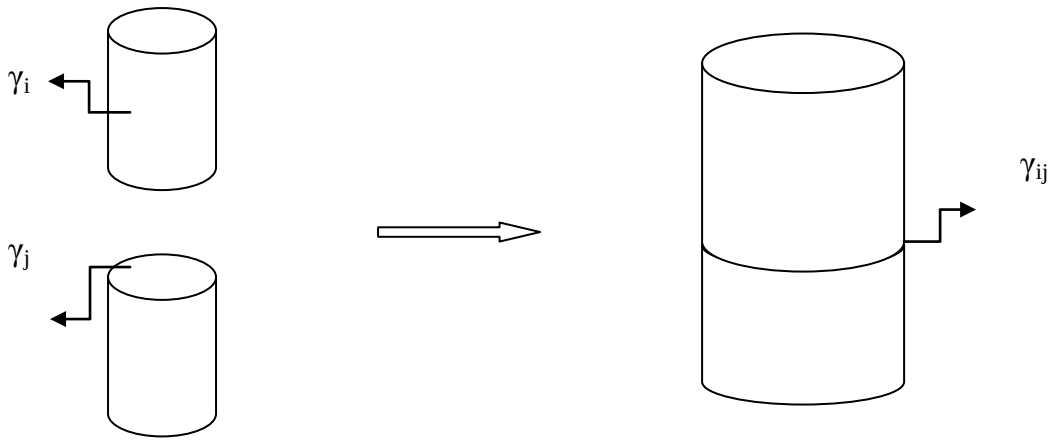

Fig 2.8b: Conceptual illustration of Adhesion Process

Figure 2.8b depicts a scenario of two unlike bodies in contact; the free energy per unit area is the free energy of adhesion or the negative of the work of adhesion.

$$\Delta G_{ij}=\gamma_{ij} - \gamma_i - \gamma_j = - F^{adh} \quad (2.6)$$

$$\Delta G_{ij}=\gamma_{lv}(1+\cos\theta) \quad (2.7)$$

To obtain a measurable contact angle, γ_{lv} must be greater than γ_{sv}, therefore when $\gamma_{lv} < \gamma_{sv}$ the liquid forms no contact angle on the solid but spread and wet it completely. But when the solid surface is in equilibrium with the liquid vapor, the reduction of the surface free energy of the solid to the vapor adsorption is termed the equilibrium spreading pressureπe.

Then equation (2.1) becomes:

$$\gamma_{lv}\cos\theta=\gamma_{sv} - \gamma_{sl} + \pi e \quad (2.8)$$

The spreading pressure S is a function of reduction in the value of free energy of the solid due to adsorption of liquid vapor. The spreading coefficient is a measure of the difference in surface energy between the dry solid and moist solid covered by microscopic film of liquid

$$S=\gamma_s - (\gamma_{sl} + \gamma_{lv}) \quad (2.9)$$

The spreading work $w_s = \gamma_{lv}(\cos\theta - 1)$ (2.10)

Wetting tension $T=F/P = \gamma_{lv}\cos\theta$ (2.11)

2.8.4 SurfaceEnergy Determination

Several thermodynamic approaches have evolved over the years for determining the values of surface energy components of solids; it is applicable to both polar and non polar systems.(Van Oss,1994). Though defined as work required tobuild a unit area, when it comes to its measurement using sessile drop technique, the surface energy is not quite as well defined. The values of contact angle obtained through the sessile drop techniques depends not only on the solid samples in use but equally on the

properties of the probe liquids being used as well as the particular theory relating mathematically to one another.

Researchers have overtime developed such numerous theories which differ from each others in terms of derivation and conventions, but most importantly they differ in the number of components which they are equipped to analyze. The simpler methods containing fewer components simplify the system by lumping surface energy into one another while the more complex methods having more components are derived to distinguish between various components of the surface energy.(Oura et al,2001).

The total surface energy of solids and liquids depends on different types of molecular interactions such as dispersion (van der Waals), polar and acid /base interactions and is taken to be the sum of these independent components. Some theories account for more of these phenomena than the others.The following are some of these theories;

2.8.4.1Van Oss-Chauhurry-Good (OCG) Approach

This approach separates the surface energy of solids and liquids into three components which includes the dispersive surface energy, acidic interaction surface energy (γ^+) and surface energy due to the base content (γ^-). The acid component theoretically describes a surface propensity to have polar interactions with a second surface that has the ability to act basic by donating electrons.

$$\gamma_{lv}(1+\cos\theta) = 2(\sqrt{\gamma_s^{lw}\gamma_l^{lw}} + \sqrt{\gamma_s^+\gamma_l^-} + \sqrt{\gamma_l^+\gamma_s^-}) \qquad (2.12)$$

The left hand side of the equation represents the part of energy of cohesion of the liquid which is in equilibrium. The right side is the energy of adhesionbetween the liquid and the solid , the value of contact angle is a competing tendencies between the energy of liquids and that of adhesion between the solid and the liquid (Yildirim,2001).

Three unknownquantitiesγ_s^{lw}, γ_s^+ , γ_l^-exist in equation (2.12)

For apolar liquids, equation (2.12) reduces to

$$\gamma_{lv}\ (1+\cos\theta) = 2(\sqrt{\gamma_s^{lw}\gamma_l^{lw}}) \qquad (2.13)$$

$\gamma_l^+ = \gamma_l^- = 0$ and $\gamma_l = \gamma_l^{lw}$

Once, the three surface tension are known, the total surface tension of the solid becomes:

$$\gamma_s^{Total}, = \gamma_s^{lw} + 2\sqrt{\gamma_s^+ \gamma_s^-} \quad (2.14)$$

Being a three component theory, it is naturally more robust than others especially in cases where there is a great imbalance between the acid and base component of the polar surface energy such as testing the surfaces energies of inorganics, and ionic surfaces.

The application of van Oss theory is not without difficulties due to the fact that there is not much of agreement in regards to a set of reference solids that can be use to characterize the acid and base components of potential probe liquids.

2.8.4.2Neumann Approach

Though there are few different models based on the equation of states, the best known is the Neumann approach (Kwok and Neumann, 1999).

The combining equation for Neumann and Young is stated as:

$$\gamma_{lv}\,(1 + \cos\theta) = 2\sqrt{\gamma_{sv}\gamma_{lv}}\exp^{-\beta(\gamma_{lv}-\gamma_{sv})2} \quad (2.15)$$

Undergoing a long development from its groundwork, the Neumann equation of state as in equation 2.15 reaches its contemporary form;

$$\cos\theta = -1 + 2\sqrt{\frac{\gamma_{sv}}{\gamma_{lv}}}\, e^{-\beta(\gamma_{lv}-\gamma_{sv})2} \quad (2.15a)$$

Other forms of equation of state was also derive from the fundamental thermodynamics of intermolecular interaction and further modification of Berthelot hypothesis respectively (Neumann et al, 1983).

$$\gamma_{sl} = \frac{(\gamma_{sv}^{1/2}-\gamma_{lv}^{1/2})^2}{1-0.015(\gamma_{sv}\gamma_{lv})^{1/2}} \quad (2.16)$$

$$\gamma_{sl} = \gamma_{sv} + \gamma_{lv} - 2\sqrt{\gamma_{sv}\gamma_{lv}}\exp 1\text{-}\beta_1(\gamma_{lv}\gamma_{sv})) \quad (2.17)$$

$$\gamma_{sl} = \gamma_{sv} + \gamma_{lv} - 2\sqrt{\gamma_{sv}\gamma_{lv}}\exp 1-\beta_2(\gamma_{lv} - \gamma_{sv})^2 \quad (2.18)$$

The value of β_1 and β_2 as determined experimentally is 0.0001247 and 0.0001057 respectively. In principle the equation of state requires the measurement to be done only by using one liquid and regardless which liquid is chosen the surface free energy result should be the same. There is a lot of criticism against this theory. The controversy deals with the question whether the constant β is universal constant of the materials or just quantity obtained as a result of the iterative procedures applied. Equation of state theory also does not divide the surface tension into different components as the other theories. This is also the only theory which allows the calculations to be done by using just one probe liquid.

2.8.4.3Owens/Wendt Approach

This approach derived from the combination of Young and Good's equation divides the surface energy into two components; surface energy due to dispersive interactions and surface energy due to polar interactions.

$$\frac{\gamma_{lv}(1+\cos\theta)}{2\sqrt{\gamma_l^d}} = \frac{\sqrt{\gamma_s^p}\sqrt{\gamma_l^p}}{\sqrt{\gamma_l^d}} + \sqrt{\gamma_s^d} \quad (2.19)$$

Note that the above equation has the form of y=mx +c, having

$$y=\frac{\gamma_{lv}(1+\cos\theta)}{2\sqrt{\gamma_l^d}}, m=\sqrt{\gamma_s^p}, x=\frac{\sqrt{\gamma_l^p}}{\sqrt{\gamma_l^d}} \text{ and } c=\sqrt{\gamma_s^d}$$

From the foregoing, the polar and the dispersive component of the solid surface energy are determined by the slope and intercept of the resulting graph.

This approach is typically applicable to surfaces of low charges and moderate polarity such as polymers containing heteroatom such as PVC, polyesters and polyamines.

2.8.4.4Fowkes Approach

This approachis derived in a slightly different way from Owens/Wendts theory. Though, mathematically, both equations are equivalent. Fowkes summed up the

independent components of surface tension in the interaction in determining the surface energy of the solid(and of a liquid), it is given as;

$$\gamma_s = \gamma_s^0 + \gamma_s^d + \gamma_s^p + \gamma_s^h + \gamma_s^i + \gamma_s^{ab} \quad (2.19)$$

Thesubscripts represent other interactions, dispersion, polar, hydrogen bonds, induction, and acid base energies.

For non polar solids $\gamma_s = \gamma^d$

Fowkes approach generally requires the use of only two probe liquids especially glycerol which should have no polar component due to its molecular symmetry and water which is commonly known to be a polar liquid.

$$\gamma_{sl} = \gamma_s + \gamma_l - 2\sqrt{\gamma_s^d \gamma_l^d} \quad (2.20)$$

The sum of all the components occurring at the right hand side of Eq(2.19) except γ_s^d are associated with polar interaction, then the following equation was obtained;

$$\gamma_{sl} = \gamma_s + \gamma_l - 2\sqrt{\gamma_s^d \gamma_l^d} - 2\sqrt{\gamma_s^p \gamma_l^p} \quad (2.21)$$

Fowkes theory is more applicable to situations where adhesion occurs and in general works better than Owens/Wendts when dealing with higher surface energies.

2.8.4.5Wu Model

Souheng Wu theory is also similar to that of Owens/Wendt and Fowkes in that it divides surface energy into polar and dispersive component.Wu employed theharmonic mean rather than the geometric mean of known surface tension and subsequently the use of more rigorous mathematics is employed.

One major challenge encounter when using Wu's equation is the mathematical concept involved which yields two results for each component.One being the true results while the other being simply a consequence of mathematics. The challenge here lies in interpreting which is the true result, though is easier to just eliminate the negative surface energy. From equation (2.21), equation (2.22) was obtained after

dividing the surface energy into lifshitz-van der Waal components γ^{LW} and acid base component γ^{AB}

$$\gamma_{sl} = \sqrt{\gamma_s^{LW}} - \sqrt{\gamma_l^{LW}} + 2\{\sqrt{\gamma_s^+}-\gamma_l^+\}.\{\sqrt{\gamma_s^+} - \sqrt{\gamma_l^-}\} \quad (2.22)$$

2.8.4.6 **Zisman Approach**

The Zisman theory is the simplest commonly used theory as it is one component theory and it is best used for non polar surfaces. It is more useful for low energy surfaces and as such is not suitable for polymer surfaces that has been subjected to heat treatment, plasma cleaning or polymers that contains heteratoms.

The findings of Fox and Zisman,(1950) that cosθ is a linear function of γ_l by plotting the points for various liquids and fitting lines through them.The best way to determine the surface energy by Zisman approach is to acquire data points of contact angles for several probe liquids on the solid surface and then plot the cosine of that angle against the known surface energy of the probe liquids. By constructing the Zisman plot, the critical surface tension γ_c can be obtain by extrapolating the line cosθ=1. Table 2.3 shows the surface tension components and parameters of common probe liquids.The presence of surface active elements such as oxygen and sulphur will create an enormous impact on the measurement obtained with these liquids. Surface active will exist in large concentrations at the surface than in the bulk of the liquid, meaning that the total level of these elements must be carefully controlled to a very low level.

Table 2.3 Surface tension components and parameters of common probe liquids (Van Oss, 1978)

Liquid	Total Surface Tension(mN/m)	Dispersive (mN/m)	Polar (mN/m)	Acid (mN/m)	Base (mN/m)
Hexane	18.4	18.4	0	0	0
Formamide	58.0	39.0	19.0	2.28	39.6
Diiodomethane	50.8	50.8	0	0	0
Water	72.8	26.4	46.4	23.2	23.3
Glycerol	64	34	30	3.92	57.6

2.8.5 Surface Free Energy of Molecules

The atoms at the surface of the condensed phase materials are in different environment compared to those from its interior, this difference arises from the asymmetric environment .In a bulk material, each atom is surrounded by similar ones and they experience no net force.

In addition, environmental influence acts only on the outermost atoms (Van Oss and Giese,2002). These atoms consequently have a different energy distribution from the inside and are at a higher state at the surface. This excess energy can be measured. The differences in the energy of the atoms or molecules located at the surface and in the bulk of the material manifest themselves as surface energy/surface tension γ.For a non-metallic material, the surface free energy has an apolar component γ^{lw} and may also have a polar component γ^{ab}. Qualitatively, surface tension acts on any surface trying to minimize the surface area.

Thermodynamically, surface tension γ is interpreted as the increase in Gibbs free energy of a system when the area of the interface under consideration is increased reversibly by an infinitesimal amount at a constant temperature (t), pressure (p) and composition (n)

$$\gamma = \left(\frac{\delta G}{\delta A}\right)_{t,\, p,n} \qquad (2.22)$$

Surface energy of solids is dependent on the workdone on the surface area of the solid against elastic forces and plastic resistance of the solids. The difficulty of determining surface free energy of solids directly from contact angle leads to the simplification of young's equation by combing the work of adhesion from Dupre equation at the liquid interface with the surface and interfacial tensions of solid-vapor, solid -vapor and solid- liquid interfaces(Ozoihu,2014).

$$w_{sl} = \gamma_{sv} + \gamma_{lv} - \gamma_{sl} \quad (2.23)$$

Combining equation (2.1) and (2.22) yields

$$w_{sl} = \gamma_{lv} (1 + \cos\theta) \quad (2.24)$$

Equation (2.23) is the strain energy of the liquid drop and γ_{sv}, γ_{sl} can be determined.

Good and Girifalco,(1960) expressed the work of adhesion as a geometric mean of the surface tension of pure components

$$w_{sl} = 2\phi (\gamma_{sv,}\gamma_{lv})^{1/2} \quad (2.25)$$

ϕ is a correction factor for intermolecular interactions

$\phi = 1$ for similar forces

$\phi < 1$ for dissimilar forces of adhesion and cohesion

ϕ depends on the chemical properties of the solid and liquid

Combining the Young-Dupre and Good and Girifalco equations yields

$$\gamma_{lv} (1 + \cos\theta) = (\gamma_{sv,}\gamma_{lv})^{1/2} \quad (2.26)$$

When primary forces are disperse

$$\gamma_{sv} = \frac{\gamma_{lv}(1+cos\theta)^2}{4\phi^2} \quad (2.27)$$

2.8.5 Surface Tension of Blood Cells and Proteins

Pathological features of diseases vary in their nature and magnitude. Despite this diversity, the common feature of various disorders underlies the physiochemical and biochemical factors such as surface tension. Changes in the surface tension behavior of human biological fluid are characteristic for some diseases. Studying these interfaces and the changes that occur will provide valuable information relating to various diseases and help to monitor the treatment efficacy.

Biological tissues are viscoelastic materials and the cells in a tissue behave very much like molecules in a fluid. This property enables them to change their position and move against each other. The morphology and shape of the organism are driven by the events that occur at the cellular level. The shape of a cell is the result of a balance of intracellular and extrinsic forces exerted on it. This behavior is defined through surface tension which tends to minimize the exposed area of the cell aggregate and maximize the cohesive forces. The intracellular forces on the membrane are a result of the cytoskeleton reorganization. Energy at the cellular level is usually measured through physical properties such as cell adhesion, viscosity, and cortical tension

Several approaches including adhesion experiments, freezing point experiment, contact angle approach etc have been used to measure blood cells and protein surface tension and all the approach used agreed with the equation of state approach, thus establishing the impact of surface properties in biological systems.

Conclusions arrived at by these previous works of Neumann et al,(1979), Van der Smolders(1978) can be summarily outlined as follows;

- Interfacial tension founds practical applications in the closing and opening of vessels in circulation of bloods, antigens-antibodies interactions and cells adhesion and protein absorption.
- These biomaterials are hydrophilic and posses relatively a high surface tension.
- Several approaches can be used to achieve their measurements.

Works has also been done on surface tension relating to quantities likethrombocytes with regards to clotting time and platelets adsorption and the values obtained as conventional surface tension of polymers are in accordance with that obtainedfromtheequationofstate.(American Society of Microbiogy, 1984)

Table2.4: Surface tension of biological systems in erg/cm^2 at temperatureof 22^{0}C (ASM,1980)

System	Contact angle	Engulfment			Adhesion	Detachment	Suspend Stability
		Advancing Solidification	Phagocytic Ingestion				
			Granulocytes	Platelets			
Granulocytes(Human)	69.1	69.3	-	-	69.0	69.0	-
Lymphocytes(Human)	70.1	70.6	-	-	-	-	-
Erythrocytes(Human)	-	64.9	-	-	-	-	63.4
(Horse)	-	65.1	-	-	-	-	65.4
(Chicken)	-	64.8	-	-	-	-	65.2
(Turkey)	-	65.1	-	-	-	-	65.7
(Canin)	-	63.9	-	-	-	-	64.4
Platelets(Porcine)	67.2	-	-	**67.9**	-	-	-
Bacteria E-coli	69.7	-	69.6	69.3	69.6	-	-
S.Aureus	69.1	-	68.7	68.8	69.3	-	-
S.Epidemidis	67.1	-	66.9	**67.3**	66.0	-	-
L.Monocytogenes	66.3	-	66.1	-	65.5	-	-
Proteins-B.serum Albumin	70.2	-	-	-	-	-	-
H. Serum Albumin	70.3	-	-	-	70.2	-	-
H.Immunoglobulin.G	67.3	-	-	-	67.7	-	-
H.Immunoglobulin.M	69.4	-	-	-	71.0	-	-
H.Macroglobulin	71.0	-	-	-	71.0	-	-
Transferrin	66.8	-	-	-	-	-	-

Table 2.5 Surface tension of some experimental liquids (Van Oss, 1978)

Liquid in contact with air	Temperature (0^0C)	Surface Tension (mN/m) or dyn/cm)
Benzene	20	28.9
Carbon tetrachloride	20	26.8
Ethanol	20	22.3
Glycerin	20	63.1
Mercury	20	465.0
Olive oil	20	32.0
Soap solution	20	25.0
Water	0	75.6
Water	20	72.8
Water	60	66.2
Water	100	58.9
Oxygen	-193	15.7
Neon	-247	5.15
Helium	-269	0.12

2.8.6 Van der Waal Interactions in Blood Cells

The attraction and repulsion of particles in a fluid medium was made explicit in the classical works of Hamaker when he established that "if two particles are embedded in a fluid and the London van der waal forces between the particle and the fluid is greater than the particles themselves, it might be thought that it will result in repulsionrather than attraction''. Owing to a peculiar property of London van der waal forces, the resultant force is generally attractive even when the particles are surrounded by the fluid(Hamaker, 1936).When two bodiesinteract in a liquid medium, separation will occur due to dispersion forces only if the attraction of the bodies with the liquid is higher than that between the bodies themselves (Viser, 1981).

The sign of a net van der Waal interaction between two different solid bodies or between two dissolved macromolecules in a liquid is often negative even if they are electrically neutral and even in polar liquids (Omenyi et al, 1980).

Now the new capability to change the attraction between solids submerged in liquids or dissolved molecules into repulsion have a considerable impact in separation methods.

Considering Hamaker expression for the free energy for such bodies in a liquid medium;

$$\Delta F(d) = -\frac{A_{132}}{12\pi d^2} \quad (2.28)$$

Assuming a minimum separation distanced_o, and equation (2.28) still valid for small separation distance, the Hamaker coefficient can now be expressed as;

$$A_{132} = -12\pi d^2 \Delta F^{adh}(d) \quad (2.29)$$

From the foregoing, the Hamaker coefficient can be calculated once the free energy of adhesion for such particular system is known.

$$\Delta F_{132}^{adh} = \gamma_{sv} - \gamma_{sl} - \gamma_{lv} \quad (2.30)$$

However, if the values of A_{132} becomes closer to zero than$\approx \mp 3.5 \times 10^{-15}$ergs$(3.5 \times 10^{-22} J)$,an exact prediction of attraction and repulsion based on whether $A_{132}$is positive or negative may no longer be reliable and this calls for a different separation method.

γ_{sv}can be found once contact angle and the surface tension of the liquid γ_{lv} is known from ;

$$\text{Cos}\theta = \frac{(0.015\gamma_{sv} - 2.00)(\gamma_{sv}\gamma_{lv})^{1/2} + \gamma_{lv}}{\gamma_{lv} 0.0015 (\gamma_{sv}\gamma_{lv})^{1/2} - 1} \quad (2.31)$$

Having obtained γ_{sv} from equation 2.31, the corresponding value of γ_{sl} can be calculated from;

$$\gamma_{sv} - \gamma_{sl} = \gamma_{lv}\text{Cos}\theta \quad (2.32)$$

Adhesion occurs when equation (2.30) is negative and repulsion is predicted when the free energy of adhesion is positive. An experimental rig was carried out using Nylon, Polysterene, Teflon , silicon glass and acetal particles in biphenyl and naphthalene to verify this thermodynamic prediction (Omenyi et al, 1980).

Table 2.6:Changes in Free Energy and Thermodynamic Prediction(Omenyi et al, 1980)

Matrice Materials	F_{NET}(mJ/m^2)	Prediction
Biphenyl/silicon glass	-3.4	Engulfment
Biphenyl/nylon	+2.5	Rejection
Biphenyl/Teflon	-2.6	Engulfment
Biphenyl/polystyrene	-0.1	Engulfment
Biphenyl/acetal	+2.7	Rejection
Naphthalene/silicon glass	-3.5	Engulfment
Naphthalene/Teflon	-2.7	Engulfment
Naphthalene/polystyrene	-0.4	Engulfment
Naphthalene/acetal	+2.3	Rejection
Naphthalene/nylon	+2.1	Rejection

The concept of negative Hamaker is a predicted condition where the absolute Hamaker coefficient becomes negative (A_{132}<0).At this point, dissimilar particles suspended in a liquid medium is predicted to repel each other (Achebe,2010).

The following criteria must be fulfill for this situation to occur;A_{132} <0 only when

$\sqrt{A_{11}}>\sqrt{A_{33}}$and $\sqrt{A_{22}} < \sqrt{A_{33}}$ (2.33)

or$\sqrt{A_{11}}<\sqrt{A_{33}}<\sqrt{A_{22}}$ (2.34)

or $\sqrt{A_{11}}<\sqrt{A_{33}}<\sqrt{A_{22}}$ or $\sqrt{A_{11}}>\sqrt{A_{33}}>\sqrt{A_{22}}$ (2.35)

$A_{132}= (\sqrt{A_{11}}-\sqrt{A_{33}})(\sqrt{A_{22}} - \sqrt{A_{33}})$ (2.36)

In relation to this study,A_{11}, A_{22} and A_{33} are Hamaker constant for uninfected white blood cell, infected lymphocyte and serum (Ani, 2016).

2.8.7 Hydrodynamic Interactions of Particles in Blood Cells

The drag force of two interacting particles in a fluid was measured using micro force measuring system and it was found that the drag force of an isolated particle depends on the power law index.The drag coefficient ratio of the interacting particle is independent of the power law index but strongly depends on the separation distance and the particle Reynolds number (Zhu, 2003).

Neumann et al (1983) studied van der waal interactions between particles of dissimilar materials using a polymeric particle in naphthalene and found that the particle are either engulfed or rejected by the solidification fronts. The motion of the particles depends on the hydrodynamic interactions which may increase the hydrodynamic drag force. The equation of motion for the drag force for a spherical particle(HCV particle) is given as;

$$F(t) = -6\pi a\mu_f(u) - 0.5m_f\frac{\delta(u)}{\delta t} - 6a^2(\pi\mu_f e_f)^{1/2}\int_0^t \frac{\delta(u)}{\delta t(t-\tau)0.5} \qquad (2.37)$$

Oscillations of the spherical particle at Reynolds number up to 62 were studied experimentally to examine the acceleration effect on the motion of the particle (Odar and Hamilton, 1964).

Modification on equation (2.37) yields;

$$F(t) = -0.5\rho_f c_D \pi a^2 \mu^2 - c_{vm}\, m_f\frac{\delta(u)}{\delta t} - c_H\, a^2(\pi\mu_f\rho_f)^{1/2}\int_0^t \frac{\delta(v).\delta\tau}{\delta\tau(t-\tau)0.5} \qquad (2.38)$$

The drag coefficient correlation for the power law fluid

$$c_D = \frac{24}{\mathrm{Re}}(1 + 0.1466\mathrm{Re}^{0.378}) + \frac{0.44}{1+0.2635/Re} \qquad (2.39)$$

Where $0.1 < \mathrm{Re} < 10^3$

For an impermeable blood vessels, the drag force on the particles will be so large at small gap because large pressure will be develop in the zone of closet approach to cause entrapped blood cells to flow radially outward. As the gap between the particles

diminishes, the viscous friction increases and the corresponding stress becomes comparable to the capillary pressure (Yiantsios and Davis, 1991).

Taking h_r as the separating distance between particles interacting in the fluid(serum),

$$F = 2\pi\sigma h_r \quad (2.40)$$

$$\sigma = 2\sigma_1\sigma_2/\sigma_1 + \sigma_2 \quad (2.41)$$

F is the force applied on each particle directed along the axis of the symmetry, σ_1, σ_2 are the interfacial tension on the two boundaries .

Danov et al (1993) derived a transcendental equation forh_r, including the potential energy of the surface forces. The surface energy is increased due to area dilatation by the driving force sufficiently large to overcome the energy barrier created by electrostatic repulsion.Recent calculations on two approaching spherical particles taking into account the van der Waalforces between the particles as analyzed.

$$\delta h_r = \frac{\delta E}{F} \quad (2.42)$$

Where F is the van der waal forces, E is the interfacial energy and h_r is the separating distance.

$$\text{But } E = \lambda_{ij}/h^6 \quad (2.43)$$

H^6 is the sixth power of molecular distance, λij London constant whose values depend on the interacting atoms. The solution of equations (2.42) and (2.43) has been analyzed for van der Waal force equation (Hamaker,1936).

$$h_r = \sqrt{\frac{RA}{12F}}. \quad (2.44)$$

Where R is the reduced radius and A is Hamaker constant forthe van der Waal

for two plane surfaces

$$h_r = \sqrt[3]{\left(\frac{A}{6\pi F}\right)} \quad (2.45)$$

At low speed, particles are rejected but at high speed they are engulfed. The free energy of adhesion is given by:

$$\Delta F = \frac{2.65x10^5 \; x \; \rho^{0.847} x T^{0.280} x \; K^{0.720} x \; D^{0.407} x \; V^{0.847}}{U^{0.127 \; x} \; (P_p C_p)^{0.441}} \quad (2.46)$$

This further decomposes to;

$$\Delta F = \gamma_{sv} + \gamma_{sl} - \gamma_{lv} \quad (2.47)$$

2.8.8 Sessile Drop Measurement of Surface Free Energy of Bacterial Cell Surfaces

Ozoihu (2014) in his work reviewed the experimental determination of contact angle by Hendrik and his team using sessile drop techniques on bacteria layers deposited on cellulose triacetate filters which was completely smeared with bacteria. Water, water-n-propanol mixtures and α −bromonaphthalene was the probe liquid used and calculation of surface energies of the various bacteria was done. Methods of calculation yieldingγ_s^d, γ_s^p together with spreading pressure πe and γ_{sv} separately were employed where d and p represents dispersion and polar component of the fluid. Tables 2.7 and 2.8 shows the contact angle of some liquids and the surface free energy of some oral bacteria respectively.

Table2.7: Contact angle of some liquids deposits of oral bacteria (Hendrik et al, 2006)

Liquids	V.alcalescensVI	S.sangiusCH3	S.salivariusHB	S.mitior T6
Water	20	42	26	55
water-n-propanol mixtures	15	41	26	52
α −bromonaphthalene	57	41	44	31

Table2.8: Surface Free Energy of Oral Bacteria (Hendrik et al, 2006)

Bacteria	γ_{sv}(erg/cm^2)	γ_s^d(erg/cm^2)	γ_s^p(erg/cm^2)	γ_s(erg/cm^2)	πe(erg/cm^2)
V.alcalescensVI	60∓1	27∓4	74∓1	101∓4	42∓3
S.sangiusCH3	45∓1	34∓2	52∓2	86∓1	44∓1
S.salivariusHB	58∓2	33∓2	72∓3	105∓5	49∓2
S.mitior T6	33∓2	38∓1	30∓6	69∓6	33∓5

2.8.9 Glycerol as Probe Liquid

Glycerol is completely soluble in water and alcohol. It is slightly soluble in ether, ethyl acetate, and dioxane and insoluble in hydrocarbons. Glycerol has useful solvent properties similar to those of water and simple aliphatic alcohols because of its three-hydroxyl groups. Glycerol is a useful solvent for many solids, both organic and inorganic which is particularly important for the preparation of pharmaceuticals. The solubility of gases in glycerol, like other liquids is temperature and pressure dependent. The physical properties of glycerine is outlined in table 2.9

Table 2.9: Physical Properties of Glycerine (Retrieved from www.aciscience.org)

Molecular weight	92.09
Thermal conductivity	0.29 w/ºK
Specific heat	0.5779 cal/gm at 26ºC (99.94%glycerol)
Flash point	177ºC
Viscosity	9.34g/cm at 20ºC (100% glycerol)
Surface tension	= 63.4 dyne/cm at 20ºC(100% glycerol)
Density (20ºC)	1.261 g/cm3
Refractive index	1.474
Melting point	18.17ºC
Boiling point(760mm Hg)	290ºC
Compressibility (28.5ºC)	2.1×10 MPa

2.8.10 Literature Summary

The nature and economic implications of Hepatitis C virus infection has been studied as well as its global health burden on the human race. The different genotypes of the virus and their responses to treatment are relatively low and as such build up resistance to drugs. This therefore, makes the drugs ineffective. The medical approach used as a marker for determining virological and immunological clearance shows that there is no total eradication of the virus. The conventional drugs used for the treatment of HCV only provides a functional cure and moreover, they are expensive, have adverse side effects on the patients and are not available to low income earners.

This research seeks to investigate some alternatives to conventional drugs such as plants extract that are readily available and can be sourced locally. This will be achieved through thermodynamic approach as against the orthodox approach employed in the field of medicine. This forms a knowledge gap that this research intends to fill. The thermodynamic approach involves the use of surface property principles of the interacting particles (blood cells and viral particles) to investigate the mechanism of interactions. This involves the determination of the surface energy, adhesion energy and van der waal interactions of the interacting particles. The use of the concept of combined negative Hamaker coefficient will also help to determine the attraction or repulsion of the blood particles and the virus.

CHAPTER THREE

MATERIALS AND METHODS

3.1 Materials

The materials used for this study are as follows; 500mg each of herbal extracts from plant samples (*Bryophyllum pinnatum(BP)*, *Anona muricata(AM)*, *vernonia amygdalina(VA)* and *phyllantus amarus*), human blood samples, glass funnels, gloves, 150mm diameter sieve, conical flask, whattman filter paper, analytical reagent (AR) 95% methanol, 2.5 liters plastic container, ice pack container, cotton wool, spreader , slide racks.

Also used are conventional drugs(*pegylated interferon alfa(IFN)ribavirin(RBV), atazanavir/ritonavir(ATR)andefavirenz/lamivudine/tenofovir(ELT)*, disposable syringes and needles, microlitre pipette, HCV test kits, HIV test kits, masking tapes, glycerin solution, test tubes, test tube racks, Prepared slides as test surface, 5.0 μl microlitre syringe.

3.1.1 Sourcing of Plant Samples

The leaves of *Bryophyllum pinnatum*, *Anona muricata*, *vernonia amygdalina* and *phyllantus amarus*were collected from Agbor in Ika south area of Delta State. They were selected after an interview with the local medicine practitioners of the Delta State Traditional Medicine Board and were taken to the Herbarium at Agbor belonging to the State Ministry of Agriculture for identification while authentication was done by a plant taxonomist.The images of these plants were displayed in Fig 3.1

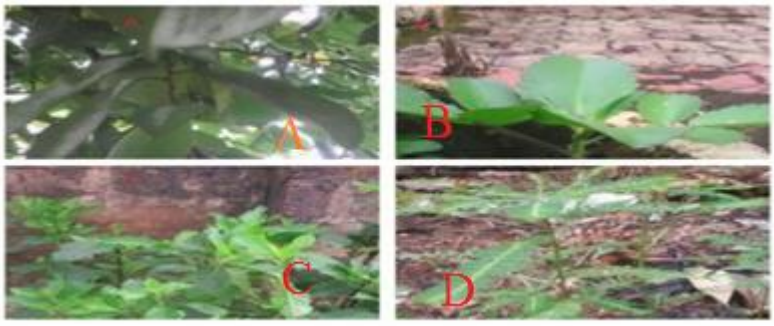

Plate 3.1: Plant samples (a)*Anona muricata* (b)*Bryophyllum pinnatum (c)vernonia amygdalina (d)phyllantus amarus*

3.1.2 Methanol

Analytical reagent methanol manufactured by Cartivalues Chemicals Ltd was used for this study. It has the following compositions tabulated in table 3.1.

Table3.1 Compositions of the Methanol used

Batch No	86.130
Lot No	16107
Volume	2.5 litres
Boiling range	64-65.5^{0}C
Non –volatile matter	0.005%
Aldehydes and Ketones	0.1%
Water	0.25%

3.1.3 Herbal Drugs

Four powdered herbal extracts from the plants mention above were prepared by extracting the bioactive agents in the plants as will be discussed in the subsequent sections.

3.1.4 Conventional Drugs

The conventional drugs considered for this study was administred to human infected blood.They are the commonly used antiviral drugs for the treatment of hepatitis C virus. They are pegylated interferon alfa (IFN), ribavirin (RBV),atazanavir/ritonavir (ATR) and efavirenz/lamivudine/tenofovir (ELT). As at the time of the experiment, the drugs have not reached its date of expiration.The table also depicts several features of the drugs like dosage, manufacturing companies with their respective batch numbers of the drugs, the size of the drugs in milligrams and also the manufacturing and expiring date.

Table 3.3 Details of the Conventional Drugs

Conventional Antiviral drugs.				
Drugs	Interferon Alfa	Ribavirin	Atazanavir/ Ritonavir	Efavirenz/Lamivudine/Tenofovir
Designation	IFN	RBV	ATR	ELT
Drug Type	Injection/Single	Tablets/Single	Tablets/DAA	Tablets /DAA
Manufactur-ing Date	June, 2015	Feb,2016	June,2015	Sept, 2015
Expiration Date	June, 2017	June,2017	May,2017	August, 2018
Dosage	Once daily	Twice daily	Once daily	Once daily
Size	0.5ml	200mg	300mg/100mg	600mg/300mg/300mg
Manufacturing Company	Roche	Teva	Mylan	Hetero
Batch Number	B3032B05	Lot3528216	3042020	E141689

Plate 3.2: Samples of Convention Drugs

Plate 3.2 shows the content of the conventional antiviral drugs used for the study. ATR and ELT are direct acting antiviral which comprises of combination therapy and are taken once on daily basis. The interferon and ribavirin are single treatment regime. RBV is taken twice daily while interferon is taken once in 3days and it is in injection form as can be seen from table 3.3.

3.1.5 Glycerin Solution

The glycerin ($C_2H_80_3$) used as probe liquid for the experiment is an analytical reagent(AR) glycerin having the following composition; minimum assay 99.7%, water insoluble matter 0.003%, Sulphate ash 0.05%, chloride 0.001%, Sulphate(So_4) 0.0025% and ammonium 0.02%. It is soluble in water and alcohol

3.1.6 Collection of Blood Samples

The blood used for this study includes ten samples of hepatitis C infected human blood and ten samples of uninfected blood. The infected samples were collected from Mount Herob Clinic and Dialysis Centre, Warri and Anambra State University Teaching Hospital, Amaku. Bloodborne pathogen and NCCLS standards were equally observed in the collection, transportation, preparation, storage and safety of the blood specimen used for the experiment. Personal protective equipment (PPE) was equally used in the course of the experiment.

3.1.7 Equipment Description

The following equipment was used for this study; rotary evaporator, refrigerator, digital electronic balance, partec cyflow counter machine, blood roll mixer, centrifuge machine, incubator, autoclave machine and Nikkon digital camera.Digital electronic balance with model number KI-313was used.The Partec Cyflow Counter Machine used for this study was manufactured by Sysmex Partec Technology with serial number 110473322.Blood roll mixer with model number KJMR-II was equally used in this study. Nikkon Digital D60 Camera with lens 18-55mm and 3.5-5.6GVR zoom lens was used for this research. Other equipment used includes; incubatorwith serial number SL 307801000, centrifuge machineBioSan Centrifuge/Vortex Multi-Spin with model number MSC-6000 and Stermite autoclave machine having a model number SM-18.

3.2 Methods

All materials used were sterilized using the autoclave machine at the beginning of the experiment. The plant extraction experiment was done at Model Laboratory, Agbor in

Delta State and the phytochemical screening and characterization of the plant extracts were carried out in Awka, Nigeria while the other experiments concerning the blood component separation, inoculation and smearing of the human blood samples were carried out at the laboratory Unit of the Anambra State University Teaching Hospital, Amaku.

3.2.1 Plant Extract Preparation

The leaves of *Bryophyllum pinnatum(BP), Anona muricata(AM), vernonia amygdalina(VA)*and *phyllantus amarus(PB)* were dried at room temperature for six weeks.The specimen were crushed into powdered substances and weighed using digital electronic balance. Methanolic extract of each of the plant specimen were prepared by soaking 500g of the dried powdered plant leaves in 1000ml of methanol for 48 hours. The needed filters, test tubes, syringes and beakers were autoclaved before the extraction experiments at the Model Laboratory, Agbor.

The soaked substances were again filtered using 150mm diameter sieve and the filtrate was again filtered using whattman filter papers with cat no: 10001-110, 110mm diameter. The whatmann paper was placed inside the glass funnel and the filtration process initiated on the specimen of the different substances.

The extracts were placed in the rotary evaporator for 10minutes at 1500rpm. The active extracts collected were stored in their respective labeled airtight containers under refrigeration below room temperature until used.

3.2.2 Phytochemical Screening

Chemical tests were carried out on the methanolic extract of the plants to identify the phytochemicals present using standard procedures.The screening test and phytochemical compositions were carried out at the laboratory section of Afrab-Chemicals Ltd, GRA-Benin city, Edo State. The Fourier transform infrared (FTIR) spectroscopy on the plant extracts was also done at springboard labouraroty, Awka in Anambra state.

3.2.2.1Determination of alkaloids

5g of plants extract were placed in a 250 ml beaker and 200 ml of 10% diethyl ether in ethanol was added. The mixture was covered and allowed to stand for 4 hours. It was then filtered using whatman filter and the filtrate was concentrated on a water bath until it reaches a quarter of its original volume. 10ml Concentrated NH_4OH was added until precipitation was complete. The mixture was allowed to settle and the precipitate collected on a weighed filter paper and washed with another 10ml diluted NH_4OH. The precipitate of alkaloid was dried and weighed.

The percentage composition of all the phytochemicals were calculated using

$$\% \text{ composition} = \frac{Weight\ of\ phytochemical\ \ tested}{weight\ of\ sample} \text{ X } 100 \qquad (3.1)$$

3.2.2.2 Determination of flavonoids

10g of each plant extracts were mixed with 100 ml of 80% aqueous methanol at room temperature. The mixture was then filtered through a filter paper into a pre-weighed beaker. The filtrate was transferred into a water bath and allowed toevaporate to dryness and weighed. A yellow coloration indicated the presence of flavonoids. The precipitate of flavonoids was dried and weighed.

3.2.2.3Determination of saponins

20g of each plant extract were weighed into a conical flaskcontaining 100 ml of 20% methanol. The mixture was heated over a hot water bath for 4 hours with continuous stirring at about 55°C. It was then filtered with a Whatman paper. The residue was re-extracted with another 200 ml of 20% methanol. The combined extract was reduced to 40 ml over a water bath at about 40°C. The concentrated extract was then transferred into a 250 ml separating funnel and 20 ml of diethyl ether was added to the extract and shaken vigorously. The aqueous layer was recovered while the diethyl ether layer was discarded. This purification process was repeated three times, and all aqueous layers were pooled.

60 ml of n-butanol was added and the combined n-butanol extract was washed twice with 10ml of 5% NaCl. The remaining solution was then heated on a water-bath in a pre-weighed 250 ml beaker. After evaporation, the residue was dried in an oven to a constant weight. The dried matter of saponin was weighed.

3.2.2.4 Determination of Tannis

10g of each plant powder were taken separately and soaked in methanol for 24 hours. Then filtered, the filtrate was extracted with petroleum ether.The formation of red violet color indicates its presence.The ether extract was treated as total tannis upon weighing

3.2.2.5 Total Phenolic content

1.5 ml of Folin-Ciocalteau reagent and 1.2 ml of 75% (w/v) sodium carbonate solution was taken in test tubes containing 5g each of plant methanolic extract. The tubes were vortexed for 15 sec and allowed to stand for 30 min at room temperature. Results were expressed as milligram of tannic acid equivalent per gram of extract weight. The results of the phytochemical screening is tabulated in table 4.1

3.2.3 Storage and screening of Blood samples

The blood samples were stored in an ethyl-diamine-tetra- acetic (EDTA) container to prevent the coagulation of the blood and kept below room temperature in the refrigerator to keep alive the living components in the blood sample before the experiment.

The samples were screened for HCV and HIV using test kits and the infection status confirmed to be HCV monoinfected for ten samples and the other ten uninfected. The blood samples were collectively gathered and transported using ice packed container surrounded with cotton wool to the laboratory Unit of the Anambra State University Teaching Hospital, Amaku.

3.2.4 Slides Preparation

A total of 400 slides were mask taped and identification codes reflecting the blood sample, treatment received and blood components written on them for recognition of the slides. For example; B_1-IFN-RBC meaning the slide will be having blood sample 1 with interferon treatment smeared with red blood cell. The slides used for the preparation of the test surface are the standard clear ground edges dimensioning 25.4mm x 76.2mm x 1.2mm

3.2.5 Cluster of Differential Cell Count (CD4+) on Blood Samples

Before the beginning of the experiment, the partec cyflow counter machine was cleaned by inserting into it 1600μl each of cleaning solution, decontamination solution and shealth fluid. 850 μl of count check beads green was used on the machine to check for quality control.

20 μl of CD mAb PE monoclonal antibody was introduced into a sample tube and 20 μl of EDTA whole blood was added to the tube and allowed tomix together. The mixture was incubated for 15 minutes in a dark field at room temperature. Added to the mixture is 800μl of no lysed buffer solution, mixed gently and run the program.

3.2.6 Serial Dilution of Drugs

The procedures employed in diluting the drugs (conventional and herbal) are:

(1) The tablets forms of the conventional drugs were crushed into powder according to the prescribed start dose required.
(2) The powdered drugs (conventional and herbal) each were mixed in labeled test tubes containing 10ml of sterile water to prepare solutions with the various drugs and thoroughly shaken to ensure even distribution of particles in the tube.
(3) With the use of a disposable syringe, an aliquot of 1ml was withdrawn from the solution and added to the second test tube containing 9ml of sterile water and the mixture thouroughly shaken.
(4) Another 1ml is taken from the solution and mixed with the third test tube containing 9ml of sterile water and the syringe disposed. The process continues

until the 7th test tube was serially diluted. The dilution factor used for this study is 10^{-6} as can be seen from table 3.3

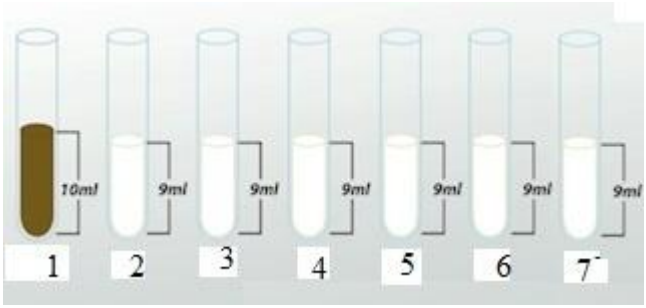

Figure 3.1: Schematic diagram of serial dilution

Table 3.4: Serial Dilution

Tubes	1	2	3	4	5	6	7
Aliquot	0	1ml	1ml	1ml	1ml	1ml	1ml
Diluent	10ml	9ml	9ml	9ml	9ml	9ml	9ml
Dilution Factor	0	1:10	1:100	1:1000	1:10000	1:100000	1:1000000

3.2.7 Inoculation and Smearing of Blood Samples

The ten uninfected blood samples kept below room temperature in an EDTA container was separated into its components using a centrifuge machine. This separated the blood samples in the order of serum, white blood cell and red blood cell at the bottom. A pipette was used to draw 1000 μl of each of the components from their boundary layer to smear the slides respectively using a spreader bent at 45^0 to achieve an even distribution on the slides. The blood samples in the container were placed in a blood roll mixer to unify the components and another 1000 μl whole blood withdrawn to smear the slide. A total of four slides were obtained from each sample and the slides were allowed to dry naturally at room temperature because exposing the slides to the sun is likely to cause oxidation and the surface energy might be increased.

3.2.7.1 Smearing of infected Blood without Treatment

100 μl each of infected blood serum, white blood cell and red blood cells was smeared on their respective slides using the method of smearing explained in section 3.3.7. and after which the blood samples were placed in the blood roll mixer and all the separated components unified so as to get the whole blood also smeared.

3.2.7.2. Inoculation and Smearing of infected Blood with Conventional and Herbal drugs

4ml ofblood samples 1 was dispensed into eight test tubes using a microlitre pipette. Inoculation of each test tube containing blood samples was done using 1000 μl of serially diluted drugs (conventional and herbal). The test tubes were kept in an incubator at room temperature for 24 hours to allow for for blood- drug interaction. The procedure was followed for the remaining blood samples. The incubated mixtures after 24hrs was loaded on the centrifuge machine and the respective blood component separated. Smearing of the slides was done and the blood components unified using blood roll mixer machine for whole blood component to be smeared.In general, a total of 400 slides was prepared to serves as test surfaces and was kept in the slide rack as shown in plate 3.3.

Plate 3.3: Smeared slides kept in slide racks

3.3Contact Angle Experiment and Measurement

The glycerin used as probe liquid for the study was dropped on the surface of the prepared slides using a microliter syringe. Contact was not made between the syringe and the test surface and the droplet volume was small enough to avoid impact effect

on the surface and gravity effect negligible. The process of spreading was captured with a high definition Nikkon digital camera and the images printed. The contact angle was measured carefully at the solid –vapour, solid- liquid and liquid interface.This was done on all the 400 slides prepared.

3.4 Response Surface Methodology

The procedures are as follows:

1. Fit the full model to the first response.
2. Use stepwise regression, forward selection, or backward elimination to identify important variables.
3. When selecting variables for inclusion in the model, follow the hierarchy principle and keep all main effects that are part of significant higher-order terms or interactions, even if the main effect *p*-value is larger than you would like (note that not all analysts agree with this principle.
4. Generate diagnostic residual plots (histograms, box plots, normal plots, etc.) for the model selected.
5. Examine the fitted model plot, interaction plots, and ANOVA statistics (R^2, adjusted R^2, lack-of-fit test, etc.). Use all these plots and statistics to determine whether the model fit is satisfactory.
6. Use contour plots of the response surface to explore the effect of changing factor levels on the response.

3.4.1 DesignMatrix for Response Surface Quadratic Model

Table 3.5: Degree of freedom for design Matrix Evaluation

Degrees of Freedom for Evaluation	
Model	5
Residuals	7
Lack of Fit	3
Pure Error	4
Corr Total	12.

A recommendation is a minimum of 3 lack of fit degree of freedom and 4 df for pure error.This ensures a valid lack of fit test.

Table 3.6: Standard Error for Design Matrix

Term	StdErr[1]	VIF	Ri-Squared	2 Std. Dev.
A	0.35	1.00	0.0000	68.1 %
B	0.35	1.00	0.0000	68.1 %
AB	0.50	1.00	0.0000	40.8 %
A^2	0.38	1.02	0.0170	99.4%

Power at 5 % alpha level to detect signal/noise ratio

Table 3.7: Design matrix information.

Run	Leverage	Space Type
1	0.6250	Axial
2	0.2000	Center
3	0.6250	Axial
4	0.6250	Axial
5	0.6250	Factorial
6	0.6250	Factorial
7	0.6250	Factorial
8	0.6250	Axial
9	0.2000	Center
10	0.6250	Factorial
11	0.2000	Center
12	0.2000	Center
13	0.2000	Center
Average =	0.4615	Watch for leverages close to 1.0. Consider replicating these pointsOr make sure they are run very carefully.

Table 3.8: Design Matrix for energy of adhesion for Infected Cells

		Factor 1	Factor 2	Response 1	Response 2
Std	Run	A:Contact Angle	B:Interfacial Energy	Surface Energy "Adh"	Hamaker Coefficient (E-17)
		(deg C)	(mJ/m^2)	(mJ/m^2)	(mJ/m^2)
5	1	58	34	-24.34	2.35E-017
9	2	62.5	34	-21.55	2.08E-017
7	3	62.5	33	-24.79	2.21E-017
6	4	67	34	-23.64	2.28E-017
2	5	66	32	-25.72	2.48E-017
1	6	59	32	-25.03	2.42E-017
4	7	66	36	-22.13	1.88E-017
8	8	62.5	37	-22.29	2.55E-017
12	9	62.5	34	-22.25	2.15E-017
3	10	59	36	-23.59	2.01E-017
13	11	62.5	34	-22.85	2.1E-017
11	12	62.5	34	-21.85	2.08E-017
10	13	62.5	34	-20.8	2.09E-017

Table 3.9: Confirmation Report.

Two-sided	**Confidence = 95%**	**n = 1**				
Factor	**Name**	**Level**	**Low Level**	**High Level**	**Std. Dev.**	**Coding**
A	Contact Angle	48.00	43.00	53.00	0.000	Actual
B	Interfacial Energy	44.00	40.00	48.00	0.000	Actual

Table 3.10: Predicted Response Matrix

	Predicted	**Predicted**							
Response	**Mean**	**Median[1]**	**Observed**	**Std Dev**	**n**	**SE Pred**	**95% PI low**	**Data Mean**	**95% PI high**
Surface Energy "Adh"	-14.456	-14.456	-	0.320501	1	0.35	-15.29		-13.63
Hamaker Coefficient (E-17)	1.3992E-017	1.3992E-017	-	5.19269E-019	1	5.688E-019	1.265E-017		1.534E-017

Table 3.11: Design Matrix for Hamaker coefficient for Infected Cells

		Factor 1	Factor 2		Response 2
Std	Run	A:Contact Angle	B:Interfacial Energy	Surface Energy "Adh"	Hamaker Coefficient (E-17)
		(deg C)	(mJ/m^2)	(mJ/m^2)	(mJ/m^2)
5	1	58	34	-24.34	2.35E-017
9	2	62.5	34	-21.55	2.08E-017
7	3	62.5	33	-24.79	2.329E-017
6	4	67	34	-23.64	2.28E-017
2	5	66	32	-25.72	2.383E-017
1	6	58	32	-25.03	2.329E-017
4	7	66	36	-22.13	2.138E-017
8	8	62.5	37	-22.29	2.182E-017
12	9	62.5	34	-22.25	2.15E-017
3	10	59	36	-23.59	2.275E-017
13	11	62.5	34	-22.85	2.1E-017
11	12	62.5	34	-21.85	2.08E-017
10	13	62.5	34	-20.8	2.09E-017

Table 3.12: Design Matrix for Uninfected cells

		Factor 1	Factor 2	Response 1	Response 2
Std	Run	A:Contact Angle	B:Interfacial Energy	Surface Energy "Adh"	Hamaker Coefficient (E-17)
		(deg C)	(mJ/m^2)	(mJ/m^2)	(mJ/m^2)
12	1	48	44	-14.07	1.366E-017
8	2	48	42	-11.5	1.11E-017
6	3	52	44	-12.32	1.23E-017
3	4	43	48	-13.5	1.156E-017
10	5	48	44	-14.06	1.36E-017
13	6	48	44	-14.72	1.42E-017
5	7	51	44	-12.63	1.231E-017
2	8	53	40	-13.41	1.29E-017
4	9	53	48	-10.28	9.9E-018
7	10	48	43	-12.63	1.42E-017
1	11	43	40	-11.92	1.41E-017
9	12	48	44	-14.7	1.43E-017
11	13	48	44	-14.73	1.42E-017

3.5 Mathematical Determination of the Interaction Process Between the Viral Particles and the Drug Particles Within the Serum

The suspension of the viral particles and that of the drug is bonded by the prevailing Van der Waal forces of attraction in the presence of the serum acting as the medium. These forces are attractive for similar bodies but can be either attractive or repulsive for dissimilar bodies.

Consider figure 3.2, the spherical particle for both the viral particle and that of the drugparticle having different radius r, and the separation distance d between the particles.

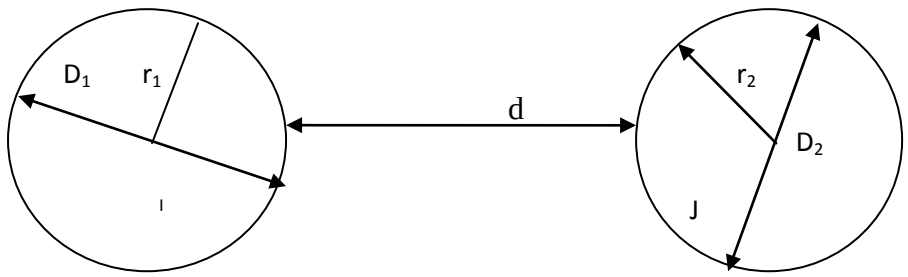

Figure 3.2: Conceptualized Geometry of virus (1) and the drug (2) suspended in a medium.

The particle 1 (i) is the viral particle, 2(j) is the drug particle and 3(k) is the interacting medium.r_1 and r_2 are the radii of the sphere while D_1 and D_2 are the diameters of the spheres.

The total energy of interaction is obtained by integration,

$$W_{vdw} = \int G_{vdw}\, dA \quad (3.2)$$

But $dA = 2\pi r dr$ (3.3)

For the two radii, r_1 and r_2

But $A = \frac{2\pi r_1 r_2}{r_1 + r_2}$ (3.4)

Putting equation (3.4) into (3.2)

$$W = \frac{2\pi r_1 r_2}{r_1 + r_2} \int G_{vdw} \quad (3.5)$$

The integration of molecules present gives the energy of attraction between molecules. The expression for Van der Waal interaction between molecules is given as

$$G_{vdw} = \frac{A}{12\pi d^2} \quad (3.6)$$

Where A is the Hamaker Constant, d is the separating distance between the molecules.

Equation (4) becomes

$$W = \frac{2\pi r_1 r_2}{r_1 + r_2} \cdot \frac{A}{12\pi d^2} \quad (3.7)$$

$$W = \frac{AR}{6d^2} \quad (3.8)$$

Where $R = \frac{r1\, r2}{r1 + r2}$ (3.9)

3.5.1 Determination of Hamaker Constantsof the InteractingParticles in the Medium.

From equation 3.8, it can be seen that Hamaker constant is a property possessed by molecules interacting with each other which depends on the material composition and the interacting medium.

For the two bodies involved, the energy of the interaction of the particle of volumes V_1 and V_2 containing atoms is given as

$$W= \frac{A12}{\pi 2}\int_{v1}\int_{v2}\frac{1}{d^6}\, d_{v1}\, d_{v2} \tag{3.10}$$

The Hamaker constant A, from equation (7) is

$$A=\pi^2\, C_L\, \rho_1\, \rho_2 \tag{3.11}$$

Where C_L is the coefficient of atoms potentials but C_L is proportional to the square of polarization α^2

$$A = \pi^2\alpha^2\, \rho_1\, \rho_2 \tag{3.12}$$

Where $\rho_1\, \rho_2$ are atomic densitiesthat are proportional to $\frac{1}{v}$

Where v is the volume, therefore A is proportional$C\rho^2$æ $\frac{v^2}{v^2}$ =Ω

$$A = \pi^2\alpha^2\Omega \tag{3.13}$$

Where Ωis the London forces

Recall the Hamaker Van der Waal force equation (Hamaker 1937)

$$E = \frac{A}{6}\left(\frac{2r_1r_2}{(2r_1+2r_2+d)d} + \frac{2r_1r_2}{(2r_1+d)(2r_2+d)} + \ln\frac{(2r_1+2r_2+d)d}{(2r_1+d)(2r_2+d)}\right) \tag{3.14}$$

Resolving mathematically yields,

$$E= \pi^2\alpha^2\Omega\frac{1}{6}\left(\frac{2r_1r_2}{d^2-(r_1+r_2)^2} + \frac{2r1r2}{d^2-(r_1-r_2)^2} + \ln\frac{d^2-(r_1+r_2)^2}{d^2-(r_1-r_2)^2}\right) \tag{3.15}$$

The total energy of particles in relation to the diameter of the viral particle and the drug is given as:

$$E =\pi^2\alpha^2\Omega\frac{1}{6}\left(\frac{D_1D_2/2}{d^2-\frac{(D_1+D)^2}{2}} + \left(\frac{D_1D_2/2}{d^2-\frac{(D_1+D)^2}{2}} + \ln\frac{d^2-\frac{(D_1+D)^2}{2}}{d^2-\frac{(D_1-D)^2}{2}}\right)\right) \tag{3.16}$$

To consider the medium in which the particles interact, we consider the Lifshitz theory to treat the Hamaker Constant A.

$$A_{132}= \frac{3KT}{4}\left(\frac{\varepsilon_1(O)-\varepsilon_3(0)}{\varepsilon_1(O)+\varepsilon_3(0}\right)\left(\frac{\varepsilon_2(O)-\varepsilon_3(0)}{\varepsilon_2(O)+\varepsilon_3(0)}\right)+ \frac{3h(ve)}{4\pi}\int_0^{\infty}\left(\frac{\varepsilon_2(iv)-\varepsilon_3(iv)}{\varepsilon_2(iv)+\varepsilon_3(iv)}\right) +$$

$$\left(\frac{\varepsilon_2(v)-\varepsilon_3(v)}{\varepsilon_2(v)+\varepsilon_3(v)}\right)dv \qquad (3.17)$$

Equations (3.6) and (3.8) remain the same in dealing with Liftshitz equation .The Hamaker constant A_{132} here becomes a function of the dielectric constant of the serum as the third body.

ε is the frequency dependent dielectric constant ε (iv) is the imaginary, T is the temperature, K is Boltzmann constant.

Considering the polarization of small spherical molecules separation by a medium.

$$\alpha\ (v) = 4\pi\varepsilon_0\varepsilon_1(v)\left(\frac{\varepsilon_1(v)-\varepsilon_3(v)}{\varepsilon_1(v)+ 2\ \varepsilon_3(v)}\right) \qquad (3.18)$$

Whereε_1 and $\varepsilon_2$are diaelectric constants but

$$\varepsilon_1\ (v) = 1+\ \frac{n^2-1}{1+(v/ve)^2} \qquad (3.19)$$

Where n is the refractive index of each medium

$$n=\sqrt{\varepsilon_1(V_n)} \qquad (3.20)$$

Using Fourier transform for the integration, equation (16) yields

$$A_{132}= \frac{3}{4}KT\left[\frac{\varepsilon_1-\varepsilon_3}{\varepsilon_{1+}\varepsilon_3}\right]\left[\frac{\varepsilon_2-\varepsilon_3}{\varepsilon_{2+}\varepsilon_3}\right]+\frac{3hve}{\sqrt[8]{2}}\frac{(n_1^2-n_3^2)(n_2^2-n_3^2)}{\sqrt{(n_1^2+n_3^2)}\sqrt{(n_2^2+n_3^2)}-\sqrt{(n_1^2+n_3^2)}+\sqrt{(n_2^2+n_3^2)}}$$

(3.21)

Where K is the Boltzmann constant

$$A_{132}= \frac{3}{4}KT\left[\frac{\varepsilon_1-\varepsilon_3}{\varepsilon_{1+}\varepsilon_3}\right]\left[\frac{\varepsilon_2-\varepsilon_3}{\varepsilon_{2+}\varepsilon_3}\right]+\frac{0.0265hv(n_2^2-n_3^2)(n_2^2-n_3^2)}{(n_1^2+n_3^2))^{0.5}(n_2^2+n_3^2))^{0.5}[(n_1^2+n_3^2)+\lceil(n_2^2+n_3^2)]\rceil^{0.5}} \qquad (3.22)$$

It should be noted that in the equation (3.22), the Van der Waal interaction is affected also by the absorbed layer of the dielectric material.

Therefore, the Hamaker constant A_{132} is also affected by the permittivity of the absorbed layer.

Considering the solid particles *i* and *j* interacting across the medium *k.*

As earlier stated for the dissimilar particles, it could be positive or negative, the general combination mixing rule can be applied.

$$A_i K_i = A_j K_j - A_i K_j + A_{ij} \quad (3.23)$$

Taking the Arithmetic mean of the particle of *i* and *j*

$$A_{ij} = \frac{A_{ii} + A_{jj}}{2} \quad (3.24)$$

$$A_{ij} = 0.5(A_{ii} + A_{jj}) \quad (3.25)$$

Also considering the geometric mean

$$A_{ij} = (A_{ii} A_{jj})^{0.5} \quad (3.26)$$

Also considering the Harmonic mean

$$A_{ij} = (A_{ii} + A_{jj}) = 2A_{ii} A_{jj} \quad (3.27)$$

Also considering the medium k, the absolute Hamaker constant becomes

$$A_{ijk} = A_{ij} + A_{kk} - A_{ik} - A_{jk} \quad (3.28)$$

From equation (3.27),

$$A_{iki} = A_{ii} + A_{kk} - 2A_{ik} \quad (3.29)$$

$$A_{iki} = \frac{(A_{ii} - A_{kk})^2}{(A_{ii} + A_{kk})} \quad (3.30)$$

Therefore

$$A_{ikj} = (A_{ii} - A_{kk})^{1/2} . (A_{jj} - A_{kk})^{1/2} \quad (3.31)$$

But when *i* = *j*

Equations (3.27) and (3.28) yields

$$A_{kk} = 2[(A_{ij})^{0.5} - A_{ikj}) . (A_{11}^{0.5} + A_{jj}^{0.5})^{-1}]^2 \quad (3.32)$$

Equation (3.31) yields

$$A_{iki} = (A_{ii} - A_{kk})^{1/2} . (A_{ii} - A_{kk})^{1/2} \quad (3.33)$$

$$A_{iki} = (A_{ii} - A_{kk})^{1/2} \quad (3.34)$$

CHAPTER FOUR

RESULTS AND DISCUSSION

This chapter contains the results of various experiments conducted and the mathematical computation of experimented data and their analysis. The resulting active plants extracts after the extraction experiments were shown in figure 4.1.

4.1 Plants Phytochemical Result

Fig 4.1: Various Plant Extracts

The extract DH is a direct acting herbal antiviral formulated from the combination *of Phyllantus amarus extract, Vernonia amygdalina extract and Anona muricata* extracts as done by practioners of complementary and alternative medicine.

Table 4.1: Details of Herbal Extracts

Plants	Abbreviations	Drug Type	Manufacturing Date	Size	Dosage
Anona Muricata	AM	Powder/Single	November, 2016	200mg	Twice daily
Vernonia Amygdalina	VA	Powder/Single	November, 2016	200mg	Twice daily
Brophyllum Pinnatum	BP	Powder/Single	November, 2016	200mg	Twice daily
Direct Acting Herbal	DH	Powder/DAA	November, 2016	100mg/200 mg/400mg	Once daily

Table 4.1 describes the detailed features of the herbal extract with respect to dosage and size. DH is taken once daily, while the rest are single regime treatment taken twice daily. The date of manufacture also is included in the table 4.1.

Table 4.2: **Characterization of Plants Extracts**

	Quantity(mg/gm)			
Phytochemicals	AM	VA	BP	Phyllantus
Alkanoids	+++	+++	++	+
Flavonoids	++	+++	+	++
Saponins	++	++	++	+++
Terpenoids	+	++	+	+
Phenolic	++	+++	++	+++
Tannis	+	+	+	++

(+++)=heavily present, (++)= moderate, (+)= low,(-)= absent

Table 4.3: **Percentage Composition of Phytochemicals in Plants Extracts**

	Quantitative Percentage Composition (%) per 200mg			
Phytochemicals	AM(%)	VA(%)	BP(%)	Phyllantus Amarus(%)
Alkanoids	5.10	3.94	0.058	1.36
Flavonoids	1.24	5.34	0.106	1.52
Saponins	2.96	12.36	2.10	0.80
Phenolic	0.005	6.86	0.64	0.08
Tannis	1.60	22.10	1.28	1.24

Tables 4.2 and 4.3 show the qualitative and quantitative compositions of the phytochemicals present in the various plants extracts. Alkaloids, flavanoids, saponins, phenols and tannis were present in the plant at different concentrations. The varied concentrations and percentage compositions explain the difference in their various antiviral efficacies.

4.2Fourier Transform Infrared analysis

4.2.1: Functional group of Bryophillum extract(see Appendix G1)

The wave numbers, functional groups of FTIR analysis on bryophillum pinnatum extracts are shown in Appendix G1 while fig. 4.2 displays its spectrum trends. The ranges of wave

numbers indicate the presence of aromatic rings (C-H bend), carboxylic acid (O-H stretch), alkanes (C-H2 stretch), amides (C-H stretch), esters(C-O band), nitriles (C-N stretch), adelhydes (C-H stretch), quinine (O-H bend) and amides(C=O stretch). Fig.4.2 shows that the active present functional groups in bryophyllum extract are amides, quinine, and carboxylic acid.These functional groups are responsible for its antiviral properties.

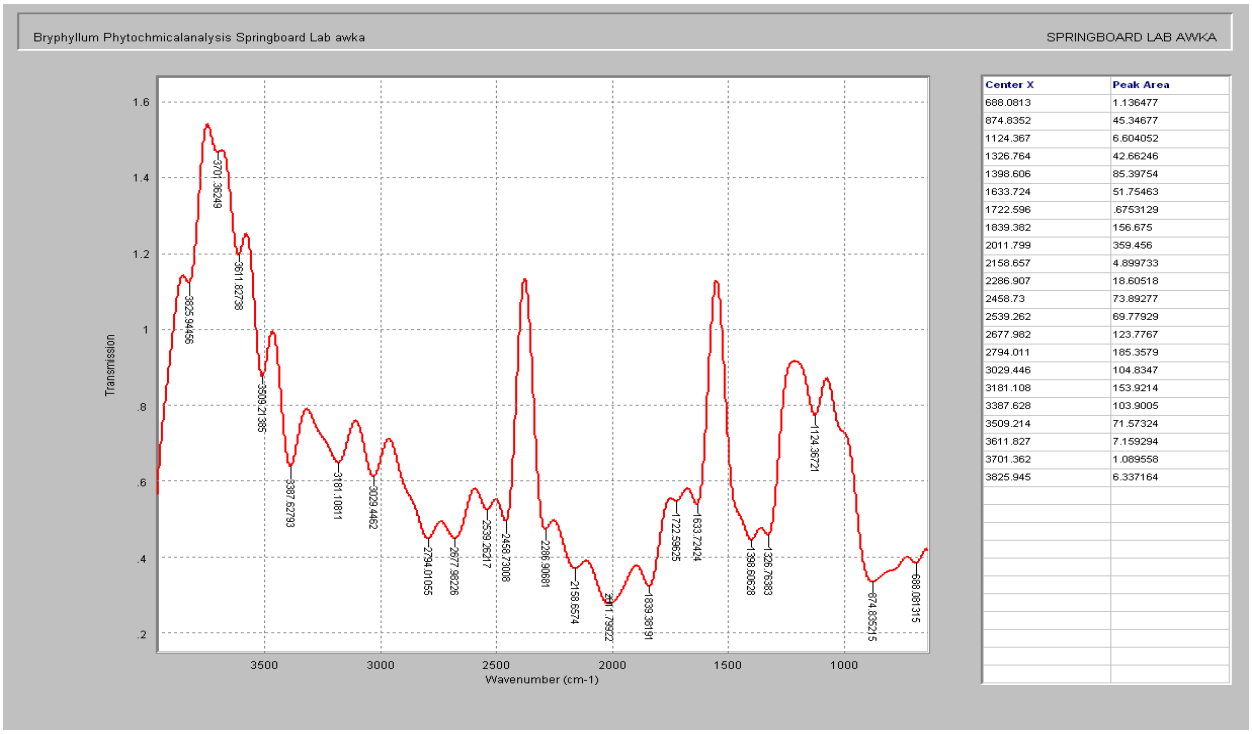

Fig. 4.2: Fourier wavelength for Bryophillum Extract

4.2.2: Functional group of phyllantus amarus extract (see Appendix G2)

Appendix G2 shows the wave numbers, functional groups of FTIR analysis of phyllantus amarus extracts. The ranges of wave numbers reveal that aromatic rings (C-H band), carboxylic acid (O-H stretch), alkanes (C-H2 stretch), amides (N-H stretch), nitriles (C-N stretch), nitriles (C-N stretch), alkanes (C-H bend), alkanes (C-H2 stretch),quinine (O-H bend) and amides (C-O stretch) are present in the methanolic extracts of phyllantus amarus. Fig 4.3 is the FTIR spectrum of phyllantus extracts showing that amides and carboxylic acid are the activefunctional group in the extract.

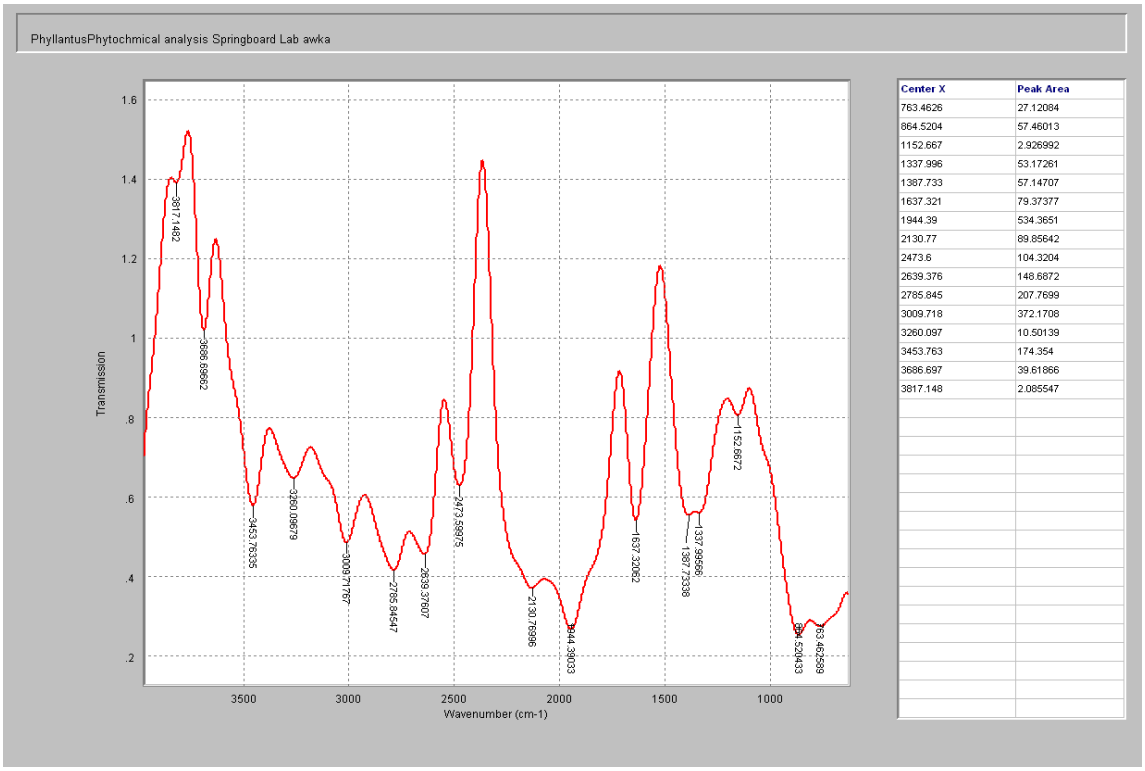

Fig. 4.3: Fourier wavelength for phyllantus amarus Extract

4.2.3Functional group of annona muricata extracts(See Appendix G3)

Appendix G3 shows the wave numbers, functional groups of FTIR analysis of Anonia muricata extracts. The range of wave numbers shows the presence of aromatic rings (C-H stretch), carboxylic acid (O-H stretch), carboxylic acid (N-H stretch), nitriles (C-N bend),adelhydes (C-H bend), quinine (O-H bend) and amides (C-O stretch) as the functional groups in the extract. Fig 4.4 is the FTIR spectrum of annona muricata extracts showing that quinine and amides are the active functional group present in the extract.

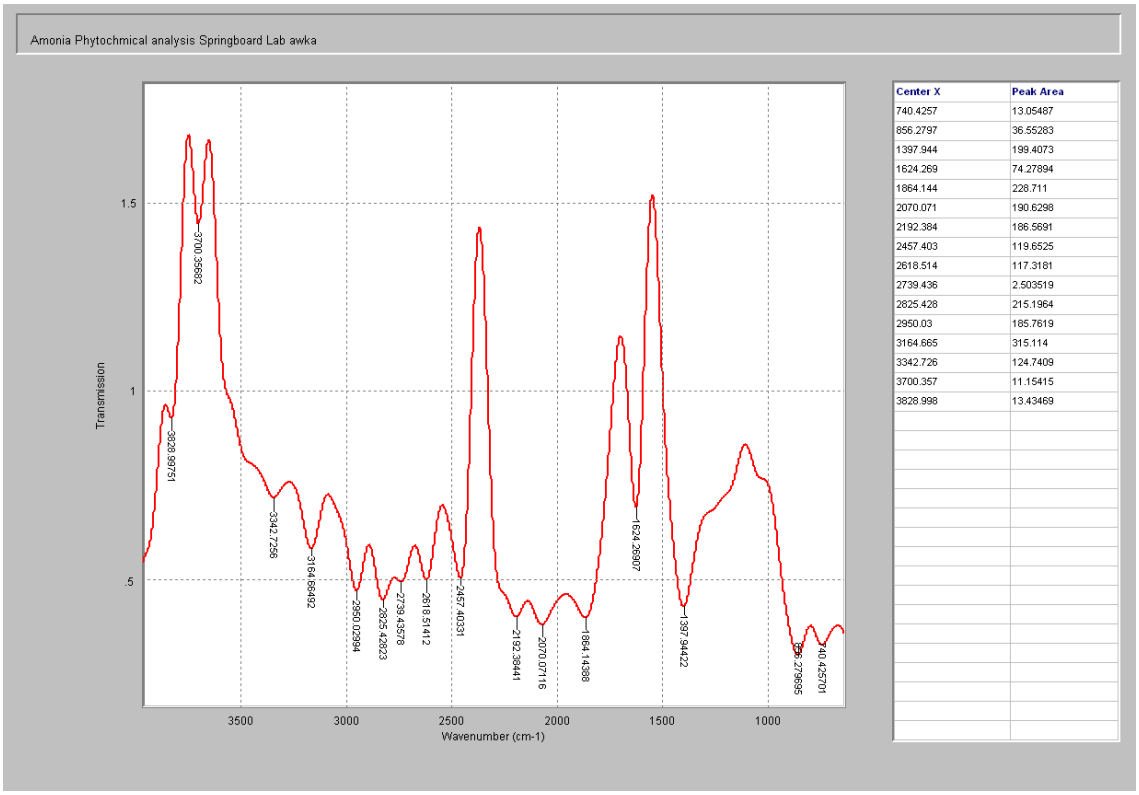

Fig. 4.4: Fourier wavelength for Annona muricata Extract

4.2.4: Functional group of vernonia amygdalina extract(see Appendix G4)

The wave numbers and functional groups of vernonia amygdalina extract as shown in Appendix G4 indicate the presence of aromatic rings (C-H stretch), alkanes (C-H2), amides (N-H stretch), nitriles (C-N stretch), adelhydes (C-H stretch), alkanes (C-H2 stretch), quinine (O-H stretch) functional groups in the extracts.Fig 4.5 is the FTIR spectrum of vernonia amygdalina extracts showing that quinine and amides are the active functional group present. The presence of quinine and amides in vernonia amygdalina extracts could be responsible for its high antiviral potentials.

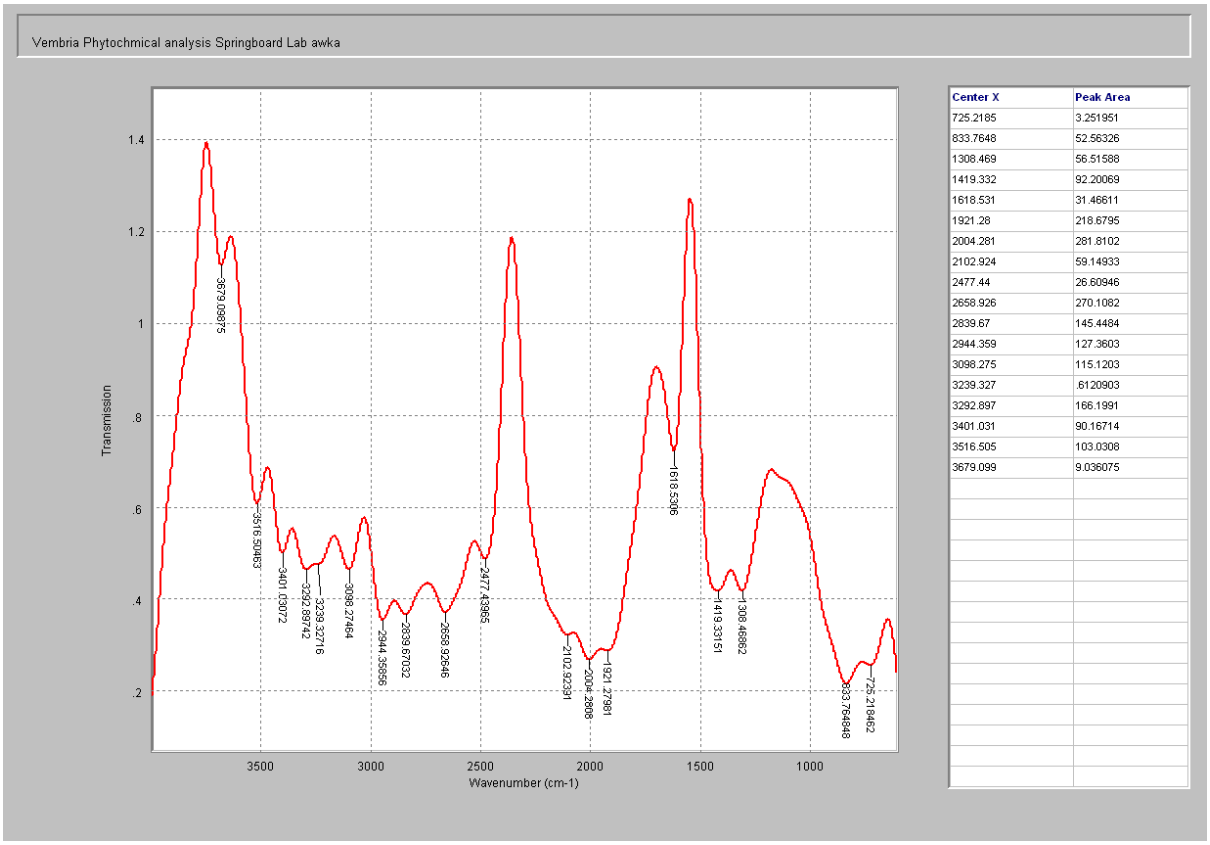

Center X	Peak Area
725.2185	3.251951
833.7648	52.56326
1308.469	56.51588
1419.332	92.20069
1618.531	31.46611
1921.28	218.6795
2004.281	281.8102
2102.924	59.14933
2477.44	26.60946
2658.926	270.1082
2839.67	145.4484
2944.359	127.3603
3098.275	115.1203
3239.327	.6120903
3292.897	166.1991
3401.031	90.16714
3516.505	103.0308
3679.099	9.036075

Fig. 4.5: Fourier wavelength for vernonia amygdalina extract

4.3 Determination of CD4 Counts on the Blood values. Samples

Table 4.8 Measured CD4 counts on both Infected and Uninfected Blood Samples

Blood samples (B)	Infected (counts/mm^3)	Uninfected(counts/mm^3)
B1	428	660
B2	600	872
B3	625	1780
B4	312	1450
B5	464	1500
B6	247	930
B7	852	1360
B8	115	1520
B9	704	1580
B10	798	1020
Average	**514.5**	**1267.2**
SD	**243.1059**	**368.2731**

Table 4.8 depicts the CD4+ results obtained from the Partec Cyflow Counter Machine for both the infected and uninfected samples.Quality of 25100 per ml was obtained which falls between standard acceptable ranges of 23270 ∓10% per ml.

In general, infected samples have low CD4 counts while the uninfected usually have high CD4 cell counts. CD4+ cell counts indicate the severity of the hepatitis c virus infection. The highest CD4 count was seen on the uninfected samples while the lowest count was noticed on the infected samples. On the average, infected samples have lower CD4 count which signifies the impact of the hepatitis C virus in the depletion of the immune system on the infected patients.

The regression trends analysis cannot be used here because the infected samples do not fit into the linear, exponential and the polynomial trends because its value cannot be approximated to 1. This is as a result of the depleted immune system of the infected patients offering different levels of resistance to the virus and also a difference in the HCV genotypes. It can also be seen that a scenario arises where an uninfected sample can have low value of CD4 count, this means that CD4 counts can also be lowered by other infections besides HCV.

4.4 Results of Measured Contact Angles and its Implications on Blood Cells

The results of contact angle measured can be seen in appendices A1-A4. The infected, uninfected and the treated samples of the blood were separated according to their respective blood components and their average results displayed in Table 4.9.

Table 4.9: Average contact angle and blood cells Infection (See Appendices A1-A4)

			Treated(θ^0)							
Blood Cells	**Infected(θ^0)**	**Uninfcted(θ^0)**	**IFN**	**RBV**	**ATR**	**ELT**	**AM**	**VA**	**BP**	**DH**
Whol. Blood	57.1± 2.38	49.5± 5.36	54.5± 3.03	55± 2.58	55.5± 3.30	54.5± 3.03	54.5± 3.03	54.5± 3.03	54.8± 3.43	53.7± 3.95
WBC	63.4± 3.21	48.5± 2.75	56.9± 4.38	56.3±4 .32	56.6± 5.25	56.5± 3.38	58.5± 4.45	55.5± 3.03	56.4± 3.57	59.6± 3.20
RBC	60.4± 2.88	50.6± 3.57	58.5± 3.03	56.1±3 .81	58.5± 3.03	58.8± 3.71	57.6± 3.20	58.2± 2.97	59.6± 3.20	53.3± 3.34
Serum	61.5± 3.03	53.1± 3.85	57.7± 4.74	56.3±3 .40	56.5± 3.38	56.5± 3.20	60.1± 3.93	55.2± 3.43	55± 3.74	53.2± 4.52

Table 4.10: CD4+ count and Contact angle

Blood Samples	Infected Blood Samples		Uninfected Blood Samples	
	CD4 Count (counts/mm^3)	Contact Angle (θ^0)	CD4 Count (counts/mm^3)	Contact Angle(θ^0)
1	428	65	660	47
2	600	61	872	46
3	625	63	1780	48
4	312	64	1450	52
5	464	67	1500	50
6	247	66	930	51
7	852	58	1360	45
8	115	68	1520	49
9	704	62	1580	44
10	798	60	1020	51
AVE	**514.5**	**63.4**	**1267.2**	**48.5**
SD	**243.1059**	**3.2045**	**368.2731**	**2.7508**

Table 4.9summarizes the effect of the hepatitis c virus on blood cellsand the various drug treatments using the average contact angle as a means of determining their surface interactions. It can be observed on critical examination of table 4.9 that infected samples have higher contact angles measured on the different components of the blood when compared to the angles measured on the uninfected and the treated samples. This is as a result of the presence of the virus on the infected surfaces which creates barrier and promotes surface roughness and heterogenity thereby reducing the spreading rate of the probe liquid.This in effect causes the surfaces to be poorly wetted(hydrophobic) by the probe liquid.The higher values of contact angle signify poorly wet surfaces(Yuan and Lee, 2013).

Ozoihu(2014) compared the contact angle of HIV infected and uninfected blood cells using different probe liquids and reported that infected samples of the blood have a higher contact angle than the uninfected.Also in table 4.9,the average contact angle of the infected white blood cells (63.4±3.21) obtained in this study is higher that the contact angle of the uninfected cells(48.5±2.75).This is in accordance with literature report on the contact angle of HIV infected surfaces where the average contact angle of the three probe liquids used yielded same result.

It is also in agreement with table 2.4 in which average contact angle of infected human lymphocytes using equation of state was reported.The assumption here is that the infected lymphocyte is an approximation of the actual virus owing to the manner the virus infuses itself to the white blood cells.

From the foregoing, it can be deduced that the hepatitis c virus has the ability of increasing the contact angles of infected surfaces. Hence, infected surfaces are poorly wetted, leading to an increase in the contact angle of such surfaces. Among the infected blood components, the white blood cell has the highest contact angle. This leads to a logical conclusion that the white blood cells are the principal target of the virus with sole action of depleting the lymphocytes (Chukwuneke, 2015).

In all the treatments administered to the blood samples, a common trend can be observed.They all have the potency required to reduce the contact angles of the infected samples (63.4^0). IFN reduced the contact angle of infected white blood to 56.9^0, RBV to 56.3^0, ATR to $56.6^0$and so on as evident in table 4.9.This suggests that continued treatment with these conventional and herbal drugs could actually lower the contact angles of the infected samples to a value closer to the uninfected contact angle measured.

Comparatively among all treatments given, *vernonia amygdalina* which is an herbal drug has the lowest contact angle on white blood cells (55.5±3.03).In principle, contact angle gives good indication of wettability and lower contact angle is an approximation of good wetting ability(Derrick et al, 2007). The lowest contact angle with blood samples treated with VA is an indication of the high interaction between the virus and the drug which showcased its effectiveness in coating the virus.

Table 4.10 details the interaction between CD4 count and contact angle of both the infected and the uninfected cells. It is clear from the table 4.10 that cells infected with HCV have lower CD4 lymphocytes counts but a higher contact angle while the uninfected cells have a higher CD4 counts but a lower contact angle. Conclusively, the presence of the virus affects the immune system of the infected patients by depleting the T4 lymphocytes cells and hence leading to an increase of the contact

angle.The white blood cells values was used to create table 4.10 since it is the principal target of the virus but in all cases of the respective blood components, the observations drawn above is same.

4.5 Surface Free Energy(γ_{sv})of Blood Cells (See B1-B60)

The measured contact angle data from experimental set up was used for Matlab computation for the surface free energy (γ_{sv}) using the equation of state (eqn 2.31). Appendix (B1-B60) shows the surface free energy(γ_{sv}) of the respective blood components of the infected, uninfected and the treated blood samples using various drugs.

Table 4.11: Average surface free energy (See AppendicesC1-C3)

			Treated(γ_{sv})							
Blood Cells	**Infected**(γ_{sv})	**Uninfected** (γ_{sv})	**IFN**	**RBV**	**ATR**	**ELT**	**AM**	**VA**	**BP**	**DH**
Whol. Blood	38.10± 1.72	43.47 ±3.70	39.87± 2.28	39.61 ±1.85	39.25± 2.18	39.97± 2.17	39.97± 2.17	39.97± 2.17	39.75 ±2.46	40.54± 2.82
WBC	33.54± 2.31	44.35 ±1.90	38.24± 3.16	38.66 ±3.08	38.45± 3.78	38.53± 2.43	37.08± 3.21	39.25± 2.18	38.60 ±2.57	36.29± 2.32
RBC	35.71± 2.08	42.74 ±2.51	37.10± 2.19	38.82 ±2.75	37.09± 2.19	36.87± 2.68	37.74± 2.32	37.31± 2.15	36.29 ±2.32	40.83± 2.38
Serum	34.92± 2.19	40.53 ±2.75	37.66± 3.42	38.± 2.45	38.53± 2.43	37.76± 3.27	35.93± 2.84	39.47± 2.46	39.61 ±2.68	40.88± 3.21

Table 4.11shows that the surface free energy of the uninfected blood component (44.35±1.90) is seen to be higher than that of the infected component (33.54±2.31) which agrees with the works of Rullison (2008) which reported that solids having

lower surface free energy exhibit high contact angles as can be seen in the case of the infected component. The surface energy of cohesion between the blood particles is reduced as soon as infection occurs which is an indicative of the fact that the presence of hepatitis c virus infection on the samples has a reduction effect on interfacial surface energy of the blood particles. The virus can be concluded to have the capability of reducing the energy at the surface.Hence infected blood components have low surface free energy and as such can be described as apolar surfaces characterized by poor wetting abilities.

The reduction of the interfacial energy in whole blood is 12.35%, white blood cell is 24.37%, red blood cell is 16% and serum is reduced by 14%. From the percentage analysis above, it can be observed that there is a reduction in the van der Waal forces of attraction between the blood particles interacting with the serum. It can be deduced that the onus of the infection is on the white blood cell component since it has the highest percentage reduction (24.37%) with its surface energy degraded from 44.35mJ/$m^2$to 33.54mJ/m^2. HCV also attacks other blood components hence a reduction in their respective surface energy as a result of the viral particles interfering with red blood cells and serum.

All the drugs used for the treatment (conventional and herbal) have shown their potency in increasing the surface free energy of all the components treated, having DH raising the surface energy of serum even beyond that of the uninfected. All treatments given were able to raise the energy of the whole blood from 38.10mJ/m^2 to 40mJ/m^2.

For the infected white blood cell being the principal target, IFN increased the surface free energy by 14%, RBV by 15%, ATR by 15%, ELT by 14%, AM by 11%, VA by 17%, BP by 15% and DH by 8%. It could be concluded that amongst all treatments given, VA is more efficient in coating the virus since it has the highest percentage efficiency in increasing the surface free energy of the infected white blood cell by 17%.For red blood, DH treatment exhibited an excellent performance in increasing the surface free energy of the infected samples by 13%. The virus reduced the surface free energy of serum by 14% but the DH treatment given was able to increase the surface free energy of the said serum by 15%. It could be deduced from the foregoing that

these treatments given have different areas in which their potency prevails, VA is the best for infected white blood cell in which the virus fuses itself to and DH is the best for infected red blood cells and serum. This could be attributed to the difference in their phytochemical compositions.

4.6Energy of Adhesion (F^{adh}) on Blood Cells

Energy of interaction is a function of van der Waal forces of adhesion which is the force of attraction between different particles suspended in a liquid medium (serum). Appendices B1-B60 show energy of adhesion of the respective blood components of the infected, uninfected and the treated blood samples using various drugs. The three models used for the study were computed for in the determination of the adhesion energy. Thermodynamically, adhesion to cell surfaces is favorable when the change in free energy of adhesion is negative. Hepatitis c virus, upon interaction with the blood cells binds itself to the surface of the lymphocytes, thereby establishing a thermodynamic relationship that can be analyzed using van der Waal forces of attraction.

Table 4.12Average Change in Surface Energy of Adhesion(See AppendicesD1-D3)

	Infected (mJ/m^2)	**Uninf-ected** (mJ/m^2)	Treated(mJ/m^2)							
			IFN	**RBV**	**ATR**	**ELT**	**AM**	**VA**	**BP**	**DH**
Neu	-23.22± 2.23	-12.99± 1.75	-18.7± 3.00	-18.34± 2.90	-18.55± 3.59	-18.45± 2.31	-19.84± 3.06	-17.77± 2.06	-18.39± 2.44	-20.59± 2.22
Fow	-35.38± 3.19	-21.47± 2.28	-29.14± 4.09	-28.59± 3.87	-28.90± 4.88	-28.73± 3.14	-30.65± 4.22	-27.80± 2.79	-28.64± 3.30	-31.66± 3.09
Wu	-85.06± 4.47	-57.23± 6.38	-69.72± 8.18	-70.83± 7.74	-70.20± 9.77	-70.54± 6.27	-72.41± 5.57	66.70± 8.43	-70.71± 6.60	-64.68± 6.18

Table 4.12 is an extract of the white blood cell data of the various models from appendices D1-D3 which will be used to explain the interaction dynamics. In all the models (Neumann, Fowkes and Wu) used for the computation of the energy of adhesion from equation 2.30, it was observed that upon infection, the virus binds itself to the surface of the cell thereby causing an increase in the energy of adhesion.

The infected surfaces have higher energy of adhesion in all models used (Neumann = -23.22±2.23, Fowkes =-35.38±3.19 and Wu= 85.06±4.47) than the uninfected blood (Neumann = -12.99±1.75, Fowkes = -21.47±2.28 and Wu= -57.23±6.38). The adhesion energy of the treated surfaces is equally higher than the uninfected samples.Achebe et al, (2012) reported that adhesion is favorable when the change in the energy of adhesion is negative. The negative sign of adhesion energies seen in table 4.12 explains the fact that there is net van der Waal force of attraction between the virus and the blood cells.The negative sense of adhesion energy of uninfected surfaces suggests the presence of other infections other than HCV binding to the blood cells, hence the reason behind the low CD4 count for some HCV uninfected blood samples. The treated surfaces also showed adhesionof the virus to the drug coated lymphocyte.

The presence of the virus causes the energy of adhesion of the infected surfaces to increase leading to an increase in contact angle and a decrease in CD4 count and surface free energy especially in white blood cells where it fuses itself to the hepatic cell and replicates alongside with the RNA. The 79% increase in adhesion energy of the infected cells causes the immune system to be depleted resulting in a low CD4 count.

In all the models used for the determination of the average adhesion energy, it was shown that the attraction between the virus and the blood cell is higher in infected white blood cell components and lower in uninfected white blood cells as seen in Appendices D1-D3.The treatments given (conventional and herbal) in all cases of the respective blood components has the tendency to reduce the surface energy of adhesion of the infected surfaces.The IFN treatment given was able to reduce the surface energy of adhesion of the infected white blood cell by 19%, RBV by 21%, ATR by 20%, ELT by 21%, AM by 15%, VA by 23.5%, BP by 21% and DH by 11%.The highest tendency to reduce the adhesion energy of the infected surfaces was observed in the herbal formulation VA(23.5%,), making it the most antiviral natural compound used for this study to effectively coat the virus as a result of the quinine present.

Neumann model is the best known equation of state. In principle, the equation of state requires the contact angle measurement to be done only with one probe liquid and regardless which liquid is chosen the surface free energy result should be the same. Equation of state theory also does not divide the surface tension into different components as the other

theories. This is also the only theory which allows the calculations to be done by using just one probe liquid (Kwok and Neumann, 1999).

The probe liquid (glycerin) used for this study is apolar in that its surfaces have low energy and Neumann model also is for low energy surfaces (Table 4.12) allowing one probe liquid to be used with high precision and prediction. It is against this backdrop that amongst other models used for this study, Neumann model will be used for further analysis.

4.7 Response Surface Analysis of Energy of Adhesion

The results obtained from matlab computations were analyzed by applying the coefficient of determination (R^2), lack of fit, response plots and analysis of variance (ANOVA) to determine the statistical significance level and generate modelequations which will express the relationship between the predicted response and independent variables in coded values.The design matrix was shown in table 3.6-3.8

Table 4.13a: Response Summary

Source	**Sequential p-value**	**Lack of Fit p-value**	**Adjusted R-Squared**	**Predicted R-Squared**
Linear	0.5637	0.0082	-0.0700	-0.7404
2FI	0.3084	0.0077	-0.0526	-0.7842
Quadratic	< 0.0001	0.5120	0.9026	0.7836
Cubic	0.2903	0.7677	0.9169	0.8932

Table 4.13b: Sequential Model Sum of Square

Source	Sum of Squares	Df	Mean Square	F Value	p-value Prob >F
Mean vs Total	6547.99	1	6547.99		
Linear vs Mean	4.85	2	2.43	0.61	0.5637
2FI vs Linear	4.58	1	4.58	1.17	0.3084
Quadratic vs 2FI	32.81	2	16.41	45.16	< 0.0001
Cubic vs Quadratic	0.99	2	0.50	1.60	0.2903
Residual	1.55	5	0.31		
Total	6592.78	13	507.14		

Table 4.13c: Lack of Fit Test

Source	Sum of Squares	Df	Mean Square	F Value	p-value Prob > F
Linear	38.42	6	6.40	16.93	0.0082
2FI	33.84	5	6.77	17.90	0.0077
Quadratic	1.03	3	0.34	0.91	0.5120
Cubic	0.038	1	0.038	0.100	0.7677
Pure Error	1.51	4	0.38		

Table 4.13d: Model Summary Statistics

Source	Std. Dev.	R-Squared	Adjusted R-Squared	Predicted R-Squared	PRESS
Linear	2.00	0.1083	-0.0700	-0.7404	77.95
2FI	1.98	0.2106	-0.0526	-0.7842	79.91
Quadratic	0.60	0.9432	0.9026	0.7836	9.69
Cubic	0.56	0.9654	0.9169	0.8932	4.78

Table4.13e: Quadratic Model Summary

Std. Dev.	0.60
Mean	-22.44
C.V. %	2.69
PRESS	9.69
R-Squared	0.9432
Adj R-Squared	0.9026
Pred R-Squared	0.7836
Adeq Precision	14.194

Table 4.13f: Analysis of Variance (ANOVA) for Surface Response Quadratic Model

Source	Sum of Squares	D*f*	Mean Square	F Value	p-value Prob > F	
Model	42.24	5	8.45	23.25	0.0003	Significant
A-Contact Angle	0.65	1	0.65	1.78	0.2237	
B-Interfacial Energy	4.20	1	4.20	11.57	0.0114	
AB	4.58	1	4.58	12.60	0.0093	
A^2	32.06	1	32.06	88.24	< 0.0001	
B^2	0.014	1	0.014	0.040	0.8474	
Residual	2.54	7	0.36			
Lack of Fit	1.03	3	0.34	0.91	0.5120	not significant
Pure Error	1.51	4	0.38			
Cor Total	44.79	12				

Tables 4.13 (a-g) are a response analysis table obtained using Neumann model for infected white blood cell (Appendix B2).The quadratic model is suggested and focus

is on the model maximizing the "Adjusted R-Squared" and the "Predicted R-Squared. The Model F-value of 23.25 implies the model is significant. There is only a 0.03% chance that an F-value this large could occur due to noise. Values of "Prob > F" less than 0.0500 indicate model terms are significant. In this case B, AB, A^2 are significant model terms. Values greater than 0.1000 indicate the model terms are not significant.

The "Lack of Fit F-value" of 0.91 implies the Lack of Fit is not significant relative to the pure error. There is a 51.20% chance that a "Lack of Fit F-value" this large could occur due to noise. Non-significant lack of fit is good.

The "Pred R-Squared" of 0.7836 is in reasonable agreement with the "Adj R-Squared" of 0.9026 since their difference is less than 0.2. "Adequate Precision" measures the signal to noise ratio. A ratio greater than 4 is desirable. Table 4.13e gives an adequate precision of 14.194 indicating an adequate interaction. This means that the model is a good one for predicting energy of adhesion in relation with contact angle and interfacial energy due to HCV infection.The equation in terms of coded factors can be used to make predictions about the response of the interacting variables. The coded equation is also useful for identifying the relative impact of the factors by comparing the factor coefficients.

Table4.13g: Surface Energy of Adhesion Model Equation

Factor	**Coefficient Estimate**	***Df***	**Standard Error**	**95% CI Low**	**95% CI High**	**VIF**
Intercept	-21.15	1	0.27	-21.79	-20.51	
A-Contact Angle	0.28	1	0.21	-0.22	0.79	1.00
B-Interfacial Energy	-0.72	1	0.21	-1.23	-0.22	1.00
AB	-1.07	1	0.30	-1.78	-0.36	1.00
A^2	-2.15	1	0.23	-2.69	-1.61	1.02
B^2	0.046	1	0.23	-0.49	0.59	1.02

Surface energy of adhesion model equation forinfected white blood is given as:

$$F^{adh} = -21.15+0.28A-0.72B-1.07AB-2.15A^2+0.046B^2 \quad (4.1)$$

The ANOVA indicates the equation and actual relationship between the response and significant variables represented by the equation 4.1 are accurate.The R^2 value of 0.9432 indicates a good measure that outcomes are likely to be predicted well by the developed model. The contour and the surface plot on Fig. 4.6 and 4.7 also reveal graphically the interaction between the independent variable and the responsesurface by visualizing with the colour coding.

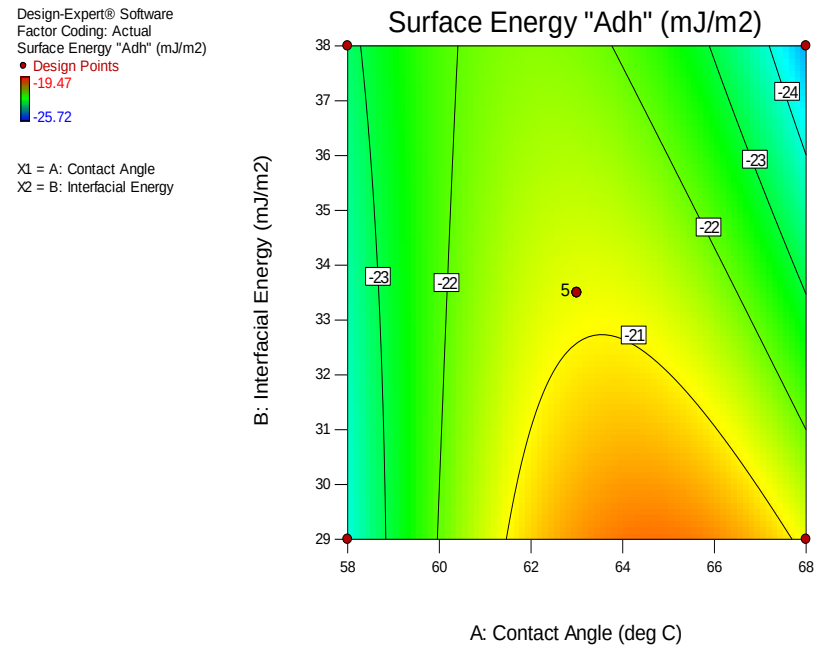

Fig 4.6: Contour plots of Infected WBC for Surface Energy of Adhesion

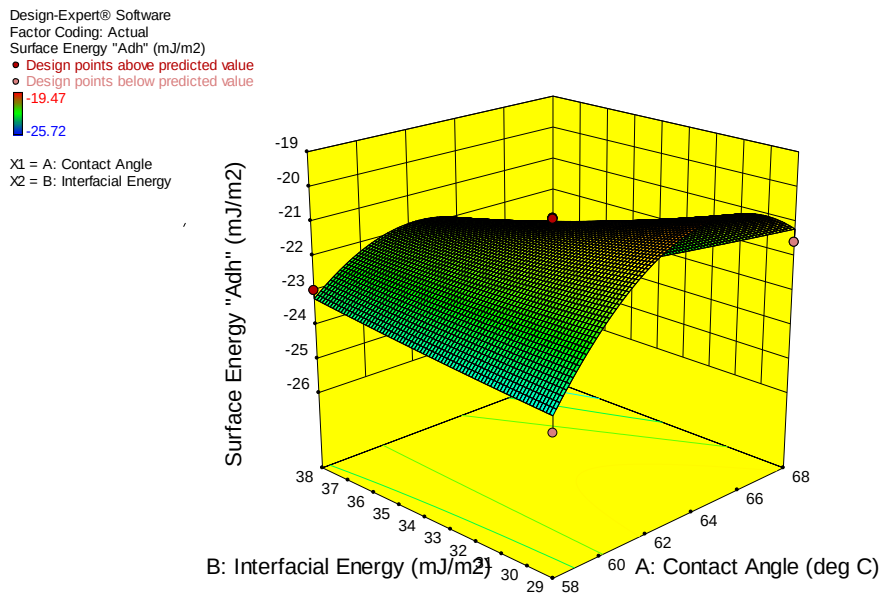

Fig 4.7: 3-D plot of Infected WBCfor Surface Energy of Adhesion

Table 4.14a: Response Summary for Unifected WBC

Source	Sequential p-value	Lack of Fit p-value	Adjusted R-Squared	Predicted R-Squared
Linear	0.0908	0.0099	0.2573	-0.1749
2FI	0.1995	0.0106	0.3197	-0.2341
Quadratic	0.0002	0.4834	0.9230	0.8238
Cubic	0.5122	0.3135	0.9175	0.4116

Table 4.14b: Sequential Model Sum of Square

Source	Sum of Squares	Df	Mean Square	F Value	p-value Prob > F
Mean vs Total	*2425.20*	*1*	*2425.20*		
Linear vs Mean	*9.26*	*2*	*4.63*	*3.08*	*0.0908*
2FI vs Linear	*2.64*	*1*	*2.64*	*1.92*	*0.1995*
Quadratic vs 2FI	*11.30*	*2*	*5.65*	*36.25*	*0.0002*
Cubic vs Quadratic	*0.26*		*0.13*	*0.77*	*0.1522*
Residual	*0.84*	*5*	*0.17*		
Total	*2449.49*	*13*	*188.42*		

Table 4.14c: Lack of Fit Test

Source	Sum of Squares	Df	Mean Square	F Value	p-value Prob > F
Linear	14.41	6	2.40	15.32	0.0099
2FI	11.77	5	2.35	15.01	0.0106
Quadratic	0.46	3	0.15	0.99	0.4834
Cubic	0.21	1	0.21	1.33	0.3135
Pure Error	0.63	4	0.16		

Table 4.14d: Model Statistics Summary

Source	Std. Dev.	R-Squared	Adjusted R-Squared	Predicted R-Squared	PRESS
Linear	1.23	0.3811	0.2573	-0.1749	28.54
2FI	1.17	0.4898	0.3197	-0.2341	29.98
Quadratic	0.39	0.9551	0.9230	0.8238	4.28
Cubic	0.41	0.9656	0.9175	0.4116	14.29

Table 4.14e: ANOVA for Response Surface QuadraticModel

Source	Sum of Squares	Df	Mean Square	F Value	p-value Prob > F	
Model	23.20	5	4.64	29.76	0.0001	Significant
A-Contact Angle	*1.07*	*1*	*1.07*	*6.85*	*0.0345*	
B-Interfacial Energy	*8.19*	*1*	*8.19*	*52.52*	*0.0002*	
AB	*2.64*	*1*	*2.64*	*16.94*	*0.0045*	
A^2	*0.17*	*1*	*0.17*	*1.07*	*0.3360*	
B^2	*11.30*	*1*	*11.30*	*72.49*	*< 0.0001*	
Residual	1.09	7	0.16			
Lack of Fit	*0.46*	*3*	*0.15*	*0.99*	*0.4834*	*not significant*
Pure Error	*0.63*	*4*	*0.16*			
Cor Total	24.29	12				

Table4.14f: Quadratic Model Summary

Std. Dev.	0.39
Mean	-13.66
C.V. %	2.89
PRESS	4.28
R-Squared	0.9551
Adj R-Squared	0.9230
Pred R-Squared	0.8238
Adeq Precision	17.672

Table 4.14(a-g) is a response analysis table obtained using Neumann model for uninfected white blood cell (Appendix B2).The quadratic model is suggested and focus is on the model maximizing the "Adjusted R-Squared" and the "Predicted R-Squared. The Model F-value of 29.76 implies the model is significant. There is only a

0.01% chance that an F-value this large could occur due to noise. Values of "Prob > F" less than 0.0500 indicate model terms are significant.

In this case A, B, AB, B^2 are significant model terms. Values greater than 0.1000 indicate the model terms are not significant.The "Lack of Fit F-value" of 0.99 implies the Lack of Fit is not significant relative to the pure error. There is a 48.34% chance that a "Lack of Fit F-value" this large could occur dueto noise. Non-significant lack of fit is good. The "Pred R-Squared" of 0.8238 is in reasonable agreement with the "Adj R-Squared" of 0.9230; since their difference is less than 0.2.

"Adeq Precision" measures the signal to noise ratio. A ratio greater than 4 is desirable.. Table 4.14e gave an adequate precision of 17.672 indicating an adequate interaction. This means that the model is a good one for predicting energy of adhesion in relation with contact angle and interfacial energy for uninfected white blood samples. The equation in terms of coded factors can be used to make predictions about the response of the interacting variables. The coded equation is also useful for identifying the relative impact of the factors by comparing the factor coefficients.

Table4.14g: Surface Energy of Adhesion Model Equation

Factor	**Coefficient Estimate**	**Df**	**Standard Error**	**95% CI Low**	**95% CI High**	**VIF**
Intercept	-14.54	1	0.18	-14.96	-14.12	
A-Contact Angle	-0.37	1	0.14	-0.70	-0.035	1.00
B-Interfacial Energy	-1.01	1	0.14	-1.34	-0.68	1.00
AB	-0.81	1	0.20	-1.28	-0.35	1.00
A^2	0.15	1	0.15	-0.20	0.51	1.02
B^2	1.27	1	0.15	0.92	1.63	1.02

Surface energy of adhesion model equation for uninfected white blood is given as:

$$F^{adh} = -14.54-0.37A-1.01B -0.81AB+0.15A^2+1.27B^2 \quad (4.2)$$

The ANOVA indicates the equation and actual relationship between the response and significant variables represented by the equation 4.2 are accurate. The R^2 value of 0.9551 indicates a good measure that outcomes are likely to be predicted well by the developed models. The contour and the surface plot on Fig 4.8 and 4.9 also reveal graphically the interaction between the independent variable and the response.

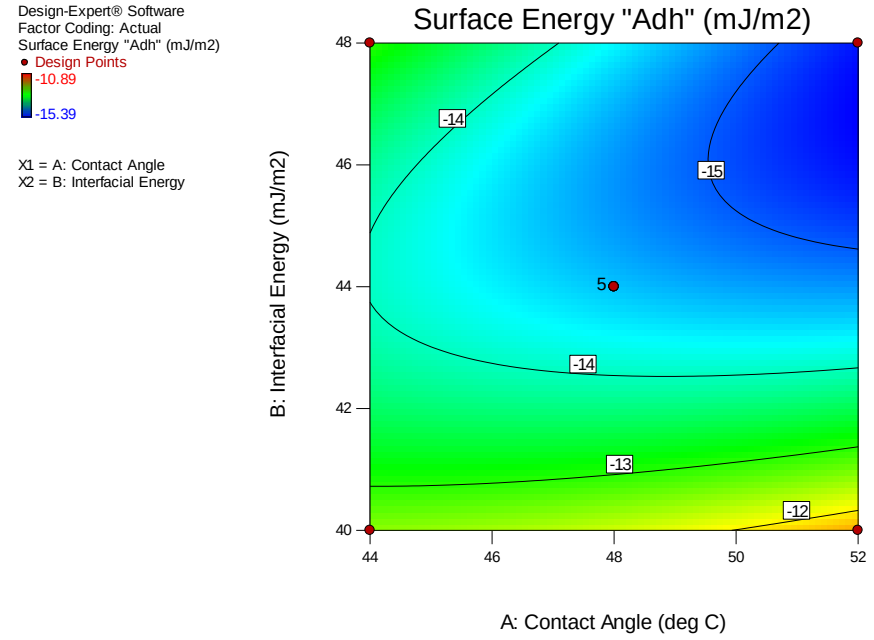

Fig 4.8: Contour Plots of Uninfected WBC for Surface Energy of Adhesion

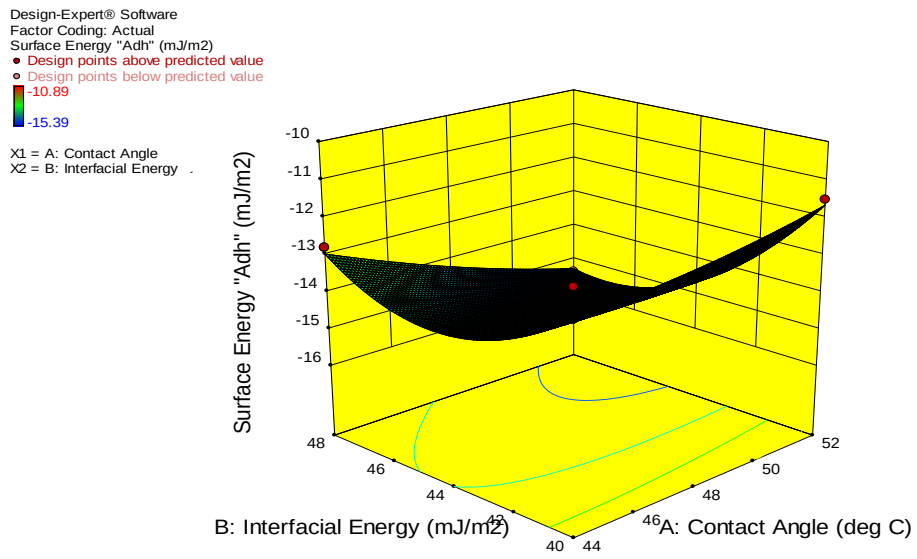

Fig 4.9: 3-D surface Plots of Uninfected WBC for Surface Energy of Adhesion

Table 4.15(a-g) is a response analysis table obtained using Neumann model for infected white blood cell treated with IFN(Appendix B14).The 2FI linear model is suggested and focus is on the model maximizing the "Adjusted R-Squared" and the "Predicted R-Squared. The Model F-value of 14.87 implies the model is significant. There is only a 0.03% chance that an F-value this large could occur due to noise. Values of "Prob > F" less than 0.0500 indicate model terms are significant.

The ANOVA indicates the equation and actual relationship between the response and significant variables represented by the equation 4.3 are accurate. The R^2 value of 0.9128indicates a good measure that outcomes are likely to be predicted well by the developed models. The contour and the surface plot on Fig 4.10 and 4.11 also reveal graphically the interaction between the independent variable and the response

Table 4.15a: Response Summary for IFN Treated

Source	Sequential p-value	Lack of Fit p-value	Adjusted R-Squared	Predicted R-Squared
Linear	0.0035	0.2215	0.6137	0.3648
2FI	0.0008	0.9648	0.8837	0.8562
Quadratic	0.9522	0.8610	0.8525	0.7914
Cubic	0.9084	0.4966	0.8013	0.2379

Table 4.15b: Sequential Model Sum of Square

Source	Sum of Squares	Df	Mean Square	F Value	p-value Prob > F
Mean vs Total	4911.71	1	4911.71		
Linear vs Mean	52.69	2	26.35	10.53	0.0035
2FI vs Linear	18.23	1	18.23	24.21	0.0008
Quadratic vs 2FI	0.094	2	0.047	0.049	0.9522
Cubic vs Quadratic	0.25	2	0.13	0.098	0.0984
Residual	6.43	5	1.29		
Total	4989.42	13	383.80		

Table 4.15c: Lack of Fit Test

Source	Sum of Squares	D*f*	Mean square	F-value	P-Value Prob>F
Linear	19.37	6	3.23	2.29	0.2215
2FI	1.13	5	0.23	0.16	0.9648
Quadratic	1.04	3	0.35	0.25	0.8610
Cubic	0.79	1	0.79	0.56	0.4966
Pure Error	5.65	4	1.41		

Table 4.15d: Model Statistics Summary

Source	Std. Dev.	R-Squared	Adjusted R-Squared	Predicted R-Squared	PRESS
Linear	1.58	0.6781	0.6137	0.3648	49.36
2FI	0.87	0.9128	0.8837	0.8562	11.17
Quadratic	0.98	0.9140	0.8525	0.7914	16.21
Cubic	1.13	0.9172	0.8013	0.2379	59.22

Table 4.15e: ANOVA for Surface Response 2FI Model

Source	Sum of Squares	Df	Mean Square	F Value	p-value Prob > F	
Model	71.02	5	14.20	14.87	0.0013	Significant
A-Contact Angle	2.60	1	2.60	2.72	0.1432	
B-Interfacial Energy	50.10	1	50.10	52.46	0.0002	
AB	18.23	1	18.23	19.09	0.0033	
A^2	0.085	1	0.085	0.089	0.7744	
B^2	3.405E-003	1	3.40E-003	3.56E-003	0.9541	
Residual	6.68	7	0.95			
Lack of Fit	1.04	3	0.35	0.25	0.8610	not significant
Pure Error	5.65	4	1.41			
Cor Total	77.71	12				

Table 4.15f: 2FI Model Summary

Std. Dev.	0.98
Mean	-19.44
C.V. %	5.03
PRESS	16.21
R-Squared	0.9128
Adj R-Squared	0.8837
Pred R-Squared	0.8562
Adeq Precision	13.970

Table 4.15g: Surface Energy of Adhesion Model Equation

Factor	**Coefficient Estimate**	**Df**	**Standard Error**	**95% CI Low**	**95% CI High**	**VIF**
Intercept	-19.49	1	0.44	-20.53	-18.46	
A-Contact Angle	0.57	1	0.35	-0.25	1.39	1.00
B-Interfacial Energy	-2.50	1	0.35	-3.32	-1.69	1.00
AB	-2.14	1	0.49	-3.29	-0.98	1.00
A^2	0.11	1	0.37	-0.77	0.99	1.02
B^2	-0.022	1	0.37	-0.90	0.85	1.02

Surface energy of adhesion model equation for white blood treated with IFN is given as:

$$F^{adh} = -19.49 - 0.57A - 2.50B - 2.14AB + 0.11A^2 - 0.22B^2 \quad (4.3)$$

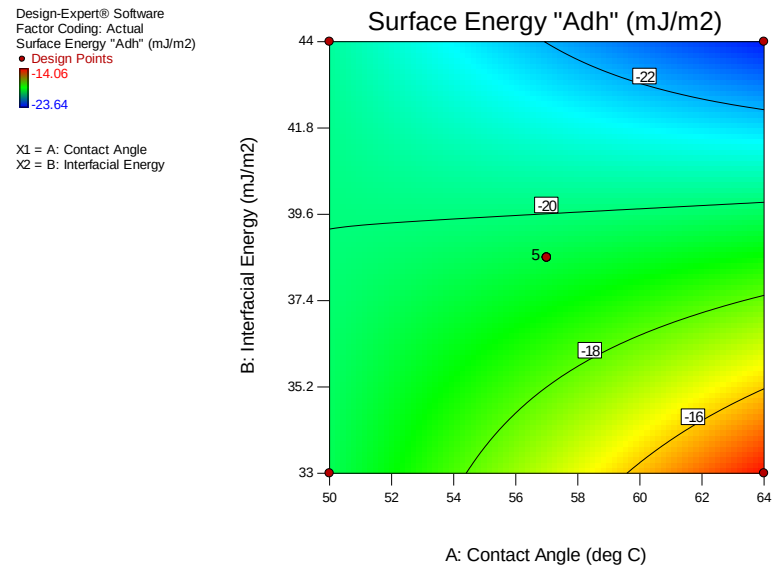

Fig 4.10: Contour Plots of infected WBC treated with IFN for Surface Energy of Adhesion

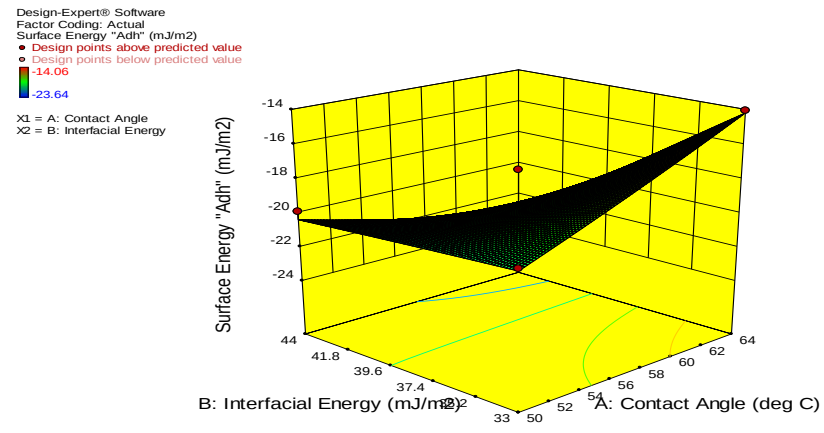

Fig 4.11: 3-D Surface Plots of infected WBC treated with IFN for Surface Energy of Adhesion.

Table 4.16(a-g) is a response analysis table obtained using Neumann model for infected white blood cell treated with RBV(Appendix B14) and Fig 4.8 and 4.9 displayed the contour and surface plots. The quadratic model is suggested and focus is on the model maximizing the "Adjusted R-Squared" and the "Predicted R-Squared. The Model F-value of 34.89 implies the model is significant. There is only a 0.01% chance that an F-value this large could occur due to noise. Values of "Prob > F" less than 0.0500 indicate model terms are significant.

The ANOVA indicates the equation and actual relationship between the response and significant variables represented by the equation 4.4 are accurate. The R^2 value of

0.9614 indicates a good measure that outcomes are likely to be predicted well by the developed models. The contour and the surface plot on Fig 4.12 and 4.13 also reveal graphically the interaction between the independent variable and the response surface.

Table 4.16a: Response Summary for RBV Treated

Source	Sequential p-value	Lack of Fit p-value	Adjusted R-Squared	Predicted R-Squared
Linear	0.3110	0.0017	0.0500	-0.3752
2FI	0.3215	0.0016	0.0594	-0.3499
Quadratic	< 0.0001	0.2002	0.9339	0.8005
Cubic	0.9275	0.0560	0.9102	-0.5541

Table 4.16b: Sequential Model Sum of Square

Source	Sum of Squares	Df	Mean Square	F Value	p-value Prob > F
Mean vs Total	4147.81	1	4147.81		
Linear vs Mean	8.22	2	4.11	1.32	0.3110
2FI vs Linear	3.40	1	3.40	1.10	0.3215
Quadratic vs 2FI	26.32	2	13.16	60.50	< 0.0001
Cubic vs Quadratic	0.045	2	0.023	0.076	0.9275
Residual	1.48	5	1.30		
Total	4187.27	13	322.10		

Table 4.16c: Lack of Fit Test

Source	Sum of Squares	df	Mean Square	F Value	p-value Prob > F
Linear	30.71	6	5.12	38.49	0.0017
2FI	27.31	5	5.46	41.07	0.0016
Quadratic	0.99	3	0.33	2.48	0.2002
Cubic	0.95	1	0.95	7.11	0.0560
Pure Error	0.53	4	0.13		

Table 4.16d: Model Summary Statistics

Source	Std. Dev.	R-Squared	Adjusted R-Squared	Predicted R-Squared	PRESS
Linear	1.77	0.2083	0.0500	-0.3752	54.27
2FI	1.76	0.2946	0.0594	-0.3499	53.27
Quadratic	0.47	0.9614	0.9339	0.8005	7.87
Cubic	0.54	0.9626	0.9102	-0.5541	61.33

Table 4.16e: Quadratic Model Summary

Std. Dev.	0.47
Mean	-17.86
C.V. %	2.61
PRESS	7.87
R-Squared	0.9614
Adj R-Squared	0.9339
Pred R-Squared	0.8005
Adeq Precision	15.803

Table 4.16f:ANOVA for Response Surface Quadratic Model

Source	**Sum of Squares**	**D*f***	**Mean Square**	**F Value**	**p-value Prob > F**	
Model	37.94	5	*7.59*	34.89	< 0.0001	Significant
A-Contact Angle	*5.93*	*1*	*5.93*	*27.26*	*0.0012*	
B-Interfacial Energy	*2.29*	*1*	*2.29*	*10.54*	*0.0141*	
AB	*3.40*	*1*	*3.40*	*15.65*	*0.0055*	
A^2	*23.79*	*1*	*23.79*	*109.37*	< *0.0001*	
B^2	*4.90*	*1*	*4.90*	*22.52*	*0.0021*	
Residual	1.52	7	0.22			
Lack of Fit	*0.99*	*3*	*0.33*	*2.48*	*0.2002*	*not significant*
Pure Error	*0.53*	*4*	*0.13*			
Cor Total	39.46	12				

Table 4.16g: Surface Energy of Adhesion Model Equation

Factor	**Coefficient Estimate**	**D*f***	**Standard Error**	**95% CI Low**	**95% CI High**	**VIF**
Intercept	-16.21	1	0.21	-16.70	-15.71	
A-Contact Angle	-0.86	1	0.16	-1.25	-0.47	1.00
B-Interfacial Energy	-0.54	1	0.16	-0.93	-0.15	1.00
AB	-0.92	1	0.23	-1.47	-0.37	1.00
A^2	-1.85	1	0.18	-2.27	-1.43	1.02
B^2	-0.84	1	0.18	-1.26	-0.42	1.02

Surface energy of adhesion model equation for white blood treated with RBV is given as:

$$F^{adh} = -16.21 - 0.86A - 0.54B - 0.92AB - 1.85A^2 - 0.84B^2 \quad (4.4)$$

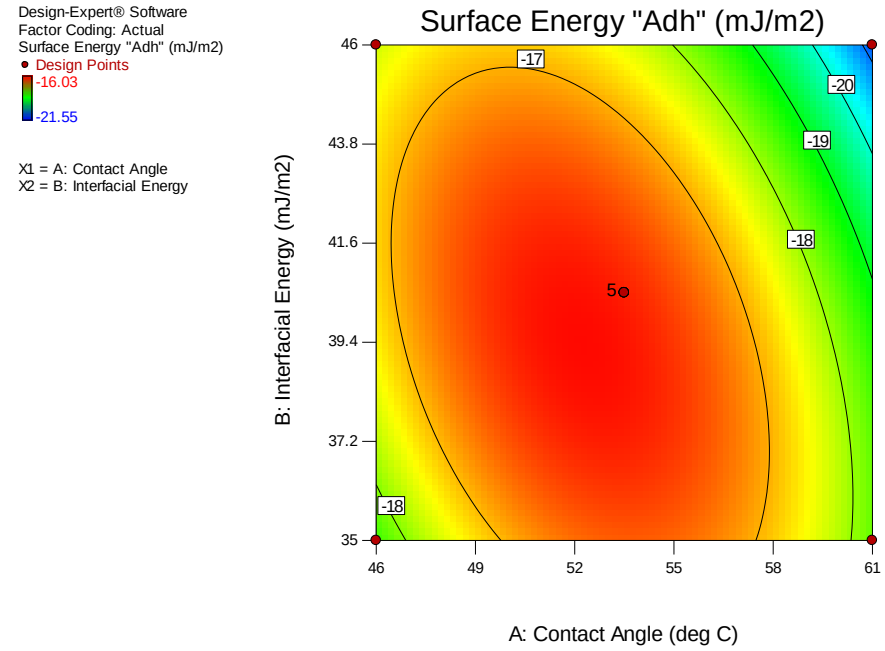

Fig.4.12: Contour Plots for Infected WBC treated with RBVfor Surface Energy of Adhesion

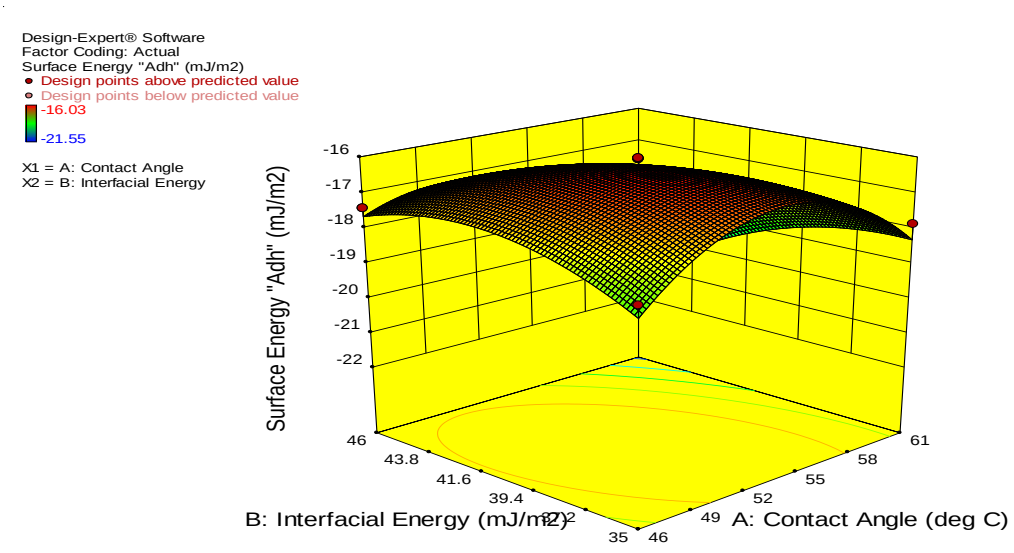

Fig.4.13: 3-D Surface Plots for Infected WBC treated with RBVfor Surface Energy of Adhesion

Table 4.17(a-g) is a response analysis table obtained using Neumann model for infected white blood cell treated with ATR(Appendix B26). The quadratic model is suggested and focus is on the model maximizing the "Adjusted R-Squared" and the "Predicted R-Squared. The Model F-value of 4.23 implies the model is significant. There is only a 0.04% chance that an F-value this large could occur due to noise. Values of "Prob > F" less than 0.0500 indicate model terms are significant.

The ANOVA indicates the equation and actual relationship between the response and significant variables represented by the equation 4.5 are accurate. The R^2 value of 0.9514 indicates a good measure that outcomes are likely to be predicted well by the developed models. The contourand the surface plot on Fig 4.14 and 4.15 also reveal graphically the interaction between the independent variable and the response surface.

Table 4.17a: Response Summary for Surface Energy of Adhesion with ATR Treatment.

Source	**Sequential p-value**	**Lack of Fit p-value**	**Adjusted R-Squared**	**Predicted R-Squared**
Linear	0.0817	0.4430	0.2728	0.0294
2FI	0.5436	0.3920	0.2263	-0.1435
Quadratic	0.0515	0.8816	0.9738	0.9401
Cubic	0.6925	0.9275	0.4848	0.6332

Table 4.17b: Sequential Model Sum of Squares

Source	Sum of Squares	Df	Mean Square	F Value	p-value Prob > F
Mean vs Total	4872.14	1	4872.14		
Linear vs Mean	13.41	2	6.70	3.25	0.0817
2FI vs Linear	0.87	1	0.87	0.40	0.5436
Quadratic vs 2FI	11.29	2	5.64	4.67	0.0515
Cubic vs Quadratic	1.16	2	0.58	0.40	0.6925
Residual	7.31	5	1.46		
Total	4906.17	13	377.40		

Table 4.17c: Lack of Fit Tests

Source	Sum of Squares	df	Mean Square	F Value	p-value Prob > F
Linear	13.34	6	2.22	1.22	0.4430
2FI	12.46	5	2.49	1.37	0.3920
Quadratic	1.17	3	0.39	0.21	0.8816
Cubic	0.017	1	0.017	9.391E-003	0.9275
Pure Error	7.29	4	1.82	1.22	

Table 4.17d: Model Summary Statistics

Source	Std. Dev.	R-Squared	Adjusted R-Squared	Predicted R-Squared	PRESS
Linear	1.44	0.3940	0.2728	0.0294	33.04
2FI	1.48	0.4197	0.2263	-0.1435	38.92
Quadratic	1.10	0.9514	0.9738	0.9401	19.74
Cubic	1.21	0.7853	0.4848	0.6332	12.48

Table 4.17e:Quadratic Model Summary

Std. Dev.	1.10
Mean	-19.36
C.V. %	5.68
PRESS	19.74
R-Squared	0.9514
Adj R-Squared	0.9738
Pred R-Squared	0.9401
Adeq Precision	5.959

Table 4.17f: Analysis of Variance (ANOVA) for Response Surface Quadratic Model for ATR

Source	**Sum of Squares**	**D*f***	**Mean Square**	**F-Value**	**P-Value Prob > F**	
Model	25.57	5	5.11	4.23	0.00431	Significant
A-Contact Angle	*13.37*	*1*	*13.37*	*11.06*	*0.0127*	
B-Interfacial Energy	*0.041*	*1*	*0.041*	*0.034*	*0.8583*	
AB	*0.87*	*1*	*0.87*	*0.72*	*0.4232*	
A^2	*11.10*	*1*	*11.10*	*9.18*	*0.0191*	
B^2	*0.75*	*1*	*0.75*	*0.62*	*0.4570*	
Residual	8.46	7	1.21			
Lack of Fit	*1.17*	*3*	*0.39*	*0.21*	*0.8816*	*not significant*
Pure Error	*7.29*	*4*	*1.82*			
Cor Total	34.03	12				

Table 4.17g: Surface Energy of Adhesion Model Equation for Infected White Blood Treated with ATR

Factor	Coefficient Estimate	*Df*	Standard Error	95% CI Low	95% CI High	VIF
Intercept	-18.38	1	0.49	-19.54	-17.22	
A-Contact Angle	-1.29	1	0.39	-2.21	-0.37	1.00
B-Interfacial Energy	0.072	1	0.39	-0.85	0.99	1.00
AB	0.47	1	0.55	-0.83	1.77	1.00
A^2	-1.26	1	0.42	-2.25	-0.28	1.02
B^2	-0.33	1	0.42	-1.31	0.66	1.02

Surface energy of adhesion model equation for white blood treated with ATR is given as:

$$F^{adh} = -18.38-1.29A+0.072B+0.47AB-1.26A^2-0.33B^2 (4.5)$$

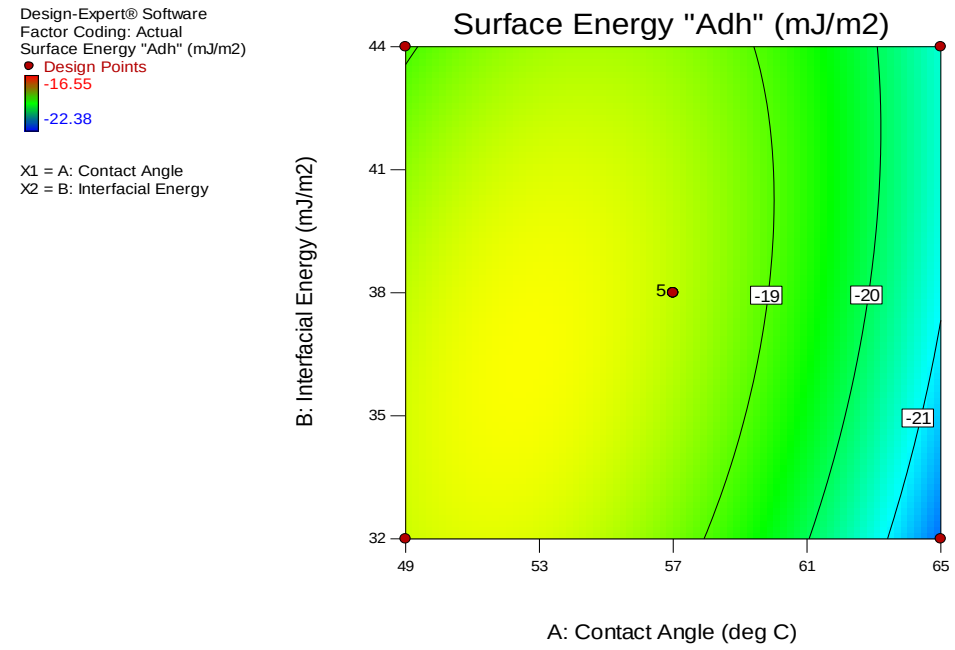

Fig 4.14: Contour Plots of ATR Treated WBCfor Adhesion Energy

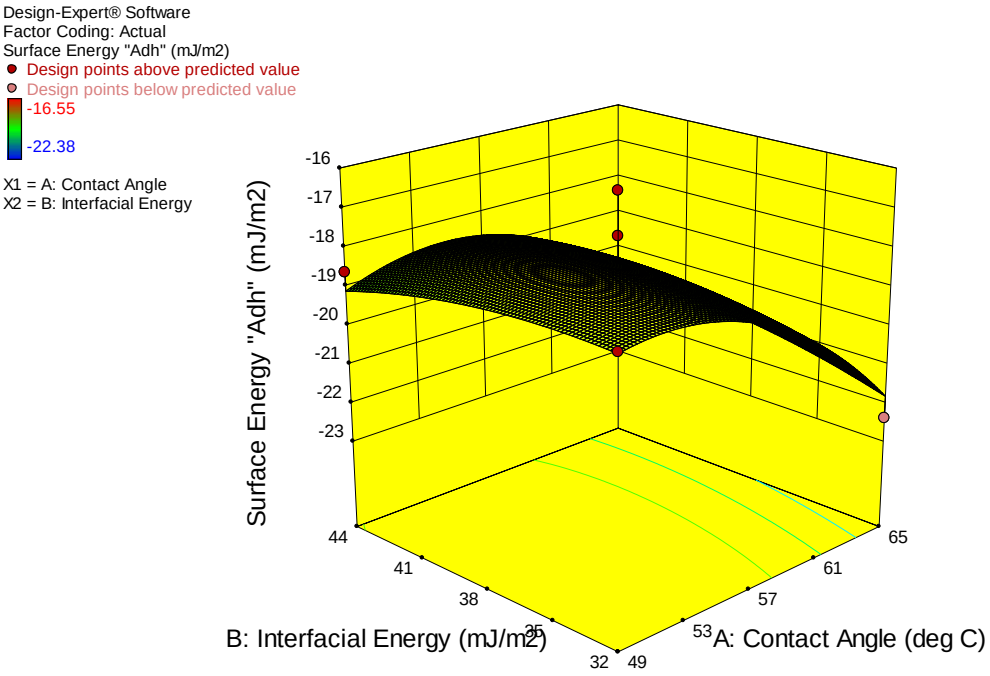

Fig 4.15: 3-D Surface Plots for ATR TreatedWBC for Adhesion Energy

Table 4.18(a-g) is a response analysis table obtained using Neumann model for infected white blood cell treated with ELT(Appendix B26). The quadratic model is suggested and focus is on the model maximizing the "Adjusted R-Squared" and the "Predicted R-Squared. The Model F-value of 9.25 implies the model is significant. There is only a 0.03% chance that an F-value this large could occur due to noise. Values of "Prob > F" less than 0.0500 indicate model terms are significant.

The ANOVA indicates the equation and actual relationship between the response and significant variables represented by the equation 4.6 are accurate. The R^2 value of 0.8686 indicates a good measure that outcomes are likely to be predicted well by the developed models. The contour and the surface plot on Fig 4.16 and 4.17 also reveal graphically the interaction between the independent variable and the response surface.

Table 4.18a: Response Summary for Surface Energy of Adhesion with ELT Treatment

Source	Sequential p-value	Lack of Fit p-value	Adjusted R-Squared	Predicted R-Squared
Linear	0.2216	0.0515	0.1123	-0.5199
2FI	0.1390	0.0630	0.2370	-0.2502
Quadratic	0.0058	0.4609	0.7747	0.8727
Cubic	0.2752	0.6277	0.8117	0.5623

Table 4.18b: Sequential Model Sum of Squares

Source	Sum of Squares	Df	Mean Square	F Value	p-value Prob > F
Mean vs Total	4333.46	1	4333.46		
Linear vs Mean	11.75	2	5.87	1.76	0.2216
2FI vs Linear	7.56	1	7.56	2.63	0.1390
Quadratic vs 2FI	19.90	2	9.95	11.74	0.0058
Cubic vs Quadratic	2.39	2	1.20	1.69	0.2752
Residual	3.54	5	0.71		
Total	4378.61	13	336.82		

Table 4.18c:Lack of Fit Tests

Source	Sum of Squares	df	Mean Square	F Value	p-value Prob > F
Linear	30.08	6	5.01	6.05	0.0515
2FI	22.52	5	4.50	5.44	0.0630
Quadratic	2.62	3	0.87	1.05	0.4609
Cubic	0.23	1	0.23	0.28	0.6277
Pure Error	3.31	4	0.83		

Table 4.18d:Model Summary Statistics

Source	Std. Dev.	R-Squared	Adjusted R-Squared	Predicted R-Squared	PRESS
Linear	1.83	0.2602	0.1123	-0.5199	68.61
2FI	1.69	0.4277	0.2370	-0.2502	56.44
Quadratic	0.92	0.8686	0.7747	0.8727	23.81
Cubic	0.84	0.9216	0.8117	0.5623	19.76

Table 4.18e:Quadratic Model Summary

Std. Dev.	0.92
Mean	-18.26
C.V. %	5.04
PRESS	23.81
R-Squared	0.8686
Adj R-Squared	0.7747
Pred R-Squared	0.8727
Adeq Precision	10.517

Table 4.18f: ANOVA for Response Surface Quadratic Model for ELT

Source	**Sum of Squares**	**D*f***	**Mean Square**	**F-Value**	**P-Value Prob > F**	
Model	39.21	5	*7.84*	9.25	0.0034	Significant
A-Contact Angle	*5.60*	*1*	*5.60*	*6.60*	*0.0370*	
B-Interfacial Energy	*6.15*	*1*	*6.15*	*7.26*	*0.0309*	
AB	*7.56*	*1*	*7.56*	*8.92*	*0.0203*	
A^2	*15.69*	*1*	*15.69*	*18.51*	*0.0036*	
B^2	*2.31*	*1*	*2.31*	*2.72*	*0.1430*	
Residual	5.93	7	0.85			
Lack of Fit	*2.62*	*3*	*0.87*	*1.05*	*0.4609*	*not significant*
Pure Error	*3.31*	*4*	*0.83*			
Cor Total	45.14	12				

Table 4.18g: Energy of Adhesion Model Equation for WBC Treated with ELT

Factor	**Coefficient Estimate**	**D*f***	**Standard Error**	**95% CI Low**	**95% CI High**	**VIF**
Intercept	-17.69	1	0.41	-18.66	-16.71	
A-Contact Angle	-0.84	1	0.33	-1.61	-0.067	1.00
B-Interfacial Energy	-0.88	1	0.33	-1.65	-0.11	1.00
AB	-1.37	1	0.46	-2.46	-0.29	1.00
A^2	-1.50	1	0.35	-2.33	-0.68	1.02
B^2	0.58	1	0.35	-0.25	1.40	1.02

Surface energy of adhesion model equation for white blood treated with ELT is:

$$F^{adh} = -17.69-0.84A-0.88B-1.37AB-1.50A^2+0.58B^2 \quad (4.6)$$

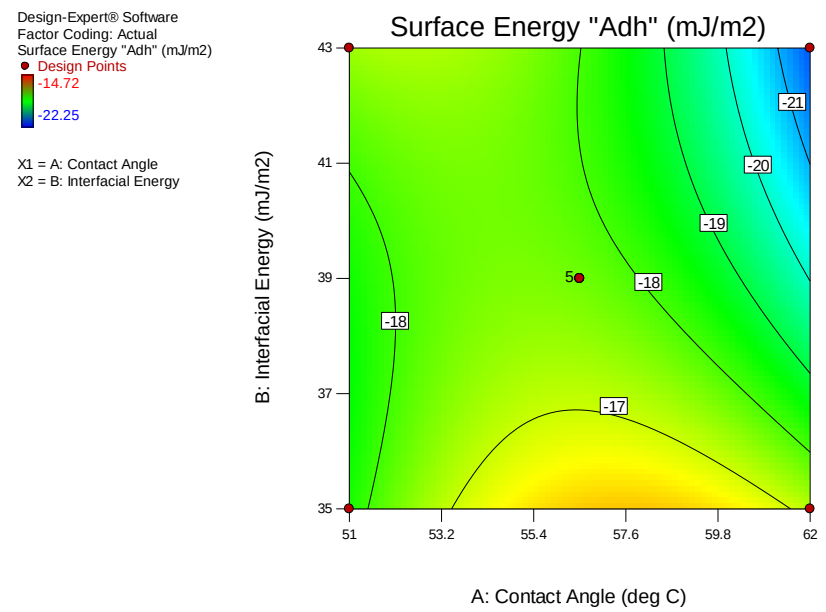

Fig.4.16: Contour plots of ELT Treated WBC for Energy of Adhesion

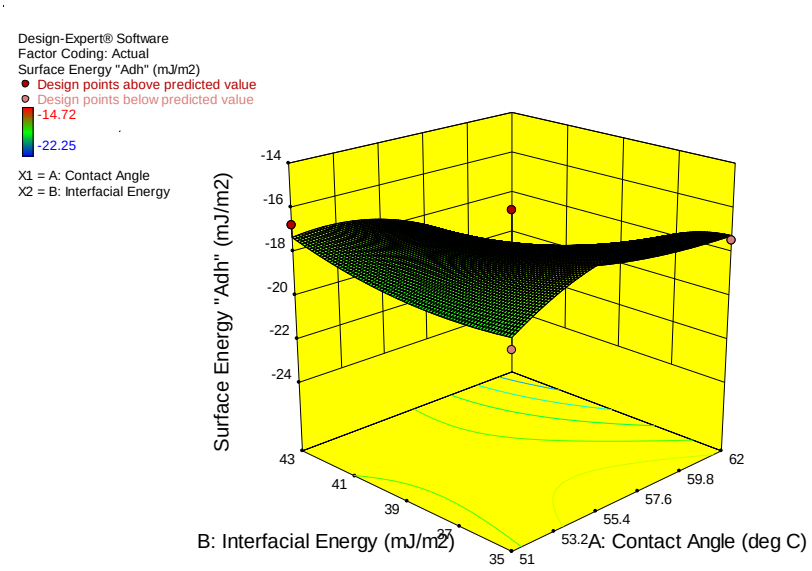

Fig.4.17: 3-DSurface Plots of ELT Treated WBC for Energy of Adhesion

Table 4.19(a-g) is a response analysis table obtained using Neumann model for infected white blood cell treated with AM (Appendix B38). The quadratic model is suggested and focus is on the model maximizing the "Adjusted R-Squared" and the "Predicted R-Squared. The Model F-value of 29.28 implies the model is significant.

There is only a 0.01% chance that an F-value this large could occur due to noise. Values of "Prob > F" less than 0.0500 indicate model terms are significant.

The ANOVA indicates the equation and actual relationship between the response and significant variables represented by the equation 4.7 are accurate. The R^2 value of 0.9522 indicates a good measure that outcomes are likely to be predicted well by the developed models. The contour and the surface plot on Fig 4.18 and 4.19 also reveal graphically the interaction between the independent variable and the response surface.

Table 4.19a: Response Summary for Surface energy of Adhesion Treated with AM

Source	Sequential p-value	Lack of Fit p-value	Adjusted R-Squared	Predicted R-Squared
Linear	0.5797	0.0050	-0.0760	-0.4684
2FI	0.8015	0.0037	-0.1867	-1.2187
Quadratic	0.0001	0.5038	0.9232	0.8278
Cubic	0.9337	0.1817	0.8953	-0.1424

Table 4.19b: Sequential Model Sum of Squares

Source	Sum of Squares	Df	Mean Square	F Value	p-value Prob > F
Mean vs Total	5361.23	1	5361.23		
Linear vs Mean	6.18	2	3.09	0.58	0.5797
2FI vs Linear	0.40	1	0.40	0.067	0.8015
Quadratic vs 2FI	50.58	2	25.29	66.01	< 0.0001
Cubic vs Quadratic	0.073	2	0.036	0.070	0.9337
Residual	2.61	5	0.52		
Total	5421.07	13	417.01		

Table 4.19c:Lack of Fit Tests

Source	Sum of Squares	df	Mean Square	F Value	p-value Prob > F
Linear	52.08	6	8.68	21.98	0.0050
2FI	51.68	5	10.34	26.17	0.0037
Quadratic	1.10	3	0.37	0.93	0.5038
Cubic	1.03	1	1.03	2.61	0.1817
Pure Error	1.58	4	0.39		

Table 4.19d:Model Summary Statistics

Source	Std. Dev.	R-Squared	Adjusted R-Squared	Predicted R-Squared	PRESS
Linear	2.32	0.1033	-0.0760	-0.4684	87.87
2FI	2.43	0.1099	-0.1867	-1.2187	132.77
Quadratic	0.62	0.9552	0.9232	0.8278	10.31
Cubic	0.72	0.9564	0.8953	-0.1424	68.36

Table 4.19e: Quadratic Model Summary

Std. Dev.	0.62
Mean	-20.31
C.V. %	3.05
PRESS	10.31
R-Squared	0.9552
Adj R-Squared	0.9232
Pred R-Squared	0.8278
Adeq Precision	13.783

Table 4.19f: ANOVA for Response Surface Quadratic Model for AM

Source	**Sum of Squares**	**D*f***	**Mean Square**	**F-Value**	**P-Value Prob > F**	
Model	57.16	5	11.43	29.84	0.0001	Significant
A-Contact Angle	*2.71*	*1*	*2.71*	*7.07*	*0.0325*	
B-Interfacial Energy	*3.47*	*1*	*3.47*	*9.06*	*0.0197*	
AB	*0.40*	*1*	*0.40*	*1.04*	*0.3426*	
A^2	*43.01*	*1*	*43.01*	*112.25*	*0.0001*	
B^2	*12.85*	*1*	*12.85*	*33.53*	*0.0007*	
Residual	2.68	7	0.38			
Lack of Fit	*1.10*	*3*	*0.37*	*0.93*	*0.5038*	*not significant*
Pure Error	*1.58*	*4*	*0.39*			
Cor Total	59.84	12				

Table 4.19g: Surface Energy of Adhesion Model Equation for Infected WBC Treated with AM

Factor	**Coefficient Estimate**	**D*f***	**Standard Error**	**95% CI Low**	**95% CI High**	**VIF**
Intercept	-22.67	1	0.28	-23.33	-22.02	
A-Contact Angle	-0.58	1	0.22	-1.10	-0.065	1.00
B-Interfacial Energy	-0.66	1	0.22	-1.18	-0.14	1.00
AB	-0.32	1	0.31	-1.05	0.42	1.00
A^2	2.49	1	0.23	1.93	3.04	1.02
B^2	1.36	1	0.23	0.80	1.91	1.02

Surface energy of adhesion model equation for white blood treated with AM is:

$$F^{adh} = -22.67-0.58A-0.66B-0.32AB+2.49A^2+1.36B^2 \quad (4.7)$$

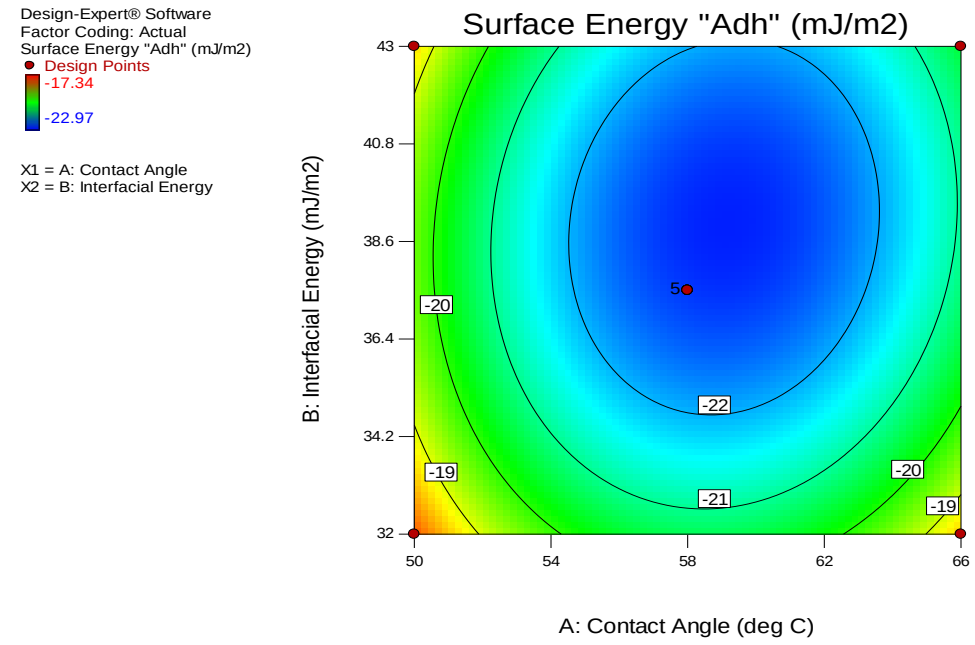

Fig 4.18: Contour Plots of AM Treated WBC for Energy of Adhesion

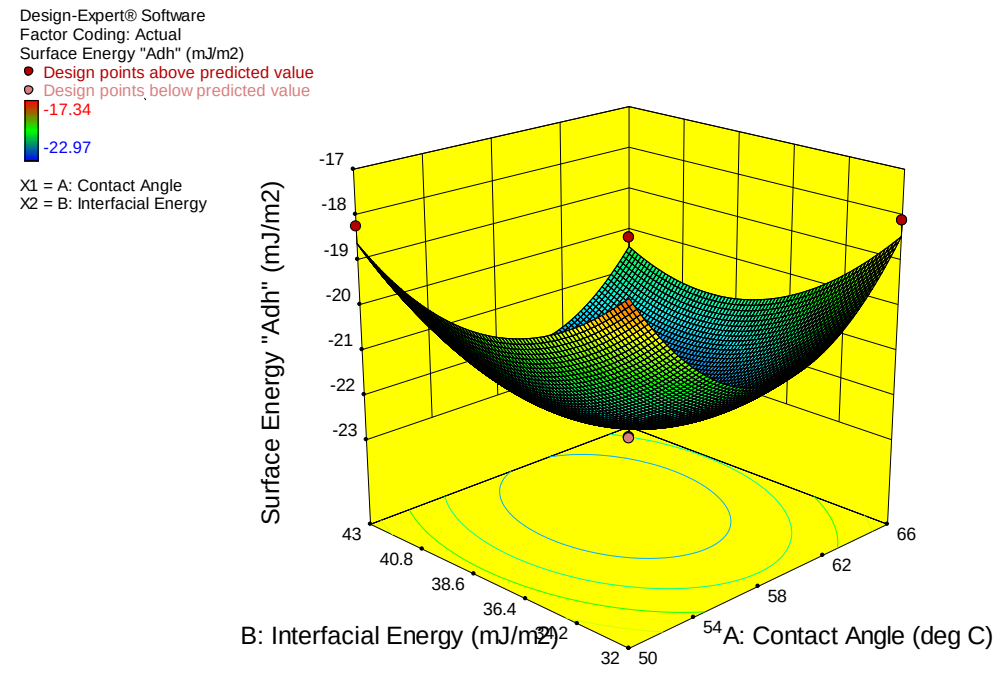

Fig 4.19: 3-D Surface Plots of AM Treated WBC for Energy of Adhesion

Table 4.20(a-g) is a response analysis table obtained using Neumann model for infected white blood cell treated with VA (Appendix B38). The quadratic model is suggested and focus is on the model maximizing the "Adjusted R-Squared" and the "Predicted R-Squared. The Model F-value of 62.67 implies the model is significant. There is only a 0.01% chance that an F-value this large could occur due to noise. Values of "Prob > F" less than 0.0500 indicate model terms are significant.

The ANOVA indicates the equation and actual relationship between the response and significant variables represented by the equation 4.8 are accurate. The R^2 value of 0.9782 indicates a good measure that outcomes are likely to be predicted well by the developed models. The contour and the surface plot on Fig 4.20 and 4.21 also reveal graphically the interaction between the independent variable and the response surface.

Table 4.20a: Response Summary for Surface energy of Adhesion Treated with VA

Source	Sequential p-value	Lack of Fit p-value	Adjusted R-Squared	Predicted R-Squared
Linear	0.0572	0.0050	0.3230	-0.0174
2FI	0.4244	0.0042	0.3021	-0.1518
Quadratic	< 0.0001	0.7454	0.9625	0.9365
Cubic	0.5000	1.0000	0.9603	0.9741

Table 4.20b: Sequential Model Sum of Squares

Source	Sum of Squares	Df	Mean Square	F Value	p-value Prob > F
Mean vs Total	3724.77	1	3724.77		
Linear vs Mean	19.22	2	9.61	3.86	0.0572
2FI vs Linear	1.80	1	1.80	0.70	0.4244
Quadratic vs 2FI	22.12	2	11.06	80.35	< 0.0001
Cubic vs Quadratic	0.23	2	0.12	0.80	0.5000
Residual	0.73	5	0.15		
Total	3768.86	13	289.91		

Table 4.20c:Lack of Fit Tests

Source	Sum of Squares	df	Mean Square	F Value	p-value Prob > F
Linear	24.15	6	4.02	22.05	0.0050
2FI	22.35	5	4.47	24.49	0.0042
Quadratic	0.23	3	0.078	0.43	0.7454
Cubic	0.000	1	0.000	0.000	1.0000
Pure Error	0.73	4	0.18		

Table 4.20d:Model Summary Statistics

Source	Std. Dev.	R-Squared	Adjusted R-Squared	Predicted R-Squared	PRESS
Linear	1.58	0.4358	0.3230	-0.0174	44.86
2FI	1.60	0.4766	0.3021	-0.1518	50.79
Quadratic	0.37	0.9782	0.9625	0.9365	2.80
Cubic	0.38	0.9834	0.9603	0.9741	1.14

Table 4.20e:Quadratic Model Summary

Std. Dev.	0.37
Mean	-16.93
C.V. %	2.19
PRESS	2.80
R-Squared	0.9782
Adj R-Squared	0.9625
Pred R-Squared	0.9365
Adeq Precision	23.859

Table 4.20f: ANOVA for Response Surface Quadratic Model for VA

Source	**Sum of Squares**	**D*f***	**Mean Square**	**F-Value**	**P-Value Prob > F**	
Model	43.13	5	8.63	62.67	< 0.0001	Significant
A-Contact Angle	*13.31*	*1*	*13.31*	*96.71*	*< 0.0001*	
B-Interfacial Energy	*5.91*	*1*	*5.91*	*42.92*	*0.0003*	
AB	*1.80*	*1*	*1.80*	*13.05*	*0.0086*	
A^2	*21.91*	*1*	*21.91*	*159.16*	*< 0.0001*	
B^2	*1.14*	*1*	*1.14*	*8.27*	*0.0238*	
Residual	0.96	7	0.14			
Lack of Fit	*0.23*	*3*	*0.078*	*0.43*	*0.7454*	*not significant*
Pure Error	*0.73*	*4*	*0.18*			
Cor Total	44.09	12				

Table 4.20g:Energy of Adhesion Model Equation for Infected White Blood Treated with VA

Factor	Coefficient Estimate	*Df*	Standard Error	95% CI Low	95% CI High	VIF
Intercept	-15.59	1	0.17	-15.98	-15.19	
A-Contact Angle	-1.29	1	0.13	-1.60	-0.98	1.00
B-Interfacial Energy	-0.86	1	0.13	-1.17	-0.55	1.00
AB	0.67	1	0.19	0.23	1.11	1.00
A^2	-1.77	1	0.14	-2.11	-1.44	1.02
B^2	-0.40	1	0.14	-0.74	-0.072	1.02

Surface energy of adhesion model equation for white blood treated with VA is:

$$F^{adh} = -15.59-1.29A-0.86B+0.67AB-1.77A^2-0.40B^2 \quad (4.8)$$

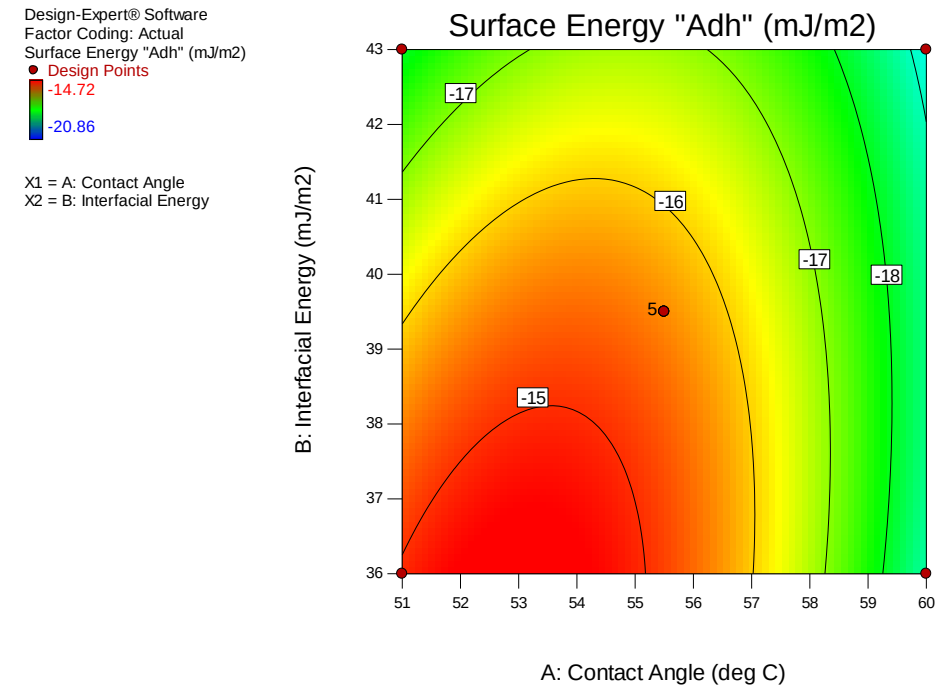

Fig 4.20: Contour Plots of VA Treated WBC for Energy of Adhesion

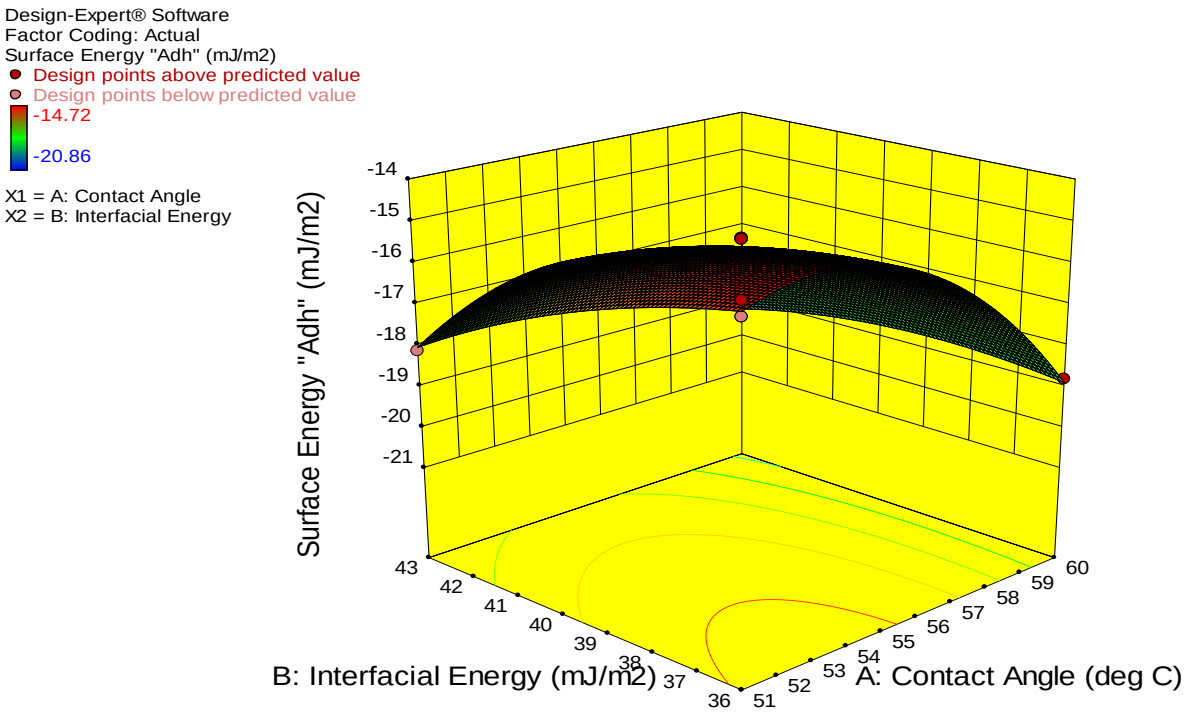

Fig 4.21: Surface Plots of VA Treated WBC for Energy of Adhesion

Table 4.21(a-g) is a response analysis table obtained using Neumann model for infected white blood cell treated with BP (Appendix B50). The quadratic model is suggested and focus is on the model maximizing the "Adjusted R-Squared" and the "Predicted R-Squared. The Model F-value of 35.88 implies the model is significant. There is only a 0.01% chance that an F-value this large could occur due to noise. Values of "Prob > F" less than 0.0500 indicate model terms are significant.

The ANOVA indicates the equation and actual relationship between the response and significant variables represented by the equation 4.9 are accurate. The R^2 value of 0.9624 indicates a good measure that outcomes are likely to be predicted well by the developed models. The contour and the surface plot on Fig 4.22 and 4.23 also reveal graphically the interaction between the independent variable and the response surface.

Table 4.21a: Response Summary for Surface energy of Adhesion Treated with BP

Source	Sequential p-value	Lack of Fit p-value	Adjusted R-Squared	Predicted R-Squared
Linear	0.2078	0.0073	0.1236	-0.4926
2FI	0.0021	0.0457	0.6788	0.5573
Quadratic	0.0015	0.6538	0.9356	0.8775
Cubic	0.9612	0.2650	0.9113	0.2605

Table 4.21b: Sequential Model Sum of Squares

Source	Sum of Squares	Df	Mean Square	F Value	p-value Prob > F
Mean vs Total	4217.40	1	4217.40		
Linear vs Mean	15.21	2	7.61	1.85	0.2078
2FI vs Linear	27.62	1	27.62	18.29	0.0021
Quadratic vs 2FI	11.47	2	5.74	18.95	0.0015
Cubic vs Quadratic	0.33	2	0.017	0.040	0.9612
Residual	2.09	5	0.42		
Total	4273.82	13	328.76		

Table 4.21c:Lack of Fit Tests

Source	Sum of Squares	df	Mean Square	F Value	p-value Prob > F
Linear	39.74	6	6.62	18.03	0.0073
2FI	12.12	5	2.42	6.60	0.0457
Quadratic	0.65	3	0.22	0.59	0.6538
Cubic	0.62	1	0.62	1.68	0.2650
Pure Error	1.47	4	0.37		

Table 4.21d:Model Summary Statistics

Source	Std. Dev.	R-Squared	Adjusted R-Squared	Predicted R-Squared	PRESS
Linear	2.03	0.2697	0.1236	-0.4926	84.21
2FI	1.23	0.7591	0.6788	0.5573	24.98
Quadratic	0.55	0.9624	0.9356	0.8775	6.91
Cubic	0.65	0.9630	0.9113	0.2605	41.72

Table 4.21e:Quadratic Model Summary

Std. Dev.	0.55
Mean	-18.01
C.V. %	3.05
PRESS	6.91
R-Squared	0.9624
Adj R-Squared	0.9356
Pred R-Squared	0.8775
Adeq Precision	21.217

Table 4.21f: ANOVA for Response Surface Quadratic Model for BP

Source	**Sum of Squares**	**D*f***	**Mean Square**	**F-Value**	**P-Value Prob > F**	
Model	54.30	5	10.86	35.88	< 0.0001	Significant
A-Contact Angle	*0.90*	*1*	*0.90*	*2.99*	*0.1275*	
B-Interfacial Energy	*14.31*	*1*	*14.31*	*47.28*	*0.0002*	
AB	*27.62*	*1*	*27.62*	*91.24*	*< 0.0001*	
A^2	*11.19*	*1*	*11.19*	*36.97*	*0.0005*	
B^2	*0.93*	*1*	*0.93*	*3.07*	*0.1230*	
Residual	2.12	7	0.30			
Lack of Fit	*0.65*	*3*	*0.22*	*0.59*	*0.6538*	*not significant*
Pure Error	*1.47*	*4*	*0.37*			
Cor Total	56.42	12				

Table 4.21g: Energy of Adhesion Model Equation for WBC Treated with BP

Factor	**Coefficient Estimate**	**D*f***	**Standard Error**	**95% CI Low**	**95% CI High**	**VIF**
Intercept	-17.01	1	0.25	-17.59	-16.42	
A-Contact Angle	0.34	1	0.19	-0.12	0.80	1.00
B-Interfacial Energy	-1.34	1	0.19	-1.80	-0.88	1.00
AB	-2.63	1	0.28	-3.28	-1.98	1.00
A^2	-1.27	1	0.21	-1.76	-0.78	1.02
B^2	-0.37	1	0.21	-0.86	0.13	1.02

Surface energy of adhesion model equation for white blood treated with BP is:

$$F^{adh} = -17.01 + 0.34A - 1.34B - 2.63AB - 1.27A^2 - 0.37B^2 \quad (4.9)$$

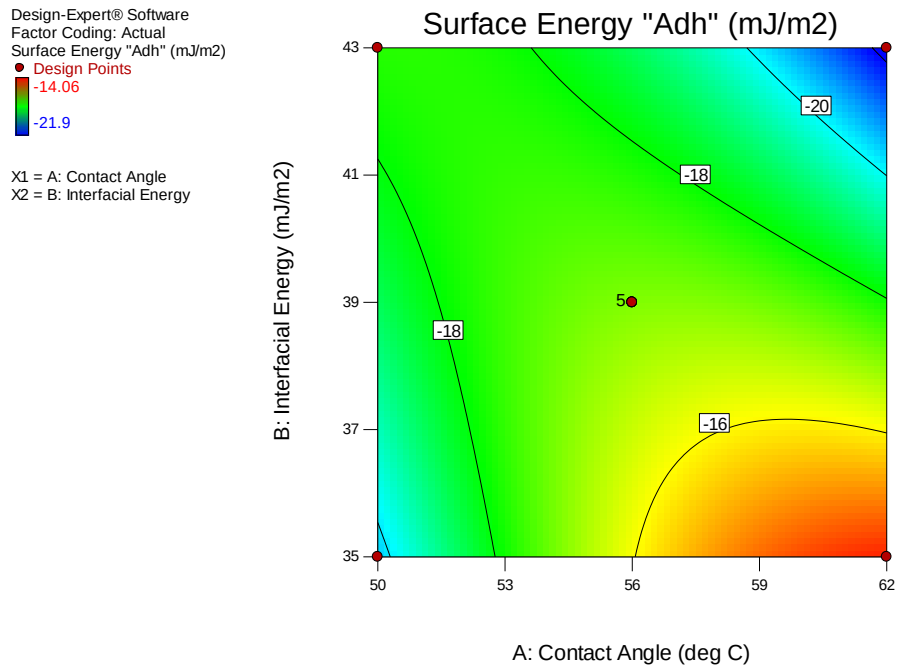

Fig 4.22:Contour plot of BP Treated WBC for Energy of Adhesion

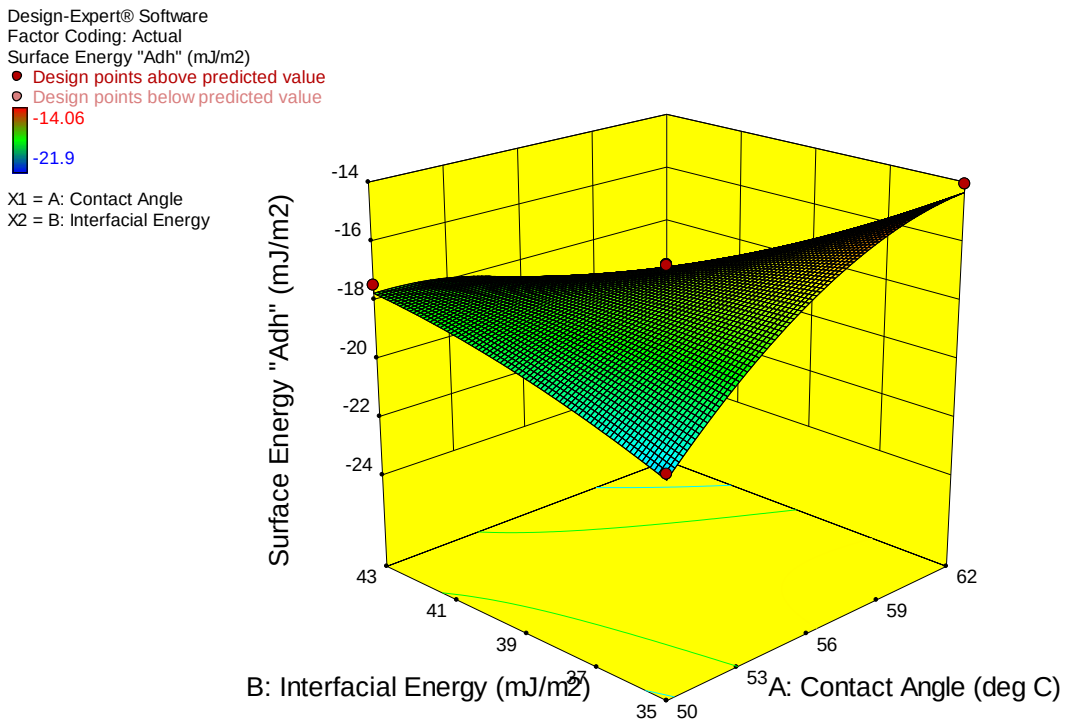

Fig 4.23: Surface Plots of BP Treated WBC for Energy of Adhesion

Table 4.22(a-g) is a response analysis table obtained using Neumann model for infected white blood cell treated with DH (Appendix B50). The quadratic model is suggested and focus is on the model maximizing the "Adjusted R-Squared" and the "Predicted R-Squared. The Model F-value of 54.51 implies the model is significant. There is only a 0.01% chance that an F-value this large could occur due to noise. Values of "Prob > F" less than 0.0500 indicate model terms are significant.

The ANOVA indicates the equation and actual relationship between the response and significant variables represented by the equation 4.10 are accurate. The R^2 value of 0.9750 indicates a good measure that outcomes are likely to be predicted well by the developed models. The contour and the surface plot on Fig 4.24 and 4.25 also reveal graphically the interaction between the independent variable and the response surface.

Table 4.22a: Response Summary for Adhesion Energy Treated with DH

Source	Sequential p-value	Lack of Fit p-value	Adjusted R-Squared	Predicted R-Squared
Linear	0.2304	0.0034	0.1053	-0.2920
2FI	0.8995	0.0025	0.0078	-0.5197
Quadratic	< 0.0001	0.6910	0.9571	0.9219
Cubic	0.9561	0.2933	0.9410	0.5507

Table 4.22b: Sequential Model Sum of Squares

Source	Sum of Squares	Df	Mean Square	F Value	p-value Prob > F
Mean vs Total	4949.10	1	4949.10		
Linear vs Mean	13.80	2	6.90	1.71	0.2304
2FI vs Linear	0.076	1	0.076	0.017	0.8995
Quadratic vs 2FI	39.01	2	19.51	100.51	< 0.0001
Cubic vs Quadratic	0.024	2	0.012	0.045	0.9561
Residual	1.33	5	0.27		
Total	5003.35	13	384.87		

Table 4.22c:Lack of Fit Tests

Source	Sum of Squares	df	Mean Square	F Value	p-value Prob > F
Linear	39.47	6	6.58	26.92	0.0034
2FI	39.39	5	7.88	32.25	0.0025
Quadratic	0.38	3	0.13	0.52	0.6910
Cubic	0.36	1	0.36	1.46	0.2933
Pure Error	0.98	4	0.24		

Table 4.22d:Model Summary Statistics

Source	Std. Dev.	R-Squared	Adjusted R-Squared	Predicted R-Squared	PRESS
Linear	2.01	0.2544	0.1053	-0.2920	70.09
2FI	2.12	0.2558	0.0078	-0.5197	82.45
Quadratic	0.44	0.9750	0.9571	0.9219	4.24
Cubic	0.52	0.9754	0.9410	0.5507	24.38

Table 4.22e:Quadratic Model Summary

Std. Dev.	0.44
Mean	-19.51
C.V. %	2.26
PRESS	4.24
R-Squared	0.9750
Adj R-Squared	0.9571
Pred R-Squared	0.9219
Adeq Precision	21.584

Table 4.22f: ANOVA for Adhesion Energy Response Surface Quadratic Model for DH

Source	**Sum of Squares**	**D*f***	**Mean Square**	**F-Value**	**P-Value Prob > F**	
Model	52.89	5	10.58	54.51	< 0.0001	Significant
A-Contact Angle	*0.89*	*1*	*0.89*	*4.56*	*0.0701*	
B-Interfacial Energy	*12.92*	*1*	*12.92*	*66.56*	*< 0.0001*	
AB	*0.076*	*1*	*0.076*	*0.39*	*0.5523*	
A^2	*3.57*	*1*	*3.57*	*18.40*	*0.0036*	
B^2	*37.81*	*1*	*37.81*	*194.83*	*< 0.0001*	
Residual	1.36	7	0.19			
Lack of Fit	*0.38*	*3*	*0.13*	*0.52*	*0.6910*	*not significant*
Pure Error	*0.98*	*4*	*0.24*			
Cor Total	54.25	12				

Table 4.22g: Surface Energy of Adhesion Model Equation for WBC Treated with DH

Factor	Coefficient Estimate	Df	Standard Error	95% CI Low	95% CI High	VIF
Intercept	-17.64	1	0.20	-18.10	-17.17	
A-Contact Angle	-0.33	1	0.16	-0.70	0.036	1.00
B-Interfacial Energy	-1.27	1	0.16	-1.64	-0.90	1.00
AB	-0.14	1	0.22	-0.66	0.38	1.00
A^2	-0.72	1	0.17	-1.11	-0.32	1.02
B^2	-2.33	1	0.17	-2.73	-1.94	1.02

Surface energy of adhesion model equation for white blood treated with DH is:

$$F^{adh} = -17.64-0.33A+1.27B-0.14AB-0.72A^2-2.33B^2 \quad (4.10)$$

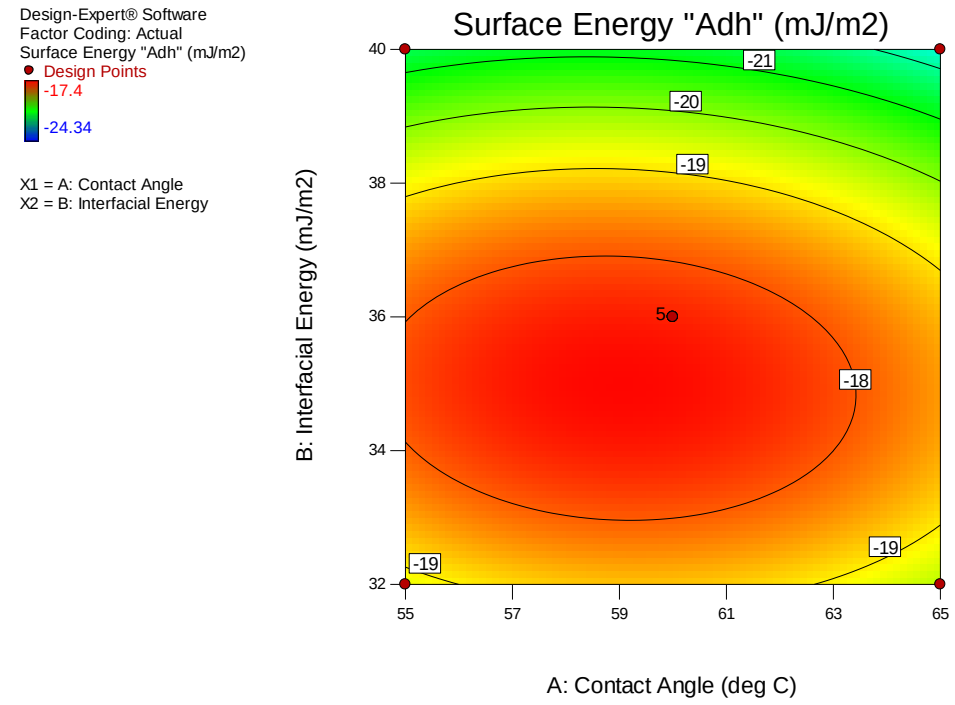

Fig 4.24: Contour Plots of DH Treated WBC for Energy of Adhesion

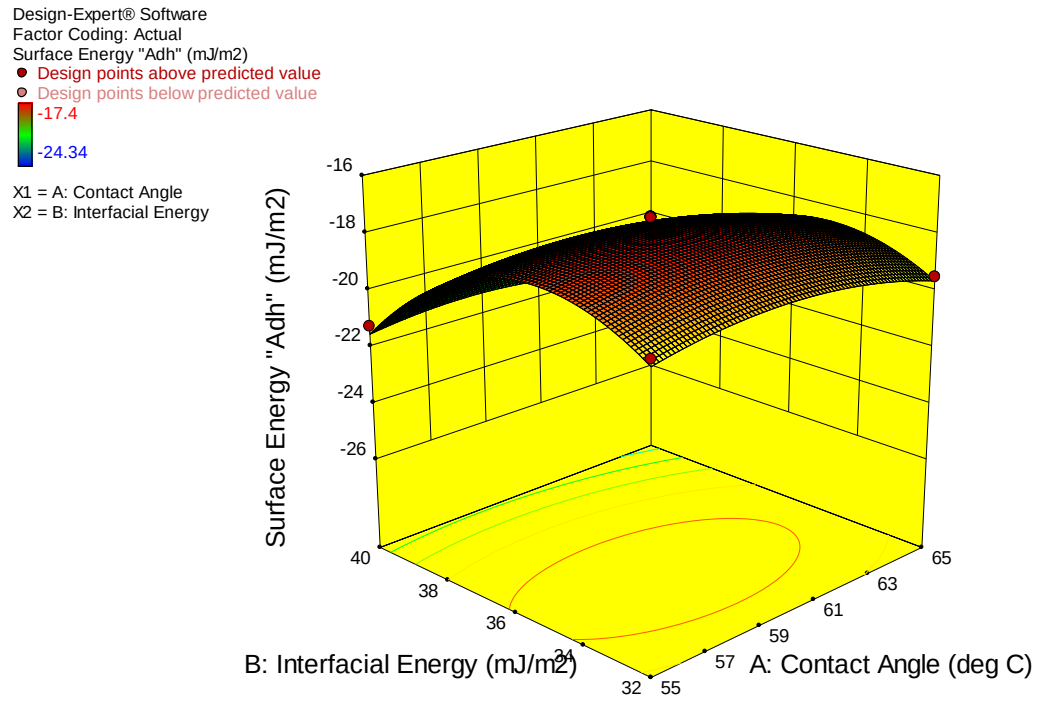

Fig 4.25:3-D Surface Plots of DH Treated WBC for Energy of Adhesion

The significance of the coefficient term is determined by the values of F and p, and the larger the value of F and the smaller the value of p, the more significant the model becomes (Kalavathy et al. 2009).

In all treatments given in this study, when analyzed using response surface (Table4.13a-4.22g) revealed that in each case considered, the larger the F-value, the smaller the p- value. The p-value in all cases is less than 0.05 suggesting the model equations (4.1-4.10) to be considered statistically significant making most of the variations in the response explainable by the model equations. The probability $p < 0.0001$ also validated the models are significant.

Also considering the R^2 values from the statistical tables, the "Predicted R^2" is in reasonable agreement with the "Adjusted R^2". "Adequacy Precision" measures the signal to noise ratio. It is reported that a ratio greater than 4 is desirable. In all scenario considered in this study, the adequacy precision ratio far above 4 was obtained, suggesting an adequate signal and also the data points were well distributed close to a straight line (R^2 close to 1), which suggested an excellent relationship between the

experimental and predicted values of the response, and the underlying assumptions of the above analysis were appropriate. The results also indicated that the selected quadratic model was adequate in assuming the response variables for the experimental data. The contour and the surface plots also in each case revealed the interaction between the independent variables and the response.

4.8: Hamaker Coefficient (A_{132}) of Blood Cells.

The concept of Hamaker coefficient is a function of the net van der Waal force of attraction or repulsion between particles suspended in a liquid. Theoretically a relationship exists between Hamaker coefficient (A_{132}) and energies of adhesion obtained from contact angle data as reported in equation 2.29.

Appendices E1-E60 show the Hamaker coefficient of the infected, uninfected and the treated samples of blood used for this study. The positive sign on the infected samples depicts attractive forces between the virus and the blood cells which connotes the HCV infection on the blood cells. The uninfected samples also have positive values though of little magnitude signifying the presence of other infections not due to HCV, hence the reason of low CD4 count in some uninfected samples. The treated samples also have positive values of Hamaker coefficient but lower than that of the infected suggesting that viral clearance maybe achieved on continued treatments. The average Hamaker coefficient for the infected, uninfected and treated samples with their respective drugs according to the models used for this study is shown in Appendices F1-F3.

Infected surfaces on the average have higher values of Hamaker coefficient than uninfected surfaces. Increase in contact angle causes an increase in Hamaker coefficient with a corresponding decrease in the CD4 counts on the infected surfaces. This increase is attributed to the presence of the HCV virus in the infected samples and the highest value was observed in the white blood cell component.

In contrast, the uninfected surfaces have lower values of Hamaker coefficient with a corresponding decrease in contact angle leading a higher CD4 counts on the uninfected surfaces. Other infections present in the HCV uninfected samples cause the

value of Hamaker coefficient to be positive but certainly not due to hepatitis C virus and the level of infection is insignificant hence a very low Hamaker coefficient value for uninfected surfaces.

The treated surfaces in all have a reduced Hamaker coefficient than the infected surfaces. This is as a result of the various treatments given to the infected surfaces which cause a reduction in Hamaker coefficient values.

Table 4.23 displays the average Hamaker coefficient of white blood cells using the different models employed in this study.

Table 4.23: Average Hamaker Coefficient using different Models(mJ/m^2)

	WBC	Neuman	Fowkes	Wu
	Infected**(A_{132})**	2.24E-17±2.15E-18	3.41E-17±3.07E-18	8.21E-17±4.43E-18
	Uninfected**(A_{132})**	1.25E-17±1.71E-18	2.07E-17±2.20E-18	5.53E-17±6.16E-18
Treated(A_{132})	IFN	1.81E-17±2.88E-18	2.81E-17±3.95E-18	6.53E-17±6.96E-18
	RBV	1.77E-17±2.80E-18	2.76E-17±3.73E-18	6.84E-17±7.46E-18
	ATR	1.79E-17±3.46E-18	2.79E-17±4.73E-18	6.80 E-17±9.96E-18
	ELT	1.81E-17±2.23E-18	2.78E-17±3.22E-18	6.81 E-17±6.05E-18
	AM	1.92E-17±2.11E-18	2.96E-17±4.06E-18	6.99 E-17±5.36E-18
	VA	1.72E-17±1.98E-18	2.68E-17±2.69E-18	6.24 E-17±5.98E-18
	BP	1.78E-17±2.35E-18	2.76E-17±3.21E-18	6.83 E-17±6.36E-18
	DH	1.99E-17±2.14E-18	3.06E-17±3.00E-18	6.44 E-17±6.96E-18

In all the categories, Wu's model recorded the highest Hamaker coefficient ($8.21x10^{-17}mJ/m^2$)for infected, ($5.53x10^{-17}mJ/m^2$) for uninfected and even for the treated while Neumann gave the lowest Hamaker coefficient of ($2.24x10^{-17}mJ/m^2$)for infected, ($1.25x10^{-17}mJ/m^2$) for the uninfected and also for the treated samples. The values of Hamaker coefficient A_{132} for particle interaction are also reported in literature ranging from $x10^{-14}$ J - $x10^{-24}$ J.

Amongst all treatments given, the infected surfaces treated with *vernonia amygdalina* VA, showed a closer Hamaker coefficient value to that of the uninfected as revealed by all the models used for the study. In general, it can be said that all drugs used have the capacity of reducing the Hamaker coefficient of HCV infected surfaces.

4.9Response Surface Analysis of Hamaker Coefficient

The results obtained from matlab computations were analyzed by applying the coefficient of determination (R^2), lack of fit, response plots and analysis of variance (ANOVA) so as to determine the statistical significance level and generate the model equation which will express the relationship between the predicted response and independent variables in coded values. The design matrix was shown table 3.7-3.11

Table 4.24a: Hamaker Response Summary for Infected WBC

Source	Sequential p-value	Lack of Fit p-value	Adjusted R-Squared	Predicted R-Squared
Linear	0.2524	0.0072	0.0888	-0.4246
2FI	0.2495	0.0072	0.1335	-0.4912
Quadratic	0.0002	0.3232	0.8987	0.7290
Cubic	0.1452	0.8163	0.9345	0.9315

Table 4.24b:Lack of Fit Tests

Source	Sum of Squares	df	Mean Square	F Value	p-value Prob > F
Linear	0.35	6	0.059	18.15	0.0072
2FI	0.30	5	0.060	18.53	0.0072
Quadratic	0.016	3	5.188E-003	1.60	0.3232
Cubic	2.000E-004	1	2.000E-004	0.062	0.8163
Pure Error	0.013	4	3.250E-003		

Table 4.24c: Hamaker Sequential Model Sum of Squares

Source	Sum of Squares	Df	Mean Square	F Value	p-value Prob > F
Mean vs Total	62.61	1	62.61		
Linear vs Mean	0.12	2	0.058	1.59	0.2524
2FI vs Linear	0.053	1	0.053	1.52	0.2495
Quadratic vs 2FI	0.29	2	0.14	34.99	0.0002
Cubic vs Quadratic	0.015	2	7.681E-003	2.91	0.1452
Residual	0.013	5	2.684 E-003		
Total	63.10	13	4.85		

Table 4.24d:Model Summary Statistics

Source	Std. Dev.	R-Squared	Adjusted R-Squared	Predicted R-Squared	PRESS
Linear	0.19	0.2407	0.0888	-0.4246	0.69
2FI	0.19	0.3502	0.1335	-0.4912	0.72
Quadratic	0.064	0.9409	0.8987	0.7290	0.13
Cubic	0.051	0.9727	0.9345	0.9315	0.033

Table 4.24e: ANOVA for Hamaker Surface Response QuadraticModel

Source	**Sum of Squares**	**D*f***	**Mean Square**	**F-Value**	**P-Value Prob > F**	
Model	0.45	5	0.091	22.29	0.0004	Significant
A-Contact Angle	*3.397E-003*	*1*	*3.397E-003*	*0.83*	*0.3919*	
B-Interfacial Energy	*0.11*	*1*	*0.11*	*27.68*	*0.0012*	
AB	*0.053*	*1*	*0.053*	*12.96*	*0.0087*	
A^2	*0.29*	*1*	*0.29*	*69.91*	*< 0.0001*	
B^2	*7.348E-003*	*1*	*7.348E-003*	*1.80*	*0.2215*	
Residual	0.029	7	4.080E-003			
Lack of Fit	*0.016*	*3*	*5.188E-003*	*1.60*	*0.3232*	*not significant*
Pure Error	*0.013*	*4*	*3.250E-003*			
Cor Total	0.48	12				

Table 4.24f:Quadratic Model Summary

Std. Dev.	0.064
Mean	2.19
C.V. %	2.91
PRESS	0.13
R-Squared	0.9409
Adj R-Squared	0.8987
Pred R-Squared	0.7290
Adeq Precision	12.703

Table 4.24(a-g) is a Hamaker coefficient response analysis obtained using Neumann model for infected white blood cell (Appendix E2)The quadratic model is suggested and focus is on the model maximizing the "Adjusted R-Squared" and the "Predicted R-Squared. The Model F-value of 22.29 implies that the model is significant. There is

only a 0.04% chance that an F-value this large could occur due to noise. Values of "Prob > F" less than 0.0500 indicate model terms are significant. In this case B, AB, A^2 are significant model terms. Values greater than 0.1000 indicate the model terms are not significant.

The "Lack of Fit F-value" of 1.60 implies the Lack of Fit is not significant relative to the pure error. There is a 32.32% chance that a "Lack of Fit F-value" this large could occur due to noise. Non-significant lack of fit is good.

The "Pred R-Squared" of 0.7290 is in reasonable agreement with the "Adj R-Squared" of 0.8987; i.e. the difference is less than 0.2. "Adeq Precision" measures the signal to noise ratio. A ratio greater than 4 is desirable. Table 4.24f predicts a ratio of 12.703 which indicates an adequate signal. This means that the model is a good one for predicting Hamaker coefficient in relation with contact angle and interfacial energy due to HCV infection. The equation in terms of coded factors can be used to make predictions about the response of the interacting variables. The coded equation is also useful for identifying the relative impact of the factors by comparing the factor coefficients.

Table 4.24g:Hamaker Coefficient Model Equation for Infected White Blood

Factor	**Coefficient Estimate**	**D*f***	**Standard Error**	**95% CI Low**	**95% CI High**	**VIF**
Intercept	2.05	1	0.029	1.98	2.12	
A-Contact Angle	-0.021	1	0.023	-0.074	0.033	1.00
B-Interfacial Energy	0.12	1	0.023	0.065	0.17	1.00
AB	0.12	1	0.032	0.039	0.19	1.00
A^2	0.20	1	0.024	0.15	0.26	1.02
B^2	0.033	1	0.024	0.025	0.090	1.02

Hamaker coefficient model equation for infected white bloodis given as:

$$A_{132}=2.05-0.021A+0.12B+0.12AB+0.20A^2+0.033B^2+0.20A^2+0.033B^2 \quad (4.11)$$

The ANOVA indicates the equation and actual relationship between the response and significant variables represented by the equation 4.11 are accurate. The R^2 value of 0.9409 indicates a good measure that outcomes are likely to be predicted well by the developed models. The contourand the surface plot on Fig 4.26 and 4.27 also reveal graphically the interaction between the independent variable and the response

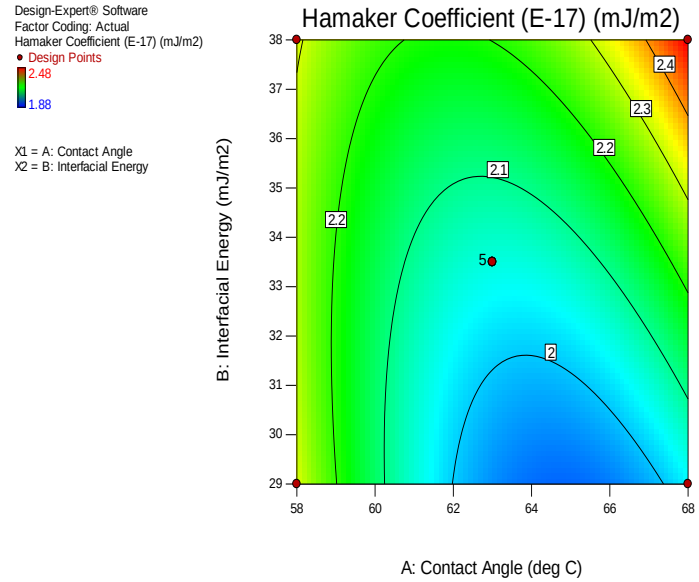

Fig. 4.26: Contour plots of Infected White blood for Hamaker Coefficient

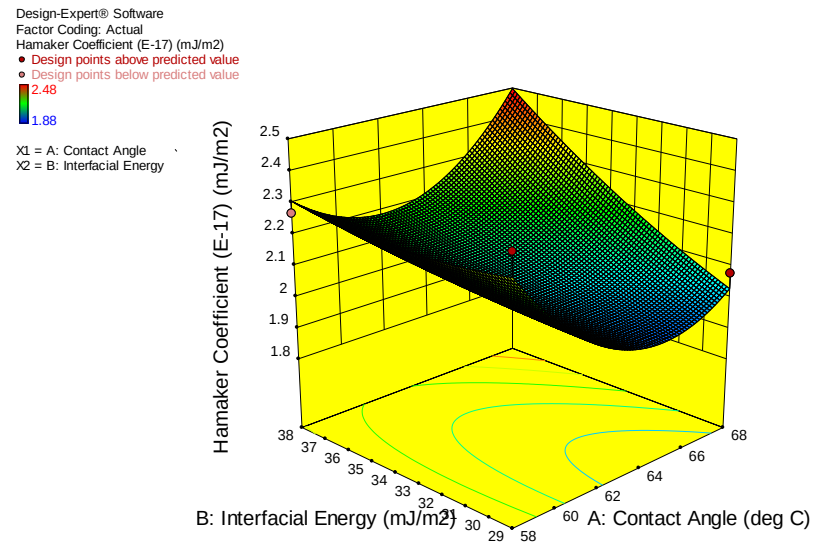

Fig4.27: 3D Surface plot of Infected White Blood for Hamaker Coefficient

Table 4.25(a-g) is a Hamaker coefficient response analysis table obtained using Neumann model for uninfected white blood cell (Appendix E2)The quadratic model is suggested and focus is on the model maximizing the "Adjusted R-Squared" and the "Predicted R-Squared.The Model F-value of 27.30 implies the model is significant. There is only a 0.02% chance that an F-value this large could occur due to noise. Values of "Prob > F" less than 0.0500 indicate model terms are significant.

In this case A, B, AB, B^2 are significant model terms.Values greater than 0.1000 indicate the model terms are not significant. The "Lack of Fit F-value" of 1.00 implies the Lack of Fit is not significant relative to the pure error. There is a 47.81% chance that a "Lack of Fit F-value" this large could occur due to noise. Non-significant lack of fit is good

The "Pred R-Squared" of 0.8076 is in reasonable agreement with the "Adj R-Squared" of 0.9164 since their difference is less than 0.2.Adequate Precision measures the signal to noise ratio. A ratio greater than 4 is desirable. Table 4.25e gave an adequate precision of 17.109 indicating an adequate interaction.

This means that the model is a good one for predicting Hamaker coefficient in relation with contact angle and interfacial energy due to HCV infection. The equation in terms

of coded factors can be used to make predictions about the response of the interacting variables. The coded equation is also useful for identifying the relative impact of the factors by comparing the factor coefficients.

Table 4.25a: Hamaker Response Summary

Source	Sequential p-value	Lack of Fit p-value	Adjusted R-Squared	Predicted R-Squared
Linear	0.0904	0.0115	0.2580	-0.1825
2FI	0.1885	0.0126	0.3270	-0.2161
Quadratic	0.0003	0.4781	0.9164	0.8076
Cubic	0.4622	0.3446	0.9140	0.4456

Table 4.25b: Hamaker Sequential Model Sum of Squares

Source	Sum of Squares	Df	Mean Square	F Value	p-value Prob > F
Mean vs Total	22.52	1	22.52		
Linear vs Mean	0.086	2	0.043	3.09	0.0904
2FI vs Linear	0.026	1	0.026	2.02	0.1885
Quadratic vs 2FI	0.10	2	0.051	32.71	0.0003
Cubic vs Quadratic	2.92E-003	2	1.46E-003	0.90	0.4622
Residual	8.08 E-003	5	1.62E-003		
Total	22.74	13	1.75		

Table 4.25c:Lack of Fit Tests

Source	Sum of Squares	df	Mean Square	F Value	p-value Prob > F
Linear	0.13	6	0.022	14.13	0.0115
2FI	0.11	5	0.022	13.70	0.0126
Quadratic	4.722E-003	3	1.574E-003	1.00	0.4781
Cubic	1.800E-003	1	1.800E-003	1.15	0.3446
Pure Error	6.280E-003	4	1.570E-003		

Table 4.25d:Model Summary Statistics

Source	Std. Dev.	R-Squared	Adjusted R-Squared	Predicted R-Squared	PRESS
Linear	0.12	0.3817	0.2580	-0.1825	0.27
2FI	0.11	0.4952	0.3270	-0.2161	0.27
Quadratic	0.040	0.9512	0.9164	0.8076	0.043
Cubic	0.040	0.9642	0.9140	0.4456	0.13

Table 4.25e:Quadratic Model Summary

Std. Dev.	0.040
Mean	1.32
C.V. %	3.01
PRESS	0.043
R-Squared	0.9512
Adj R-Squared	0.9164
Pred R-Squared	0.8076
Adeq Precision	17.109

Table 4.25f: ANOVA for Hamaker Response Surface QuadraticModel

Source	**Sum of Squares**	**D**f	**Mean Square**	**F-Value**	**P-Value Prob > F**	
Model	0.21	5	0.043	27.30	0.0002	*Significant*
A-Contact Angle	0.010	1	0.010	6.45	0.0386	
B-Interfacial Energy	0.076	1	0.076	48.31	0.0002	
AB	0.026	1	0.026	16.29	0.0050	
A^2	9.200E-004	1	9.200E-004	0.59	0.4692	
B^2	0.10	1	0.10	65.34	< 0.0001	
Residual	0.011	7	1.572E-003			
Lack of Fit	4.722E-003	3	1.574E-003	1.00	0.4781	*not significant*
Pure Error	6.280E-003	4	1.570E-003			
Cor Total	0.23	12				

Table4.25g:Hamaker Coefficient Model Equation for uninfected White Blood

Factor	**Coefficient Estimate**	**D*f***	**Standard Error**	**95% CI Low**	**95% CI High**	**VIF**
Intercept	1.40	1	0.018	1.36	1.44	
A-Contact Angle	0.036	1	0.014	2.46E-003	0.069	1.00
B-Interfacial Energy	0.097	1	0.014	0.064	0.13	1.00
AB	0.080	1	0.020	0.033	0.13	1.00
A^2	-0.011	1	0.015	-0.047	0.024	1.02
B^2	-0.12	1	0.015	-0.16	-0.086	1.02

Hamaker coefficient model equation for uninfected white bloodis given as:

$$A_{132} = 1.40+0.036A+0.097B+0.080AB-0.0011A^2-0.12B^2 \quad (4.12)$$

The ANOVA indicates the equation and actual relationship between the response and significant variables represented by the equation 4.12 are accurate. The R^2 value of 0.9512 indicates a good measure that outcomes are likely to be predicted well by the developed models. The contour and the surface plot on Fig 4.28 and 4.29 also revealed graphically the interaction between the independent variable and response.

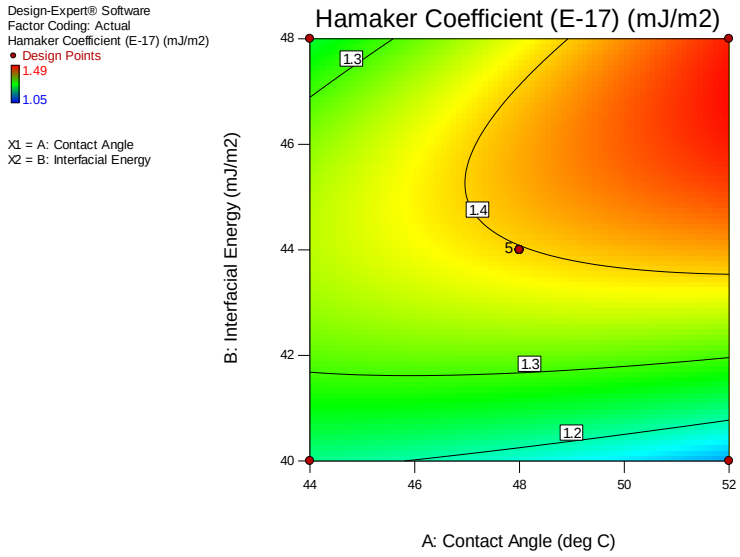

Fig 4.28: Contour plot of uninfected WBC for Hamaker Coefficient

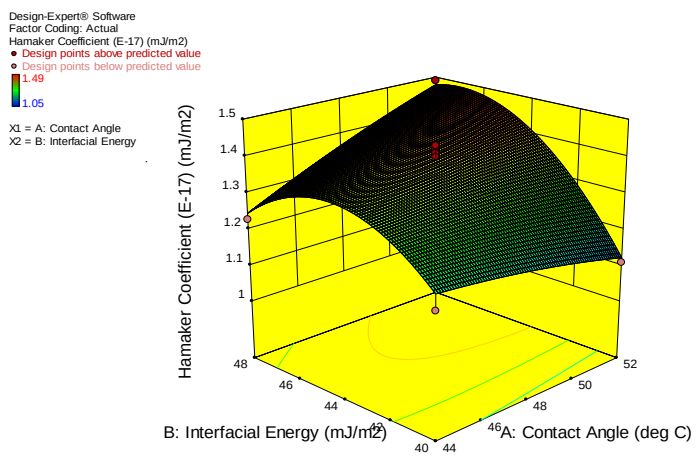

Fig 4.29: 3-D surface plot for uninfected white blood cellfor Hamaker Coefficient

Table 4.26(a-g) is a Hamaker response analysis obtained using Neumann model for infected white blood cell treated with IFN(Appendix E14) and Fig 4.30 and 4.31 displayed the contour and surface plots. The quadratic model is suggested and focus is on the model maximizing the "Adjusted R-Squared" and the "Predicted R-Squared. The Model F-value of 14.94 implies the model is significant. There is only a 0.013% chance that an F-value this large could occur due to noise. Values of "Prob > F" less than 0.0500 indicate model terms are significant.

The ANOVA indicates the equation and actual relationship between the response and significant variables represented by the equation 4.13 are accurate. The R^2 value of 0.9143 indicates a good measure that outcomes are likely to be predicted well by the developed models. The contour and the surface plot also reveal graphically the interaction between the independent variable and the response surface.

Table 4.26a: Hamaker Response Summary

Source	**Sequential p-value**	**Lack of Fit p-value**	**Adjusted R-Squared**	**Predicted R-Squared**
Linear	0.0051	0.2401	0.5832	0.3203
2FI	0.0007	0.9927	0.8798	0.8737
Quadratic	0.8364	0.9811	0.8531	0.8475
Cubic	0.9989	0.7088	0.7944	0.6593

Table 4.26b: Hamaker Sequential Model Sum of Squares

Source	Sum of Squares	Df	Mean Square	F Value	p-value Prob > F
Mean vs Total	45.38	1	45.38		
Linear vs Mean	0.42	2	0.21	9.39	0.0051
2FI vs Linear	0.16	1	0.16	25.67	0.0007
Quadratic vs 2FI	2.862E-003	2	1.43E-003	0.18	0.8364
Cubic vs Quadratic	2.35E-005	2	1.18E-005	1.08E-003	0.9989
Residual	0.055	5	0.011		
Total	46.02	13	3.54		

Table 4.26c:Lack of Fit Tests

Source	Sum of Squares	df	Mean Square	F Value	p-value Prob > F
Linear	0.17	6	0.028	2.15	0.2401
2FI	4.998E-003	5	9.995E-004	0.076	0.9927
Quadratic	2.136E-003	3	7.120E-004	0.054	0.9811
Cubic	2.112E-003	1	2.112E-003	0.16	0.7088
Pure Error	0.053	4	0.013		

Table 4.26d:Model Summary Statistics

Source	Std. Dev.	R-Squared	Adjusted R-Squared	Predicted R-Squared	PRESS
Linear	0.15	0.6526	0.5832	0.3203	0.43
2FI	0.080	0.9098	0.8798	0.8737	0.081
Quadratic	0.088	0.9143	0.8531	0.8475	0.097
Cubic	0.10	0.9143	0.7944	0.6593	0.22

Table 4.21e:Quadratic Model Summary

Std. Dev.	0.088
Mean	1.87
C.V. %	4.73
PRESS	0.097
R-Squared	0.9143
Adj R-Squared	0.8531
Pred R-Squared	0.8475
Adeq Precision	14.104

Table 4.26f: ANOVA for Hamaker Response Surface Quadratic Model

Source	**Sum of Squares**	**D*f***	**Mean Square**	**F-Value**	**P-Value Prob > F**	
Model	0.58	5	0.12	14.94	0.0013	Significant
A-Contact Angle	*0.026*	*1*	*0.026*	*3.33*	*0.1107*	
B-Interfacial Energy	*0.39*	*1*	*0.39*	*49.97*	*0.0002*	
AB	*0.16*	*1*	*0.16*	*21.01*	*0.0025*	
A^2	*1.827E-004*	*1*	*1.827E-004*	*0.023*	*0.8827*	
B^2	*2.818E-003*	*1*	*2.818E-003*	*0.36*	*0.5670*	
Residual	0.055	7	7.808E-003			
Lack of Fit	*2.14E-003*	*3*	*7.120E-003*	*0.054*	*0.9811*	*not significant*
Pure Error	*0.053*	*4*	*0.013*			
Cor Total	0.64	12				

Table4.26g:Hamaker Coefficient Model Equation for White Blood Treated with IFN

Factor	Coefficient Estimate	Df	Standard Error	95% CI Low	95% CI High	VIF
Intercept	1.88	1	0.040	1.79	1.98	
A-Contact Angle	-0.057	1	0.031	-0.13	0.017	1.00
B-Interfacial Energy	0.22	1	0.031	0.15	0.29	1.00
AB	0.20	1	0.044	0.098	0.31	1.00
A^2	-5.125E-003	1	0.034	-0.084	0.074	1.02
B^2	-0.020	1	0.034	-0.099	0.059	1.02

Hamaker coefficient model equation for infected white blood treated with IFNis given as:

$$A_{132} = 1.88-0.057A+0.22B+0.20AB-5.125E-003A^2-0.020B^2 \quad (4.13)$$

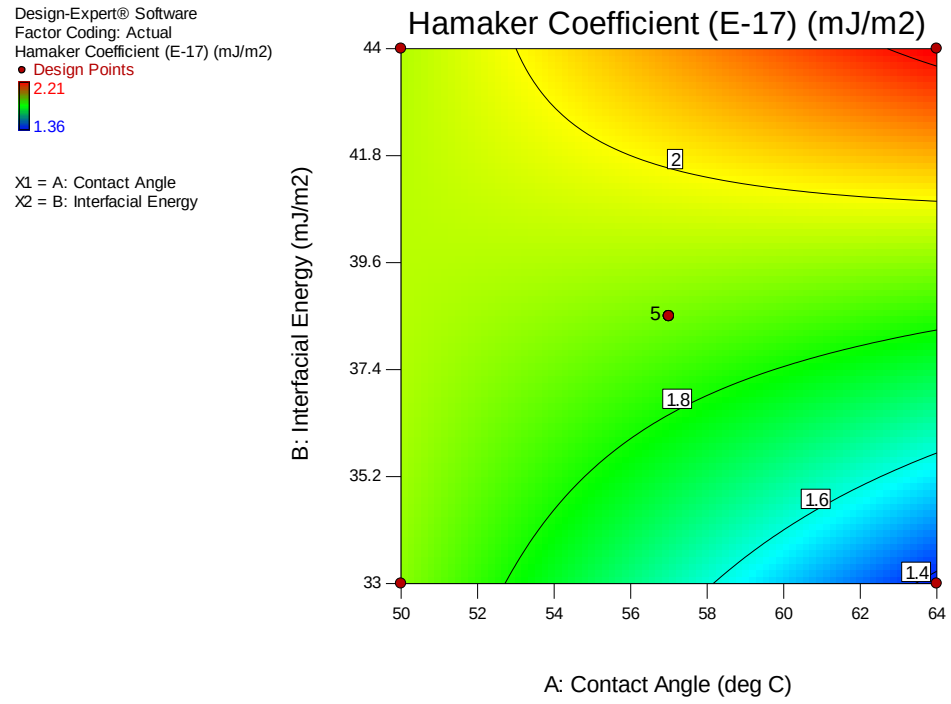

Fig 4.30: Contour plot of infected WBC IFN Treated for Hamaker Coefficient

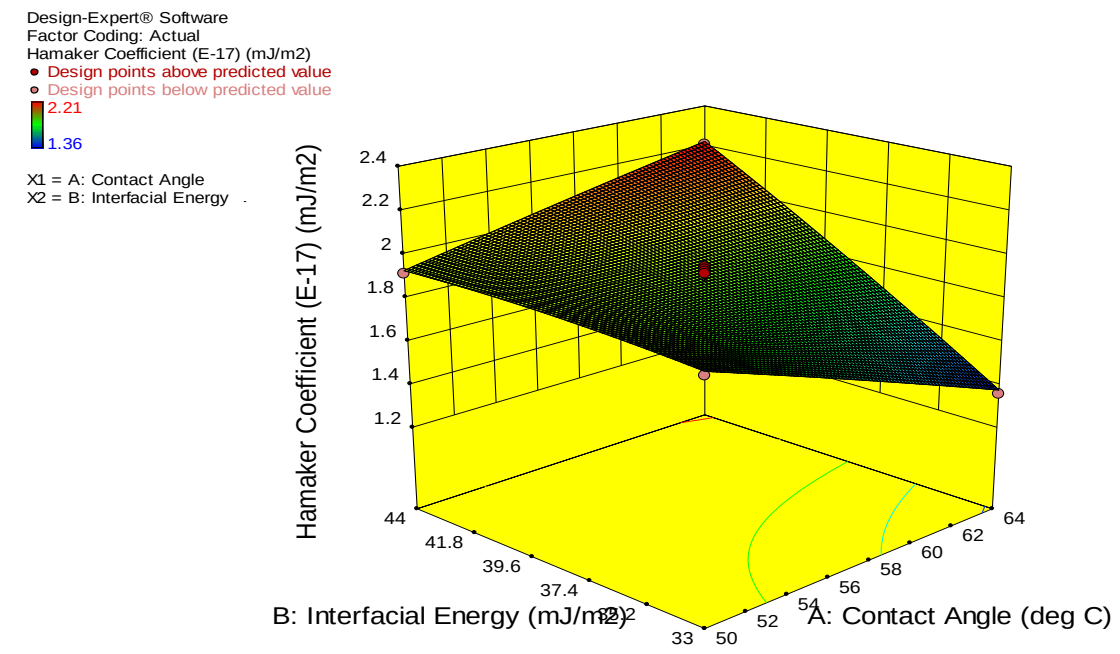

Fig 4.31: 3-D Surface plot of WBC IFN Treated for Hamaker Coefficient

Table 4.27(a-g) is a Hamaker response analysis obtained using Neumann model for infected white blood cell treated with RBV(Appendix E14) and Fig 4.32 and 4.33 displayed the contour and surface plots. The quadratic model is suggested and focus is on the model maximizing the "Adjusted R-Squared" and the "Predicted R-Squared. The Model F-value of 31.45 implies the model is significant. There is only a 0.001% chance that an F-value this large could occur due to noise. Values of "Prob > F" less than 0.0500 indicate model terms are significant.

The ANOVA indicates the equation and actual relationship between the response and significant variables represented by the equation 4.14 are accurate. The R^2 value of 0.9574 indicates a good measure that outcomes are likely to be predicted well by the developed models. The contour and the surface plot also reveal graphically the interaction between the independent variable and the response surface.

Table 4.27a: Hamaker Response Summary

Source	Sequential p-value	Lack of Fit p-value	Adjusted R-Squared	Predicted R-Squared
Linear	0.1253	0.0024	0.2079	-0.2777
2FI	0.0238	0.0056	0.5163	0.3383
Quadratic	0.0006	0.1611	0.9269	0.7704
Cubic	0.9133	0.0441	0.9014	-0.8034

Table 4.27b: Hamaker Sequential Model Sum of Squares

Source	Sum of Squares	Df	Mean Square	F Value	p-value Prob > F
Mean vs Total	36.69	1	36.69		
Linear vs Mean	0.13	2	0.064	2.57	0.1253
2FI vs Linear	0.11	1	0.11	7.38	0.0238
Quadratic vs 2FI	0.12	2	0.060	26.29	0.0006
Cubic vs Quadratic	5.73E-004	2	2.87E-004	0.092	0.9133
Residual	0.016	5	3.10E-003		
Total	37.07	13	2.85		

Table 4.27c:Lack of Fit Tests

Source	Sum of Squares	df	Mean Square	F Value	p-value Prob > F
Linear	0.24	6	0.041	32.55	0.0024
2FI	0.13	5	0.026	21.10	0.0056
Quadratic	0.011	3	3.695E-003	2.96	0.1611
Cubic	0.011	1	0.011	8.41	0.0441
Pure Error	5.000E-003	4	1.250E-003		

Table 4.27d:Model Summary Statistics

Source	Std. Dev.	R-Squared	Adjusted R-Squared	Predicted R-Squared	PRESS
Linear	0.16	0.3399	0.2079	-0.2777	0.48
2FI	0.12	0.6373	0.5163	0.3383	0.25
Quadratic	0.048	0.9574	0.9269	0.7704	0.087
Cubic	0.056	0.9589	0.9014	-0.8034	0.68

Table 4.27e:Quadratic Model Summary

Std. Dev.	0.048
Mean	1.68
C.V. %	2.85
PRESS	0.087
R-Squared	0.9574
Adj R-Squared	0.9269
Pred R-Squared	0.7704
Adeq Precision	18.046

Table 4.27f: ANOVA for Hamaker Response Surface Quadratic Model

Source	**Sum of Squares**	**D*f***	**Mean Square**	**F-Value**	**P-Value Prob > F**	
Model	0.36	5	0.072	31.45	0.0001	Significant
A-Contact Angle	*5.539E-004*	*1*	*5.539E-004*	*0.24*	*0.6385*	
B-Interfacial Energy	*0.13*	*1*	*0.13*	*55.58*	*0.0001*	
AB	*0.11*	*1*	*0.11*	*48.84*	*0.0002*	
A^2	*0.11*	*1*	*0.11*	*48.73*	*0.0002*	
B^2	*0.019*	*1*	*0.019*	*8.15*	*0.0245*	
Residual	0.016	7	2.298E-003			
Lack of Fit	*0.011*	*3*	*3.695E-003*	*2.96*	*0.1611*	*not significant*
Pure Error	*5.000E-003*	*4*	*1.250E-003*			
Cor Total	0.38	12				

Table4.27g: Hamaker Coefficient Model Equation for White Blood Treated with RBV.

Factor	**Coefficient Estimate**	**D*f***	**Standard Error**	**95% CI Low**	**95% CI High**	**VIF**
Intercept	1.57	1	0.021	1.52	1.62	
A-Contact Angle	-8.321E-003	1	0.017	-0.048	0.032	1.00
B-Interfacial Energy	0.13	1	0.017	0.086	0.17	1.00
AB	0.17	1	0.024	0.11	0.22	1.00
A^2	0.13	1	0.018	0.084	0.17	1.02
B^2	0.052	1	0.018	8.898E-003	0.095	1.02

Hamaker coefficient model equation for infected white blood treated with RBVis given as:

$$A_{132}=1.57-8.32E-003A+0.13B+0.17AB+0.13A^2-0.052B^2 \quad (4.14)$$

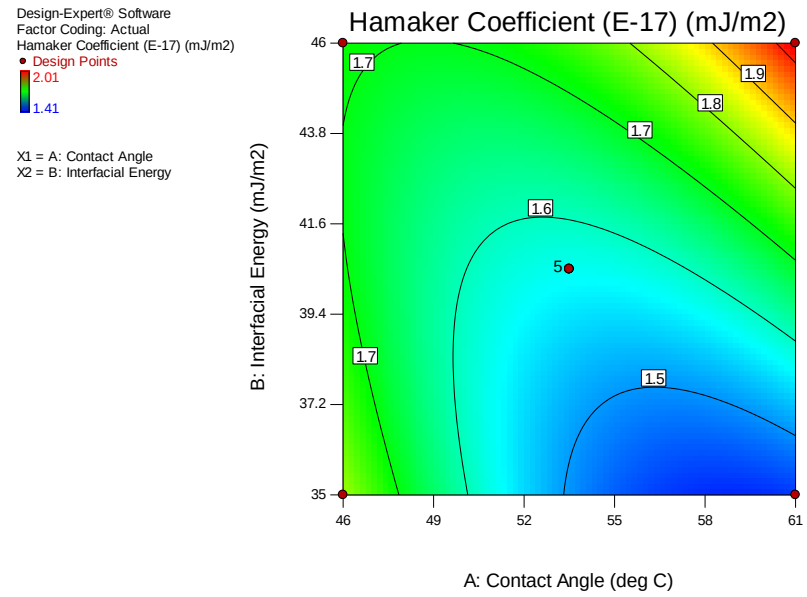

Fig 4.32: Contour plot of infected WBC Treated with RBV for Hamaker Coefficient

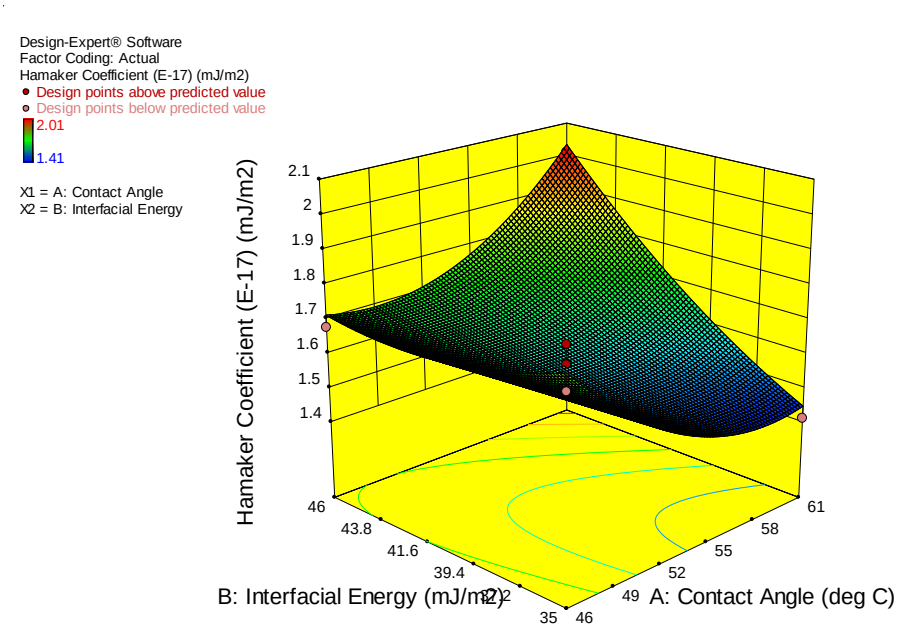

Fig 4.33: 3-D Hamaker Coefficient Surface plot of Infected WBC Treated with RBV

Table 4.28(a-g) is a Hamaker response analysis obtained using Neumann model for infected white blood cell treated with ATR(Appendix E26) and Fig 4.34 and 4.35 displayed the contour and surface plots. The 2FI linear model is suggested and focus is on the model maximizing the "Adjusted R-Squared" and the "Predicted R-Squared. The Model F-value of 6.49 implies the model is significant. There is only a 0.001% chance that an F-value this large could occur due to noise. Values of "Prob > F" less than 0.0500 indicate model terms are significant.

The ANOVA indicates the equation and actual relationship between the response and significant variables represented by the equation 4.15 are accurate. The R^2 value of 0.9839 indicates a good measure that outcomes are likely to be predicted well by the developed models. The contour and the surface plot also reveal graphically the interaction between the independent variable and the response surface.

Table 4.28a: Hamaker Response Summary for ATR

Source	**Sequential p-value**	**Lack of Fit p-value**	**Adjusted R-Squared**	**Predicted R-Squared**
Linear	0.1046	0.4614	0.2361	-0.1658
2FI	0.0145	0.8954	0.9786	0.9950
Quadratic	0.5046	0.9158	0.5544	0.4364
Cubic	0.9715	0.5441	0.3833	-0.9863

Table 4.28b: Sequential Model Sum of Squares

Source	Sum of Squares	Df	Mean Square	F Value	p-value Prob > F
Mean vs Total	45.12	1	45.12		
Linear vs Mean	0.27	2	0.14	2.85	0.1046
2FI vs Linear	0.24	1	0.24	9.13	0.0145
Quadratic vs 2FI	0.042	2	0.021	0.76	0.5046
Cubic vs Quadratic	2.238E-003	2	1.119E-003	0.029	0.9715
Residual	0.19	5	0.038		
Total	45.87	13	3.53		

Table 4.28c:Lack of Fit Tests

Source	Sum of Squares	df	Mean Square	F Value	p-value Prob > F
Linear	0.30	6	0.051	1.17	0.4614
2FI	0.063	5	0.013	0.29	0.8954
Quadratic	0.021	3	7.084E-003	0.16	0.9158
Cubic	0.019	1	0.019	0.44	0.5441
Pure Error	0.17	4	0.043		

Table 4.28d: Model Summary Statistics

Source	Std. Dev.	R-Squared	Adjusted R-Squared	Predicted R-Squared	PRESS
Linear	0.22	0.3634	0.2361	-0.1658	0.87
2FI	0.16	0.9839	0.9786	0.9950	0.38
Quadratic	0.17	0.7400	0.5544	0.4364	0.42
Cubic	0.20	0.7430	0.3833	-0.9863	1.49

Table 4.28e:ANOVA for Response Surface 2FI Model for Hamaker ATR

Source	Sum of Squares	D*f*	Mean Square	F-Value	P-Value Prob > F	
Model	0.51	5	0.17	6.49	0.0125	Significant
A-Contact Angle	*0.065*	*1*	*0.065*	*2.48*	*0.1501*	
B-Interfacial Energy	*0.21*	*1*	*0.21*	*7.87*	*0.0205*	
AB	*0.24*	*1*	*0.24*	*9.13*	*0.0145*	
Residual	0.24	7	0.026			
Lack of Fit	*0.063*	*3*	*0.013*	*0.29*	*0.8954*	*not significant*
Pure Error	*0.17*	*4*	*0.043*			
Cor Total	0.75	12				

Table 4.28f:2FI Model Summary

Std. Dev.	0.16
Mean	1.86
C.V. %	8.71
PRESS	0.38
R-Squared	0.9839
Adj R-Squared	0.9786
Pred R-Squared	0.9950
Adeq Precision	9.023

Table 4.28g: Hamaker Coefficient Model Equation for ATR Treated White Blood.

Factor	Coefficient Estimate	D*f*	Standard Error	95% CI Low	95% CI High	VIF
Intercept	1.86	1	0.045	1.76	1.96	
A-Contact Angle	0.090	1	0.057	-0.039	0.22	1.00
B-Interfacial Energy	0.16	1	0.057	0.031	0.29	1.00
AB	0.25	1	0.081	0.062	0.43	1.00

Hamaker coefficient model equation for infected white blood treated with ATRis given as:

$$A_{132}=18 +0.090A+0.16B+0.25AB \quad (4.15)$$

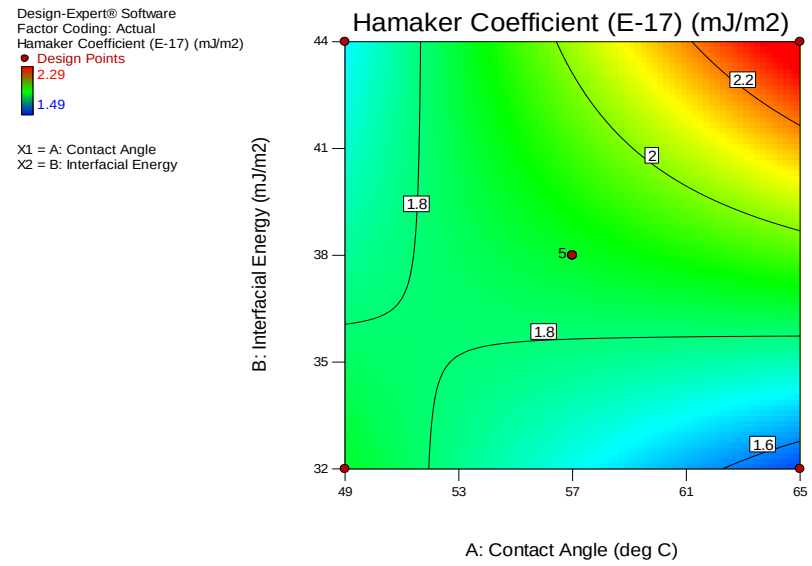

Fig 4.34: Hamaker contour plot for infected white blood cell treated with ATR

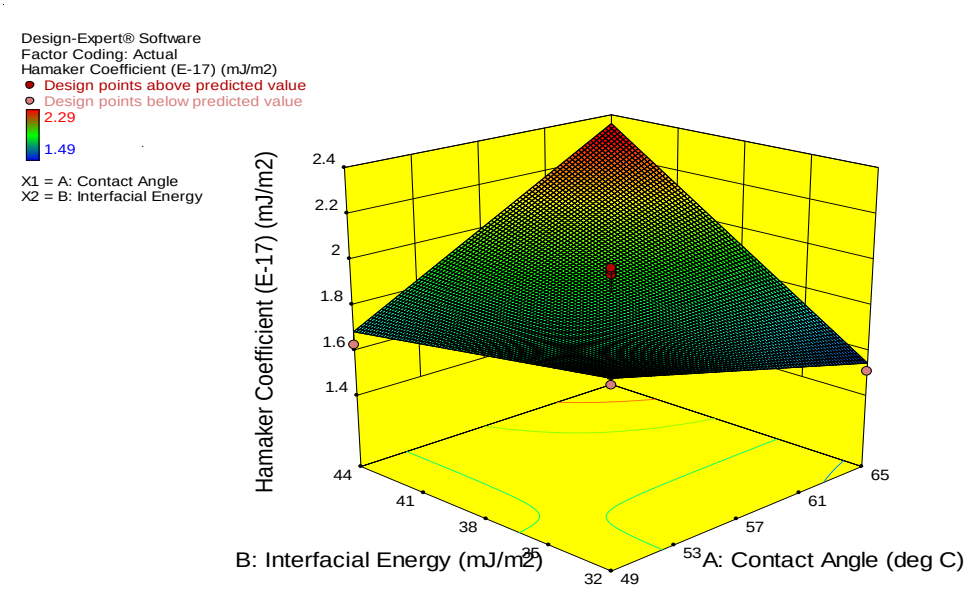

Fig 4.35: Hamaker 3-D surface plot for ATR treated

Table 4.29(a-g) is a Hamaker response analysis obtained using Neumann model for infected white blood cell treated with ELT(Appendix E26) and Fig 4.36 and 4.37 displayed the contour and surface plots. The quadratic model is suggested and focus is on the model maximizing the "Adjusted R-Squared" and the "Predicted R-Squared. The Model F-value of 11.26 implies the model is significant. There is only a 0.003% chance that an F-value this large could occur due to noise. Values of "Prob > F" less than 0.0500 indicate model terms are significant.

The ANOVA indicates the equation and actual relationship between the response and significant variables represented by the equation 4.16 are accurate. The R^2 value of 0.8894 indicates a good measure that outcomes are likely to be predicted well by the developed models. The contour and the surface plot also reveal graphically the interaction between the independent variable and the response surface

Table 4.29a: Hamaker Response Summary for ELT Treated

Source	Sequential p-value	Lack of Fit p-value	Adjusted R-Squared	Predicted R-Squared
Linear	0.2930	0.0562	0.0612	-0.6184
2FI	0.1608	0.0655	0.1718	-0.3257
Quadratic	0.0024	0.7139	0.8104	0.6648
Cubic	0.4747	0.8575	0.8029	0.8252

Table 4.29b: Sequential Model Sum of Squares

Source	Sum of Squares	Df	Mean Square	F Value	p-value Prob > F
Mean vs Total	40.20	1	40.20		
Linear vs Mean	0.091	2	0.046	1.39	0.2930
2FI vs Linear	0.068	1	0.068	2.34	0.1608
Quadratic vs 2FI	0.21	2	0.11	16.15	0.0024
Cubic vs Quadratic	0.012	2	5.978E-003	0.87	0.4747
Residual	0.034	5	6.886E-003		
Total	40.62	13	3.12		

Table 4.29c:Lack of Fit Tests

Source	Sum of Squares	df	Mean Square	F Value	p-value Prob > F
Linear	0.29	6	0.049	5.74	0.0562
2FI	0.23	5	0.045	5.31	0.0655
Quadratic	0.012	3	4.090E-003	0.48	0.7139
Cubic	3.125E-004	1	3.125E-004	0.037	0.8575
Pure Error	0.034	4	8.530E-003		

Table 4.29d:Model Summary Statistics

Source	Std. Dev.	R-Squared	Adjusted R-Squared	Predicted R-Squared	PRESS
Linear	0.18	0.2177	0.0612	-0.6184	0.68
2FI	0.17	0.3789	0.1718	-0.3257	0.56
Quadratic	0.081	0.8894	0.8104	0.6648	0.14
Cubic	0.083	0.9179	0.8029	0.8252	0.073

Table 4.29e:Quadratic Model Summary

Std. Dev.	0.081
Mean	1.76
C.V. %	4.63
PRESS	0.14
R-Squared	0.8894
Adj R-Squared	0.8104
Pred R-Squared	0.6648
Adeq Precision	11.902

Table 4.29f: ANOVA for Hamaker Response Surface Quadratic Model for ELT

Source	**Sum of Squares**	**D*f***	**Mean Square**	**F-Value**	**P-Value Prob > F**	
Model	0.37	5	0.075	11.26	0.0031	Significant
A-Contact Angle	*0.051*	*1*	*0.051*	*7.77*	*0.0270*	
B-Interfacial Energy	*0.040*	*1*	*0.040*	*6.01*	*0.0441*	
AB	*0.068*	*1*	*0.068*	*10.20*	*0.0152*	
A^2	*0.15*	*1*	*0.15*	*22.80*	*0.0020*	
B^2	*0.039*	*1*	*0.039*	*5.92*	*0.0452*	
Residual	0.046	7	6.627E-003			
Lack of Fit	*0.012*	*3*	*4.090E-003*	*0.48*	*0.7139*	*not significant*
Pure Error	*0.034*	*4*	*8.530E-003*			
Cor Total	0.42	12				

Table 4.29g: Hamaker Model Equation for Infected White Blood Treated with ELT

Factor	Coefficient Estimate	D*f*	Standard Error	95% CI Low	95% CI High	VIF
Intercept	1.71	1	0.036	1.63	1.80	
A-Contact Angle	0.080	1	0.029	0.012	0.15	1.00
B-Interfacial Energy	0.071	1	0.029	2.476E -003	0.14	1.00
AB	0.13	1	0.041	0.034	0.23	1.00
A^2	0.15	1	0.031	0.074	0.22	1.02
B^2	-0.075	1	0.031	-0.15	-2.14E-003	1.02

Hamaker coefficient model equation for infected white blood treated with ATRis given as:

$$A_{132}= 1.71+0.080A+0.071B+0.13AB+0.15A^2-0.075B^2 \quad (4.16)$$

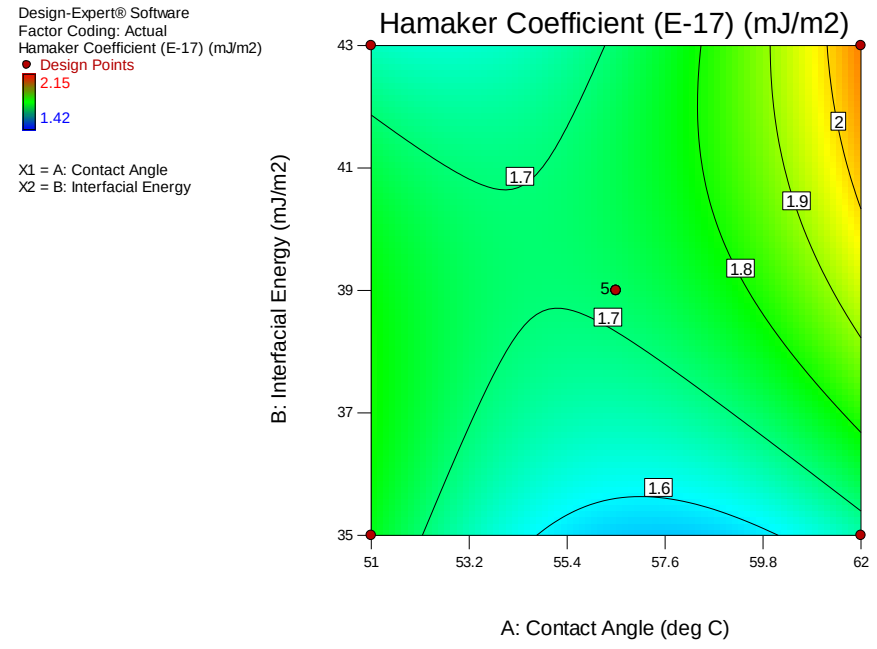

Fig 4.36: Hamaker contour plot for infected white blood cell treated with ELT

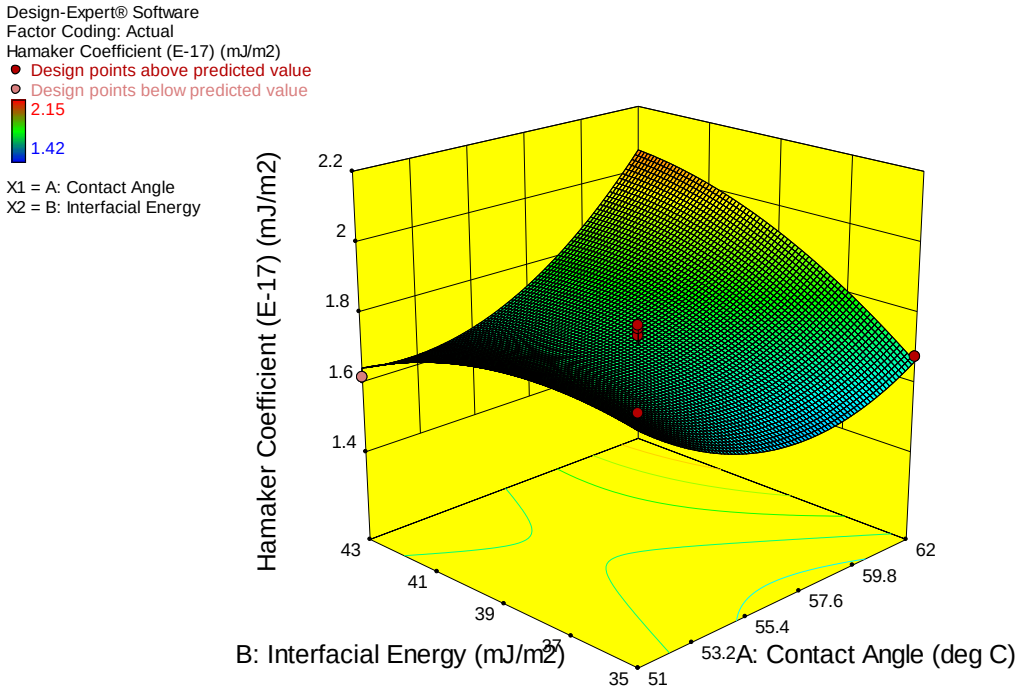

Fig 4.37: 3-D Hamaker Coefficient Surface plot of Infected WBC Treated with ELT

Table 4.30(a-g) is a Hamaker response analysis obtained using Neumann model for infected white blood cell treated with AM(Appendix E38) and Fig 4.38 and 4.39 displayed the contour and surface plots. The quadratic model is suggested and focus is on the model maximizing the "Adjusted R-Squared" and the "Predicted R-Squared. The Model F-value of 27.37 implies the model is significant. There is only a 0.002% chance that an F-value this large could occur due to noise. Values of "Prob > F" less than 0.0500 indicate model terms are significant.

The ANOVA indicates the equation and actual relationship between the response and significant variables represented by the equation 4.17 are accurate. The R^2 value of 0.9513 indicates a good measure that outcomes are likely to be predicted well by the developed models. The contour and the surface plot also reveal graphically the interaction between the independent variable and the response surface.

Table 4.30a: Response Summary for Hamaker Coefficient with AM

Source	Sequential p-value	Lack of Fit p-value	Adjusted R-Squared	Predicted R-Squared
Linear	0.5290	0.0053	-0.0565	-0.4582
2FI	0.8040	0.0039	-0.1654	-1.2078
Quadratic	< 0.0001	0.4438	0.9166	0.8014
Cubic	0.9539	0.1488	0.8854	-0.3967

Table 4.30b: Sequential Model Sum of Squares

Source	Sum of Squares	Df	Mean Square	F Value	p-value Prob > F
Mean vs Total	50.14	1	50.14		
Linear vs Mean	0.068	2	0.034	0.68	0.5290
2FI vs Linear	3.600E-003	1	3.600E-003	0.065	0.8040
Quadratic vs 2FI	0.47	2	0.23	59.36	< 0.0001
Cubic vs Quadratic	5.167E-004	2	2.584E-004	0.0048	0.9539
Residual	0.027	5	5.419E-003		
Total	50.70	13	3.90		

Table 4.30c:Lack of Fit Tests

Source	Sum of Squares	df	Mean Square	F Value	p-value Prob > F
Linear	0.48	6	0.081	21.41	0.0053
2FI	0.48	5	0.096	25.51	0.0039
Quadratic	0.013	3	4.176E-003	1.11	0.4438
Cubic	0.012	1	0.012	3.19	0.1488
Pure Error	0.015	4	3.770E-003		

Table 4.30d:Model Summary Statistics

Source	Std. Dev.	R-Squared	Adjusted R-Squared	Predicted R-Squared	PRESS
Linear	0.22	0.1196	-0.0565	-0.4582	0.83
2FI	0.23	0.1259	-0.1654	-1.2078	1.25
Quadratic	0.063	0.9513	0.9166	0.8014	0.11
Cubic	0.074	0.9522	0.8854	-0.3967	0.79

Table 4.30e:Quadratic Model Summary

Std. Dev.	0.063
Mean	1.96
C.V. %	3.20
PRESS	0.11
R-Squared	0.9513
Adj R-Squared	0.9166
Pred R-Squared	0.8014
Adeq Precision	13.306

Table 4.30f: ANOVA for Hamaker Response Surface Quadratic Model for AM

Source	Sum of Squares	D*f*	Mean Square	F-Value	P-Value Prob > F	
Model	0.54	5	0.11	27.37	0.0002	Significant
A-Contact Angle	*0.026*	*1*	*0.026*	*6.65*	*0.0366*	
B-Interfacial Energy	*0.042*	*1*	*0.042*	*10.55*	*0.0141*	
AB	*3.600E-003*	*1*	*3.600E-003*	*0.91*	*0.3712*	
A^2	*0.41*	*1*	*0.41*	*104.47*	*< 0.0001*	
B^2	*0.10*	*1*	*0.10*	*25.77*	*0.0014*	
Residual	0.028	7	3.944E-003			
Lack of Fit	*0.013*	*3*	*4.176E-003*	*1.11*	*0.4438*	*not significant*
Pure Error	*0.015*	*4*	*3.770E-003*			
Cor Total	0.57	12				

Table 4.30g:Hamaker Coefficient Model Equation for Infected White Blood Treated with AM

Factor	Coefficient Estimate	D*f*	Standard Error	95% CI Low	95% CI High	VIF
Intercept	2.19	1	0.028	2.12	-22.02	
A-Contact Angle	0.057	1	0.022	4.744E-003	-0.065	1.00
B-Interfacial Energy	0.072	1	0.022	0.020	-0.14	1.00
AB	0.030	1	0.031	-0.044	0.42	1.00
A^2	-0.24	1	0.024	-0.30	3.04	1.02
B^2	-0.12	1	0.024	-0.18	1.91	1.02

Hamaker coefficient model equation for infected white blood treated with AMis given as:

$$A_{132}= 2.19+0.057A+0.072B+0.030AB-0.24A^2-0.12B^2 \quad (4.17)$$

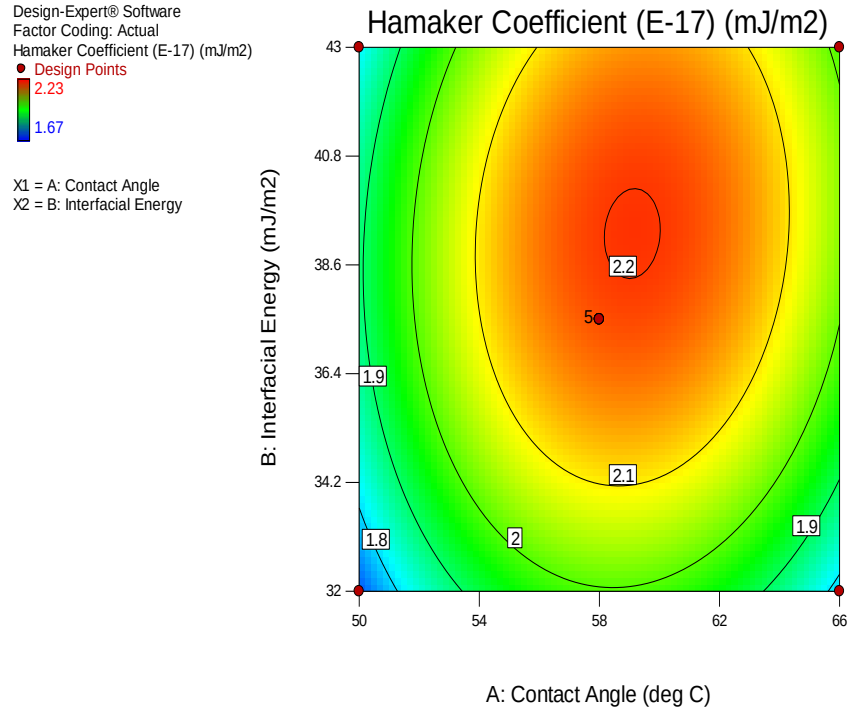

Fig 4.38: Hamaker Coefficient Contour plot for infected white blood cell treated with AM

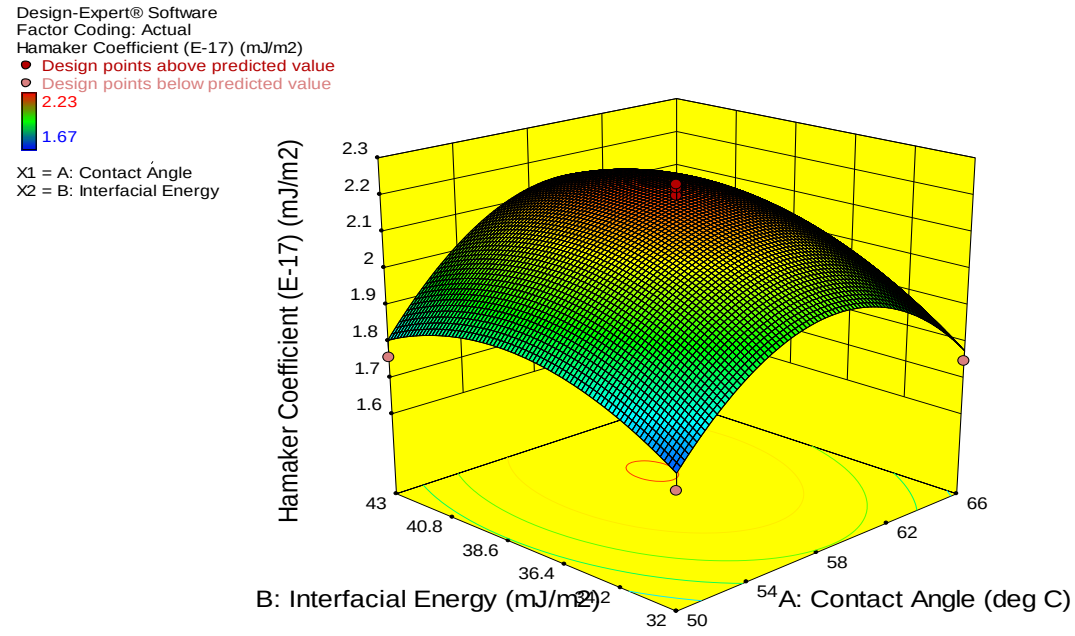

Fig 4.39:3-D Hamaker Coefficient Surface plot of Infected WBC Treated with AM

Table 4.31(a-g) is a Hamaker response analysis obtained using Neumann model for infected white blood cell treated with VA(Appendix E38) and Fig 4.40 and 4.41 displayed the contour and surface plots. The quadratic model is suggested and focus is on the model maximizing the "Adjusted R-Squared" and the "Predicted R-Squared. The Model F-value of 52.88 implies the model is significant. There is only a 0.001% chance that an F-value this large could occur due to noise. Values of "Prob > F" less than 0.0500 indicate model terms are significant.

The ANOVA indicates the equation and actual relationship between the response and significant variables represented by the equation 4.18 are accurate. The R^2 value of 0.9742 indicates a good measure that outcomes are likely to be predicted well by the developed models. The contour and the surface plot also reveal graphically the interaction between the independent variable and the response surface.

Table 4.31a: Response Summary for Hamaker Coefficient with VA

Source	**Sequential p-value**	**Lack of Fit p-value**	**Adjusted R-Squared**	**Predicted R-Squared**
Linear	0.0514	0.0071	0.3373	0.0005
2FI	0.4082	0.0061	0.3205	-0.1198
Quadratic	< 0.0001	0.7409	0.9558	0.9246
Cubic	0.4947	1.0000	0.9533	0.9696

Table 4.31b: Sequential Model Sum of Squares

Source	Sum of Squares	Df	Mean Square	F Value	p-value Prob > F
Mean vs Total	34.87	1	34.87		
Linear vs Mean	0.18	2	0.089	4.05	0.0514
2FI vs Linear	0.017	1	0.017	0.75	0.4082
Quadratic vs 2FI	0.19	2	0.096	65.66	< 0.0001
Cubic vs Quadratic	2.510E-003	2	1.255E-003	0.81	0.4947
Residual	7.720E-003	5	1.544E00-3		
Total	35.26	13	2.71		

Table 4.31c: Lack of Fit Tests

Source	Sum of Squares	df	Mean Square	F Value	p-value Prob > F
Linear	0.21	6	0.035	18.25	0.0071
2FI	0.19	5	0.039	20.15	0.0061
Quadratic	2.510E-003	3	8.367E-004	0.43	0.7409
Cubic	0.000	1	0.000	0.000	1.0000
Pure Error	7.720E-003	4	1.930E-003		

Table 4.31d:Model Summary Statistics

Source	Std. Dev.	R-Squared	Adjusted R-Squared	Predicted R-Squared	PRESS
Linear	0.15	0.4477	0.3373	0.0005	0.40
2FI	0.15	0.4904	0.3205	-0.1198	0.44
Quadratic	0.038	0.9742	0.9558	0.9246	0.030
Cubic	0.039	0.9805	0.9533	0.9696	0.012

Table 4.31e:Quadratic Model Summary

Std. Dev.	0.038
Mean	1.64
C.V. %	2.33
PRESS	0.030
R-Squared	0.9742
Adj R-Squared	0.9558
Pred R-Squared	0.9246
Adeq Precision	22.192

Table 4.31f: ANOVA for Hamaker Response Surface Quadratic Model for VA

Source	Sum of Squares	Df	Mean Square	F-Value	P-Value Prob > F	
Model	0.39	5	0.077	52.88	< 0.0001	Significant
A-Contact Angle	0.12	1	0.12	83.27	< 0.0001	
B-Interfacial Energy	0.056	1	0.056	38.25	0.0005	
AB	0.017	1	0.017	11.56	0.0114	
A^2	0.19	1	0.19	130.38	< 0.0001	
B^2	8.767E-003	1	8.767E-003	6.00	0.0442	
Residual	0.010	7	1.461E-003			
Lack of Fit	2.510E-003	3	8.367E-004	0.43	0.7409	not significant
Pure Error	7.720E-003	4	1.930E-003			
Cor Total	0.40	12				

Table 4.31g: Hamaker Coefficient Model Equation for Infected White Blood Treated with VA

Factor	Coefficient Estimate	Df	Standard Error	95% CI Low	95% CI High	VIF
Intercept	1.51	1	0.017	1.47	1.55	
A-Contact Angle	0.12	1	0.014	0.091	0.16	1.00
B-Interfacial Energy	0.084	1	0.014	0.052	0.12	1.00
AB	-0.065	1	0.019	-0.11	-0.020	1.00
A^2	0.17	1	0.014	0.13	0.20	1.02
B^2	0.036	1	0.014	1.226E-003	0.070	1.02

Hamaker coefficient model equation for infected white blood treated with VAis given as:

$$A_{132}= 1.51+ 0.12A+0.084B-0.065AB+0.17A^2+0.036B^2 \quad (4.18)$$

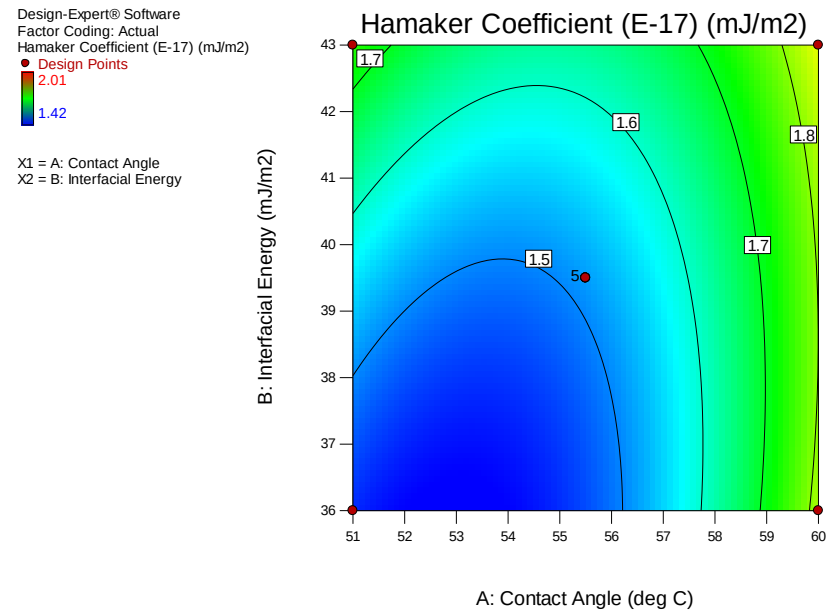

Fig 4.40: Hamaker contour plot for infected white blood cell treated with VA

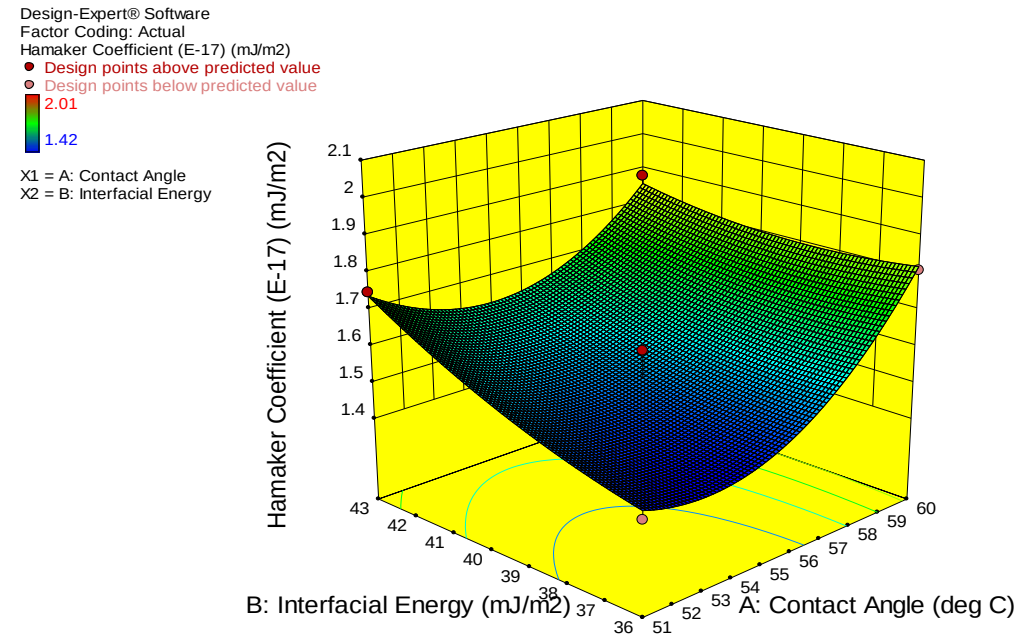

Fig 4.41: 3-D Hamaker Coefficient Surface plot of Infected WBC Treated with VA

Table 4.32(a-g) is a Hamaker response analysis obtained using Neumann model for infected white blood cell treated with BP(Appendix E50) and Fig 4.42 and 4.43 displayed the contour and surface plots. The quadratic model is suggested and focus is on the model maximizing the "Adjusted R-Squared" and the "Predicted R-Squared. The Model F-value of 346.67 implies the model is significant. There is only a 0.001% chance that an F-value this large could occur due to noise. Values of "Prob > F" less than 0.0500 indicate model terms are significant.

The ANOVA indicates the equation and actual relationship between the response and significant variables represented by the equation 4.19 are accurate. The R^2 value of 0.9960 indicates a good measure that outcomes are likely to be predicted well by the developed models. The contour and the surface plot also reveal graphically the interaction between the independent variable and the response surface.

Table 4.32a: Response SummaryHamaker with BP

Source	**Sequential p-value**	**Lack of Fit p-value**	**Adjusted R-Squared**	**Predicted R-Squared**
Linear	0.2034	< 0.0001	0.1273	-0.5060
2FI	0.0038	0.0002	0.6361	0.4293
Quadratic	< 0.0001	0.3307	0.9931	0.9817
Cubic	0.8292	0.1145	0.9910	0.8769

Table 4.32b: Sequential Model Sum of Squares

Source	Sum of Squares	Df	Mean Square	F Value	p-value Prob > F
Mean vs Total	38.94	1	38.94		
Linear vs Mean	0.15	2	0.074	1.88	0.2034
2FI vs Linear	0.25	1	0.25	14.98	0.0038
Quadratic vs 2FI	0.15	2	0.073	233.98	< 0.0001
Cubic vs Quadratic	1.566E-004	2	7.830E-005	0.19	0.8292
Residual	2.012E-003	5	4.025E-004		
Total	39.48	13	3.04		

Table 4.32c:Lack of Fit Tests

Source	Sum of Squares	df	Mean Square	F Value	p-value Prob > F
Linear	0.39	6	0.065	260.80	< 0.0001
2FI	0.15	5	0.029	116.94	0.0002
Quadratic	1.169E-003	3	3.897E-004	1.56	0.3307
Cubic	1.012E-003	1	1.012E-003	4.05	0.1145
Pure Error	1.000E-003	4	2.500E-004		

Table 4.32d: Model Summary Statistics

Source	Std. Dev.	R-Squared	Adjusted R-Squared	Predicted R-Squared	PRESS
Linear	0.20	0.2728	0.1273	-0.5060	0.81
2FI	0.13	0.7271	0.6361	0.4293	0.31
Quadratic	0.018	0.9960	0.9931	0.9817	9.876E-003
Cubic	0.020	0.9963	0.9910	0.8769	0.066

Table 4.32e:Quadratic Model Summary

Std. Dev.	0.018
Mean	1.73
C.V. %	1.02
PRESS	9.876E-003
R-Squared	0.9960
Adj R-Squared	0.9931
Pred R-Squared	0.9817
Adeq Precision	63.114

Table 4.32f: ANOVA for Hamaker Response Surface Quadratic Model for BP

Source	**Sum of Squares**	**D*f***	**Mean Square**	**F-Value**	**P-Value Prob > F**	
Model	0.54	5	0.11	346.67	< 0.0001	Significant
A-Contact Angle	*0.012*	*1*	*0.012*	*39.12*	*0.0004*	
B-Interfacial Energy	*0.13*	*1*	*0.13*	*435.57*	*< 0.0001*	
AB	*0.25*	*1*	*0.25*	*790.73*	*< 0.0001*	
A^2	*0.15*	*1*	*0.15*	*467.94*	*< 0.0001*	
B^2	*2.611E-003*	*1*	*2.611E-003*	*8.43*	*0.0229*	
Residual	2.169E-003	7	3.099E-004			
Lack of Fit	*1.169E-003*	*3*	*3.897E-004*	*1.56*	*0.3307*	*not significant*
Pure Error	*1.000E-003*	*4*	*2.500E-004*			
Cor Total	0.54	12				

Table 4.32g: Hamaker CoefficientModel Equation for Infected White Blood Treated with BP

Factor	Coefficient Estimate	Df	Standard Error	95% CI Low	95% CI High	VIF
Intercept	1.63	1	7.872E-003	1.61	1.65	
A-Contact Angle	-0.039	1	6.224E-003	-0.054	-0.024	1.00
B-Interfacial Energy	0.13	1	6.224E-003	0.12	0.14	1.00
AB	0.25	1	8.802E-003	0.23	0.27	1.00
A^2	0.14	1	6.674E-003	0.13	0.16	1.02
B^2	0.019	1	6.674E-003	3.593E-003	0.035	1.02

Hamaker coefficient model equation for infected white blood treated with BPis given as:

$$A_{132} = 1.63 - 0.039A + 0.13B + 0.25AB + 0.14A^2 + 0.019B^2 \quad (4.19)$$

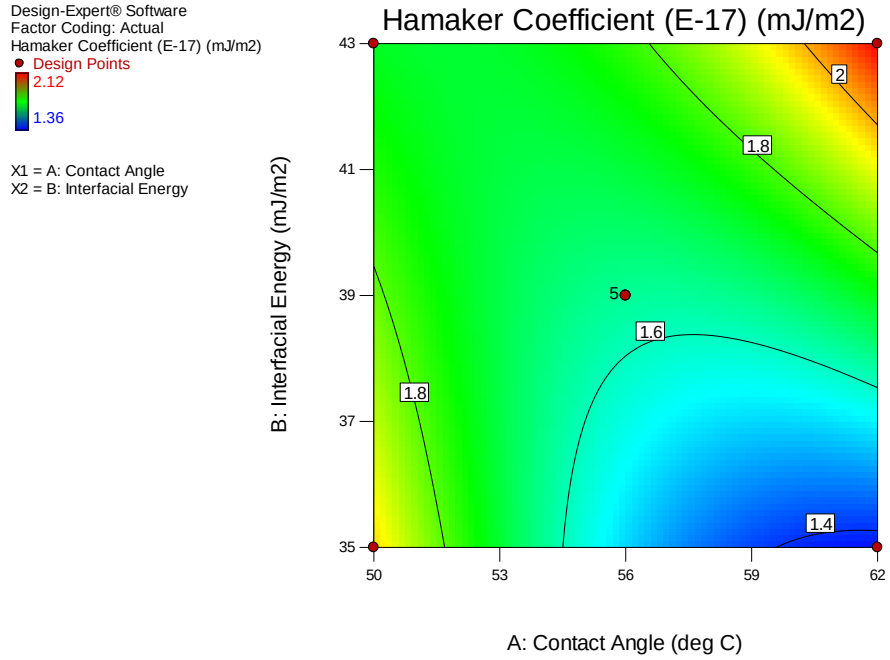

Fig 4.42: Hamaker contour plot for infected white blood cell treated with BP

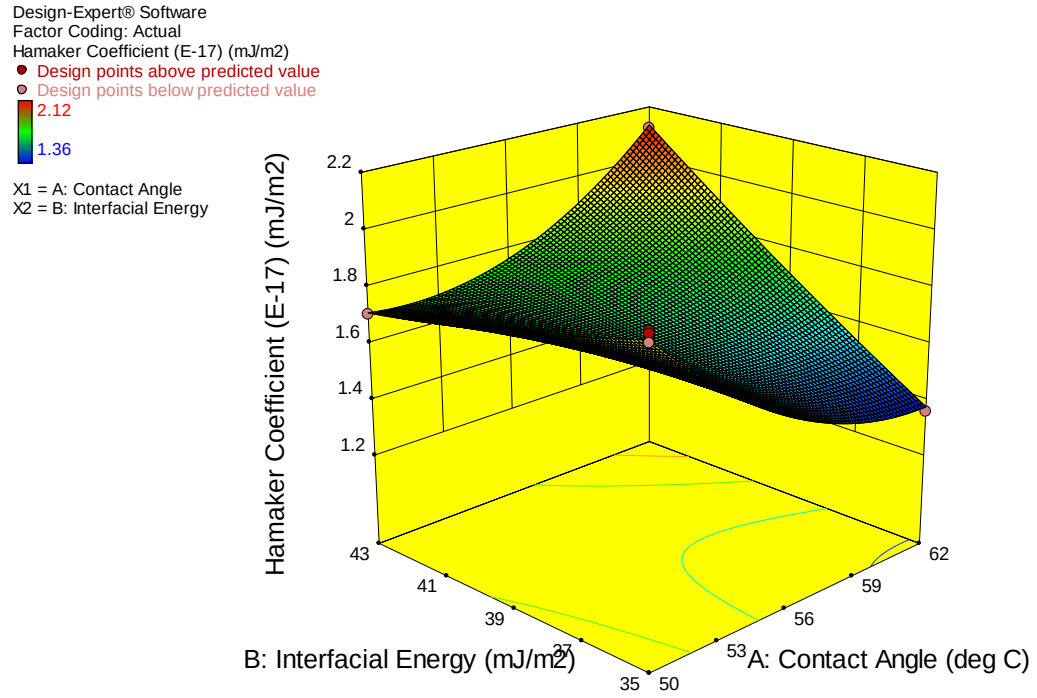

Fig 4.43:3-D Hamaker Coefficient Surface plot of Infected WBC Treated with BP

Table 4.33(a-g) is a Hamaker response analysis obtained using Neumann model for infected white blood cell treated with DH(Appendix E50) and Fig 4.44 and 4.45 displayed the contour and surface plots. The quadratic model is suggested and focus is on the model maximizing the "Adjusted R-Squared" and the "Predicted R-Squared. The Model F-value of 350.85 implies the model is significant. There is only a 0.001% chance that an F-value this large could occur due to noise. Values of "Prob > F" less than 0.0500 indicate model terms are significant.

The ANOVA indicates the equation and actual relationship between the response and significant variables represented by the equation 4.20 are accurate. The R^2 value of 0.9960 indicates a good measure that outcomes are likely to be predicted well by the developed models. The contour and the surface plot also reveal graphically the interaction between the independent variable and the response surface.

Table 4.33a: Hamaker Response Summary with DH Treatment

Source	**Sequential p-value**	**Lack of Fit p-value**	**Adjusted R-Squared**	**Predicted R-Squared**
Linear	0.3309	< 0.0001	0.0381	-0.3686
2FI	0.9594	< 0.0001	-0.0684	-0.7133
Quadratic	< 0.0001	0.5392	0.9932	0.9853
Cubic	0.9751	0.1926	0.9906	0.9005

Table 4.33b: Sequential Model Sum of Squares

Source	Sum of Squares	Df	Mean Square	F Value	p-value Prob > F
Mean vs Total	45.35	1	45.35		
Linear vs Mean	0.081	2	0.041	1.24	0.3309
2FI vs Linear	1.000E-004	1	1.000E-004	2.741E-003	0.9594
Quadratic vs 2FI	0.33	2	0.16	702.14	< 0.0001
Cubic vs Quadratic	1.636E-005	2	8.180E-006	0.025	0.9751
Residual	1.613E-003	5	3.225E-004		
Total	45.76	13	3.52		

Table 4.33c: Lack of Fit Tests

Source	Sum of Squares	df	Mean Square	F Value	p-value Prob > F
Linear	0.33	6	0.055	218.33	< 0.0001
2FI	0.33	5	0.065	261.92	< 0.0001
Quadratic	6.289E-004	3	2.096E-004	0.84	0.5392
Cubic	6.125E-004	1	6.125E-004	2.45	0.1926
Pure Error	1.000E-003	4	2.500E-004		

Table 4.33d:Model Summary Statistics

Source	Std. Dev.	R-Squared	Adjusted R-Squared	Predicted R-Squared	PRESS
Linear	0.18	0.1985	0.0381	-0.3686	0.56
2FI	0.19	0.1987	-0.0684	-0.7133	0.70
Quadratic	0.015	0.9960	0.9932	0.9853	6.034E-003
Cubic	0.018	0.9961	0.9906	0.9005	0.041

Table 4.33e:Quadratic Model Summary

Std. Dev.	0.015
Mean	1.87
C.V. %	0.82
PRESS	6.034E-003
R-Squared	0.9960
Adj R-Squared	0.9932
Pred R-Squared	0.9853
Adeq Precision	54.226

Table 4.33f: ANOVA for Hamaker Response Surface Quadratic Model for DH

Source	**Sum of Squares**	**D*f***	**Mean Square**	**F-Value**	**P-Value Prob > F**	
Model	0.41	5	0.082	350.85	< 0.0001	Significant
A-Contact Angle	*2.136E-003*	*1*	*2.136E-003*	*9.18*	*0.0191*	
B-Interfacial Energy	*0.079*	*1*	*0.079*	*340.35*	*< 0.0001*	
AB	*1.000E-004*	*1*	*1.000E-004*	*0.43*	*0.5331*	
A^2	*0.042*	*1*	*0.042*	*182.47*	*< 0.0001*	
B^2	*0.31*	*1*	*0.31*	*1326.25*	*< 0.0001*	
Residual	1.629E-003	7	2.327E-004			
Lack of Fit	*6.289E-004*	*3*	*2.096E-004*	*0.84*	*0.5392*	*not significant*
Pure Error	*1.000E-003*	*4*	*2.500E-004*			
Cor Total	0.41	12				

Table 4.33g: Hamaker Model Equation for Infected White Blood Treated with DH

Factor	Coefficient Estimate	D*f*	Standard Error	95% CI Low	95% CI High	VIF
Intercept	1.69	1	6.822E-003	1.67	1.71	
A-Contact Angle	0.016	1	5.393E-003	3.586E-003	0.029	1.00
B-Interfacial Energy	0.099	1	5.393E-003	0.087	0.11	1.00
AB	5.000E-003	1	7.627E-003	-0.013	0.023	1.00
A^2	0.078	1	5.784E-003	0.064	0.092	1.02
B^2	0.21	1	5.784E-003	0.20	0.22	1.02

Hamaker coefficient model equation for infected white blood treated with BPis given as:

$$A_{132}=1.69+0.016A+0.099B+5.00E\text{-}003AB+0.078A^2+0.21B^2 \quad (4.20)$$

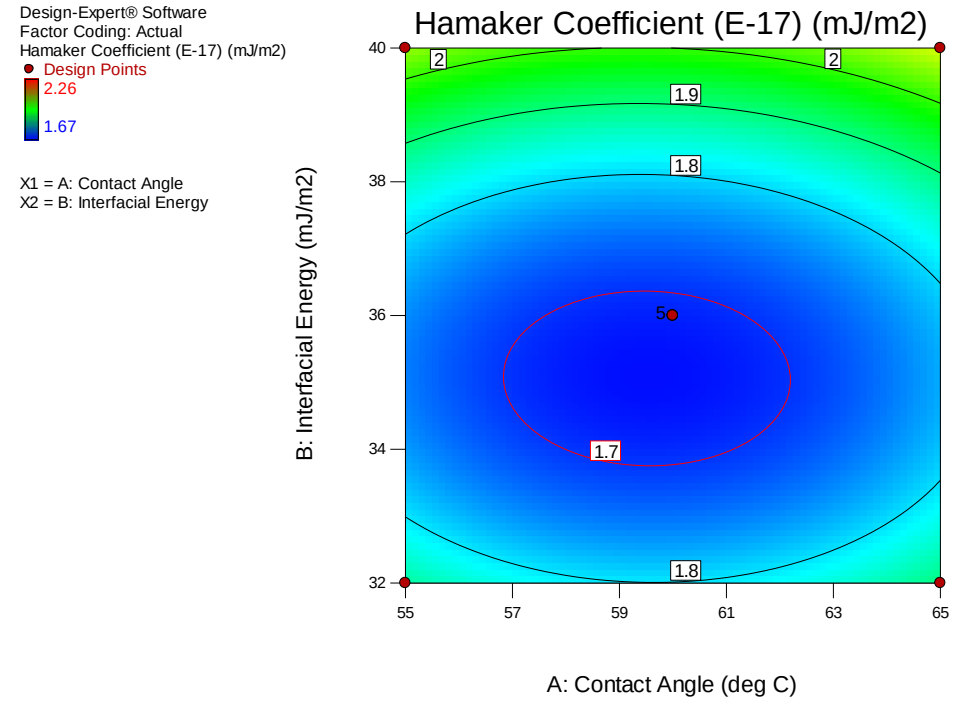

Fig 4.44: Hamaker contour plot for infected white blood cell treated with DH

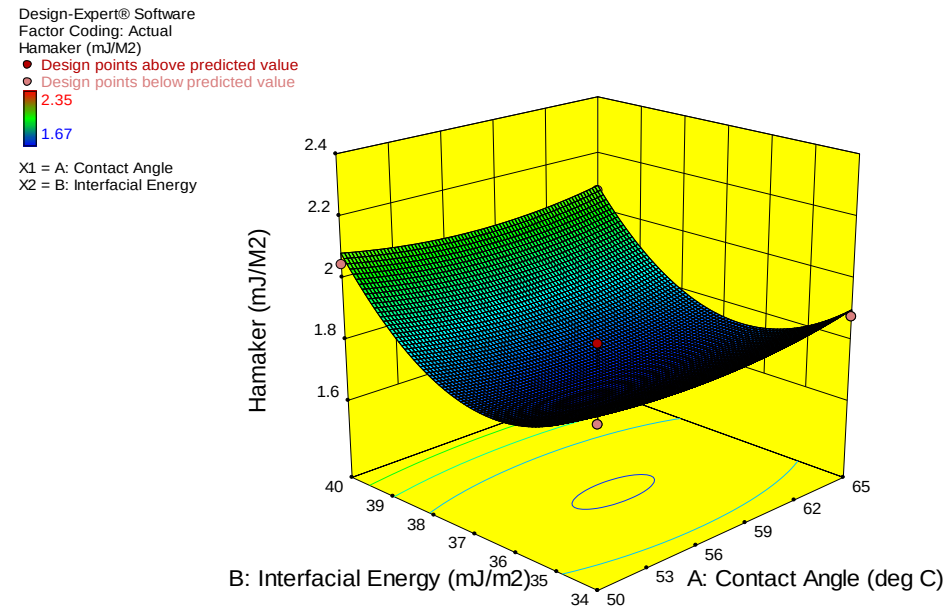

Fig 4.45:3-D Hamaker Coefficient Surface plot of Infected WBC Treated with DH

The significance of the coefficient term is determined by the values of *F* and *p*, and the larger the value of *F* and the smaller the value of *p*, the more significant the model becomes (Kalavathy et al. 2009).

In all treatments given in this study for the determination of Hamaker coefficien, when analyzed using response surface (Table4.26a-4.33g) revealed that in each case considered, the larger the F-value, the smaller the p- value. The p-value in all cases is less than 0.05 suggesting the model equations (4.11-4.20) to be considered statistically significant making most of the variations in the response explainable by the model equations. The probability $p < 0.0001$ also validated the models are significant.

Also considering the R^2 values from Table (4.26-4.33), the "Predicted R^2" is in reasonable agreement with the "Adjusted R^2". "Adequacy Precision" measures the signal to noise ratio. It is reported that a ratio greater than 4 is desirable. In all scenario considered in this study, the adequacy precision ratio far above 4 was obtained, suggesting an adequate signal and also the data points were well distributed close to a straight line (R^2 close to 1), which suggested an excellent relationship between the experimental and predicted values of the response, and the underlying assumptions of the above analysis were appropriate. The results also indicated that the selected quadratic model was adequate in assuming the response variables for the experimental data. The contour and the surface plots also in each case revealed the interaction between the independent variables and the response

4.10 Determination of the Negative Concept of Hamaker Coefficient.

The concept of negative Hamaker is employed in this study to check the feasibility of separating the lymphocytes and the hepatitis c virus. As earlier stated in the preceding chapters, it is a principle rooted on the net van der Waal forces of attraction and repulsion. The Hamaker constant on each blood samples is used to predict the attraction or possibly rejection of particulate matters interacting in a given system. Any of the treatments administered in this study that have the ability of rendering the combine Hamaker coefficient(A_{132}) negative is proposed as an additive(s) to the serum which will separate hepatitis C virus from the lymphocyte cells.

Table 4.34 is the mean of the individualHamaker constantsA_{11}, A_{22}, and A_{33} of the total of ten samples of the blood used for this study to yield the average A_{132} of infected, uninfected and the various treatments administered.

Table 4.34: Average Hamaker Coefficient (A_{132}) using Neumann Model for WBC

			Treated(A_{132})$\varkappa$**10^{-17}**							
Blood Cells	**Infected**(A_{132}) $\varkappa$**10^{-17}**	**Uninfected** (A_{132}) $\varkappa$ **10^{-17}**	**IFN**	**RBV**	**ATR**	**ELT**	**AM**	**VA**	**BP**	**DH**
WBC	2.24± 2.15	1.25± 1.71	1.81 ± 2.88	1.77 ± 2.80	1.62± 3.16	1.81± 2.23	1.92± 2.11	1.72± 1.98	1.78± 2.35	1.99± 2.14
Serum	2.11± 2.04	1.60± 2.48	1.86 ±3.13	1.77 ± 2.23	1.78± 2.23	1.79± 2.11	2.02± 2.62	1.73± 2.01	1.68± 2.44	1.57± 2.93

As stated in eqn (3.31-3.34), the condition for rendering combined Hamaker coefficient negative is that Hamaker constant A_{ii} is greater than A_{kk} which is also greater than A_{jj}. The infected lymphocytes are assumed to be an approximation of the virus A_{jj}. The energies of the interactionseen in table 4.30were computed using equations (3.31-3.34). Taking i=1,j=2 and k=3

Table 4.35: Computation for Combined Negative Hamaker Coefficient (mJ/m^2)

		$A_{11}(mJ/m^2)$	$A_{22}(mJ/m^2)$	$A_{33}(mJ/m^2)$	$A_{131}(mJ/m^2)$	$A_{232}(mJ/m^2)$	$A_{132}(mJ/m^2)$
	Infected		$0.224x10^{-16}$	$0.211\ x10^{-16}$	-	$1.103\ x10^{-18}$	$-0.150\ x10^{-18}$
	Uninfected	$0.125\ x10^{-16}$	-	$0.160\ x10^{-16}$	$0.21\ x10^{-18}$	-	-
Treated	IFN	-	$0.181\ x10^{-16}$	$0.186\ x10^{-16}$	$0.593\ x10^{-18}$	$0.36\ x10^{-20}$	$0.462\ x10^{-19}$
	RBV	-	$0.177\ x10^{-16}$	$0.176\ x10^{-16}$	$0.423\ x10^{-18}$	$0.40\ x10^{-21}$	$-0.132\ x10^{-19}$
	ATR	-	$0.162\ x10^{-16}$	$0.178\ x10^{-16}$	$0.463\ x10^{-18}$	$0.36\ x10^{-20}$	$1.291\ x10^{-19}$
	ELT	-	$0.181\ x10^{-16}$	$0.179\ x10^{-16}$	$0.476\ x10^{-18}$	$0.40\ x10^{-21}$	$-0.138\ x10^{-19}$
	AM	-	$0.192\ x10^{-16}$	$0.202\ x10^{-16}$	$0.903\ x10^{-18}$	$1.20\ x10^{-20}$	$1.045\ x10^{-19}$
	VA	-	$0.172\ x10^{-16}$	$0.171\ x10^{-16}$	$0.348\ x10^{-18}$	$0.10\ x10^{-21}$	$-0.592\ x10^{-20}$
	BP	-	$0.178\ x10^{-16}$	$0.168\ x10^{-16}$	$0.314\ x10^{-18}$	$1.44\ x10^{-20}$	$-0.672\ x10^{-19}$
	DH	-	$0.199\ x10^{-16}$	$0.157\ x10^{-16}$	$0.176\ x10^{-18}$	$2.50\ x10^{-19}$	$-0.210\ x10^{-18}$

The combined negative Hamaker coefficientof the different treatments administered to the blood samples are shown in table 4.35. The A_{132} of the infected sample was seen to be -0.150 $x10^{-18}mJ/m^2$ = - 0.150 $x10^{-25}J$. This is in agreement with the value reported in literature in the work of Achebe(2013) stating that HIV infected cell using the Hamaker approach has a combined negative Hamaker of -0.281 $x10^{-25}J$. Both results have suggested the possibility of applying the concept of negative Hamaker as a method of separation.

The interaction energyA_{131} and A_{232} are all positive indicating the dominance of van der Waal forces of attraction as the particles interacts with the serum. The energy of interaction of the lymphocytes 0.21 $x10^{-18}mJ/m^2$ is observed to be less than that of the infected cell 1.103 $x10^{-18}mJ/m^2$. This is due to the presence of the virus in increasing the interaction energy of the infected cells. The near zero value of the uninfected sample (0.21 $x10^{-18}$ mJ/m^2=0.21 $x10^{-25}J$) indicates absence of infection on the samples and also buttresses the relevance of the concept.

The treatments given in each case as can be seen from table 4.35 tries to reduce the interaction energy of the virus (A_{232}) by boosting that of the lymphocytes(A_{131}).

This action of the treatments can lead to a reduction in viral loads and also an increase in CD4 count of the infected cells but cannot guarantee virological clearance or total separation of the virus from the lymphocytes. This is known as functional cure as is the case of most conventional drugs used for the treatment of hepatitis C virus. As times goes on, the viral replication will still over power the immune system security of the lymphocyte. That is the reason why most conventional antiviral drugs used for this study even when they reduce the interaction energy of the virus but are still unable to render the combined Hamaker coefficient negative.

RBV and ELT are the only conventional treatment that rendered combined Hamaker negative out of the four conventional drugs used for this study but they have a lot of psychological effects like suicidal urge, mental disorder and above all are very expensive thereby making it inaccessible for patients of low income(Calland et al, 2012;AASLD, 2015).

Three herbal drugs (VA,BP and DH) out of the four used for this study were able to render combined Hamaker coefficient(A_{132}) negative as can be seen from table 4.35.This implies that these herbal drugs could be effective for the treatment of hepatitis c virus as claimed by practitioners of complementary and alternative medicine. The negative combined Hamaker coefficient guarantees van der Waal forces of repulsion will prevail causing the drug coated lymphocytes to repel the virus.The marker for accessing treatment success medically is shown as proposed criteria for HCV-drug interaction in table 4.36.

Table 4.36: Medical and thermodynamic Criteria for HCV clearance

Efficacy	**Virological**		**Immunological**	**Clinical**	**Thermodynamic**	
Marker	**Viral Load**		**CD4 Cells Count**	**Clinical Stage**	**Absolute Combined Hamaker Coefficient of HCV-Drug Coated Blood Interaction.**	
Time	24weeks	48weeks	24-48weeks	12weeks	24weeks	48weeks
Suggested Range	<400copies/ml of HCV	<50copies/ml of HCV	Increase from baseline by atleast50-100cell/mm^3	Acute or Chronic	Negative value for combine A_{132} of HCV infected blood	Increase negative value for combine A_{132} for HCV positive blood.
Response	Reduced viral load to clinically undetectable levels.		Increased CD4 cells counts to atleast 350cells/mm^3	Symptoms of HCV infection subside	Net Repulsive van der Waals forces between HCV and drug coated lymphocytes resulting in increasein surface energy of HCV positive blood.	

4.11 Validation of Results

The results obtained in this study were compared with those in existing literature as seen in table 4.37. The contact angle obtained from this study ($63.4^0 \pm 3.20$) is in agreement with the work of Ozoihu (2014) and also with that obtained by the American Society of Microbiology (1984) for Bacteria infected Human cells using the equation of state.

The surface free energy obtained from this study (33.54 ±2.31 mJ/m^2) was also compared with the values of 34 mJ/m^2 obtained from the work of ASM (1984), 31.81 mJ/m^2 obtained from Ozoihu (2014), Ani et al (2015) obtained a value of 39.5 mJ/m^2 and Chukwuneke et al (2015) got a value 38.5 mJ/m^2. Table 4.37 shows that the value obtained for surface free energy in this study is in reasonable agreement with the values obtained from the works of these pioneer researchers.

The value of critical Hamaker constant $0.211x10^{-23}J$ for serum and the combined Negative Hamaker coefficient values obtained from this study ($-0.150x10^{-25}J$) were also compared with the existing literature and the results abtained are in agreement as can be seen from Table 4.37. Achebe (2013) obtained the values of $0.976x10^{-21}$ J and $-0.281x10^{-25}$ J for Hamaker constant for serum and combined negative Hamaker coefficient respectively. Values of $0.190x10^{-23}J$ for Hamaker constant for serum and $-0.664x10^{-26}J$ for combined negative Hamaker coefficient were obtained from the work of Ozoihu (2014). Chukwuneke et al (2015) obtained $0.957x10^{-21}J$ for Hamaker constant for serum and $-0.23x10^{-26}J$ for combined negative Hamaker coefficient as can be seen from Table 4.37

Table 4.37: Validation data

References	Neumann et al, (1974)	Iweriolor, (2019)	ASM, (1984)	Achebe et al,(2013)	Ozoihu (2014)	Ani et al,(2015)	Chukwuneke et al,(2015)
Method		Contact Angle	State equation	UV photometer	Contact Angle	UVphotometer	UV photometer
Organism		HCV	Bacteria	HIV	HIV	HIV	M-TB/HIV
Θ^0		63.4±3.20	67		63.7		
γ_{sv} (mJ/m^2)		33.54 ±2.31	34 ±3.45		31.81	39.5	38.5
A_{33c} (J)	$\times 10^{-14}$--$\times 10^{-24}$	$0.211x10^{-23}$		$0.976x10^{-21}$	$0.190x10^{-23}$		$0.957x10^{-21}$
Combined Neg. Hamaker (A_{132})		$-0.150x10^{-25}$J		$-0.281x10^{-25}$ J	$-0.664x10^{-26}$J		$-0.23x10^{-26}$J

Table 4.38: Thermodynamic Response Predicted Treatment for HCV Infected Patients

Drug Name	Drug Size	Prescri-bed Dose	Drug Type	Combine Hamaker Coeff. Value(A_{132})	Van der Waal Interaction sign	Thermo-dynamic Response	Treatment Prediction
IFN	0.5ml	Once daily	Injection / Single	0.462×10^{-19}	positive	Attraction	Treatment success unpredicted
RBV	200mg	Twice daily	Tablet/ single	-0.132×10^{-19}	Negative	Repulsion	Treatment success predicted
ATR	300mg/ 100mg	Once daily	Tablet/ single	1.291×10^{-19}	positive	Attraction	Treatment success unpredicted
ELT	600mg/ 300mg/ 300mg	Once Daily	Tablet/ DAA	-0.138×10^{-19}	Negative	Repulsion	Treatment success predicted
AM	200mg	Twice Daily	Powder/s ingle	1.045×10^{-19}	positive	Attraction	Treatment success unpredicted
VA	200mg	Twice Daily	Powder/s ingle	-0.592×10^{-20}	Negative	Repulsion	Treatment success predicted
BP	200mg	Twice Daily	Powder/s ingle	-0.672×10^{-19}	Negative	Repulsion	Treatment success predicted
DH	100mg/ 200mg/ 400mg	Once Daily	Powder/ DAA	-0.210×10^{-18}	Negative	Repulsion	Treatment success predicted

The summary of thermodynamic response as regards to various treatments used for this study is depicted in Table 4.38. In all the treatments given, the increase in CD4 count and also reduced viral load is predicted but treatment success is only predicted for drugs capable of rendering combined Hamaker coefficient negative.

CHAPTER FIVE

CONCLUSION AND RECOMMENDATIONS

5.1 Conclusion

This study has in no doubt brought to limelight the essence of collaboration between engineers and practitioners in medical field for the purpose of interpreting and implementing this research result.The findings of this research has proved that the efficacy of some antiviral drugs are only limited to boosting the immune system of the infected patients by reducing the interaction energy of the virus (A_{232}) but cannot totally isolate the virus from the host(lymphocytes) as seen in samples treated with IFN, ATR and herbal drug AM.

The negative value of the combined Hamaker coefficient (A_{132}) for HCV infected sample (- 0.150 $x10^{-25}$J) signifiesthat van der Waal repulsion in the interacting particles is attainable. By this, the virus can be isolated from the lymphocyte when the serum acting as the intervening medium is altered.The negative values of the combine Hamaker coefficient obtained for each drug is as follows; RBV(-0.132 $x10^{-19}$=-0.132 $x10^{-26}$ J), ELT (-0.138 $x10^{-19}$=-0.138 $x10^{-26}$J), VA is (-0.592 $x10^{-20}$ =-0.592 $x10^{-27}$J), BP (-0.672 $x10^{-19}$=-0.672 $x10^{-26}$J) and that of DH is given as (-0.210 $x10^{-18}$=-0.210 $x10^{-25}$J).

It can also be concluded that additives administered to infected surfaces (63.4^0±3.20) in the form of drugs constitute better weting ability and have the capacity of reducing the contact angle of infected cells(IFN measured 56.9^0± 4.38, RBV is 56.3^0± 4.32, ATR measured contact angle is 56.6^0±5.25, ELT is 56.5^0±3.37 while 58.5^0±4.45, 55.5^0±3.02, 56.4^0±3.57 and 59.6^0±3.20 were measured for AM, VA, BP and DH respectively).The presence of the virus in the infected sample causes the surfaces to be poorly wetted and as such leads to an increase in the contact angle.

The investigation of the ethnomedicinal uses of the selected plants revealed that three out of the four plants used indicated separation of the virus from the blood cells, thereby making them candidates for clinical trials.

The energies of interaction (adhesion) are increased by the virus.The presence of the virus in infected cells causes an increase in the van der Waal forces of attraction. The energy of adhesionof the infected cells (-23.22±2.22mJ/m^2)wasobserved to be higher than that of the uninfected (-12.99 ±1.76mJ/m^2).

The negative sense of combined Hamaker coefficient on natural compounds under study suggests that they can be considered in the design of drugs since they are cheap and readily available and can be a better alternative for the ever expensive conventional antiviral drugs.

5.2 Contribution to Knowledge

- This research has verified the efficacy of herbal therapies for HCV treatments using contact angle approach.
- Model equations for the relationship between predicted response and variables in the interaction mechanism of HCV and blood cells have been proposed.
- The negative sense of the combined hamaker coefficient derived from the herbal extracts is a good indicator that these natural compounds will be effective for drug design.

5.3 Recommendations

- Thermodynamic response should be added to immunological and virological clearance used as a marker for determining efficacy of antiviral drugs on infected patients.
- Further experimentation of this work should be conducted *in vivo* since this study is totally *in vitro* based and results obtained should be compared.
- Hepatitis c virus and the various treatments given in this study should be further investigated using an alternative method to contact angle where absorbance measurement will be taken with Ultraviolet Visible Spectrophometer.
- The concept of negative Hamaker coefficient should also be employed in the determination of the efficacy of other antiviral drugs used for the treatment of

other deadly viral diseases like herpes simplex virus, mump virus, coscakie virus, avo virus etc.

- Pharmacist, engineers and other medical personnels should form an alliance in the manufacturing of some of these antiviral drugs for the purpose of calculating the interfacial surface energies and negative Hamaker coefficients of various drugs before marketing it so that the effectiveness of such drugs can be known.
- Surface thermodynamics investigation on herbal drugs should be extended to other viral diseases to check for their effectiveness in coating the virus.

REFERENCES

AASLD, (2015).Recommendations for testing, managing and treatment of hepatitis C. American Association for the Study of Liver Disease. Infectious Disease Society of America.

Abdelwahab, K.S. and Ahmed, Z.N. (2018). Status of hepatitis C virus vaccination. World Journal of Gastroenterology 22(2): 862-873

Achebe, C.H and Omenyi, S.N.(2013). Mathematical Determination of Critical Absolute Hamaker constant which favours repulsion in HIV-Blood Interactions.Proceedings of World Congress 0n Engineering Vol.2, London.

Achebe, C.H., Omenyi, S.N., Manafa, O.P., Okoli, D. (2012). HIV-blood interactions; surface thermodynamics approach. Proceedings of the International Conference of Engineers and Computer Scientist, Hong Kong.

Adeneye, A.A., Benebo, A.S. and Agbaje, E.O. (2006). Protective effect of aqueous extract and seed extract of phyllantus amarus on alcohol induced hepatoxicitty in rats. West African Journal of Pharmacol. Drug Res.22: 42-50

Agoha, R.C. (1974). Medicinal plants in Nigeria. Offset Arakkenji Faculfeider Wis Kunde, Netherlands 33: 41-42

Almeida, A.P., Da Silva, S.A.G., Souza, M.L., Bergmann, B.(2006).1-octen-3-0-aplha-l arabinopyranosyl-[1-6]-β- glucopyranosides; amino substance from leaves of pinnatum. Brazilian Journal of Pharmacognoosy 16(4): 485-489

Andreo, U., Millard, P., kalinina, O., Wallic, M., Meurs, E. (2007). Lipoprotein lipase mediates HCV entry and inhibits HCV infections. Cell Microbiol. 9: 2445-2456

Ani,O.I.(2016). Surface Energetics study of the interaction between HIV-Blood Blood Cells Treated with Antiretroviral Drugs. Ph.D thesis, UNIZIK, Nigeria

Anonymous(2000).Http://www.chemie.unibonn.de/oc/ak/br/analytical/Nigeria/vernonia/vern.inf.html.

Awomukwu D. A., Nyananyo B. L., Onukwube N. D. , Uka C. J. , Okeke C. U. , Ikpeama A. I. (2014). Comparative Phytochemical Constituents and Pharmacognistic Importance of the Vegetative Organs of Some Phyllanthus Species in South Eastern Nigeria, International Journal of Modern Botany 2014, 4(2): 29-39 DOI: 10.5923/j.ijmb.20140402.01

Balunas, M.J. and Kinghorn, A.D. (2006). Drug discovery from medicinal plants. Life Sci. 78: 431-441

Barbose-Filho, J.M., Mederiros, C.P., Diruz, F.M., Batista, L. M.(2006). Natural products inhibitors of the enzyme acetylcholine sterase. Rev. Bvas farmacogn 16: 258-265

Bartenschlager, R., Penin, F., Lohmann, V., Andre, P. (2011). Assembly of infectious hepatitis C virus particles. Trends Microbiol. 19: 95-103

Barth, H., Liang, T.J. and Baurnert, T.F. (2006). Hepatitis C virus entry; molecular biology anf clinical implications. Hepatology 44: 527-535

Barth, H., Ulsenheimer, A., Schafer, C., Adah, M.I. (2003). The cellular binding of hepatitis C virus envelope glycoprotein E2 requires cell surface heparan sulfate . Journal of Biol. Chem 278: 41003-41012

Basu, A., Kanda, T., Beyene, A., Saito, K., Meryer, K.(2007). Sulfated homologous of heparin inhibit HCV into mammalian cells 81: 3933-3941

Bellantani, S., Pozzato, G., and Saccoccio, G.(1999).Clinical course and risk factorsof hepatitis c virus related liver disease in the general population . J Virol.44(6): 870-80

Belouzard, S.,Cocquerel, L. and Dubuisson , J. (2011).Hepatitis C virus entry into the hepatocyte. Cent. Eur. J of Biol.6: 1-13

Benedicto, I., Molina-Jimenez, F., Bartosch, B., Prieto, J.(2009).Tight junction associated protein occluding is required for post binding step in hepatitis C virus entry and infection . J Virol. 83 : 8012-8020

Blanchard, E., Belouzard, C., Goueslain, L., Rouille, Y., Wakita, T. (2006). Hepatitis C virus entry depends on clathrin-mediated endocytosis. J Virol. 80: 6964-6972

Boyer, J.L.(2011). Liver cirrhosis and its development. Proceedings of falk symposium 115, Springer. Pp 344. ISBN 978-0-7923-8760-2

Brazzzoli, M., Bianchi, A. and Fillipini, C.(2008). CD81 is a central regulator of cellular events required for hepatitis C virus entry. J Virol. 82: 5007-5020

Brok, J.,Gluud, L. L. and Gluud, C.(2010).Ribavirin plus interferon versus interferon for hepatitis C . Cochrane Database System Review 1: CD005445

Calland, N., Dubuisson, J. and Rouilley, Y.(2012). Hepatitis C virus and natural compound, a new antiviral approach. Viruses

Cambi, A., Koopman, M. and Fidgdor, C.G.(2005). How C-type lectins detects pathogens. Cell Microbiol. 7: 481-488

Carreno, V. (2006). Occult hepatitis C virus infection; a new form of hepatitis C. World Journal of Gastroenterology 12(43): 6922-6925

Castera, L., Sabastiani, G.,Le Bail, B., Haaser, M., Alberti, A.(2010). Prospective comparison of two algorithm combining non invasive method of staging liver fibrosis in chronic hepatitis C. J. Hepatol. 52:191-198

Catanese, M.T., Uryu, K., Kopp, M.,Andre, P.(2013). Ultrastructural analysis of hepatitis C virus particles. Proc. Natl. Acad. Sci.USA. 110, 9505-9510

Cavallaro,L., Garcia, G. and Broussalis, A. (1995).Anti- herpetic in vitro activity of gamochaeta simplicicaulis extracts. Phytother. Res. 9: 176-179

Chapel, H.M., Christie, J.M., Peach, V., Chapman, R.W. (2001). Five years follow up of patients with deficiencies following an outbreak of acute hepatitis C. Clinical Immunol. 99 :320-324 . Science 244(4902): 359-362.

Chukwuneke, J.L.(2015) Surface Energetic Study of MTB. Ph.D thesis, UNIZIK.

Connely, M.A. and Williams, D.L.(2003). Scavenger receptor class B type 1 and cholesterol uptake into steroidogenic cells. Trends Endocrinol. Metab.14 (10): 467-472.

Cukierman, L., Meertens, L., Bertanx, C., Kajumo, F., Dragil, T.(2009). Residues in a highly conserved claudin-1 motif are required for HCV entry and mediate cell to cell formation. J Virol. 83: 5477-5484

Danov, K.D., Denkov, N.D.,Petsev, D.N., Ivanov, I.B.(1993).Coalescene dynamics of deformable Brownian emulsion droplets. Langmuir 9: 1731-1740

Dao Thi, V.L., Granier, C. and Ziesel, M.B. (2012). Characterization of hepatitis C virus particles sub-populations reveals multiple usage of SR-B1 for entry step. J Biol Chem.287:31242-31257

Dao Thi, V.L., Granier, C. and Zeisel, M.B.(2012). Characterization of hepatitis C virus particles sub populations reveals multiple usage of the scavenger receptor B1 for entry step. J Biol Chem.287: 31424-31257

De Clercq, E. (2013). Dancing with chemical formulae of antiviral; a panoramic view (part2). Biochemical Pharmacol 86(10):1907-1917

Den Brinker, M., Wit, F. and Dillen, P.M.(2000).Hepatitis B and C viral co-infection and the risk of hepatocixity of HAARTs in HIV-1 infection. AIDS 14: 2895-2902

Derrick, O., Esio, O., and Rhoda, H. (2007).Determination of contact angle from comtact area of liquid droplets spreading on solid substrate. Journal of Practices and Tech. 10: 29-38

Dervis, J. and Serez, K.(2005). The prevalence of dermatologic manifestation related to chronic hepatitis c infection in a study from a single centre in Turkey.Acta Dermatovenerol Alp Panonica Adriat. 14(3):93-8

Dienstag, J.L. and McHutchiso, J.G.(2006). American gastroenterological Association technical review on the management of hepatitis C. Gastroenterol. 130: 231-264

Dreux, M., Boson, B., Ricard-Blum, S., Molle, J., Lavilette, D., Pecheur, E.I.(2007). The exchangeable apolipoproteins Apo-C1 promotes membrane fusion of hepatitis c virus . J Biol Chem. 282, 32537-32369

Duraipandiyan, V., Ayyanar, M. and Igancimuthu, S. (2006). Antimicrobial activity of some ethmomedicinal plants used by Indian tribes. BMC Complementary and Alternative Med. 635EASL,(2015). European Association for the Study of Liver; recommendations on treatment of HCV infection.

El-Khourly, A.C., Klimack,W.K.,Wallace, C.,Razovi, H.(2011). Economic burden of hepatitis C associated disease in the United States.Journal of Viral Hepatitis 19(3):153-160

Eurosurvillance Editorial Team , (2011)"World Hepatitis Day 2011." Eurosurvillance 16(30)

Evans, M.J., VonHann, T., Tscherme, D.M., Syder, A.J., panis, M.(2007). Claudin-1 is a hepatitis C virus co-receptor required for late step in entry. Nature 446: 801-805

Farci, P., Shimoda, A., Wong, D., Cabeson, T. (1994).Prevention of hepatitis C virus infection in chimpanzees after antibody- mediated in vitro neutralization. Proc. Natl. Acad. Sci.USA. 91, 7792-7796

Faustino, A. F., Carvelho, F.A., Martins, I.C., Castanho, M.A., Almeida, F.C.(2014). Dengue virus capsid proteins interacts specifically with LDL. Nanomedicine 10(1): 247- 255

Feray, C., Gigou, M., Samuel, D., Ducot, B., Reynes, M. (1998). Incidences of hepatitis C in patients receiving different preparations of hepatitis B immunoglobulin after liver transplantation . Ann Intern Med. 128: 810-816

Flint, M., Manders, C., Shatton, C.,Monk, R.(199). Characterization of hepatitis C virus E2 glycoprotein interaction with putative cellular receptor, CD81. J.Virol. 73: 6235-6244

Flint, M., VonHahn, T., Zhang , J.,Farquhar, M., Jones, C.T.(2006). Diverse CD81 protein supports hepatitis C virus infection. J Virol 80: 11331-11342

Flori, N., Funakoshi, N. and Duny, Y. (2013). Pegylated interferon alpha 2a and ribavirin versus pegylated interferon alpha 2b and ribavirin in chronic hepatitis C;a metal analysis. Drugs 73(3): 263-277

Fukuhara, T., Kambara, H., Shiokawa, M., Ono, C., Kato, H.,Matsuura, Y.(2012). Expression of micro RNA facilitates an efficient replication in non hepatic cells upon HCV infection. J. Virol. 86: 7918-7933

Garg, G. and Kar, P.(2009). Management of hepatitis C infection ; current issues and future option. Trop. Gastroenterol.30: 11-18

Good, R. J. (1992).Contact angle, wetting and adhesion;a critical review. Journal of Adhesion Science and Technology 6 (12): 1269-1302

Good, R. J. and Girifalco, L. A.(1960). Surface and colloidal science, Phys. Chem. 64:561

Greber, U.F. and Gastaldelli, M.(2007). Junctional gating; the archilles heels of epithelial cells in pathogen infection . Cell Host Microbes 2 :143- 146

Grove, J., Huby, T., Stamataki, Z., Vanwollenghem, T., Mulleman, P.(2007). Scavenger receptor class B type 1 and B11 expression levels modulates hepatitis C virus infectivity. J Virol. 81: 3162-3169

Haid, S.,Novodomska, A., Gentzsch, J., Grethe, C.(2012). A plant derived flavonoid inhibits entry of all HCV genotypes into human hepatocytes. Gastroenterol. 143: 213-222

Hajarizadeh, B., Grebely, J. and Dore, G.J.(2013). Epidemology and natural history of HCV infection.Nat. Rev. Gastroenterol Hepatol 10: 553-562

Hamaker, H.C.(1936). The London/Van der wall attraction between spherical particles. Physics 4: 1058

Harbone, J.B., (1998) . Phytochemical methods. A grade to morden technologies of plant analysis, champaman and Hall, London.

Hargartner, l., Zinkernagel, R.M. and Hengartner, H.(2006). Antiviral antibody responses;the two examples of a wide spectrum. Natl. Rev Immunol. 6: 231-243

Helle, F., Wychoswski, C., Vu-Dac, N., Gustafson, K.R., Dubuisson, J.(2006). Cyanovirin-N inhibits hepatitis C virus by binding to envelop protein glycans. J Biol Chem 281: 25177- 25183

Hendrik, J., Anton , H., Henry, C., Van der Mel, Y. (1984). Applied and Enviromental Microbiology; University of Groningen,Antonius Deusinglam,Netherlands

Igeh, I.I. and Ejike, C.C. (2011).Current perspectives on the medicinal potentials of vernonia amygdalina. J Med. Plant Res. 5(7): 1051-1061

Illoh, E.O., Onyema-Illoh, O.B., Omogo, S.E., Agbafor, K.N., (2015) Preliminary Phytochemical screening of Ethanol extract of vernonia amygdalina,America-Eurasian Journal of Scientific research 10(4), 206-209

Ince, N. and Wands, J.R.(1999). The increasing incidences of hepatocellular carcinoma. N Engl. J Med. 340: 798-799

Jacob, J.R., Korba, B.E., You, J.E., Tenant, B.C., Kim, Y.H. (2004). Korean medicinal plant extracts exhibits potency against viral hepatitis. Journal of Alter. Complement. Med. 10: 1019-1026

Jacobson,T.M., Gordon, S.C. and Kowdley, K.V.(2013). Sofosbuvir for hepatitis C genotype 2 or 3 in patients without treatment option. N Engl J Med. 368(20):1867-1877

Jiang, J., Wu, X., Tang, H., Luo, G.(2013). Apolipoproteins-E mediates attachment of clinical hepatitis C virus to hepatocytes by binding to cell surface heparan sulfate proteoglycan receptor. PLOS (1): 8 e 67982

Joseph, B. and Raj, S.J. (2010). Phytopharmacological properties of ficcus racemesa linn; an overview. Int. J. Pharma. Sci. Rev. Res. 3: 134-138

Kalavathy, M.H., Regupathi, I., Pillai, M.G., Miranda, L.R., (2009). Modelling, analysis and optimization of adsorption parameters for H_3PO_4 activated rubber wood sawdust using response surface methodology (RSM). Colloids Surf B: 7035–45

Kapadia, S.B., Barth, H.,Baumert, T., McKeating, J.A., Chisari, F.V.(2007). Initiation of hepatitis C virus infection is dependent on cholesterol and cooperativity between CD81 and SB-R1. J Virol. 81: 374-383

Keck, Z.y., Li, T., Xia, J., Olson, O., Li, S., Ball, J.K.(2008). Definition of a conserved immunodormonant on hepatitis C virus E2 glycoprotein by neutralizing human monoclonal antibodies. Journal of Virol. 82: 6061-6066

Kondo, Y., Ueno, Y., Kakazu, E., Kobayashi,K., Inoue, J.(2011). Lymphotropic HCV strain can infect human CD4+ cells and affects their proliferation and IFN-alpha secretion activity. Journal of Gastroenterolo. 46:232-241

Koutosoudakis, G., Hermann, E., Kallis, S., Bartenschlager, R., Pietschmann, T. (2006).The level of CD81 cell surface expression is a key determinant for productive entry of hepatitis C virus into host cell. J Virol 60: 3004-3009

Krumpfer, J.W.,McCarthy, T.J. and Gao, L. (2010). Wetting properties of fluids. Physics of Fluids, Faraday discuss 146:103

Kwok ,D.Y.,and Neumann,A.W.,(1999).Contact angle measurements and contact angle interpretation" , Advances in colloid and interface science 81(167).

Kwok, D.Y and Neumann, A.W. (2003). Contact angle wettability and adhesion.Vol 3,VSP Int. Science, Boston. Pp117

Lai, M.E.,Mazzoleni, A.P., Argiolu, F., Devirgilis, S.,Balestrieri, A., Purcelli, R.H. (1994).Hepatitis C virus in multiple episode of acute hepatitis polytransfused thalassaemic children. Haul. 343:388-390

Lanvanchy, D (2009). The global of hepatitis C. WHO, Geneve, Switzerland.Liver Int.Medical research;

Lau, J.Y., Tam, R.C., Liang, T.J., Hong, Z. (2002). Mechanism of action of ribavirin in the combination treatment of chronic HCV infection. Hepatol.35:1002-1009

Laus, C.A (2006). Ethnomedicine used in Trinidad and Tobago for urinaryproblems and diabetics mellitus. J Ethnobiol. Ethnomed. 2:45

Lavillette, D., Tarr, A.W., Voisset, C., Bartosch, B., Barin, C. (2005). Characterization of host- range and cell entry properties of a major genotype and sub-genotypes of HCV. Hepatology 41:265-274

Lefevre, M., Felmlee, D.J., Parnot, M., Baumert,T. F., Schuster,C.(2014). Syndecan-4 is involved in mediating HCV entry through interactions with lipoviral particle-associated alipoprotein –E. Plos 1: 9 e 95550

Liang, T.J. and Ghany, M.G. (2013). Current and future therapy for HCV infection. N Engl J Med. 368(20):1907-1917

Lieber, C.S. (2001).Liver disease by alcohol and hepatitis C ; early detection and insight in pathogenesis leads to improved treatment . American Journal of Addictions 10:29-50

Lindenbach, B.D., Meuleman, P., Ploss, A., Vanwolleghem, T., McKeating, J.A., Major, M.E. (2006). Cells cultured –grown hepatitis C virus is infectious in vivo and can be recultured in vitro. Proc. Natl. Acad. Sci.USA. 103, 3805-09

Liu, M. M., Zhou, L., Zhang, Y.N.,Shen, Q.,Zuo, J. (2012). Discovery of flavonoid derivatives as anti-HCV agent via pharmacophore searching combining molecular docking strategy. Eur J Med. Chem. 52: 33-43

Liu, S., Yang, W., Shen, L., Coyne, C.B.(2009).Tight junction claudin-1 and occludin controls hepatitis C virus entry and are down regulated during infection to prevent superinfection. J Virol. 83: 1207-1212

Maheshwari, A. and Thuluvath, P.J.(2010). Management of acute hepatitis C. Clinics in Liver Disease. 14(1) :169-176

Marsh, M. and Helenius, A. (2006). Viral entry open sesame. Cell 124: 729-740McHutchison, M.G.(2000). Therapy of Chronic hepatitis C; standard treatment of standard patients. AASLD Postgraduate Course 136-142

Meertens, L., Bertaux,C. and Dragic, T. (2006). Hepatitis C virus entry requires a critical post-internalization step and delivery to early endosomes via clathrin coated vesicles. J Virol.80: 11571-11578

Mehrotra, R.S., Rawat, S., Goyal, P., Kulshreshtha, D.K.(1991).In vitro effects of phyllantus amarus on hepatitis B virus. Indian Journal of Med. Res 93: 71-73

Merz, A., Long, G. and Hiet, M.S. (2011). Biochemical and morphological properties of hepatitis C virus particle and determination of their lipidome.J Biol Chem 286: 3018-3032

Meunier, J.C., Engle, R.E., Faulk, K., Zhoa, M., Emerson, H.U. (2005). Evidence of cross-neutralization of hepatitis C virus pseudo-particles and enhancement of infectivity by apolipopreteinsC-1. Proc. Natl. Acad. Sci.USA.102: 4560-5

Miller, M.H., Agarwal, K. and Austin, A. (2015).British viral hepatitis group; British Society of Gastroenterology Liver Committee; British Association for the Study of Liver Disease, 2014 United Kingdom Consensus guidelines; hepatitis C management and DAAs. Pharmacol. Therapy 39(12): 1363-1375

Mohira, S., Castet, V., Fournier-Wirth, C., Avner, R., Harats, D., Coste, J. (2007). The LDL-R plays a role in the infection of primary human hepatocytes by HCV. Hepatology 46: 411-419

Momoh, M., Adikwu, M. and Oyi, A. (2010). Vernonia amygdalina and CD4 + cell counts; an immune study. Global Journal of Biotechnology and Biochemistry 5: 92-96

Monga, H.K., Rodrignez-Barradas, M.C., Breaux, K. (2001). Hepatitis C virus infection related morbidity and mortality among patients with HIV infections. Clin Infect. Dis. 33: 240-247

Morikawa, K., Zhao, Z., Date, T., Miyamoto, M., Murayama, A., Sone, S.(2007). The role of CD81 and glycosaminoglycans in the adsorption and uptake of infectious HCV particles. J Med. Virol. 79: 664-671

Mudi, S.Y. and Ibrahim, H. (2008). Brine shrimp lethality and antimicrobial susceptibility test from leaft extraxt of bryophyllium pinnatum and cassia occidentalis on respiratory tract infection causing bacteria. Proc. Chem Soc. Nig. 592-598

Murao, K., Imachi, H., Yu, X., Ahmed, R.A., Wong, N.C.(2008). Interferon alpha decreases the expression levels of human SB-R1 ; a possible HCV receptor in hepatocytes. Gut 57: 664-671

Naithani, R., Huma, L.C., Holland, L.E.,Shukla, D.,Mehta, R.G., Moriarty, R.M. (2008). Antiviral activity of phytochemicals; a comprehensive review.Mini Rev. Med.Chem 8: 1106-1133

National Institute of Health Consensus Development (1997). Management of hepatitis C infection; conference panel statement. Hepatology and Gastroenterology 45: 797-804

National Patients Safety Agency (2007). Safety in doses medication safety incidents in NHS. www.nrls.npsa .nhs.uk (accessed 2nd July 2018)

National Prescribing centre (2012), single competency framework for allprescribers, www.yurl.com accessed (02- July, 2018).

Neumann, A.W., Good, R.J., Hope C.J.,Segpal, M. (1974).Colloids and interfaces; equation of state approach to determine the surface tension of low energy fluids from contact angle. Colloid Interface Sci. 49: 291-304

Newmann, D.J. and Cragg, M.G. (2012). Natural products as sources of new drugs over the past 30 years from 1981 to 2010. Journal of Nat. Prod. 75: 311-335

Nomoto, A., Tsukiyama-Kohara, K., Linzuka, N., Kohara, M.(1992). Internal ribosomal entry site within hepatitis C virus RNA. Journal of Virol. 66: 1476-1483

Nursing and midwifery council (2015). The code:Professional Standards of practice and medicine management www.nmc.org.uk/global assets. (2ndJuly, 2018)

Nwanjo, H.U. (2005). Efficacy of aqueous leaf extract of vernonia amygdalina on plasma lipoprotein and oxidation status in diabetic rat models. Nigerian Journal of Physiological Science 20 (1-2):30-42

Odar, F. and Hamilton, W.S. (1964). Forces on a sphere accelerating a viscous fluid. J Fliud Mech. 18: 302-314 haemagylutinin. Anti microb Agents Chemotherapy 47: 2518-2525

Okoye E.J., Anyaegbunam, L.C, and Obi, Z.C. (2015) Pharmaceutical Constituents of leaf of bryophyllum pinnatum, journal of health medicine and nursing, vol 16

Okwu, D.E. (2008). Citrus fruits; a rich source of phytochemicals and other role in human health . A Review Int. J. Chem Sci.6 (2):451-471.

Okwu, D.E. and Ezenagu, V. (2008). Evaluation of the phytochemical composition of mango stem bark and leaves. Int. J Chem. Sci 6(2) : 705-716

Oluwafemi, F. and Debris, F. (2008). Antimicrobial effects of phyllantus amarus and parquetina nigrescens on salmonella typhi. African Journal of Biomed. Res. 11: 215-219

Omenyi, S.N., Newmann, A.W., Van Oss,C.J.,Absolom, D.R., Viser, J.(1980). Advance colloid interface Sci. 18:133

Omolara, J.O, Mathew O.O. and Abiola M.A 2016 comparative phytochemistry and antioxidant activities of Ethanol Extract of Anona muricata leaf.Advances in Biological Research 10(4), 230-235

Oura, K.,Lifshits, V.G.,Saranin,A.A., Zotov, A.V.(2001). Surface Science: An Introduction. Springer-Verlag: Berlin,223

Ozoihu, E.M. (2014). Human immunodeficiency virus; contact angle approach. Ph.D thesis, Unizik, Awka, Nigeria.

Pacific Island Ecosystem at Risk (2008)."Results set for anona muricata". United States Geological Survey and Forest Service

Page, K., Morris, M. D. and Maher, L. (2013). Injection drug use and hepatitis C virus in young adult injectors. Clin. Infect. Dis. Suppl 2:32-38

Pathak, P., Saraswathy, D.R. and Vora, A.(2010).In vitro antimicrobial activity and phytochemical analysis of the leaves of anona muricata. Int. J Pharm. Res. Dev. 2(5)

Pawlotsky, J.M. (2014). New HCV drugs and hope for a cure; concepts in anti-HCV drug development. Semin. Liver Dis. 34: 22-29

Perez-Olmeda, M., Garcia-samaniego, J. and Sorrianno, V. (2000). Hepatitis C viremia in HIV-HCV co-infected patients having immune restoration with HAARTs. AIDS 14:212

Pessione, F.,Degos, F. and Marcellin, P.(1998). Effects of alcohol consumption on serum hepatitis virus RNA and histological lessons in chronic hepatitis C. Hepatol 28: 805-809

Pestka, J.M., Zeisel, M.B.,Blaser, E., Schurmann, P., Bartosch , B., Cosset,F.L. (2007).Rapid induction of virus neutralizing antibodies and viralclearance in a single source outbreak of hepatitis C. Proc. Natl. Acad. Sci.USA. 104: 6025-6030

Pham, T.N., Coffin,C.S. and Michalak, T.I .(2010). Occult hepatitis C virus infection; what does it mean.Liver International, Official Journal of the International Association for the Study of Liver. 30(4):502-511

Poordad, F., McCone, J., Bacon, B. R., Bruno, S.,Manns, M.P.,Reddy, K.R.(2011). Boceprevir for untreated chronic HCV genotype infection. N Engl. J Med. 304: 1195-1206

Powell, E.E., Edwards-Smit, C.J. and Hary, L.J.(2010).Host factors influences disease progression in chronic hepatitis C . Hepatol 31: 828-833

Preetha R, Jayaprakash SN, Rosamma P, Bright Singh IS. (2007). Optimization of carbon and nitrogen sources and growth factors for the production of an

aquaculture probiotic (Pseudomonas MCCB 103) using response surface methodology. J Appl Microbiol102:1043–10

Public Health Agency of Canada, (2006). Hepatitis C prevention, support and research program health. Canada. Retreieved 24th sept, 2016

Puoti, M., Gargiulo, F. and Rolden, E.Q. (2000).Liver damage and kinetics of hepatitis C virus and HIV replication during the early phase of combination of antiretroviral treatment. Journal of Infectious Dis. 181: 2035-2036

Purcell, R. H. and Bukh, J.(2006). A milestone for hepatitis C virus research; avirus generated in cultured cell is fully viable invivo. Proc. Natl. Acad.Sci.USA. 103, 3500-3501

Ray, S.C. and Thomas, D.L.(2010). Principles and practices of infectious disease. Churchill Livingstone, Elsevier Publishers, Philadephia. Pg 2157-2185

Reading, S.A and Dimmock, N.J (2007). Neutralization of animal virus infectivity by antibody by antibody. Arch Virol. 152: 1047-1059

Reason, J.(1990) Human Error Cambridge University press Cambridge

Rhainds, D. and Brissette, L.(2004). The role of Scavenger receptor class B type 1 in lipid trafficking; defining the rules for lipid traders. Int. J BioChem Cell Biol. 36:39-77

Rice, C.M. and Saeed, M. (2014). Hepatitis C; treatment triumphi. Nature 510:43-44

Robinson, J.L. (2008).Vertical transmission of hepatitis C virus; current knowledge and issues. Review of Medical Virology 18(3): 137-157

Rosmann, A.S.,Wariach, A., Galvin, K., Casino, J.(1993).Hepatitis C virusantibody in alcoholic patients. Archievers of Internal Med. 153: 965-969

Rullison, C.(2008). Comparison of different methods to measure contact angles of Soil colloids. Journal of Colloids and Interface Science.328:299-307

Samuelsson, G. and Bohlin, L.(2004). Drugs of natural origin; a textbook on pharmacognosy. 5th Edition, Swedish Pharmaceutical Press, Stockholm, Sweden.

Sandmann, L. and Ploss, A.(2013). Barriers of hepatitis C virus interspecies transmission. Journal of Virology 435(1) 70-80

Sansonno, D., Lauletta, G. and De Re, V. (2004). Intra hepatic B-cells clonal expansion and extrahepatic manifestation of chronic HCV infection. European Journal of Immunol.34:126-136

Scheel, T.K. and Rice, C.M. (2013). Understanding HCV life cycle paves the way for high effective therapies. Natl. Med. 19:837-849

Sharma, N.R., Marten, G., Druex, M., Grakoui, A., Melikyan, G.B.(2011).Hepatitis C virus is primed by CD81 protein for low-pH dependent fusion. J Biol Chem 286:30361-30371

Shiao, J., Guo, L. and McLaws, M.L. (2000).Estimation of the risk of blood borne pathogens to health care workers after needlestick injury in Taiwan. American Journal of Infection Control 30: 15-20

Shiffman, M.I.,Salvatore, J. and Hubbard, S.(2007). Treatment of chronic hepatitis C virus with peg-interferon , ribavirin and epotein alpha. Hepatol 46:371-379

Shin, K., Fogg, V.C. and Margolis, B. (2006). Tight junctions and cells polarity. Annu. Rev. Cell. Dev. Biol.22: 207-235

Shoham, T., Rajapaksa, R., Kuo, C.C., Haimovich, J.,Levi, S.(2006). Building the tetraspanin web; distinct structural domain for CD81 functions in different cellular compartments. Mol .Cell Biol. 26: 1373-1385

Simmonds ,P., Bukh, J. and Combet,C.(2005). Concensus proposal of unified system of nomenclature of hepatitis C virus genotype. Hepatology 42:967-73

Simmonds, P., Beacher, P., Monaths, T., Rice, C.M., Stiansny, K.(2011). Classification of hepatitis C virus into six major genotype and a series of subtypes by phylogenetic analysis of the NS-5 region. Journal of Gen. Virol. 74(11): 2391-2399

Smith, A. E and Helenius, A. (2004). How virus enters animal cells. Science 304: 237-247

Solo, B., Sanchez-Quijano, A. and Rodrigo, L. (1997). HIV infection modifies the natural history of chronic parenterally-acquired hepatitis C with an unusual rapid progression to cirrhosis. Journal of Hepatol. 26: 1-5

Sulkowski, M.S., Cooper, C. and Hunyady, B. (2011). Management of adverseeffects of peg-IFN and ribavirin therapy for hepatitis C. Natl. Rev. Gastroenterol. Hepatol. 8(4): 212-223

Sweeney, C.J., Mehotra, S., Sadaria, M.R.,Kumar, S.(2008). The sesquiterpene lactone parthenolide in combination with doceterxel reduces metastasis and improves survival in xenograft models of breast cancer. Mole. Cancer Ther. 4(6): 1004

Thomas, C., David, L. and Stuart,C.(2009). Hepatitis C; principles and practices of infectious disease, 7th Edition,Philadelphia Churchill,Livingstone .ISBN 978-0-443-06839-3

Thyagarajan, S.P., Subramanian, T. and Thirumalasunri, P.S.(1998). Effects of phyllantus amarus on the chronic carriers of hepatitis B virus. Lancet 2:764-766

Timpe, J.M., Stamataki, Z., Jennings, A., Hu,K., Harris, H.J.(2007). Hepatitis Cvirus cell to cell transmission of neutralizing antibodies. Hepatol(in press)

Torriani, F.J and Sorriano, V.(2000). Chronic hepatitis C in HIV infectedindividuals. AIDS Reviews 2:168-177

Trease, G .E and Evans, W.C (1989).Pharmacognsy. 11th edition. BrailliarTiridel. Macmillian Publishers, U.S.A

Tscherne, D. M., Jones, C.T.,Evans, M.J., Lindenbach, B.D., McKeating, J.A.(2006). Time and temperature dependent activation of hepatitis C virus for low-pH triggered entry. J Virol 80: 1734-1741

Van Eck, M., Hoekstra, M., Out, R., Bos, I.S.,Kruijt, J.K., Hildebrand, R.B., Van Berkel, T.J. (2008). Scavenger receptor class B type 1 facilitates the metabolism of VLDL in vivo. J Res.49: 136-146

Van Oss, C.J 1994). Interfacial forces in aqueous media, New York. Marcel Deker

Van Oss, C.J. and Giese, R.F. (2002). Colloids and surface properties of clay and related minerals, New York.

Venkateswaran, P.S., Millman, I. and Blumberg, B.S (1987). Effects of an extracts from phyllantus on hepatitis B and woodchuck hepatitis viruses; in vitro and in vivo studies. Proc. Natl. Acad. Sci.USA. 84: 274-278

Vieyres, G., Dubuisson, J. and Pietschmann, T. (2014). Incoporation of hepatitis C virus E1-E2 glycoproteins; the keystone on a particular virion. Viruses 6: 1149-1187

Von Hann, T., Yoon, J.C., Alter, H., Rice, C.M. (2007). Hepatitis C viruscontinuously escapes from neutralizing antibodies and T- cell responses during chronic infection in vivo. Gastroenterol 132: 667-678

VonHann, T. and Rice, C.M. (2008). Hepatitis C entry. J Biol Chem. 283:3689-3693

Wahyuni, T.S., Tumewu, L., Permanasari, A.A., Apriani, E. (2013). Antiviralactivity of Indonesia medicinal plant in the east region against hepatitis Cvirus. Journal of Virol . 10:259

Wakita, K., Pietschmann, T., Kato, T., Date, T., Miyamoto, M.(2005).Productionof infectious hepatitis C virus in tissue cultured from a cloned viral genome. Natl. Med. 11:791-796

Walker, M. A. (1999). Hepatitis C virus; an overview of current approaches and progress. Drug Discovering Today 4: 518- 529

Wilkins, T., Malcolm, J.K. and Raina, D. (2010).Hepatitis C;diagnosis andtreatment. American Family physician 81(11):1351-1357

Willey, T.E., McCarthy, M.,Breidi, L.,Layden, T.J.(1998). Impact of alcohol onthe histological and clinical progression of hepatitis C infection. Hepatol 28:805-809

Witteveldt, J., Evans, M.J., Bitzegeio, J., Owsianka, A.M., (2009).CD81 isdispensable for hepatitis C virus cell to cell transmission in hepatoma cells. J Gen. Virol. 90:48-50

Wong, J.B. (2006). Hepatitis C; cost of illness and consideration for economic evaluation of antiviral therapies. Pharmacoeconomics 24(7): 661-72World Health Organization (2013). Hepatitis C facts sheet. No: 164

www.laskerfoundation.org/awards,(2012). Albert Lasker Awards for Clinical Medical research; year 2000 winners. Retreieved 24th sept, 2016

Yi, M.K. and Lemon, S.M. (2003). 3' UTR RNA signals required for replication of hepatitis C virus RNA. J.Virol.77: 3557-3568

Yiantsios, S.G. and Davis, R.H.(1991). Surface and colloids chemistry. J Colloid Interface Sci.144: 412-413

Yildrim, I. (2001).Surface free energy characterization of powders. Virginia Tech.

Yuan, Y. and Lee, R. (2013). Contact angle and wetting properties, University of Houston,Texas. TX 77204-5003

Zeisel, M.B., Koutsoudakis, G., Schnober, E.K., Blum, H.E.(2007). Scavenger receptor class B type 1 is a key host factor for hepatitis C virus infection required for an entry step closely linked to CD81. Hepatology 46: 1722-1731

Zhang, P., Wu, C.G., Mihalik, K., Yu, M.Y., Feinstone, M.J. (2007). Hepatitis C virus epitope-specific antibodies in immunoglobulin prepared from human plasma. Proc. Natl. Acad. Sci.USA. 104: 8449-8454

Zheng, J., Randall, G., Higginbottom, A., Monk, P., Rice, C.M.(2007). Claudin-6and Claudin-9 functions as additional co-receptors for HCV. J Virol. 81: 12465-12471

Zhu, J. (2003). Drag forces of interacting spheres in power law fluids. J Mech. Res.Comm. 30: 651-6

APPENDIX

Appendix A1:

Whole Blood Contact Angles

Blood Samples	Infected(θ^0)	Uninfected(θ^0)	Treated(θ^0)							
			IFN	RBV	ATR	ELT	AM	VA	BP	DH
1	60	50	51	51	53	52	50	53	60	50
2	55	51	52	52	55	50	56	52	50	55
3	58	40	57	53	56	53	51	57	52	58
4	60	50	59	58	59	59	59	58	56	59
5	60	45	56	59	57	58	57	56	59	49
6	56	56	58	57	54	56	53	55	51	56
7	55	55	50	55	60	55	54	50	55	54
8	58	50	54	56	58	57	58	59	58	57
9	54	43	53	54	52	54	52	54	53	48
10	55	55	55	55	51	51	55	51	54	51
AVE	**57.1**	**49.5**	**54.5**	**55**	**55.5**	**54.5**	**54.5**	**54.5**	**54.8**	**53.7**
SD	**2.3781**	**5.3593**	**3.0277**	**2.5820**	**3.0276**	**3.0277**	**3.0277**	**3.0277**	**3.4254**	**3.9455**

Appendix A2:

White Blood Cells Contact Angles

Blood Samples	Infected (θ^0)	Uninfected (θ^0)	Treated(θ^0)							
			IFN	RBV	ATR	ELT	AM	VA	BP	DH
1	65	47	58	56	54	57	55	51	58	56
2	61	46	50	46	49	55	56	57	50	58
3	63	48	52	55	50	54	50	56	55	57
4	64	52	60	60	60	60	59	58	57	60
5	67	50	61	58	58	58	60	55	60	62
6	66	51	57	61	62	62	57	60	59	59
7	58	45	53	57	57	51	58	54	53	61
8	68	49	64	58	65	59	66	53	62	65
9	62	44	55	59	52	53	61	59	56	63
10	60	51	59	53	59	56	63	52	54	55
AVE	**63.4**	**48.5**	**56.9**	**56.3**	**56.6**	**56.5**	**58.5**	**55.5**	**56.4**	**59.6**
SD	**3.2045**	**2.7508**	**4.3831**	**4.3218**	**5.2534**	**3.3747**	**4.4535**	**3.0277**	**3.5653**	**3.2042**

Appendix A3:

Red Blood Cells Contact Angles

Blood Samples	Infected (θ^0)	Uninfected (θ^0)	Treated(θ^0)							
			IFN	RBV	ATR	ELT	AM	VA	BP	DH
1	59	48	55	52	57	58	57	59	58	55
2	64	57	54	53	55	60	56	56	57	53
3	58	45	58	50	56	54	58	54	56	56
4	57	50	59	59	59	59	59	57	59	49
5	56	52	57	58	58	57	55	58	62	58
6	62	51	60	57	60	63	60	64	60	57
7	63	49	61	54	63	53	61	60	55	51
8	61	54	63	60	61	61	54	61	61	54
9	60	47	56	62	62	65	63	58	65	52
10	64	53	62	56	54	58	53	55	63	48
AVE	**60.4**	**50.6**	**58.5**	**56.1**	**58.5**	**58.8**	**57.6**	**58.2**	**59.6**	**53.3**
SD	**2.8752**	**3.5653**	**3.0277**	**3.8137**	**3.0277**	**3.7059**	**3.2042**	**2.9740**	**3.2042**	**3.335**

Appendix A4:

Serum Contact Angles

Blood Samples	Infected (θ^0)	Uninfected (θ^0)	Treated(θ^0)							
			IFN	RBV	ATR	ELT	AM	VA	BP	DH
1	60	58	50	55	53	53	56	58	58	55
2	62	55	61	50	57	57	55	55	55	56
3	63	45	53	54	55	55	58	52	56	57
4	61	56	60	60	56	56	60	60	59	59
5	59	53	59	56	59	59	63	50	57	46
6	64	57	63	58	51	58	59	59	54	58
7	58	54	55	53	58	54	57	54	50	48
8	65	52	65	59	60	60	61	51	49	53
9	66	50	57	57	62	62	65	57	60	51
10	57	51	54	61	54	52	67	56	52	49
AVE	**61.5**	**53.1**	**57.7**	**56.3**	**56.5**	**56.6**	**60.1**	**55.2**	**55**	**53.2**
SD	**3.0277**	**3.8427**	**4.7387**	**3.4010**	**3.3747**	**3.2042**	**3.9285**	**3.4254**	**3.7417**	**4.5166**

NEUMANN MODEL ANALYSIS

Appendix B1:

Neumann: Whole Blood

	(a) Neumann: Whole Blood Infected				(b) **Neumann: Whole Blood Uninfected**			
SN	$CD4^+$ count ($cells/mm^3$)	$\theta(^0C)$	γ_{sv} (mJ/m^2)	F^{adh} (mJ/m^2)	CD4+ count ($cells/mm^3$)	$\theta(^0C)$	γ_{sv} (mJ/m^2)	F^{adh} (mJ/m^2)
1	428	60	36.00	-20.86	1660	50	43.18	-14.06
2	600	55	39.62	-17.41	1572	51	42.48	-14.72
3	625	58	37.45	-19.47	1780	40	49.90	-7.95
4	312	60	36.00	-20.86	1450	50	43.18	-14.06
5	464	60	36.00	-20.86	1500	45	46.63	-10.89
6	247	56	38.90	-18.09	1193	56	38.90	-18.09
7	852	55	39.62	-17.41	1360	55	39.62	-17.41
8	115	58	37.45	-19.47	1520	50	43.18	-14.06
9	704	54	40.34	-16.73	1580	43	47.96	-9.68
10	798	55	39.62	-17.41	1020	55	39.62	-17.41
AVE	**514.5**	**57.1**	**38.10**	**-18.86**	**1267.2**	**49.5**	**43.47**	**-13.833**
SD	**243.1059**	**2.378141**	**1.721233**	**1.639153**	**368.2731**	**5.359312**	**3.70064**	**3.41844**

Appendix B2:

Neumann: WBC

	(a) Neumann: White Blood Infected				(b) **Neumann: White Blood Uninfected**			
SN	$CD4^+$ count ($cells/mm^3$)	$\theta(^0C)$	γ_{sv} (mJ/m^2)	F^{adh} (mJ/m^2)	CD4+ count ($cells/mm^3$)	$\theta(^0C)$	γ_{sv} (mJ/m^2)	F^{adh} (mJ/m^2)
1	428	65	32.38	-24.34	1660	47	45.27	-12.13
2	600	61	35.27	-21.55	1572	46	45.95	-11.50
3	625	63	33.83	-22.95	1780	48	44.58	-12.77
4	312	64	33.10	-23.64	1450	52	41.77	-15.39
5	464	67	30.95	-25.72	1500	50	43.18	-14.06
6	247	66	31.66	-25.03	1193	51	42.48	-14.72
7	852	58	37.45	-19.47	1360	45	46.63	-10.89
8	115	68	30.23	-26.41	1520	49	43.88	-13.41
9	704	62	34.55	-22.25	1580	44	47.30	-10.28
10	798	60	36.00	-20.86	1020	51	42.48	-14.72
AVE	**514.5**	**63.4**	**33.54**	**-23.222**	**1267.2**	**48.5**	**44.35**	**-12.99**
SD	**243.1059**	**3.204164**	**2.313597**	**2.225303**	**368.2731**	**2.750757**	**1.903218**	**1.758447**

Appendix B3:

Neumann: RBC

	(a) **Neumann: Red Blood Infected**				(b) **Neumann: Red Blood Uninfected**			
SN	$CD4^+$ count (cells/mm^3)	$\theta(^0C)$	γ_{sv} (mJ/m^2)	F^{adh} (mJ/m^2)	CD4+ count (cells/mm^3)	$\theta(^0C)$	γ_{sv} (mJ/m^2)	F^{adh} (mJ/m^2)
1	428	59	36.73	-20.16	1660	48	44.58	-12.77
2	600	64	33.10	-23.64	1572	57	38.17	-18.78
3	625	58	37.45	-19.47	1780	45	46.63	-10.89
4	312	57	38.17	-18.78	1450	50	43.18	-14.06
5	464	56	38.90	-18.09	1500	52	41.77	-15.39
6	247	62	34.55	-22.25	1193	51	42.48	-14.72
7	852	63	33.83	-22.94	1360	49	43.88	-13.41
8	115	61	35.27	-21.55	1520	54	40.34	-16.73
9	704	60	36.00	-20.86	1580	47	45.27	-12.13
10	798	64	33.10	-23.64	1020	53	41.05	-16.06
AVE	**514.5**	**60.4**	**35.71**	**-21.14**	**1267.2**	**50.6**	**42.735**	**-14.494**
SD	**243.1059**	**2.875181**	**2.083736**	**1.995549**	**368.2731**	**3.565265**	**2.514868**	**2.347307**

Appendix B4:

Neumann: Serum

	(a) **Neumann: Serum Infected**				(b) **Neumann: Serum Uninfected**			
SN	$CD4^+$ count (cells/mm^3)	$\theta(^0C)$	γ_{sv} (mJ/m^2)	F^{adh} (mJ/m^2)	CD4+ count (cells/mm^3)	$\theta(^0C)$	γ_{sv} (mJ/m^2)	F^{adh} (mJ/m^2)
1	428	60	36.00	-20.86	1660	58	37.45	-19.47
2	600	62	34.55	-22.25	1572	55	39.62	-17.41
3	625	63	33.83	-22.94	1780	45	46.63	-10.89
4	312	61	35.27	-21.55	1450	56	38.90	-18.09
5	464	59	36.73	-20.16	1500	53	41.05	-16.06
6	247	64	33.10	-23.64	1193	57	38.17	-18.78
7	852	58	37.45	-19.47	1360	54	39.62	-17.41
8	115	65	32.38	-24.34	1520	52	41.77	-15.39
9	704	66	31.66	-25.03	1580	50	43.18	-14.06
10	798	57	38.17	-18.78	1020	51	38.90	-14.72
AVE	**514.5**	**61.5**	**34.92**	**-21.902**	**1267.2**	**53.1**	**40.53**	**-16.23**
SD	**243.1059**	**3.02765**	**2.192022**	**2.1043**	**368.2731**	**3.842742**	**2.750081**	**2.570081**

FOWKES MODEL ANALYSIS

Appendix B5:

Fowkes: Whole Blood

	(a) **Fowkes: Whole Blood Infected**				(b) **Fowkes: Whole Blood Uninfected**			
SN	$CD4^+$ count (cells/mm^3)	$\theta(^0C)$	γ_{sv} (mJ/m^2)	F^{adh} (mJ/m^2)	CD4+ count (cells/mm^3)	$\theta(^0C)$	γ_{sv} (mJ/m^2)	F^{adh} (mJ/m^2)
1	428	60	36.00	-32.00	1660	58	43.18	-22.862
2	600	55	39.62	-27.29	1572	55	42.48	-23.724
3	625	58	37.45	-30.09	1780	45	49.90	-16.75
4	312	60	36.00	-32.00	1450	56	43.18	-22.86
5	464	60	36.00	-32.00	1500	53	46.63	-18.75
6	247	56	38.90	-28.21	1193	57	38.90	-28.21
7	852	55	39.62	-27.29	1360	54	39.62	-27.29
8	115	58	37.45	-30.09	1520	52	43.18	-22.862
9	704	54	40.34	-26.38	1580	50	47.96	-17.86
10	798	55	39.62	-27.29	1020	51	39.62	-27.29
AVE	**514.5**	**57.1**	**38.10**	**-29.264**	**1267.2**	**53.1**	**43.465**	**-22.8458**
SD	**243.1059**	**2.378141**	**1.721233**	**2.234578**	**368.2731**	**3.842742**	**3.70064**	**4.052996**

Appendix B6:

Fowkes: WBC

	(a) **Fowkes: White Blood Infected**				(b) **Fowkes: White Blood Uninfected**			
SN	$CD4^+$ count (cells/mm^3)	$\theta(^0C)$	γ_{sv} (mJ/m^2)	F^{adh} (mJ/m^2)	CD4+ count (cells/mm^3)	$\theta(^0C)$	γ_{sv} (mJ/m^2)	F^{adh} (mJ/m^2)
1	428	65	32.38	-36.95	1660	47	45.27	-20.35
2	600	61	35.27	-32.97	1572	46	45.95	-19.54
3	625	63	33.83	-34.95	1780	48	44.58	-21.18
4	312	64	33.10	-35.94	1450	52	41.77	-24.60
5	464	67	30.95	-38.99	1500	50	43.18	-22.86
6	247	66	31.66	-37.97	1193	51	42.48	-23.72
7	852	58	37.45	-30.09	1360	45	46.63	-18.75
8	115	68	30.23	-40.03	1520	49	43.88	-22.01
9	704	62	34.55	-33.95	1580	44	47.30	-17.96
10	798	60	36.00	-32.00	1020	51	42.48	-23.72
AVE	**514.5**	**63.4**	**33.54**	**-35.384**	**1267.2**	**48.5**	**44.35**	**-21.469**
SD	**243.1059**	**3.204164**	**2.313597**	**3.190044**	**368.2731**	**2.750757**	**1.903218**	**2.283455**

Appendix B7:

Fowkes: RBC

	(a) **Fowkes: Red Blood Infected**				(b) **Fowkes: Red Blood Uninfected**			
SN	$CD4^+$ count (cells/mm^3)	$\theta(^0C)$	γ_{sv} (mJ/m^2)	F^{adh} (mJ/m^2)	CD4+ count (cells/mm^3)	$\theta(^0C)$	γ_{sv} (mJ/m^2)	F^{adh} (mJ/m^2)
1	428	59	36.73	-31.04	1660	48	44.58	-21.18
2	600	64	33.10	-35.94	1572	57	38.17	-29.14
3	625	58	37.45	-30.09	1780	45	46.63	-18.75
4	312	57	38.17	-29.14	1450	50	43.18	-22.86
5	464	56	38.90	-28.21	1500	52	41.77	-24.60
6	247	62	34.55	-33.95	1193	51	42.48	-23.72
7	852	63	33.83	-34.95	1360	49	43.88	-22.01
8	115	61	35.28	-32.97	1520	54	40.34	-26.38
9	704	60	36.00	-32.00	1580	47	45.27	-20.35
10	798	64	33.10	-35.94	1020	53	41.05	-25.48
AVE	**514.5**	**60.4**	**35.71**	**-32.423**	**1267.2**	**50.6**	**42.74**	**-23.447**
SD	**243.1059**	**2.875181**	**2.083504**	**2.785223**	**368.2731**	**3.565265**	**2.514868**	**3.086742**

Appendix B8:

Fowkes: Serum

	(a) **Fowkes: Serum Infected**				(b) **Fowkes: Serum Uninfected**			
SN	$CD4^+$ count (cells/mm^3)	$\theta(^0C)$	γ_{sv} (mJ/m^2)	F^{adh} (mJ/m^2)	CD4+ count (cells/mm^3)	$\theta(^0C)$	γ_{sv} (mJ/m^2)	F^{adh} (mJ/m^2)
1	428	60	36.00	-32.00	1660	58	37.45	-30.09
2	600	62	34.55	-33.95	1572	55	39.62	-27.29
3	625	63	33.83	-34.95	1780	45	46.63	-18.75
4	312	61	35.28	-32.97	1450	56	38.90	-28.21
5	464	59	36.73	-31.04	1500	53	41.05	-25.48
6	247	64	33.10	-35.94	1193	57	38.17	-29.14
7	852	58	37.45	-30.09	1360	54	40.34	-26.38
8	115	65	32.38	-36.95	1520	52	41.77	-24.60
9	704	66	31.66	-37.97	1580	50	43.18	-22.86
10	798	57	38.18	-29.14	1020	51	42.48	-23.72
AVE	**514.5**	**61.5**	**34.92**	**-33.5**	**1267.2**	**53.1**	**40.96**	**-25.652**
SD	**243.1059**	**3.02765**	**2.193856**	**2.969515**	**368.2731**	**3.842742**	**2.719879**	**3.365184**

WU MODEL ANALYSIS

Appendix B9:

Wu: Whole Blood

	(a) **Wu: Whole Blood Infected**				(b) **Wu: Whole Blood Uninfected**			
SN	$CD4^+$ count ($cells/mm^3$)	$\theta(^0C)$	γ_{sv} (mJ/m^2)	F^{adh} (mJ/m^2)	CD4+ count ($cells/mm^3$)	$\theta(^0C)$	γ_{sv} (mJ/m^2)	F^{adh} (mJ/m^2)
1	428	60	36.00	-82.28	1660	50	43.18	-64.00
2	600	55	39.62	-80.55	1572	51	42.48	-73.42
3	625	58	37.45	-98.05	1780	40	49.90	-67.83
4	312	60	36.00	-90.51	1450	50	43.18	-64.00
5	464	60	36.00	-90.51	1500	45	46.63	-64.00
6	247	56	38.90	-71.58	1193	56	38.90	-71.58
7	852	55	39.62	-73.42	1360	55	39.62	-73.42
8	115	58	37.45	-82.28	1520	50	43.18	-67.83
9	704	54	40.34	-93.61	1580	43	47.96	-75.24
10	798	55	39.62	-73.42	1020	55	39.62	-73.42
AVE	**514.5**	**57.1**	**38.10**	**-82.80**	**1267.2**	**49.5**	**43.47**	**-69.47**
SD	**243.1059**	**2.378141**	**1.721233**	**8.92309**	**368.2731**	**5.359312**	**3.70064**	**4.468336**

Appendix B10:

Wu: WBC

	(a) **Wu: White Blood Infected**				(b) **Wu: White Blood Uninfected**			
SN	$CD4^+$ count ($cells/mm^3$)	$\theta(^0C)$	γ_{sv} (mJ/m^2)	F^{adh} (mJ/m^2)	CD4+ count ($cells/mm^3$)	$\theta(^0C)$	γ_{sv} (mJ/m^2)	F^{adh} (mJ/m^2)
1	428	65	32.38	-87.30	1660	47	45.27	-54.10
2	600	61	35.28	-88.92	1572	46	45.95	-62.06
3	625	63	33.83	-85.65	1780	48	44.58	-58.11
4	312	64	33.10	-78.81	1450	52	41.77	-56.11
5	464	67	30.95	-82.28	1500	50	43.18	-50.01
6	247	66	31.66	-80.55	1193	51	42.48	-52.06
7	852	58	37.45	-90.51	1360	45	46.63	-67.83
8	115	68	30.23	-83.98	1520	49	43.88	-47.95
9	704	62	34.55	-92.08	1580	44	47.30	-60.09
10	798	60	36.00	-80.55	1020	51	42.48	-64.00
AVE	**514.5**	**63.4**	**33.54**	**-85.06**	**1267.2**	**48.5**	**44.35**	**-57.23**
SD	**243.1059**	**3.204164**	**2.314428**	**4.569046**	**368.2731**	**2.750757**	**1.903218**	**6.38142**

Appendix B11:

Wu: RBC

	(a) **Wu: Red Blood Infected**				(b) **Wu: Red Blood Uninfected**			
SN	$CD4^+$ count ($cells/mm^3$)	$\theta(^0C)$	γ_{sv} (mJ/m^2)	F^{adh} (mJ/m^2)	CD4+ count ($cells/mm^3$)	$\theta(^0C)$	γ_{sv} (mJ/m^2)	F^{adh} (mJ/m^2)
1	428	59	36.73	-85.65	1660	48	44.58	-65.93
2	600	64	33.10	-69.71	1572	57	38.18	-56.11
3	625	58	37.45	-90.51	1780	45	46.63	-67.83
4	312	57	38.18	-82.28	1450	50	43.18	-69.71
5	464	56	38.90	-78.80	1500	52	41.77	-71.58
6	247	62	34.55	-80.55	1193	51	42.48	-60.09
7	852	63	33.83	-83.98	1360	49	43.88	-58.11
8	115	61	35.28	-75.24	1520	54	40.34	-62.06
9	704	60	36.00	-87.30	1580	47	45.27	-64.00
10	798	64	33.10	-77.03	1020	53	41.05	-56.11
AVE	**514.5**	**60.4**	**35.71**	**-81.105**	**1267.2**	**50.6**	**42.74**	**-63.153**
SD	**243.1059**	**2.875181**	**2.084817**	**6.178873**	**368.2731**	**3.565265**	**2.512852**	**5.57303**

Appendix B12:

Wu: Serum

	(a) **Wu: Serum Infected**				(b) **Wu: Serum Uninfected**			
SN	$CD4^+$ count ($cells/mm^3$)	$\theta(^0C)$	γ_{sv} (mJ/m^2)	F^{adh} (mJ/m^2)	CD4+ count ($cells/mm^3$)	$\theta(^0C)$	γ_{sv} (mJ/m^2)	F^{adh} (mJ/m^2)
1	428	60	36.00	-67.83	1660	58	37.45	-64.00
2	600	62	34.55	-73.42	1572	55	39.62	-60.09
3	625	63	33.83	-90.51	1780	45	46.63	-58.11
4	312	61	35.28	-71.58	1450	56	38.90	-62.06
5	464	59	36.73	-77.03	1500	53	41.05	-65.92
6	247	64	33.10	-69.71	1193	57	38.18	-56.11
7	852	58	37.45	-75.24	1360	54	40.34	-67.83
8	115	65	32.38	-78.80	1520	52	41.77	-54.10
9	704	66	31.66	-82.28	1580	50	43.18	-52.06
10	798	57	38.18	-80.55	1020	51	42.48	-69.71
AVE	**514.5**	**61.5**	**34.92**	**-76.70**	**1267.2**	**53.1**	**40.96**	**-60.999**
SD	**243.1059**	**3.02765**	**2.193856**	**6.731642**	**368.2731**	**3.842742**	**2.718742**	**5.93922**

INFECTED SAMPLES WITH IFN TREATMENT AND RBV TREATMENT

NEUMANN MODEL ANALYSIS

Appendix B13:

Neumann: Whole Blood Infected

	Neumann: Whole Blood Treated With IFN				**Neumann: Whole Blood Treated With RBV**			
SN	$CD4^+$ count (cells/mm^3)	$\theta(^0C)$	γ_{sv} (mJ/m^2)	F^{adh} (mJ/m^2)	CD4+ count (cells/mm^3)	$\theta(^0C)$	γ_{sv} (mJ/m^2)	F^{adh} (mJ/m^2)
1	428	51	42.48	-14.72	428	51	42.47	-14.72
2	600	52	41.77	-15.39	600	52	41.77	-15.39
3	625	57	3.18	-18.78	625	53	41.05	-16.06
4	312	59	36.73	-20.16	312	58	37.45	-19.47
5	464	56	38.90	-18.09	464	59	36.73	-20.16
6	247	58	37.45	-19.47	247	57	38.18	-18.78
7	852	50	43.18	-14.06	852	55	39.62	-17.41
8	115	54	40.34	-16.73	115	56	38.90	-18.09
9	704	53	41.05	-16.06	704	54	40.34	-16.73
10	798	55	39.62	-17.41	798	55	39.62	-17.41
AVE	**514.5**	**54.5**	**39.87**	**-17.09**	**514.5**	**55**	**39.613**	**-17.42**
SD	**243.1059**	**3.02765**	**2.28393**	**2.05280**	**243.1059**	**2.581989**	**1.85474**	**1.7558**

Appendix B14:

Neumann: WBC Infected

	(a) Neumann: WBC Treated With IFN				(b) **Neumann: WBC Treated With RBV**			
SN	$CD4^+$ count (cells/mm^3)	$\theta(^0C)$	γ_{sv} (mJ/m^2)	F^{adh} (mJ/m^2)	CD4+ count (cells/mm^3)	$\theta(^0C)$	γ_{sv} (mJ/m^2)	F^{adh} (mJ/m^2)
1	428	58	37.45	-19.47	428	56	38.90	-18.09
2	600	50	43.18	-14.06	600	46	45.95	-11.50
3	625	52	41.77	-15.39	625	55	39.62	-17.41
4	312	60	36.00	-20.86	312	60	36.00	-20.86
5	464	61	35.28	-21.55	464	58	37.45	-19.47
6	247	57	38.18	-18.78	247	61	35.28	-21.55
7	852	53	41.05	-16.06	852	57	38.18	-18.78
8	115	64	33.10	-23.64	115	58	37.45	-19.47
9	704	55	39.62	-17.41	704	59	36.73	-20.16
10	798	59	36.78	-20.16	798	53	41.05	-16.06
AVE	**514.5**	**56.9**	**38.24**	**-18.74**	**514.5**	**56.3**	**38.66**	**-18.34**
SD	**243.1059**	**4.383048**	**3.15565**	**3.00051**	**243.1059**	**4.32178**	**3.07714**	**2.89876**

Appendix B15:

Neumann: RBC Infected

	(a) Neumann: RBC Treated With IFN				(b) **Neumann: RBC Treated With RBV**			
SN	$CD4^+$ count ($cells/mm^3$)	$\theta(^0C)$	γ_{sv} (mJ/m^2)	F^{adh} (mJ/m^2)	CD4+ count ($cells/mm^3$)	$\theta(^0C)$	γ_{sv} (mJ/m^2)	F^{adh} (mJ/m^2)
1	428	55	39.62	-17.41	428	52	41.77	-15.39
2	600	54	40.34	-16.73	600	53	41.05	-16.06
3	625	58	37.54	-19.47	625	50	43.18	-14.06
4	312	59	36.73	-20.16	312	59	36.73	-20.16
5	464	57	38.18	-18.78	464	58	37.45	-19.47
6	247	60	36.00	-20.86	247	57	38.18	-18.78
7	852	61	35.28	-21.55	852	54	40.34	-16.73
8	115	63	33.83	-22.95	115	60	36.00	-20.86
9	704	56	38.90	-18.09	704	62	34.55	-22.25
10	798	62	34.55	-22.25	798	56	38.90	-18.09
AVE	**514.5**	**58.5**	**37.10**	**-19.83**	**514.5**	**56.1**	**38.82**	**-18.19**
SD	**243.1059**	**3.02765**	**2.1935**	**2.0935**	**243.1059**	**3.81372**	**2.74553**	**2.60459**

Appendix B16:

Neumann: Serum Infected

	(a) Neumann: Serum Treated With IFN				(b) **Neumann: Serum Treated With RBV**			
SN	$CD4^+$ count ($cells/mm^3$)	$\theta(^0C)$	γ_{sv} (mJ/m^2)	F^{adh} (mJ/m^2)	CD4+ count ($cells/mm^3$)	$\theta(^0C)$	γ_{sv} (mJ/m^2)	F^{adh} (mJ/m^2)
1	428	50	43.18	-14.06	428	55	39.62	-17.41
2	600	61	35.28	-21.55	600	50	43.18	-14.06
3	625	53	41.05	-16.06	625	54	40.34	-16.73
4	312	60	36.00	-20.86	312	60	36.00	-20.86
5	464	59	36.73	-20.16	464	56	38.90	-18.09
6	247	63	33.83	-22.95	247	58	37.45	-19.47
7	852	55	39.62	-17.41	852	53	41.05	-16.06
8	115	65	32.38	-24.34	115	59	36.73	-20.16
9	704	57	38.18	-18.78	704	57	38.18	-18.78
10	798	54	40.34	-16.73	798	61	35.28	-21.55
AVE	**514.5**	**57.7**	**37.66**	**-19.29**	**514.5**	**56.3**	**38.67**	**-18.32**
SD	**243.1059**	**4.73872**	**3.4171**	**3.25511**	**243.1059**	**3.40098**	**2.44635**	**2.32064**

FOWKES MODEL ANALYSIS

Appendix B17:

Fowkes: Whole Blood Infected

	Fowkes: Whole Blood Infected With IFN				**Fowkes: Whole Blood Infected With RBV**			
SN	$CD4^+$ count ($cells/mm^3$)	$\theta(^0C)$	γ_{sv} (mJ/m^2)	F^{adh} (mJ/m^2)	CD4+ count ($cells/mm^3$)	$\theta(^0C)$	γ_{sv} (mJ/m^2)	F^{adh} (mJ/m^2)
1	428	51	42.48	-23.72	428	51	42.48	-23.72
2	600	52	41.77	-24.60	600	52	41.77	-24.60
3	625	57	38.18	-29.14	625	53	41.05	-25.48
4	312	59	36.73	-31.04	312	58	37.45	-30.09
5	464	56	38.90	-28.21	464	59	36.73	-31.04
6	247	58	37.45	-30.09	247	57	38.18	-29.14
7	852	50	43.18	-22.86	852	55	39.62	-27.29
8	115	54	40.34	-26.38	115	56	38.90	-28.21
9	704	53	41.05	-25.48	704	54	40.34	-26.38
10	798	55	39.62	-27.29	798	55	39.62	-27.29
AVE	**514.5**	**54.5**	**39.97**	**-26.88**	**514.5**	**55**	**39.61**	**-27.32**
SD	**243.1059**	**3.02765**	**2.17222**	**2.7530**	**243.1059**	**2.5820**	**1.85646**	**2.36279**

Appendix B18:

Fowkes: WBC Infected

	(a) Fowkes: WBC Infected With IFN				(b) **Fowkes: WBC Infected With RBV**			
SN	$CD4^+$ count ($cells/mm^3$)	$\theta(^0C)$	γ_{sv} (mJ/m^2)	F^{adh} (mJ/m^2)	CD4+ count ($cells/mm^3$)	$\theta(^0C)$	γ_{sv} (mJ/m^2)	F^{adh} (mJ/m^2)
1	428	58	37.45	-30.09	428	56	38.90	-28.21
2	600	50	43.18	-22.86	600	46	45.95	-19.54
3	625	52	41.77	-24.60	625	55	39.62	-27.29
4	312	60	36.00	-32.00	312	60	36.00	-32.00
5	464	61	35.28	-32.97	464	58	37.45	-30.09
6	247	57	38.18	-29.14	247	61	35.28	-32.97
7	852	53	41.05	-25.48	852	57	38.18	-29.14
8	115	64	33.10	-35.94	115	58	37.45	-30.09
9	704	55	39.62	-27.29	704	59	36.73	-31.04
10	798	59	36.73	-31.04	798	53	41.05	-25.48
AVE	**514.5**	**56.9**	**38.24**	**-29.14**	**514.5**	**56.3**	**38.66**	**-28.59**
SD	**243.1059**	**4.3830**	**3.1583**	**4.08886**	**243.1059**	**4.32178**	**3.07714**	**3.8714**

Appendix B19:

Fowkes: RBC Infected

	(a) **Fowkes: RBC Infected With IFN**				(b) **Fowkes: RBC Infected With RBV**			
SN	$CD4^+$ count ($cells/mm^3$)	$\theta(^0C)$	γ_{sv} (mJ/m^2)	F^{adh} (mJ/m^2)	CD4+ count ($cells/mm^3$)	$\theta(^0C)$	γ_{sv} (mJ/m^2)	F^{adh} (mJ/m^2)
1	428	55	39.62	-27.29	428	52	41.77	-24.60
2	600	54	40.34	-26.38	600	53	41.05	-25.48
3	625	58	37.45	-30.09	625	50	43.18	-22.86
4	312	59	36.73	-31.04	312	59	36.73	-31.04
5	464	57	38.18	-29.14	464	58	37.45	-30.09
6	247	60	36.00	-32.00	247	57	38.18	-29.14
7	852	61	35.28	-32.97	852	54	40.34	-26.38
8	115	63	33.83	-34.95	115	60	36.00	-32.00
9	704	56	38.90	-28.21	704	62	34.55	-33.95
10	798	62	34.55	-33.95	798	56	38.90	-28.21
AVE	**514.5**	**58.5**	**37.09**	**-30.60**	**514.5**	**56.1**	**38.82**	**-28.38**
SD	**243.1059**	**3.02765**	**2.19166**	**2.88259**	**243.1059**	**3.81371**	**2.745531**	**3.52614**

Appendix B20:

Fowkes: Serum Infected

	(a) **Fowkes: Serum Infected With IFN**				(b) **Fowkes: Serum Infected With RBV**			
SN	$CD4^+$ count ($cells/mm^3$)	$\theta(^0C)$	γ_{sv} (mJ/m^2)	F^{adh} (mJ/m^2)	CD4+ count ($cells/mm^3$)	$\theta(^0C)$	γ_{sv} (mJ/m^2)	F^{adh} (mJ/m^2)
1	428	50	43.18	-22.86	428	55	39.62	-27.29
2	600	61	35.28	-32.97	600	50	43.18	-22.86
3	625	53	41.05	-25.48	625	54	40.34	-26.38
4	312	60	36.00	-32.00	312	60	36.00	-32.00
5	464	59	36.73	-31.04	464	56	38.90	-28.21
6	247	63	33.83	-34.95	247	58	37.45	-30.09
7	852	55	39.62	-27.29	852	53	41.05	-25.48
8	115	65	32.38	-36.95	115	59	36.73	-31.04
9	704	57	38.18	-29.14	704	57	38.18	-29.14
10	798	54	40.34	26.38	798	61	35.28	-32.97
AVE	**514.5**	**57.7**	**37.67**	**-29.91**	**514.5**	**56.3**	**38.67**	**-28.55**
SD	**243.1059**	**4.73873**	**3.41710**	**4.46240**	**243.1059**	**3.4010**	**2.44635**	**3.13708**

WU MODEL ANALYSIS

Appendix B21:

Wu: Whole Blood Infected

	(a) Wu: Whole Blood Infected With IFN				(b) **Wu: Whole Blood Infected With RBV**			
SN	$CD4^+$ count ($cells/mm^3$)	$\theta(^0C)$	γ_{sv} (mJ/m^2)	F^{adh} (mJ/m^2)	CD4+ count ($cells/mm^3$)	$\theta(^0C)$	γ_{sv} (mJ/m^2)	F^{adh} (mJ/m^2)
1	428	51	42.48	-80.55	428	51	42.48	-80.55
2	600	52	41.77	-78.80	600	52	41.77	-78.80
3	625	57	38.18	-69.71	625	53	41.05	-77.03
4	312	59	36.73	-65.93	312	58	37.45	-67.83
5	464	56	38.90	-71.58	464	59	36.73	-65.93
6	247	58	37.45	-67.83	247	57	38.17	-69.71
7	852	50	43.18	-82.28	852	55	39.62	-73.42
8	115	54	40.34	-75.24	115	56	38.90	-71.58
9	704	53	41.05	-77.03	704	54	40.34	-75.24
10	798	55	39.62	-73.42	798	55	39.62	-73.42
AVE	**514.5**	**54.5**	**39.97**	**-74.24**	**514.5**	**55**	**39.61**	**-73.35**
SD	**243.1059**	**3.02765**	**2.17222**	**5.50200**	**243.1059**	**2.58199**	**1.85732**	**4.72083**

Appendix B22:

Wu: WBC Infected

	(a) Wu: WBC Treated With IFN				(b) **Wu: WBC Treated With RBV**			
SN	$CD4^+$ count ($cells/mm^3$)	$\theta(^0C)$	γ_{sv} (mJ/m^2)	F^{adh} (mJ/m^2)	CD4+ count ($cells/mm^3$)	$\theta(^0C)$	γ_{sv} (mJ/m^2)	F^{adh} (mJ/m^2)
1	428	58	37.45	-67.83	428	56	38.90	-71.58
2	600	50	43.18	-82.28	600	46	45.95	-88.92
3	625	52	41.77	-78.81	625	55	39.62	-73.42
4	312	60	36.00	-64.00	312	60	36.00	-64.00
5	464	61	35.28	-62.06	464	58	37.45	-67.83
6	247	57	38.18	-69.71	247	61	35.28	-62.06
7	852	53	41.05	-77.03	852	57	38.18	-69.71
8	115	64	33.10	-56.11	115	58	37.45	-67.83
9	704	55	39.62	-73.42	704	59	36.73	-65.93
10	798	59	36.73	-65.93	798	53	41.05	-77.03
AVE	**514.5**	**56.9**	**38.24**	**-69.72**	**514.5**	**56.3**	**38.66**	**-70.83**
SD	**243.1059**	**4.38305**	**3.15826**	**8.17904**	**243.1059**	**4.32178**	**3.07714**	**7.74442**

Appendix B23:

Wu: RBC Infected

	(a) **Wu: RBC Treated With IFN**				(b) **Wu: RBC Treated With RBV**			
SN	$CD4^+$ count ($cells/mm^3$)	$\theta(^0C)$	γ_{sv} (mJ/m^2)	F^{adh} (mJ/m^2)	CD4+ count ($cells/mm^3$)	$\theta(^0C)$	γ_{sv} (mJ/m^2)	F^{adh} (mJ/m^2)
1	428	55	39.62	-73.42	428	52	41.77	-78.81
2	600	54	40.34	-75.24	600	53	41.05	-77.03
3	625	58	37.45	-67.83	625	50	43.18	-82.28
4	312	59	36.73	-65.93	312	59	36.73	-65.93
5	464	57	38.18	-69.71	464	58	37.45	-67.83
6	247	60	36.00	-64.00	247	57	38.18	-69.71
7	852	61	35.28	-62.06	852	54	40.34	-75.24
8	115	63	33.83	-58.11	115	60	36.00	-64.00
9	704	56	38.90	-71.58	704	62	34.55	-60.09
10	798	62	34.55	-60.09	798	56	38.90	-71.58
AVE	**514.5**	**58.5**	**37.09**	**-66.80**	**514.5**	**56.1**	**38.82**	**-71.25**
SD	**243.1059**	**3.02765**	**2.19166**	**5.76426**	**243.1059**	**3.81372**	**2.74553**	**7.05321**

Appendix B24:

Wu: Serum Infected

	(a) **Wu: Serum Treated With IFN**				(b) **Wu: Serum Treated With RBV**			
SN	$CD4^+$ count ($cells/mm^3$)	$\theta(^0C)$	γ_{sv} (mJ/m^2)	F^{adh} (mJ/m^2)	CD4+ count ($cells/mm^3$)	$\theta(^0C)$	γ_{sv} (mJ/m^2)	F^{adh} (mJ/m^2)
1	428	50	43.18	-82.28	428	55	39.62	-73.42
2	600	61	35.28	-62.06	600	50	43.18	-82.28
3	625	53	41.05	-77.03	625	54	40.34	-75.24
4	312	60	36.00	-64.00	312	60	36.00	-64.00
5	464	59	36.73	-65.93	464	56	38.90	-71.58
6	247	63	33.83	-58.11	247	58	37.45	-67.83
7	852	55	39.62	-73.42	852	53	41.05	-77.03
8	115	65	32.38	-54.10	115	59	36.73	-65.93
9	704	57	38.18	-69.71	704	57	38.18	-69.71
10	798	54	40.34	-75.24	798	61	35.28	-62.06
AVE	**514.5**	**57.7**	**37.66**	**-68.19**	**514.5**	**56.3**	**38.67**	**-70.91**
SD	**243.1059**	**4.73873**	**3.41710**	**8.92197**	**243.1059**	**3.40098**	**2.44635**	**6.27187**

INFECTED SAMPLES WITH ATR AND ELT TREATMENT

NEUMANN MODEL ANALYSIS

Appendix B25:

Neumann: Whole Blood Infected

	Neumann: Whole Blood Treated With ATR				**Neumann: Whole Blood Treated With ELT**			
SN	$CD4^+$ count (cells/mm^3)	$\theta(^0C)$	γ_{sv} (mJ/m^2)	F^{adh} (mJ/m^2)	CD4+ count (cells/mm^3)	$\theta(^0C)$	γ_{sv} (mJ/m^2)	F^{adh} (mJ/m^2)
1	428	53	41.05	-16.06	428	52	41.77	-15.39
2	600	55	39.62	-17.41	600	50	43.18	-14.06
3	625	56	38.90	-18.09	625	53	41.05	-16.06
4	312	59	36.73	-20.16	312	59	36.73	-20.16
5	464	57	38.18	-18.78	464	58	37.45	-19.47
6	247	54	40.34	-16.73	247	56	38.90	-18.09
7	852	60	36.00	-20.86	852	55	39.62	-17.41
8	115	58	37.45	-19.47	115	57	38.18	-18.78
9	704	52	41.77	-15.39	704	54	40.34	-16.73
10	798	51	42.48	-14.72	798	51	42.48	-14.72
AVE	**514.5**	**55.5**	**39.25**	**-17.77**	**514.5**	**54.5**	**39.97**	**-17.09**
SD	**243.1059**	**3.02765**	**2.17992**	**2.06491**	**243.1059**	**3.02765**	**2.17222**	**2.05280**

Appendix B 26:

Neumann: WBC Infected

	(a) Neumann: WBC Treated With ATR				(b) **Neumann: WBC Treated With ELT**			
SN	$CD4^+$ count (cells/mm^3)	$\theta(^0C)$	γ_{sv} (mJ/m^2)	F^{adh} (mJ/m^2)	CD4+ count (cells/mm^3)	$\theta(^0C)$	γ_{sv} (mJ/m^2)	F^{adh} (mJ/m^2)
1	428	54	40.34	-16.73	428	57	38.18	-18.78
2	600	49	43.88	-13.41	600	55	39.62	-17.41
3	625	50	43.18	-14.06	625	54	40.34	-16.73
4	312	60	36.00	-20.86	312	60	36.00	-20.86
5	464	58	37.45	-19.47	464	58	37.45	-19.47
6	247	62	34.55	-22.25	247	62	34.55	-22.25
7	852	57	38.18	-18.78	852	51	42.48	-14.72
8	115	65	32.38	-24.34	115	59	36.73	-20.16
9	704	52	41.77	-15.39	704	53	41.05	-16.06
10	798	59	36.73	-20.16	798	56	38.90	-18.09
AVE	**514.5**	**56.6**	**38.45**	**-18.55**	**514.5**	**56.5**	**38.53**	**-18.45**
SD	**243.1059**	**5.253**	**3.779195**	**3.588857**	**243.1059**	**3.374743**	**2.434114**	**2.31219**

Appendix B27:

Neumann: RBC Infected

	(a) **Neumann: RBC Treated With ATR**				(b) **Neumann: RBC Treated With ELT**			
SN	$CD4^+$ count (cells/mm^3)	$\theta(^0C)$	γ_{sv} (mJ/m^2)	F^{adh} (mJ/m^2)	CD4+ count (cells/mm^3)	$\theta(^0C)$	γ_{sv} (mJ/m^2)	F^{adh} (mJ/m^2)
1	428	57	38.18	-18.78	428	58	37.45	-19.47
2	600	55	39.62	-17.41	600	60	36.00	-20.86
3	625	56	38.90	-18.09	625	54	40.34	-16.73
4	312	59	36.73	-20.16	312	59	36.73	-20.16
5	464	58	37.45	-19.47	464	57	38.18	-18.78
6	247	60	36.00	-20.86	247	63	33.83	-22.95
7	852	63	33.83	-22.95	852	53	41.05	-16.06
8	115	61	35.28	-21.55	115	61	35.28	-21.55
9	704	62	34.55	-22.25	704	65	32.38	-24.34
10	798	54	40.34	-16.73	798	58	37.45	-19.47
AVE	**514.5**	**58.5**	**37.09**	**-19.825**	**514.5**	**58.8**	**36.87**	**-20.04**
SD	**243.1059**	**3.02765**	**2.191655**	**2.093505**	**243.1059**	**3.705851**	**2.679314**	**2.559488**

Appendix B28:

Neumann: Serum Infected

	(a) **Neumann: Serum Treated With ATR**				(b) **Neumann: Serum Treated With ELT**			
SN	$CD4^+$ count (cells/mm^3)	$\theta(^0C)$	γ_{sv} (mJ/m^2)	F^{adh} (mJ/m^2)	CD4+ count (cells/mm^3)	$\theta(^0C)$	γ_{sv} (mJ/m^2)	F^{adh} (mJ/m^2)
1	428	53	41.05	-16.06	428	53	41.05	-16.06
2	600	57	38.17	-18.78	600	57	31.18	-18.78
3	625	55	39.62	-17.41	625	55	39.62	-17.41
4	312	56	38.90	-18.09	312	56	38.90	-18.09
5	464	59	36.73	-20.16	464	59	36.73	-20.16
6	247	51	42.48	-14.72	247	58	37.45	-19.47
7	852	58	37.45	-19.47	852	54	40.34	-16.73
8	115	60	36.00	-20.86	115	60	36.00	-20.86
9	704	62	34.55	-22.25	704	62	34.55	-22.25
10	798	54	40.34	-16.73	798	52	41.77	-15.39
AVE	**514.5**	**56.5**	**38.53**	**-18.45**	**514.5**	**56.6**	**37.76**	**-18.52**
SD	**243.1059**	**3.374743**	**2.434276**	**2.31219**	**243.1059**	**3.204164**	**3.26896**	**2.198934**

Appendix B29:

Fowkes: Whole Blood Infected

	Fowkes:Whole Blood Treated With ATR				**Fowkes: Whole Blood Treated With ELT**			
SN	$CD4^+$ count ($cells/mm^3$)	$\theta(^0C)$	γ_{sv} (mJ/m^2)	F^{adh} (mJ/m^2)	CD4+ count ($cells/mm^3$)	$\theta(^0C)$	γ_{sv} (mJ/m^2)	F^{adh} (mJ/m^2)
1	428	53	41.05	-25.48	428	52	41.77	-24.60
2	600	55	39.62	-27.29	600	50	43.18	-22.86
3	625	56	38.90	-28.21	625	53	41.05	-25.48
4	312	59	36.73	-31.04	312	59	36.73	-31.04
5	464	57	38.18	-29.14	464	58	37.45	-30.09
6	247	54	40.34	-26.38	247	56	38.90	-28.21
7	852	60	36.00	-32.00	852	55	39.62	-27.29
8	115	58	37.45	-30.09	115	57	38.18	-29.14
9	704	52	41.77	-24.60	704	54	40.34	-26.38
10	798	51	42.48	-23.72	798	51	42.18	-23.72
AVE	**514.5**	**55.5**	**39.25**	**-27.795**	**514.5**	**54.5**	**39.94**	**-26.881**
SD	**243.1059**	**3.02765**	**2.179923**	**2.786684**	**243.1059**	**3.02765**	**2.135468**	**2.752952**

Appendix B30:

Fowkes: WBC Infected

	(c) Fowkes: WBC Treated With ATR				(d) **Fowkes: WBC Treated With ELT**			
SN	$CD4^+$ count ($cells/mm^3$)	$\theta(^0C)$	γ_{sv} (mJ/m^2)	F^{adh} (mJ/m^2)	CD4+ count ($cells/mm^3$)	$\theta(^0C)$	γ_{sv} (mJ/m^2)	F^{adh} (mJ/m^2)
1	428	54	40.34	-26.38	428	57	38.18	-29.14
2	600	49	43.88	-22.01	600	55	39.62	-27.29
3	625	50	43.18	-22.86	625	54	40.34	-26.38
4	312	60	36.00	-32.00	312	60	36.00	-32.00
5	464	58	37.45	-30.09	464	58	37.45	-30.09
6	247	62	34.55	-33.95	247	62	34.55	-33.95
7	852	57	38.18	-29.14	852	51	42.48	-23.72
8	115	65	32.38	-36.95	115	59	36.73	-31.04
9	704	52	41.77	-24.60	704	53	41.05	-25.48
10	798	59	36.73	-31.04	798	56	38.90	-28.21
AVE	**514.5**	**56.6**	**38.45**	**-28.902**	**514.5**	**56.5**	**38.53**	**-28.73**
SD	**243.1059**	**5.25357**	**3.779195**	**4.884924**	**243.1059**	**3.374743**	**2.434114**	**3.141553**

Appendix B31:

Fowkes: RBC Infected

	(c) **Fowkes: RBC Infected With ATR**				(d) **Fowkes: RBC Infected With ELT**			
SN	$CD4^+$ count (cells/mm^3)	$\theta(^0C)$	γ_{sv} (mJ/m^2)	F^{adh} (mJ/m^2)	CD4+ count (cells/mm^3)	$\theta(^0C)$	γ_{sv} (mJ/m^2)	F^{adh} (mJ/m^2)
1	428	57	38.18	-29.14	428	58	37.45	-30.09
2	600	55	39.62	-27.29	600	56	38.90	-28.21
3	625	56	38.90	-28.21	625	54	40.34	-26.38
4	312	59	36.73	-31.04	312	59	36.73	-31.04
5	464	58	37.45	-30.09	464	55	39.62	-27.29
6	247	60	36.00	-32.00	247	60	36.00	-32.00
7	852	61	35.27	-32.97	852	57	38.17	-29.14
8	115	54	40.34	-26.38	115	61	35.27	-32.97
9	704	63	33.83	-34.95	704	53	41.05	-25.48
10	798	52	41.77	-24.60	798	51	42.48	-23.72
AVE	**514.5**	**57.5**	**37.81**	**-29.67**	**514.5**	**56.4**	**38.60**	**-28.632**
SD	**243.1059**	**3.374743**	**2.43921**	**3.17728**	**243.1059**	**3.204164**	**2.311038**	**2.971295**

Appendix B32:

Fowkes: Serum Infected

	(a) **Fowkes: Serum Infected With ATR**				(b) **Fowkes: Serum Infected With ELT**			
SN	$CD4^+$ count (cells/mm^3)	$\theta(^0C)$	γ_{sv} (mJ/m^2)	F^{adh} (mJ/m^2)	CD4+ count (cells/mm^3)	$\theta(^0C)$	γ_{sv} (mJ/m^2)	F^{adh} (mJ/m^2)
1	428	53	41.05	-25.48	428	58	37.45	-30.09
2	600	57	38.17	-29.14	600	53	41.05	-25.48
3	625	55	39.62	-27.29	625	51	42.48	-23.72
4	312	56	38.90	-28.21	312	55	39.62	-27.29
5	464	59	36.73	-31.04	464	59	36.73	-31.04
6	247	61	35.27	-32.97	247	57	38.18	-29.14
7	852	52	41.77	-24.60	852	56	38.90	-28.21
8	115	60	36.00	-32.00	115	60	36.00	-32.00
9	704	54	40.34	-26.38	704	54	40.34	-26.38
10	798	51	42.48	-23.72	798	52	41.77	-24.60
AVE	**514.5**	**55.8**	**39.03**	**-28.08**	**514.5**	**55.5**	**39.25**	**-27.80**
SD	**243.1059**	**3.425395**	**2.470259**	**3.172356**	**243.1059**	**3.02765**	**2.179923**	**2.786684**

Appendix B33:

Wu: Whole Blood Infected

	(a) **Wu: Whole Blood Treated With ATR**				(b) **Wu: Whole Blood Treated With ELT**			
SN	$CD4^+$ count ($cells/mm^3$)	$\theta(^0C)$	γ_{sv} (mJ/m^2)	F^{adh} (mJ/m^2)	CD4+ count ($cells/mm^3$)	$\theta(^0C)$	γ_{sv} (mJ/m^2)	F^{adh} (mJ/m^2)
1	428	53	41.05	-77.03	428	52	41.77	-78.81
2	600	55	39.62	-73.42	600	50	43.18	-82.28
3	625	56	38.90	-71.58	625	53	41.05	-77.03
4	312	59	36.73	-65.93	312	59	36.73	-65.93
5	464	57	38.18	-69.71	464	58	37.45	-67.83
6	247	54	40.34	-75.24	247	56	38.90	-71.58
7	852	60	36.00	-64.00	852	55	39.62	-73.42
8	115	58	37.45	-67.83	115	57	38.18	-69.71
9	704	52	41.77	-78.81	704	54	40.34	-75.24
10	798	51	42.48	-80.55	798	51	42.48	-80.55
AVE	**514.5**	**55.5**	**39.25**	**-72.41**	**514.5**	**54.5**	**39.97**	**-74.238**
SD	**243.1059**	**3.02765**	**2.179923**	**5.570426**	**243.1059**	**3.02765**	**2.172224**	**5.502926**

Appendix B34:

Wu: WBC Infected

	(e) **Wu: WBC Treated With ATR**				(f) **Wu: WBC Treated With ELT**			
SN	$CD4^+$ count ($cells/mm^3$)	$\theta(^0C)$	γ_{sv} (mJ/m^2)	F^{adh} (mJ/m^2)	CD4+ count ($cells/mm^3$)	$\theta(^0C)$	γ_{sv} (mJ/m^2)	F^{adh} (mJ/m^2)
1	428	54	40.34	-75.24	428	57	38.18	-69.71
2	600	49	43.88	-83.98	600	55	39.62	-73.42
3	625	50	43.18	-82.28	625	54	40.34	-75.24
4	312	60	36.00	-64.00	312	60	36.00	-64.00
5	464	58	37.45	-67.83	464	58	37.45	-67.83
6	247	62	34.55	-60.09	247	62	34.55	-60.09
7	852	57	38.18	-69.71	852	51	42.48	-80.55
8	115	65	32.38	-54.10	115	59	36.73	-65.93
9	704	52	41.77	-78.81	704	53	41.05	-77.03
10	798	59	36.73	-65.93	798	56	38.90	-71.58
AVE	**514.5**	**56.6**	**38.45**	**-70.197**	**514.5**	**56.5**	**38.53**	**-70.54**
SD	**243.1059**	**5.25357**	**3.779195**	**9.771275**	**243.1059**	**3.3747**	**2.434114**	**6.280882**

Appendix B35:

Wu: RBC Infected

	(e) **Wu: RBC Infected With ATR**				(f) **Wu: RBC Infected With ELT**			
SN	$CD4^+$ count ($cells/mm^3$)	$\theta(^0C)$	γ_{sv} (mJ/m^2)	F^{adh} (mJ/m^2)	CD4+ count ($cells/mm^3$)	$\theta(^0C)$	γ_{sv} (mJ/m^2)	F^{adh} (mJ/m^2)
1	428	57	38.18	-69.71	428	58	37.45	-67.83
2	600	55	39.62	-73.42	600	56	38.90	-71.58
3	625	56	38.90	-71.58	625	54	40.34	-75.24
4	312	59	36.73	-65.93	312	59	36.73	-65.93
5	464	58	37.45	-67.83	464	55	39.62	-73.42
6	247	60	36.00	-64.00	247	60	36.00	-64.00
7	852	61	35.28	-62.06	852	57	38.18	-69.71
8	115	54	40.34	-75.24	115	61	35.28	-62.06
9	704	63	33.83	-58.11	704	53	41.05	-77.03
10	798	52	41.77	-78.81	798	51	42.48	-80.55
AVE	**514.5**	**57.5**	**37.81**	**-68.67**	**514.5**	**56.4**	**38.60**	**-70.74**
SD	**243.1059**	**3.374743**	**2.438055**	**6.353691**	**243.1059**	**3.204164**	**2.309233**	**5.938322**

Appendix B36:

Wu: Serum Infected

	(c) **Wu: Serum Infected With ATR**				(d) **Wu: Serum Infected With ELT**			
SN	$CD4^+$ count ($cells/mm^3$)	$\theta(^0C)$	γ_{sv} (mJ/m^2)	F^{adh} (mJ/m^2)	CD4+ count ($cells/mm^3$)	$\theta(^0C)$	γ_{sv} (mJ/m^2)	F^{adh} (mJ/m^2)
1	428	53	41.05	-77.03	428	58	37.45	-67.83
2	600	57	38.18	-69.72	600	53	41.05	-77.03
3	625	55	39.62	-73.42	625	51	42.48	-80.55
4	312	56	38.90	-71.58	312	55	39.62	-73.42
5	464	59	36.73	-65.93	464	59	36.73	-65.93
6	247	61	35.28	-62.06	247	57	38.18	-69.71
7	852	52	41.77	-78.81	852	56	38.90	-71.58
8	115	60	36.00	-64.00	115	60	36.00	-64.00
9	704	54	40.34	-75.24	704	54	40.34	-75.24
10	798	51	42.48	-80.55	798	52	41.77	-78.81
AVE	**514.5**	**55.8**	**39.04**	**-71.83**	**514.5**	**55.5**	**39.25**	**-72.41**
SD	**243.1059**	**3.425395**	**2.468181**	**6.34246**	**243.1059**	**3.02765**	**2.179923**	**5.570426**

INFECTED SAMPLES WITH AM AND VA TREATMENT

NEUMANN MODEL ANALYSIS

Appendix B37:

Neumann: Whole Blood Infected

	Neumann: Whole Blood Treated With AM				**Neumann: Whole Blood Treated With VA**			
SN	$CD4^+$ count (cells/mm^3)	$\theta(^0C)$	γ_{sv} (mJ/m^2)	F^{adh} (mJ/m^2)	CD4+ count (cells/mm^3)	$\theta(^0C)$	γ_{sv} (mJ/m^2)	F^{adh} (mJ/m^2)
1	428	50	43.18	-14.06	428	53	41.05	-16.06
2	600	56	38.90	-18.09	600	52	41.77	-15.39
3	625	51	42.48	-14.72	625	57	38.18	-18.78
4	312	59	36.73	-20.16	312	58	37.45	-19.47
5	464	57	38.18	-18.78	464	56	38.90	-18.09
6	247	53	41.05	-16.06	247	55	39.62	-17.41
7	852	54	40.34	-16.73	852	50	43.18	-14.06
8	115	58	37.45	-19.47	115	59	36.73	-20.16
9	704	52	41.77	-15.39	704	54	40.34	-16.73
10	798	55	39.62	-17.41	798	51	42.48	-14.72
AVE	**514.5**	**54.5**	**39.97**	**-17.09**	**514.5**	**54.5**	**39.97**	**-17.09**
SD	**243.1059**	**3.02765**	**2.172224**	**2.052803**	**243.1059**	**3.02765**	**2.172224**	**2.052803**

Appendix B38:

Neumann: WBC Infected

	(a) Neumann: WBC Treated With AM				(b) **Neumann: WBC Treated With VA**			
SN	$CD4^+$ count (cells/mm^3)	$\theta(^0C)$	γ_{sv} (mJ/m^2)	F^{adh} (mJ/m^2)	CD4+ count (cells/mm^3)	$\theta(^0C)$	γ_{sv} (mJ/m^2)	F^{adh} (mJ/m^2)
1	428	55	39.62	-17.41	428	51	42.48	-14.72
2	600	56	38.90	-18.09	600	57	38.18	-18.78
3	625	50	43.18	-14.06	625	56	38.90	-18.09
4	312	59	36.73	-20.16	312	58	37.45	-19.47
5	464	60	36.00	-20.86	464	55	39.62	-17.41
6	247	57	38.18	-18.78	247	60	36.00	-20.86
7	852	58	37.45	-19.47	852	54	40.34	-16.73
8	115	66	31.66	-25.03	115	53	41.05	-16.06
9	704	61	35.28	-21.55	704	59	36.73	-20.16
10	798	63	33.83	-22.95	798	52	41.77	-15.39
AVE	**514.5**	**58.5**	**37.08**	**-19.84**	**514.5**	**55.5**	**39.25**	**-17.77**
SD	**243.1059**	**4.453463**	**3.210895**	**3.060705**	**243.1059**	**3.02765**	**2.179923**	**2.064914**

Appendix B39:

Neumann: RBC Infected

	(a)Neumann: RBC Treated With AM				(b)Neumann: RBC Treated With VA			
SN	$CD4^+$ count ($cells/mm^3$)	$\theta(^0C)$	γ_{sv} (mJ/m^2)	F^{adh} (mJ/m^2)	CD4+ count ($cells/mm^3$)	$\theta(^0C)$	γ_{sv} (mJ/m^2)	F^{adh} (mJ/m^2)
1	428	57	38.18	-18.78	428	59	36.73	-20.16
2	600	56	38.90	-18.09	600	56	38.90	-18.09
3	625	58	37.45	-19.47	625	54	40.34	-16.73
4	312	59	36.73	-20.16	312	57	38.18	-18.78
5	464	55	39.62	-17.41	464	58	37.45	-19.47
6	247	60	36.00	-20.86	247	64	33.10	-23.64
7	852	61	35.28	-21.55	852	60	36.00	-20.86
8	115	54	40.34	-16.73	115	61	35.28	-21.55
9	704	63	33.83	-22.95	704	58	37.45	-19.47
10	798	53	41.05	-16.06	798	55	39.62	-17.41
AVE	**514.5**	**57.6**	**37.74**	**-19.21**	**514.5**	**58.2**	**37.31**	**-19.62**
SD	**243.1059**	**3.204164**	**2.315675**	**2.208766**	**243.1059**	**2.973961**	**2.15351**	**2.055941**

Appendix B40:

Neumann: Serum Infected

	Neumann: Serum Treated With AM				Neumann: Serum Treated With VA			
SN	$CD4^+$ count ($cells/mm^3$)	$\theta(^0C)$	γ_{sv} (mJ/m^2)	F^{adh} (mJ/m^2)	CD4+ count ($cells/mm^3$)	$\theta(^0C)$	γ_{sv} (mJ/m^2)	F^{adh} (mJ/m^2)
1	428	56	38.90	-18.094	428	58	37.45	-19.47
2	600	55	39.62	-17.411	600	55	39.62	-17.41
3	625	58	37.45	-19.471	625	52	41.77	-15.39
4	312	60	36.00	-20.857	312	60	36.00	-20.86
5	464	63	33.83	-22.945	464	50	43.18	-14.06
6	247	59	36.73	-20.163	247	59	36.73	-20.16
7	852	57	38.18	-18.781	852	54	40.34	-16.73
8	115	61	35.28	-21.552	115	51	42.48	-14.72
9	704	65	32.38	-24.336	704	57	38.18	-18.78
10	798	67	30.95	-25.723	798	56	38.90	-18.09
AVE	**514.5**	**60.1**	**35.93**	**-20.93**	**514.5**	**55.2**	**39.47**	**-17.57**
SD	**243.1059**	**3.928528**	**2.841951**	**2.724119**	**243.1059**	**3.425395**	**2.461058**	**2.328634**

Appendix B41:

Fowkes: Whole Blood Infected

	Fowkes: Whole Blood Treated With AM				**Fowkes: Whole Blood Treated With VA**			
SN	$CD4^+$ count (cells/mm^3)	$\theta(^0C)$	γ_{sv} (mJ/m^2)	F^{adh} (mJ/m^2)	CD4+ count (cells/mm^3)	$\theta(^0C)$	γ_{sv} (mJ/m^2)	F^{adh} (mJ/m^2)
1	428	50	43.18	-22.86	428	53	41.053	-25.484
2	600	56	38.90	-28.21	600	52	41.7658	-24.598
3	625	51	42.48	-23.72	625	57	38.1746	-29.143
4	312	59	36.73	-31.04	312	58	37.4504	-30.085
5	464	57	38.18	-29.14	464	56	38.8973	-28.212
6	247	53	41.05	-25.48	247	55	39.6183	-27.291
7	852	54	40.34	-26.38	852	50	43.18	-22.862
8	115	58	37.45	-30.09	115	59	36.7254	-31.038
9	704	52	41.77	-24.60	704	54	40.337	-26.382
10	798	55	39.62	-27.29	798	51	42.475	-23.724
AVE	**514.5**	**54.5**	**39.97**	**-26.88**	**514.5**	**54.5**	**39.97**	**-26.88**
SD	**243.1059**	**3.02765**	**2.172224**	**2.752952**	**243.1059**	**3.02765**	**2.172689**	**2.75145**

Appendix B42:

Fowkes: WBC Infected

	(c) Fowkes: WBC Treated With AM				(d) **Fowkes: WBC Treated With VA**			
SN	$CD4^+$ count (cells/mm^3)	$\theta(^0C)$	γ_{sv} (mJ/m^2)	F^{adh} (mJ/m^2)	CD4+ count (cells/mm^3)	$\theta(^0C)$	γ_{sv} (mJ/m^2)	F^{adh} (mJ/m^2)
1	428	55	39.62	-27.29	428	51	42.475	-23.724
2	600	56	38.90	-28.21	600	57	38.1746	-29.143
3	625	50	43.18	-22.86	625	56	38.8973	-28.212
4	312	59	36.73	-31.04	312	58	37.4504	-30.085
5	464	60	36.00	-32.00	464	55	39.6183	-27.291
6	247	57	38.18	-29.14	247	60	36.00	-32.00
7	852	58	37.45	-30.09	852	54	40.337	-26.382
8	115	66	31.66	-37.97	115	53	41.053	-25.484
9	704	61	35.28	-32.97	704	59	36.7254	-31.038
10	798	63	33.83	-34.95	798	52	41.7658	-24.598
AVE	**514.5**	**58.5**	**37.08**	**-30.65**	**514.5**	**55.5**	**39.25**	**-27.80**
SD	**243.1059**	**4.453463**	**3.210895**	**4.215716**	**243.1059**	**3.02765**	**2.179537**	**2.785265**

Appendix B43:

Fowkes: RBC Infected

	(g) Fowkes: RBC Infected With AM				(h) **Fowkes: RBC Infected With VA**			
SN	$CD4^+$ count ($cells/mm^3$)	$\theta(^0C)$	γ_{sv} (mJ/m^2)	F^{adh} (mJ/m^2)	CD4+ count ($cells/mm^3$)	$\theta(^0C)$	γ_{sv} (mJ/m^2)	F^{adh} (mJ/m^2)
1	428	57	38.18	-29.14	428	59	36.73	-31.04
2	600	56	38.90	-28.21	600	56	38.90	-28.21
3	625	58	37.45	-30.09	625	54	40.34	-26.38
4	312	59	36.73	-31.04	312	57	38.18	-29.14
5	464	55	39.62	-27.29	464	58	37.45	-30.09
6	247	60	36.00	-32.00	247	64	33.10	-35.94
7	852	61	35.28	-32.97	852	60	36.00	-32.00
8	115	54	40.34	-26.38	115	61	35.28	-32.97
9	704	63	33.83	-34.95	704	58	37.45	-30.09
10	798	53	41.05	-25.48	798	55	39.62	-27.29
AVE	**514.5**	**57.6**	**37.74**	**-29.76**	**514.5**	**58.2**	**37.31**	**-30.32**
SD	**243.1059**	**3.204164**	**2.315675**	**3.030135**	**243.1059**	**2.973961**	**2.15351**	**2.840232**

Appendix B44:

Fowkes: Serum Infected

	(e) Fowkes: Serum Infected With AM				(f) **Fowkes: Serum Infected With VA**			
SN	$CD4^+$ count ($cells/mm^3$)	$\theta(^0C)$	γ_{sv} (mJ/m^2)	F^{adh} (mJ/m^2)	CD4+ count ($cells/mm^3$)	$\theta(^0C)$	γ_{sv} (mJ/m^2)	F^{adh} (mJ/m^2)
1	428	56	38.90	-28.21	428	58	37.45	-30.09
2	600	55	39.62	-27.29	600	55	39.62	-27.29
3	625	58	37.45	-30.09	625	52	41.77	-24.60
4	312	60	36.00	-32.00	312	60	36.00	-32.00
5	464	63	33.83	-34.95	464	50	43.18	-22.86
6	247	59	36.73	-31.04	247	59	36.73	-31.04
7	852	57	38.18	-29.14	852	54	40.34	-26.38
8	115	61	35.28	-32.97	115	51	42.48	-23.72
9	704	65	32.38	-36.95	704	57	38.18	-29.14
10	798	67	30.95	-38.99	798	56	38.90	-28.21
AVE	**514.5**	**60.1**	**35.93**	**-32.16**	**514.5**	**55.2**	**39.47**	**-27.53**
SD	**243.1059**	**3.928528**	**2.84195**	**3.830257**	**243.1059**	**3.425395**	**2.461058**	**3.130478**

Appendix B45:

Wu: Whole Blood Infected

	(a) Wu: Whole Blood Infected With AM				(b) **Wu: Whole Blood Infected With VA**			
SN	$CD4^+$ count ($cells/mm^3$)	$\theta(^0C)$	γ_{sv} (mJ/m^2)	F^{adh} (mJ/m^2)	CD4+ count ($cells/mm^3$)	$\theta(^0C)$	γ_{sv} (mJ/m^2)	F^{adh} (mJ/m^2)
1	428	50	43.18	-82.28	428	53	41.05	-77.03
2	600	56	38.90	-71.58	600	52	41.77	-78.81
3	625	51	42.48	-80.55	625	57	38.18	-69.71
4	312	59	36.73	-65.93	312	58	37.45	-67.83
5	464	57	38.18	-69.71	464	56	38.90	-71.58
6	247	53	41.05	-77.03	247	55	39.62	-73.42
7	852	54	40.34	-75.24	852	50	43.18	-82.28
8	115	58	37.45	-67.83	115	59	36.73	-65.93
9	704	52	41.77	-78.80	704	54	40.34	-75.24
10	798	55	39.62	-73.42	798	51	42.48	-80.55
AVE	**514.5**	**54.5**	**39.97**	**-74.24**	**514.5**	**54.5**	**39.97**	**-74.24**
SD	**243.1059**	**3.02765**	**2.172224**	**5.502004**	**243.1059**	**3.02765**	**2.172224**	**5.502926**

Appendix B46:

Wu: WBC Infected

	(e) Wu: WBC Treated With AM				(f) **Wu: WBC Treated With VA**			
SN	$CD4^+$ count ($cells/mm^3$)	$\theta(^0C)$	γ_{sv} (mJ/m^2)	F^{adh} (mJ/m^2)	CD4+ count ($cells/mm^3$)	$\theta(^0C)$	γ_{sv} (mJ/m^2)	F^{adh} (mJ/m^2)
1	428	55	39.62	-80.55	428	51	42.48	-73.42
2	600	56	38.90	-69.71	600	57	38.18	-71.58
3	625	50	43.18	-71.58	625	56	38.90	-82.28
4	312	59	36.73	-67.83	312	58	37.45	-65.93
5	464	60	36.00	-73.42	464	55	39.62	-64.00
6	247	57	38.18	-64.00	247	60	36.00	-69.71
7	852	58	37.45	-75.24	852	54	40.34	-67.83
8	115	66	31.66	-77.03	115	53	41.05	-52.06
9	704	61	35.28	-65.93	704	59	36.73	-62.06
10	798	63	33.83	-78.81	798	52	41.77	-58.11
AVE	**514.5**	**58.5**	**37.08**	**-72.41**	**514.5**	**55.5**	**39.25**	**-66.70**
SD	**243.1059**	**4.453463**	**3.210895**	**5.570426**	**243.1059**	**3.02765**	**2.179923**	**8.42995**

Appendix B47:

Wu: RBC Infected

	(i) **Wu: RBC Treated With AM**				(j) **Wu: RBC Treated With VA**			
SN	$CD4^+$ count ($cells/mm^3$)	$\theta(^0C)$	γ_{sv} (mJ/m^2)	F^{adh} (mJ/m^2)	CD4+ count ($cells/mm^3$)	$\theta(^0C)$	γ_{sv} (mJ/m^2)	F^{adh} (mJ/m^2)
1	428	57	38.18	-69.71	428	59	36.73	-65.93
2	600	56	38.90	-71.58	600	56	38.90	-71.58
3	625	58	37.45	-67.83	625	54	40.34	-75.24
4	312	59	36.73	-65.93	312	57	38.18	-69.71
5	464	55	39.62	-73.42	464	58	37.45	-67.83
6	247	60	36.00	-64.00	247	64	33.10	-56.11
7	852	61	35.28	-62.06	852	60	36.00	-64.00
8	115	54	40.34	-75.24	115	61	35.28	-62.06
9	704	63	33.83	-58.11	704	58	37.45	-67.83
10	798	53	41.05	-77.03	798	55	39.62	-73.42
AVE	**514.5**	**57.6**	**37.74**	**-68.49**	**514.5**	**58.2**	**37.31**	**-67.37**
SD	**243.1059**	**3.204164**	**2.315675**	**6.05598**	**243.1059**	**2.973961**	**2.15351**	**5.682101**

Appendix B48:

Wu: Serum Infected

	(g) **Wu: Serum Treated With AM**				(h) **Wu: Serum Treated With VA**			
SN	$CD4^+$ count ($cells/mm^3$)	$\theta(^0C)$	γ_{sv} (mJ/m^2)	F^{adh} (mJ/m^2)	CD4+ count ($cells/mm^3$)	$\theta(^0C)$	γ_{sv} (mJ/m^2)	F^{adh} (mJ/m^2)
1	428	56	38.90	-71.58	428	58	37.45	-67.83
2	600	55	39.62	-73.42	600	55	39.62	-73.42
3	625	58	37.45	-67.83	625	52	41.77	-78.81
4	312	60	36.00	-64.00	312	60	36.00	-64.00
5	464	63	33.83	-58.11	464	50	43.18	-82.28
6	247	59	36.73	-65.93	247	59	36.73	-65.93
7	852	57	38.18	-69.71	852	54	40.34	-75.24
8	115	61	35.28	-62.06	115	51	42.48	-80.55
9	704	65	32.38	-54.10	704	57	38.18	-69.71
10	798	67	30.95	-50.01	798	56	38.90	-71.58
AVE	**514.5**	**60.1**	**35.93**	**-63.68**	**514.5**	**55.2**	**39.47**	**-72.94**
SD	**243.1059**	**3.928528**	**2.841951**	**7.661739**	**243.1059**	**3.425395**	**2.461058**	**6.259065**

INFECTED SAMPLES WITH BP TREATMENT AND DH TREATMENT

NEUMANN MODEL ANALYSIS

Appendix B49:

Neumann: Whole Blood Infected

	Neumann: Whole Blood Treated With BP				**Neumann: Whole Blood Treated With DH**			
SN	$CD4^+$ count (cells/mm^3)	$\theta(^0C)$	γ_{sv} (mJ/m^2)	F^{adh} (mJ/m^2)	CD4+ count (cells/mm^3)	$\theta(^0C)$	γ_{sv} (mJ/m^2)	F^{adh} (mJ/m^2)
1	428	60	36.00	-20.86	428	50	43.18	-14.06
2	600	50	43.18	-14.06	600	55	39.62	-17.41
3	625	52	41.77	-15.39	625	58	37.45	-19.47
4	312	56	38.90	-18.09	312	59	36.73	-20.16
5	464	59	36.73	-20.16	464	49	43.89	-13.41
6	247	51	42.48	-14.72	247	56	38.90	-18.09
7	852	55	39.62	-17.41	852	54	40.34	-16.73
8	115	58	37.45	-19.47	115	57	38.18	-18.78
9	704	53	41.05	-16.06	704	48	44.58	-12.77
10	798	54	40.34	-16.73	798	51	42.48	-14.72
AVE	**514.5**	**54.8**	**39.75**	**-17.30**	**514.5**	**53.7**	**40.54**	**-16.56**
SD	**243.1059**	**3.425395**	**2.4619**	**2.330061**	**243.1059**	**3.945462**	**2.81833**	**2.65353**

Appendix B50:

Neumann: WBC Infected

	(a)Neumann: WBC Treated With BP				(g) **Neumann: WBC Treated With DH**			
SN	$CD4^+$ count (cells/mm^3)	$\theta(^0C)$	γ_{sv} (mJ/m^2)	F^{adh} (mJ/m^2)	CD4+ count (cells/mm^3)	$\theta(^0C)$	γ_{sv} (mJ/m^2)	F^{adh} (mJ/m^2)
1	428	58	37.45	-19.47	428	56	38.90	-18.09
2	600	50	43.18	-14.06	600	58	37.45	-19.47
3	625	55	39.62	-17.41	625	57	38.18	-18.78
4	312	57	38.18	-18.78	312	60	36.00	-20.86
5	464	60	36.00	-20.86	464	62	34.55	-22.25
6	247	59	36.73	-20.16	247	59	36.73	-20.16
7	852	53	41.05	-16.06	852	61	35.28	-21.55
8	115	62	34.55	-22.25	115	65	32.38	-24.34
9	704	56	38.90	-18.09	704	63	33.83	-22.95
10	798	54	40.34	-16.73	798	55	39.62	-17.41
AVE	**514.5**	**56.4**	**38.6**	**-18.39**	**514.5**	**59.6**	**36.29**	**-20.59**
SD	**243.1059**	**3.565265**	**2.566779**	**2.436655**	**243.1059**	**3.204164**	**2.321009**	**2.222607**

Appendix B51:

Neumann: RBC Infected

	(k) Neumann: RBC Treated With BP				(l) Neumann: RBC Treated With DH			
SN	$CD4^+$ count (cells/mm^3)	$\theta(^0C)$	γ_{sv} (mJ/m^2)	F^{adh} (mJ/m^2)	CD4+ count (cells/mm^3)	$\theta(^0C)$	γ_{sv} (mJ/m^2)	F^{adh} (mJ/m^2)
1	428	58	37.45	-19.47	428	55	39.62	-17.411
2	600	57	38.18	-18.78	600	53	41.05	-16.06
3	625	56	38.90	-18.09	625	56	38.90	-18.09
4	312	59	36.73	-20.16	312	49	43.88	-13.41
5	464	62	34.55	-22.25	464	58	37.45	-19.47
6	247	60	36.00	-20.86	247	57	38.18	-18.78
7	852	55	39.62	-17.41	852	51	42.48	-14.72
8	115	61	35.28	-21.55	115	54	40.34	-16.73
9	704	65	32.38	-24.34	704	52	41.77	-15.39
10	798	63	33.83	-22.95	798	48	44.58	-12.77
AVE	**514.5**	**59.6**	**36.29**	**-20.59**	**514.5**	**53.3**	**40.83**	**-16.28**
SD	**243.1059**	**3.204164**	**2.321009**	**2.222607**	**243.1059**	**3.335**	**2.37803**	**2.236437**

Appendix B52:

Neumann: Serum Infected

	(c) Neumann: Serum Treated With BP				(d) Neumann: Serum Treated With DH			
SN	$CD4^+$ count (cells/mm^3)	$\theta(^0C)$	γ_{sv} (mJ/m^2)	F^{adh} (mJ/m^2)	CD4+ count (cells/mm^3)	$\theta(^0C)$	γ_{sv} (mJ/m^2)	F^{adh} (mJ/m^2)
1	428	58	37.45	-19.47	428	55	39.62	-17.41
2	600	55	39.62	-17.41	600	56	38.90	-18.09
3	625	56	38.90	-18.09	625	57	38.18	-18.78
4	312	59	36.73	-20.16	312	59	36.73	-20.16
5	464	57	38.18	-18.78	464	46	45.95	-11.50
6	247	54	40.34	-16.73	247	58	37.45	-19.47
7	852	50	43.18	-14.06	852	48	44.58	-12.77
8	115	49	43.88	-13.41	115	53	41.05	-16.06
9	704	60	36.00	-20.86	704	51	42.48	-14.72
10	798	52	41.77	-15.39	798	49	43.88	-13.41
AVE	**514.5**	**55**	**39.61**	**-17.436**	**514.5**	**53.2**	**40.88**	**-16.24**
SD	**243.1059**	**3.741657**	**2.681568**	**2.534352**	**243.1059**	**4.516636**	**3.210558**	**3.016665**

Appendix B53:

Fowkes: Whole Blood Infected

	(c) **Fowkes: Whole Blood Treated With BP**				(d) **Fowkes: Whole Blood Treated With DH**			
SN	$CD4^+$ count ($cells/mm^3$)	$\theta(^0C)$	γ_{sv} (mJ/m^2)	F^{adh} (mJ/m^2)	CD4+ count ($cells/mm^3$)	θowkes(^{0}C)	γ_{sv} (mJ/m^2)	F^{adh} (mJ/m^2)
1	428	60	36.00	-32.00	428	50	43.18	-22.86
2	600	50	43.18	-22.86	600	55	39.62	-27.29
3	625	52	41.77	-24.60	625	58	37.45	-30.09
4	312	56	38.90	-28.21	312	59	36.73	-31.04
5	464	59	36.73	-31.04	464	49	43.88	-22.01
6	247	51	42.48	-23.72	247	56	38.90	-28.21
7	852	55	39.62	-27.29	852	54	40.34	-26.38
8	115	58	37.45	-30.09	115	57	38.18	-29.14
9	704	53	41.05	-25.48	704	48	44.58	-21.18
10	798	54	40.34	-26.38	798	51	42.48	-23.72
AVE	**514.5**	**54.8**	**39.75**	**-27.17**	**514.5**	**53.7**	**40.53**	**-26.19**
SD	**243.1059**	**3.425395**	**2.4619**	**3.13567**	**243.1059**	**3.945462**	**2.817009**	**3.535907**

Appendix B54:

Fowkes: WBC Infected

	(h) **Fowkes: WBC Treated With BP**				(i) **Fowkes: WBC Treated With DH**			
SN	$CD4^+$ count ($cells/mm^3$)	$\theta(^0C)$	γ_{sv} (mJ/m^2)	F^{adh} (mJ/m^2)	CD4+ count ($cells/mm^3$)	$\theta(^0C)$	γ_{sv} (mJ/m^2)	F^{adh} (mJ/m^2)
1	428	58	37.45	-30.09	428	56	38.90	-28.21
2	600	50	43.18	-22.86	600	58	37.45	-30.09
3	625	55	39.62	-27.29	625	57	38.18	-29.14
4	312	57	38.18	-29.14	312	60	36.00	-32.00
5	464	60	36.00	-32.00	464	62	34.55	-33.95
6	247	59	36.73	-31.04	247	59	36.73	-31.04
7	852	53	41.05	-25.48	852	61	35.28	-32.97
8	115	62	34.55	-33.95	115	65	32.38	-36.95
9	704	56	38.90	-28.21	704	63	33.83	-34.95
10	798	54	40.34	-26.38	798	55	39.62	-27.29
AVE	**514.5**	**56.4**	**38.6**	**-28.64**	**514.5**	**59.6**	**36.29**	**-31.66**
SD	**243.1059**	**3.565265**	**2.566779**	**3.301633**	**243.1059**	**3.204164**	**2.321009**	**3.092699**

Appendix B55:

Fowkes: RBC Infected

	(m)Fowkes: RBC Treated With BP				(n) Fowkes: RBC Treated With DH			
SN	$CD4^+$ count (cells/mm^3)	$\theta(^0C)$	γ_{sv} (mJ/m^2)	F^{adh} (mJ/m^2)	CD4+ count (cells/mm^3)	$\theta(^0C)$	γ_{sv} (mJ/m^2)	F^{adh} (mJ/m^2)
1	428	58	37.45	-30.09	428	55	39.62	-27.29
2	600	57	38.18	-29.14	600	53	41.05	-25.48
3	625	56	38.90	-28.21	625	56	38.90	-28.21
4	312	59	36.73	-31.04	312	49	43.88	-22.01
5	464	62	34.55	-33.95	464	58	37.45	-30.09
6	247	60	36.00	-32.00	247	57	38.18	-29.14
7	852	55	39.62	-27.29	852	51	42.48	-23.72
8	115	61	35.28	-32.97	115	54	40.34	-26.38
9	704	65	32.38	-36.95	704	52	41.77	-24.60
10	798	63	33.83	-34.95	798	48	44.58	-21.18
AVE	**514.5**	**59.6**	**36.29**	**-31.66**	**514.5**	**53.3**	**40.83**	**-25.81**
SD	**243.1059**	**3.204164**	**2.321009**	**3.092699**	**243.1059**	**3.335**	**2.37803**	**2.972104**

Appendix B56:

Fowkes: Serum Infected

	(i) Fowkes: Serum Treated With BP				(j) Fowkes: Serum Treated With DH			
SN	$CD4^+$ count (cells/mm^3)	$\theta(^0C)$	γ_{sv} (mJ/m^2)	F^{adh} (mJ/m^2)	CD4+ count (cells/mm^3)	$\theta(^0C)$	γ_{sv} (mJ/m^2)	F^{adh} (mJ/m^2)
1	428	58	37.45	-30.09	428	55	39.62	-27.29
2	600	55	39.62	-27.29	600	56	38.90	-28.21
3	625	56	38.90	-28.21	625	57	38.18	-29.14
4	312	59	36.73	-31.04	312	59	36.73	-31.04
5	464	57	38.18	-29.14	464	46	45.95	-19.54
6	247	54	40.34	-26.38	247	58	37.45	-30.09
7	852	50	43.18	-22.86	852	48	44.58	-21.18
8	115	49	43.88	-22.01	115	53	41.05	-25.48
9	704	60	36.00	-32.00	704	51	42.48	-23.72
10	798	52	41.77	-24.60	798	49	43.88	-22.01
AVE	**514.5**	**55**	**39.61**	**-27.36**	**514.5**	**53.2**	**40.88**	**-25.77**
SD	**243.1059**	**3.741657**	**2.681568**	**3.39724**	**243.1059**	**4.5166**	**3.2106**	**4.0050**

Appendix B57:

Wu: Whole Blood Infected

	(e) **Wu: Whole Blood Treated With BP**				(f) **Wu: Whole Blood Treated With DH**			
SN	$CD4^+$ count ($cells/mm^3$)	$\theta(^0C)$	γ_{sv} (mJ/m^2)	F^{adh} (mJ/m^2)	CD4+ count ($cells/mm^3$)	$\theta(^0C)$	γ_{sv} (mJ/m^2)	F^{adh} (mJ/m^2)
1	428	60	36.00	-64.00	428	50	43.18	-82.28
2	600	50	43.18	-82.28	600	55	39.62	-73.42
3	625	52	41.77	-78.81	625	58	37.45	-67.83
4	312	56	38.90	-71.58	312	59	36.73	-65.93
5	464	59	36.73	-65.93	464	49	43.88	-83.98
6	247	51	42.48	-80.55	247	56	38.90	-71.58
7	852	55	39.62	-73.42	852	54	40.34	-75.24
8	115	58	37.45	-67.83	115	57	38.18	-69.71
9	704	53	41.05	-77.03	704	48	44.58	-85.65
10	798	54	40.34	-75.24	798	51	42.48	-80.55
AVE	**514.5**	**54.8**	**39.75**	**-73.67**	**514.5**	**53.7**	**40.53**	**-75.62**
SD	**243.1059**	**3.425395**	**2.4619**	**6.268025**	**243.1059**	**3.945462**	**2.81701**	**7.07079**

Appendix B58:

Wu: WBC Infected

	(j) **Wu: WBC Treated With BP**				(k) **Wu: WBC Treated With DH**			
SN	$CD4^+$ count ($cells/mm^3$)	$\theta(^0C)$	γ_{sv} (mJ/m^2)	F^{adh} (mJ/m^2)	CD4+ count ($cells/mm^3$)	$\theta(^0C)$	γ_{sv} (mJ/m^2)	F^{adh} (mJ/m^2)
1	428	58	37.45	-67.83	428	56	38.90	-71.58
2	600	50	43.18	-82.28	600	58	37.45	-67.83
3	625	55	39.62	-73.42	625	57	38.18	-69.71
4	312	57	38.18	-69.71	312	60	36.00	-64.00
5	464	60	36.00	-64.00	464	62	34.55	-60.09
6	247	59	36.73	-65.93	247	59	36.73	-65.93
7	852	53	41.05	-77.03	852	61	35.28	-62.06
8	115	62	34.55	-60.09	115	65	32.38	-54.10
9	704	56	38.90	-71.58	704	63	33.83	-58.11
10	798	54	40.34	-75.24	798	55	39.62	-73.42
AVE	**514.5**	**56.4**	**38.60**	**-70.71**	**514.5**	**59.6**	**36.29**	**-64.68**
SD	**243.1059**	**3.565265**	**2.566779**	**6.602865**	**243.1059**	**3.204164**	**2.32101**	**6.18492**

Appendix B59:

Wu: RBC Infected

	(o) **Wu: RBC Treated With BP**				(p) **Wu: RBC Treated With DH**			
SN	$CD4^+$ count ($cells/mm^3$)	$\theta(^0C)$	γ_{sv} (mJ/m^2)	F^{adh} (mJ/m^2)	CD4+ count ($cells/mm^3$)	$\theta(^0C)$	γ_{sv} (mJ/m^2)	F^{adh} (mJ/m^2)
1	428	58	37.45	-67.83	428	55	39.62	-73.42
2	600	57	38.18	-69.71	600	53	41.05	-77.03
3	625	56	38.90	-71.58	625	56	38.90	-71.58
4	312	59	36.73	-65.93	312	49	43.88	-83.98
5	464	62	34.55	-60.09	464	58	37.45	-67.83
6	247	60	36.00	-64.00	247	57	38.18	-69.71
7	852	55	39.62	-73.42	852	51	42.48	-80.55
8	115	61	35.28	-62.06	115	54	40.34	-75.24
9	704	65	32.38	-54.10	704	52	41.77	-78.81
10	798	63	33.83	-58.11	798	48	44.58	-85.65
AVE	**514.5**	**59.6**	**36.29**	**-64.68**	**514.5**	**53.3**	**40.83**	**-76.38**
SD	**243.1059**	**3.204164**	**2.321009**	**6.184924**	**243.1059**	**3.335**	**2.37803**	**5.94514**

Appendix B60:

Wu: Serum Infected

	(k) **Wu: Serum Treated With BP**				(l) **Wu: Serum Treated With DH**			
SN	$CD4^+$ count ($cells/mm^3$)	$\theta(^0C)$	γ_{sv} (mJ/m^2)	F^{adh} (mJ/m^2)	CD4+ count ($cells/mm^3$)	$\theta(^0C)$	γ_{sv} (mJ/m^2)	F^{adh} (mJ/m^2)
1	428	58	37.45	-67.83	428	55	39.62	-73.42
2	600	55	39.62	-73.42	600	56	38.90	-71.58
3	625	56	38.90	-71.58	625	57	38.18	-69.71
4	312	59	36.73	-65.93	312	59	36.73	-65.93
5	464	57	38.18	-69.71	464	46	45.95	-88.92
6	247	54	40.34	-75.24	247	58	37.45	-67.83
7	852	50	43.18	-82.28	852	48	44.58	-85.65
8	115	49	43.88	-83.98	115	53	41.05	-77.03
9	704	60	36.00	-64.00	704	51	42.48	-80.55
10	798	52	41.77	-78.81	798	49	43.88	-83.98
AVE	**514.5**	**55**	**39.61**	**-73.28**	**514.5**	**53.2**	**40.88**	**-76.46**
SD	**243.1059**	**3.741657**	**2.681568**	**6.793873**	**243.1059**	**4.516636**	**3.210558**	**8.008935**

Appendix C1:

Average Interfacial Surface Free Energy(γ_{sv}) in (mJ/m^2)

Neumann Model

			Treated(γ_{sv})							
Blood Cells	**Infected** (γ_{sv})	**Uninfecte** (γ_{sv})	**IFN**	**RBV**	**ATR**	**ELT**	**AM**	**VA**	**BP**	**DH**
Whol. Blood	38.10 ± 1.72	43.47± 3.70	39.87 ± 2.28	39.61±1.85	39.25 ±2.18	39.97 ±2.17	39.97 ±2.17	39.97 ±2.17	39.75 ±2.46	40.54± 2.82
WBC	33.54 ±2.31	44.35± 1.90	38.24 ±3.16	38.66±3.08	38.45 ±3.78	38.53 ±2.43	37.08 ±3.21	39.25 ± 2.18	38.6± 2.57	36.29± 2.32
RBC	35.71 ±2.08	42.74± 2.51	37.10 ±2.19	38.82±2.75	37.09 ±2.19	36.87 ±2.68	37.74 ±2.32	37.31 ± 2.15	36.29 ±2.32	40.83± 2.38
Serum	34.92 ±2.19	40.53± 2.75	37.66 ±3.42	38.67±2.45	38.53 ±2.43	37.76 ±3.27	35.93 ±2.84	39.47 ±2.46	39.61 ±2.68	40.88± 3.21

Appendix C2:

Average Interfacial Surface Free Energy(γ_{sv}) in (mJ/m^2)

Fowkes Model

			Treated(γ_{sv})							
Blood Cells	**Infected** (γ_{sv})	**Uninfected** (γ_{sv})	**IFN**	**RBV**	**ATR**	**ELT**	**AM**	**VA**	**BP**	**DH**
Whol. Blood	38.10 ±1.72	43.47± 3.70	39.97 ±2.17	39.61 ±1.86	39.25± 2.18	39.94± 2.18	39.97± 2.17	39.97± 2.17	39.75± 2.46	40.53 ±2.82
WBC	33.54 ±2.31	44.35±1 .90	38.24 ±3.16	38.66 ±3.08	38.45± 3.78	38.53± 2.43	37.08± 3.21	39.25± 2.18	38.6±2 .57	36.29 ±2.32
RBC	35.71 ±2.08	42.74±2 .51	37.09 ±2.19	38.82 ±2.75	37.81± 2.44	38.60± 2.31	37.74± 2.32	37.31± 2.15	36.29± 2.32	40.83 ±2.37
Serum	34.92 ±2.19	40.96±2 .72	37.67 ±3.42	38.67 ±2.45	39.03± 2.47	39.25± 2.18	35.93± 2.84	39.47± 2.46	39.61± 2.68	40.88 ±3.21

Appendix C3:

Average Interfacial Surface Free Energy(γ_{sv}) in (mJ/m^2)

Wu Model

			Treated(γ_{sv})							
Blood Cells	**Infected** (γ_{sv})	**Uninfect**(γ_{sv})	**IFN**	**RBV**	**ATR**	**ELT**	**AM**	**VA**	**BP**	**DH**
Whol. Blood	38.10± 1.72	43.47± 3.70	39.97± 2.17	39.61 ±1.86	39.25± 2.18	39.97± 2.17	39.97± 2.17	39.97± 2.17	39.75± 2.46	40.53 ±2.81
WBC	33.54± 2.31	44.35± 1.90	38.24± 3.15	38.66 ±3.08	38.45± 3.78	38.53± 2.43	37.08± 3.21	39.25± 2.17	38.60± 2.57	36.29 ±2.32
RBC	35.71± 2.08	42.74± 2.51	37.09± 2.19	38.82 ±2.75	37.81± 2.44	38.60± 2.31	37.74± 2.32	37.31± 2.15	36.29± 2.32	40.83 ±2.38
Serum	34.92± 2.19	40.96± 2.72	37.66± 3.42	38.67 ±2.45	39.04± 2.47	39.25± 2.18	35.93± 2.84	39.47± 2.46	39.61± 2.68	40.88 ± 3.21

Appendix D1:

Average Surface Energy of Adhesion (F^{adh}) in (mJ/m^2)

Neumann Model

			Treated(F^{adh})							
Blood Cells	**Infected**(F^{adh})	**Uninfect.**(F^{adh})	**IFN**	**RBV**	**ATR**	**ELT**	**AM**	**VA**	**BP**	**DH**
Whole. Blood	-18.86± 1.64	-13.83± 3.42	-17.09± 2.05	-17.42± 1.75	-17.77± 2.06	-17.09± 2.05	-17.09± 2.05	-17.09± 2.05	-17.30± 2.05	-16.56± 2.65
WBC	-23.22± 2.23	-12.99± 1.75	-18.74± 3.00	-18.34± 2.90	-18.55± 3.59	-18.45± 2.31	-19.84± 3.06	-17.77± 2.06	-18.39± 2.44	-20.59± 2.22
RBC	-21.14± 2.00	-14.49± 2.35	-19.83± 2.09	-18.19± 2.60	-19.83± 2.09	-20.04± 2.56	-19.21± 2.21	-19.62± 2.06	-20.59± 2.22	-16.28± 2.24
Serum	-21.90± 2.10	-16.23± 2.57	-19.29± 3.26	-18.32± 2.32	-18.45± 2.31	-18.52± 2.20	-20.93± 2.72	-17.57± 2.32	-17.44± 2.53	-16.24± 3.02

Appendix D2: Average Surface Energy of Adhesion (F^{adh}) in (mJ/m^2)

Fowkes Model

			Treated(F^{adh})							
Blood Cells	**Infected**(F^{adh})	**Uninfected**(F^{adh})	**IFN**	**RBV**	**ATR**	**ELT**	**AM**	**VA**	**BP**	**DH**
WholeBlood	-29.26± 2.23	-22.85± 4.05	-26.88± 2.75	-27.32± 2.36	-27.80± 2.79	-26.88± 2.75	-26.88± 2.75	-26.88± 2.75	-27.17± 3.14	-26.19± 3.53
WBC	-35.38± 3.19	-21.47± 2.28	-29.14± 4.09	-28.59± 3.87	-28.90± 4.88	-28.73± 3.14	-30.65± 4.22	-27.80± 2.79	-28.64± 3.30	-31.66± 3.09
RBC	-32.42± 2.79	-23.45± 3.09	-30.60± 2.88	-28.38± 3.52	-29.67± 3.18	-28.63± 2.97	-29.76± 3.03	-30.32± 2.28	-31.66± 3.09	-25.81± 2.97
Serum	-33.5± 2.97	-25.65± 3.37	-29.91± 4.46	-28.55± 3.14	-28.08± 3.17	-27.80± 2.79	-32.16± 3.83	-27.53± 3.13	-27.36± 3.40	-25.77± 3.40

Appendix D3: Average Surface Energy of Adhesion (F^{adh}) in (mJ/m^2)

Wu Model

			Treated(F^{adh})							
Blood Cells	**Infected**(F^{adh})	**Uninfected**(F^{adh})	**IFN**	**RBV**	**ATR**	**ELT**	**AM**	**VA**	**BP**	**DH**
WholBlood	-82.80± 8.94	-69.47± 4.47	-74.24 ± 5.50	-73.35± 4.72	-72.41± 5.57	-74.24± 5.50	-74.24± 5.50	-74.24± 5.50	-73.67± 6.27	-75.62± 7.07
WBC	-85.06± 4.47	-57.23± 6.38	-69.72 ± 8.18	-70.83± 7.74	-70.20± 9.77	-70.54± 6.27	-72.41± 5.57	66.70± 8.43	-70.71± 6.60	-64.68± 6.18
RBC	-81.11± 6.18	-63.15± 5.57	-66.80 ± 5.76	-71.25± 7.05	-68.67± 6.35	-70.74± 5.94	-68.49± 6.05	-67.37± 5.68	-64.68± 6.18	-76.38± 5.95
Serum	-76.70± 6.73	-60.99± 5.93	-68.19 ± 8.92	-70.91± 6.27	-71.83± 6.34	-72.41± 5.57	-63.68± 7.66	-72.94± 6.26	-73.28± 6.79	-76.46± 8.00

NEUMANN MODEL ANALYSIS

Appendix E1:

Neumann: Whole Blood

	Neumann: Infected Whole Blood				**Neumann: Uninfected Whole Blood**			
SN	$CD4^+$ count (cells/mm^3)	$\theta(^0C)$	γ_{sv} (mJ/m^2)	A_{132} (mJ/m^2)	CD4+ count (cells/mm^3)	$\theta(^0C)$	γ_{sv} (mJ/m^2)	A_{132} (mJ/m^2)
1	428	60	36.00	2.01E-17	1660	50	43.18	1.36E-17
2	600	55	39.62	1.68E-17	1572	51	42.48	1.42E-17
3	625	58	37.45	1.88E-17	1780	40	49.90	0.77E-17
4	312	60	36.00	2.01E-17	1450	50	43.18	1.36E-17
5	464	60	36.00	2.01E-17	1500	45	46.63	1.05E-17
6	247	56	38.90	1.75E-17	1193	56	38.90	1.75E-17
7	852	55	39.62	1.68E-17	1360	55	39.62	1.68E-17
8	115	58	37.45	1.88E-17	1520	50	43.18	1.36E-17
9	704	54	40.34	1.62E-17	1580	43	47.96	0.93E-17
10	798	55	39.62	1.68E-17	1020	55	39.62	1.68E-17
AVE	**514.5**	**57.1**	**38.10**	**1.82E-17**	**1267.2**	**49.5**	**43.465**	**1.34E-17**
SD	**243.1059**	**2.378141**	**1.721233**	**1.56E-18**	**368.2731**	**5.359312**	**3.70064**	**3.31E-18**

Appendix E2:

Neumann: WBC

	(c) Neumann: White Blood Infected				(d) **Neumann: White Blood Uninfected**			
SN	$CD4^+$ count (cells/mm^3)	$\theta(^0C)$	γ_{sv} (mJ/m^2)	A_{132} (mJ/m^2)	CD4+ count (cells/mm^3)	$\theta(^0C)$	γ_{sv} (mJ/m^2)	A_{132} (mJ/m^2)
1	428	65	32.38	2.35E-17	1660	47	45.27	1.17E-17
2	600	61	35.27	2.08E-17	1572	46	45.95	1.11E-17
3	625	63	33.83	2.21E-17	1780	48	44.58	1.23E-17
4	312	64	33.10	2.28E-17	1450	52	41.77	1.49E-17
5	464	67	30.95	2.48E-17	1500	50	43.18	1.36E-17
6	247	66	31.66	2.42E-17	1193	51	42.48	1.42E-17
7	852	58	37.45	1.88E-17	1360	45	46.63	1.05E-17
8	115	68	30.23	2.55E-17	1520	49	43.88	1.29E-17
9	704	62	34.55	2.15E-17	1580	44	47.30	0.99E-17
10	798	60	36.00	2.01E-17	1020	51	42.48	1.42E-17
AVE	**514.5**	**63.4**	**33.542**	**2.24E-17**	**1267.2**	**48.5**	**44.352**	**1.25E-17**
SD	**243.1059**	**3.204164**	**2.313597**	**2.15E-18**	**368.2731**	**2.750757**	**1.903218**	**1.71E-18**

Appendix E3:

Neumann: RBC

	(c) **Neumann: Red Blood Infected**				(d) **Neumann: Red Blood Uninfected**			
SN	$CD4^+$ count (cells/mm^3)	$\theta(^0C)$	γ_{sv} (mJ/m^2)	A_{132} (mJ/m^2)	CD4+ count (cells/mm^3)	$\theta(^0C)$	γ_{sv} (mJ/m^2)	A_{132} (mJ/m^2)
1	428	59	36.73	1.95E-17	1660	48	44.58	1.23E-17
2	600	64	33.10	2.28E-17	1572	57	38.17	1.81E-17
3	625	58	37.45	1.88E-17	1780	45	46.63	1.05E-17
4	312	57	38.17	1.81E-17	1450	50	43.18	1.36E-17
5	464	56	38.90	1.75E-17	1500	52	41.77	1.49E-17
6	247	62	34.55	2.15E-17	1193	51	42.48	1.42E-17
7	852	63	33.83	2.21E-17	1360	49	43.88	1.29E-17
8	115	61	35.27	2.08E-17	1520	54	40.34	1.62E-17
9	704	60	36.00	2.01E-17	1580	47	45.27	1.17E-17
10	798	64	33.10	2.28E-17	1020	53	41.05	1.55E-17
AVE	**514.5**	**60.4**	**35.71**	**2.04E-17**	**1267.2**	**50.6**	**42.735**	**1.4E-17**
SD	**243.1059**	**2.875181**	**2.083736**	**1.91E-18**	**368.2731**	**3.565265**	**2.514868**	**2.27E-18**

Appendix E4:

Neumann: Serum

	(c) **Neumann: Serum Infected**				(d) **Neumann: Serum Uninfected**			
SN	$CD4^+$ count (cells/mm^3)	$\theta(^0C)$	γ_{sv} (mJ/m^2)	A_{132} (mJ/m^2)	CD4+ count (cells/mm^3)	$\theta(^0C)$	γ_{sv} (mJ/m^2)	A_{132} (mJ/m^2)
1	428	60	36.00	2.01E-17	1660	58	37.45	1.88E-17
2	600	62	34.55	2.15E-17	1572	55	39.62	1.68E-17
3	625	63	33.83	2.21E-17	1780	45	46.63	1.05E-17
4	312	61	35.27	2.08E-17	1450	56	38.90	1.75E-17
5	464	59	36.73	1.95E-17	1500	53	41.05	1.55E-17
6	247	64	33.10	2.28E-17	1193	57	38.17	1.81E-17
7	852	58	37.45	1.88E-17	1360	54	39.62	1.68E-17
8	115	65	32.38	2.35E-17	1520	52	41.77	1.49E-17
9	704	66	31.66	2.42E-17	1580	50	43.18	1.36E-17
10	798	57	38.17	1.81E-17	1020	51	38.90	1.75E-17
AVE	**514.5**	**61.5**	**34.92**	**2.11E-17**	**1267.2**	**53.1**	**40.529**	**1.6E-17**
SD	**243.1059**	**3.02765**	**2.192022**	**2.04E-18**	**368.2731**	**3.842742**	**2.750081**	**2.48E-18**

FOWKES MODEL ANALYSIS

Appendix E5:

Fowkes: Whole Blood

	(c) Fowkes: Whole Blood Infected				(d) Fowkes: Whole Blood Uninfected			
SN	$CD4^+$ count ($cells/mm^3$)	$\theta(^0C)$	γ_{sv} (mJ/m^2)	A_{132} (mJ/m^2)	CD4+ count ($cells/mm^3$)	$\theta(^0C)$	γ_{sv} (mJ/m^2)	A_{132} (mJ/m^2)
1	428	60	36.00	3.09E-17	1660	50	43.18	2.21 E-17
2	600	55	39.62	2.63 E-17	1572	51	42.48	2.29 E-17
3	625	58	37.45	2.90 E-17	1780	40	49.90	1.91E-17
4	312	60	36.00	3.08 E-17	1450	50	43.18	2.21 E-17
5	464	60	36.00	3.08 E-17	1500	45	46.63	2.11E-17
6	247	56	38.90	2.72E-17	1193	56	38.90	2.72E-17
7	852	55	39.62	2.63 E-17	1360	55	39.62	2.63E-17
8	115	58	37.45	2.90 E-17	1520	50	43.18	2.21 E-17
9	704	54	40.34	2.55 E-17	1580	43	47.96	2.01E-17
10	798	55	39.62	2.63 E-17	1020	55	39.62	2.63E-17
AVE	**514.5**	**57.1**	**38.10**	**2.82E-17**	**1267.2**	**49.5**	**43.465**	**2.29E-17**
SD	**243.1059**	**2.378141**	**1.721233**	**2.14E-18**	**368.2731**	**5.359312**	**3.70064**	**2.77E-18**

Appendix E6:

Fowkes: WBC

	(c) Fowkes: White Blood Infected				(d) Fowkes: White Blood Uninfected			
SN	$CD4^+$ count ($cells/mm^3$)	$\theta(^0C)$	γ_{sv} (mJ/m^2)	A_{132} (mJ/m^2)	CD4+ count ($cells/mm^3$)	$\theta(^0C)$	γ_{sv} (mJ/m^2)	A_{132} (mJ/m^2)
1	428	65	32.38	3.57E-17	1660	47	45.27	1.96E-17
2	600	61	35.27	3.18E-17	1572	46	45.95	1.89E-17
3	625	63	33.83	3.37E-17	1780	48	44.58	2.04E-17
4	312	64	33.10	3.47E-17	1450	52	41.77	2.37E-17
5	464	67	30.95	3.76E-17	1500	50	43.18	2.21E-17
6	247	66	31.66	3.66E-17	1193	51	42.48	2.29E-17
7	852	58	37.45	2.90E-17	1360	45	46.63	1.81E-17
8	115	68	30.23	3.86E-17	1520	49	43.88	2.12E-17
9	704	62	34.55	3.28E-17	1580	44	47.30	1.73E-17
10	798	60	36.00	3.09E-17	1020	51	42.48	2.29E-17
AVE	**514.5**	**63.4**	**33.542**	**3.41E-17**	**1267.2**	**48.5**	**44.352**	**2.07E-17**
SD	**243.1059**	**3.204164**	**2.313597**	**3.07E-18**	**368.2731**	**2.750757**	**1.903218**	**2.2E-18**

Appendix E7:

Fowkes: RBC

	(c) **Fowkes: Red Blood Infected**				(d) **Fowkes: Red Blood Uninfected**			
SN	$CD4^+$ count ($cells/mm^3$)	$\theta(^0C)$	γ_{sv} (mJ/m^2)	A_{132} (mJ/m^2)	CD4+ count ($cells/mm^3$)	$\theta(^0C)$	γ_{sv} (mJ/m^2)	A_{132} (mJ/m^2)
1	428	59	36.73	3.00E-17	1660	48	44.58	2.04E-17
2	600	64	33.10	3.47E-17	1572	57	38.17	2.81E-17
3	625	58	37.45	2.90E-17	1780	45	46.63	1.81E-17
4	312	57	38.17	2.81E-17	1450	50	43.18	2.21E-17
5	464	56	38.90	2.72E-17	1500	52	41.77	2.37E-17
6	247	62	34.55	3.28E-17	1193	51	42.48	2.29E-17
7	852	63	33.83	3.37E-17	1360	49	43.88	2.12E-17
8	115	61	35.28	3.18E-17	1520	54	40.34	2.55E-17
9	704	60	36.00	3.09E-17	1580	47	45.27	1.96E-17
10	798	64	33.10	3.47E-17	1020	53	41.05	2.46E-17
AVE	**514.5**	**60.4**	**35.711**	**3.13E-17**	**1267.2**	**50.6**	**42.735**	**2.26E-17**
SD	**243.1059**	**2.875181**	**2.083504**	**2.7E-18**	**368.2731**	**3.565265**	**2.514868**	**2.99E-18**

Appendix E8:

Fowkes: Serum

	(c) **Fowkes: Serum Infected**				(d) **Fowkes: Serum Uninfected**			
SN	$CD4^+$ count ($cells/mm^3$)	$\theta(^0C)$	γ_{sv} (mJ/m^2)	A_{132} (mJ/m^2)	CD4+ count ($cells/mm^3$)	$\theta(^0C)$	γ_{sv} (mJ/m^2)	A_{132} (mJ/m^2)
1	428	60	36.00	3.09E-17	1660	58	37.45	2.90E-17
2	600	62	34.55	3.28E-17	1572	55	39.62	2.63E-17
3	625	63	33.83	3.37E-17	1780	45	46.63	1.81E-17
4	312	61	35.28	3.18E-17	1450	56	38.90	2.72E-17
5	464	59	36.73	3.00E-17	1500	53	41.05	2.46E-17
6	247	64	33.10	3.47E-17	1193	57	38.17	2.81E-17
7	852	58	37.45	2.90E-17	1360	54	40.34	2.55E-17
8	115	65	32.38	3.57E-17	1520	52	41.77	2.37E-17
9	704	66	31.66	3.66E-17	1580	50	43.18	2.21E-17
10	798	57	38.18	2.81E-17	1020	51	42.48	2.29E-17
AVE	**514.5**	**61.5**	**34.916**	**3.23E-17**	**1267.2**	**53.1**	**40.959**	**2.48E-17**
SD	**243.1059**	**3.02765**	**2.193856**	**2.87E-18**	**368.2731**	**3.842742**	**2.719879**	**3.23E-18**

WU MODEL ANALYSIS

Appendix E9:

Wu: Whole Blood

	(c) **Wu: Whole Blood Infected**				(d) **Wu: Whole Blood Uninfected**			
SN	$CD4^+$ count ($cells/mm^3$)	$\theta(^0C)$	γ_{sv} (mJ/m^2)	A_{132} (mJ/m^2)	CD4+ count ($cells/mm^3$)	$\theta(^0C)$	γ_{sv} (mJ/m^2)	A_{132} (mJ/m^2)
1	428	60	36.00	7.94E-17	1660	50	43.18	6.18E-17
2	600	55	39.62	7.78E-17	1572	51	42.48	7.09E-17
3	625	58	37.45	9.46E-17	1780	40	49.90	6.55E-17
4	312	60	36.00	8.74E-17	1450	50	43.18	6.18E-17
5	464	60	36.00	8.74E-17	1500	45	46.63	6.18E-17
6	247	56	38.90	6.91E-17	1193	56	38.90	6.91E-17
7	852	55	39.62	7.09E-17	1360	55	39.62	7.09E-17
8	115	58	37.45	7.94E-17	1520	50	43.18	6.55E-17
9	704	54	40.34	9.04E-17	1580	43	47.96	7.26E-17
10	798	55	39.62	7.09E-17	1020	55	39.62	7.09E-17
AVE	**514.5**	**57.1**	**38.10**	**7.99E-17**	**1267.2**	**49.5**	**43.465**	**6.71E-17**
SD	**243.1059**	**2.378141**	**1.721233**	**8.60E-18**	**368.2731**	**5.359312**	**3.70064**	**4.31E-18**

Appendix E10:

Wu: WBC

	(c) **Wu: White Blood Infected**				(d) **Wu: White Blood Uninfected**			
SN	$CD4^+$ count ($cells/mm^3$)	$\theta(^0C)$	γ_{sv} (mJ/m^2)	A_{132} (mJ/m^2)	CD4+ count ($cells/mm^3$)	$\theta(^0C)$	γ_{sv} (mJ/m^2)	A_{132} (mJ/m^2)
1	428	65	32.38	8.43E-17	1660	47	45.27	5.22E-17
2	600	61	35.28	8.58E-17	1572	46	45.95	5.99E-17
3	625	63	33.83	8.27E-17	1780	48	44.58	5.61E-17
4	312	64	33.10	7.61E-17	1450	52	41.77	5.42E-17
5	464	67	30.95	7.94E-17	1500	50	43.18	4.83E-17
6	247	66	31.66	7.77E-17	1193	51	42.48	5.03E-17
7	852	58	37.45	8.74E-17	1360	45	46.63	6.55E-17
8	115	68	30.23	8.10E-17	1520	49	43.88	4.63E-17
9	704	62	34.55	8.89E-17	1580	44	47.30	5.80E-17
10	798	60	36.00	7.77E-17	1020	51	42.48	6.18E-17
AVE	**514.5**	**63.4**	**33.543**	**8.21E-17**	**1267.2**	**48.5**	**44.352**	**5.53E-17**
SD	**243.1059**	**3.204164**	**2.314428**	**4.43E-18**	**368.2731**	**2.750757**	**1.903218**	**6.16E-18**

Appendix E11:

Wu: RBC

	(c) Wu: Red Blood Infected				(d) **Wu: Red Blood Uninfected**			
SN	$CD4^+$ count ($cells/mm^3$)	$\theta(^0C)$	γ_{sv} (mJ/m^2)	A_{132} (mJ/m^2)	CD4+ count ($cells/mm^3$)	$\theta(^0C)$	γ_{sv} (mJ/m^2)	A_{132} (mJ/m^2)
1	428	59	36.73	8.27E-17	1660	48	44.58	6.36E-17
2	600	64	33.10	6.73E-17	1572	57	38.18	5.42E-17
3	625	58	37.45	8.74E-17	1780	45	46.63	6.55E-17
4	312	57	38.18	7.94E-17	1450	50	43.18	6.73E-17
5	464	56	38.90	7.61E-17	1500	52	41.77	6.91E-17
6	247	62	34.55	7.77E-17	1193	51	42.48	5.80E-17
7	852	63	33.83	8.10E-17	1360	49	43.88	5.61E-17
8	115	61	35.28	7.26E-17	1520	54	40.34	5.99E-17
9	704	60	36.00	8.43E-17	1580	47	45.27	6.18E-17
10	798	64	33.10	7.43E-17	1020	53	41.05	5.42E-17
AVE	**514.5**	**60.4**	**35.712**	**7.83E-17**	**1267.2**	**50.6**	**42.736**	**6.10E-17**
SD	**243.1059**	**2.875181**	**2.084817**	**5.98E-18**	**368.2731**	**3.565265**	**2.512852**	**5.37E-18**

Appendix E12:

Wu: Serum

	(c) Wu: Serum Infected				(d) **Wu: Serum Uninfected**			
SN	$CD4^+$ count ($cells/mm^3$)	$\theta(^0C)$	γ_{sv} (mJ/m^2)	A_{132} (mJ/m^2)	CD4+ count ($cells/mm^3$)	$\theta(^0C)$	γ_{sv} (mJ/m^2)	A_{132} (mJ/m^2)
1	428	60	36.00	6.55E-17	1660	58	37.45	6.18E-17
2	600	62	34.55	7.09E-17	1572	55	39.62	5.80E-17
3	625	63	33.83	8.74E-17	1780	45	46.63	5.61E-17
4	312	61	35.28	6.91E-17	1450	56	38.90	5.99E-17
5	464	59	36.73	7.43E-17	1500	53	41.05	6.36E-17
6	247	64	33.10	6.73E-17	1193	57	38.18	5.42E-17
7	852	58	37.45	7.26E-17	1360	54	40.34	6.55E-17
8	115	65	32.38	7.61E-17	1520	52	41.77	5.22E-17
9	704	66	31.66	7.94E-17	1580	50	43.18	5.03E-17
10	798	57	38.18	7.77E-17	1020	51	42.48	6.73E-17
AVE	**514.5**	**61.5**	**34.92**	**7.40E-17**	**1267.2**	**53.1**	**40.96**	**5.89E-17**
SD	**243.1059**	**3.02765**	**2.193856**	**6.49E-18**	**368.2731**	**3.842742**	**2.718742**	**5.73E-18**

INFECTED SAMPLES WITH IFN TREATMENT AND RBV TREATMENT

NEUMANN MODEL ANALYSIS

Appendix E13:

Neumann: Whole Blood Infected

	Neumann: Whole Blood Treated With IFN				**Neumann: Whole BloodTreated With RBV**			
SN	$CD4^+$ count (cells/mm^3)	$\theta(^0C)$	γ_{sv} (mJ/m^2)	A_{132} (mJ/m^2)	CD4+ count (cells/mm^3)	$\theta(^0C)$	γ_{sv} (mJ/m^2)	A_{132} (mJ/m^2)
1	428	51	42.48	1.42E-17	428	51	42.47	1.42E-17
2	600	52	41.77	1.49E-17	600	52	41.77	1.49E-17
3	625	57	3.18	1.81E-17	625	53	41.05	1.56E-17
4	312	59	36.73	1.95E-17	312	58	37.45	1.88E-17
5	464	56	38.90	1.75E-17	464	59	36.73	1.95E-17
6	247	58	37.45	1.88E-17	247	57	38.18	1.81E-17
7	852	50	43.18	1.36E-17	852	55	39.62	1.68E-17
8	115	54	40.34	1.62E-17	115	56	38.90	1.78E-17
9	704	53	41.05	1.55E-17	704	54	40.34	1.62E-17
10	798	55	39.62	1.68E-17	798	55	39.62	-1.68E-17
AVE	**514.5**	**54.5**	**39.87**	**1.65E-17**	**514.5**	**55**	**39.613**	**1.69E-17**
SD	**243.1059**	**3.02765**	**2.28393**	**1.98E-18**	**243.1059**	**2.581989**	**1.85474**	**1.72E-18**

Appendix E14:

Neumann: WBC Infected

	(c) Neumann: WBC Treated With IFN				(d) **Neumann: WBC Treated With RBV**			
SN	$CD4^+$ count (cells/mm^3)	$\theta(^0C)$	γ_{sv} (mJ/m^2)	A_{132} (mJ/m^2)	CD4+ count (cells/mm^3)	$\theta(^0C)$	γ_{sv} (mJ/m^2)	A_{132} (mJ/m^2)
1	428	58	37.45	1.88E-17	428	56	38.90	1.75E-17
2	600	50	43.18	1.36E-17	600	46	45.95	1.11E-17
3	625	52	41.77	1.49E-17	625	55	39.62	1.68E-17
4	312	60	36.00	2.01E-17	312	60	36.00	2.01E-17
5	464	61	35.28	2.08E-17	464	58	37.45	1.88E-17
6	247	57	38.18	1.81E-17	247	61	35.28	2.08E-17
7	852	53	41.05	1.55E-17	852	57	38.18	1.81E-17
8	115	64	33.10	2.28E-17	115	58	37.45	1.88E-17
9	704	55	39.62	1.68E-17	704	59	36.73	1.95E-17
10	798	59	36.78	1.95E-17	798	53	41.05	1.55E-17
AVE	**514.5**	**56.9**	**38.24**	**1.81E-17**	**514.5**	**56.3**	**38.66**	**1.77E-17**
SD	**243.1059**	**4.383048**	**3.15565**	**2.88E-18**	**243.1059**	**4.32178**	**3.07714**	**2.80E-18**

Appendix E15:

Neumann: RBC Infected

	(c) Neumann: RBC Treated With IFN				(d) **Neumann: RBC Treated With RBV**			
SN	$CD4^+$ count ($cells/mm^3$)	$\theta(^0C)$	γ_{sv} (mJ/m^2)	A_{132} (mJ/m^2)	CD4+ count ($cells/mm^3$)	$\theta(^0C)$	γ_{sv} (mJ/m^2)	A_{132} (mJ/m^2)
1	428	55	39.62	1.68E-17	428	52	41.77	1.49E-17
2	600	54	40.34	1.62E-17	600	53	41.05	1.55E-17
3	625	58	37.54	1.88E-17	625	50	43.18	1.36E-17
4	312	59	36.73	1.95E-17	312	59	36.73	1.95E-17
5	464	57	38.18	1.81E-17	464	58	37.45	1.88E-17
6	247	60	36.00	2.01E-17	247	57	38.18	1.81E-17
7	852	61	35.28	2.08E-17	852	54	40.34	1.62E-17
8	115	63	33.83	2.21E-17	115	60	36.00	2.01E-17
9	704	56	38.90	1.75E-17	704	62	34.55	2.15E-17
10	798	62	34.55	2.15E-17	798	56	38.90	1.75E-17
AVE	**514.5**	**58.5**	**37.10**	**1.91E-17**	**514.5**	**56.1**	**38.82**	**1.76E-17**
SD	**243.1059**	**3.02765**	**2.1935**	**2.0E-18**	**243.1059**	**3.81372**	**2.74553**	**2.50E-18**

Appendix E16:

Neumann: Serum Infected

	Neumann: Serum Treated With IFN				**Neumann: SerumTreated With RBV**			
SN	$CD4^+$ count ($cells/mm^3$)	$\theta(^0C)$	γ_{sv} (mJ/m^2)	A_{132} (mJ/m^2)	CD4+ count ($cells/mm^3$)	$\theta(^0C)$	γ_{sv} (mJ/m^2)	A_{132} (mJ/m^2)
1	428	50	43.18	1.36E-17	428	55	39.62	1.68E-17
2	600	61	35.28	2.08E-17	600	50	43.18	1.36E-17
3	625	53	41.05	1.55E-17	625	54	40.34	1.62E-17
4	312	60	36.00	2.01E-17	312	60	36.00	2.01E-17
5	464	59	36.73	1.95E-17	464	56	38.90	1.75E-17
6	247	63	33.83	2.21E-17	247	58	37.45	1.88E-17
7	852	55	39.62	1.68E-17	852	53	41.05	1.55E-17
8	115	65	32.38	2.35E-17	115	59	36.73	1.95E-17
9	704	57	38.18	1.81E-17	704	57	38.18	1.81E-17
10	798	54	40.34	1.62E-17	798	61	35.28	2.08E-17
AVE	**514.5**	**57.7**	**37.66**	**1.86E-17**	**514.5**	**56.3**	**38.67**	**1.76E-17**
SD	**243.1059**	**4.73872**	**3.4171**	**3.13E-18**	**243.1059**	**3.40098**	**2.44635**	**2.23E-18**

FOWKES MODEL ANALYSIS

Appendix E17:

Fowkes: Whole Blood Infected

	Fowkes: Whole Blood Treated With IFN				**Fowkes: Whole BloodTreated With RBV**			
SN	$CD4^+$ count ($cells/mm^3$)	$\theta(^0C)$	γ_{sv} (mJ/m^2)	A_{132} (mJ/m^2)	CD4+ count ($cells/mm^3$)	$\theta(^0C)$	γ_{sv} (mJ/m^2)	A_{132} (mJ/m^2)
1	428	51	42.48	2.29E-17	428	51	42.48	2.29E-17
2	600	52	41.77	2.37E-17	600	52	41.77	2.37E-17
3	625	57	38.18	2.81E-17	625	53	41.05	2.46E-17
4	312	59	36.73	3.00E-17	312	58	37.45	2.90E-17
5	464	56	38.90	2.72E-17	464	59	36.73	3.00E-17
6	247	58	37.45	2.90E-17	247	57	38.18	2.81E-17
7	852	50	43.18	2.21E-17	852	55	39.62	2.63E-17
8	115	54	40.34	2.55E-17	115	56	38.90	2.72E-17
9	704	53	41.05	2.46E-17	704	54	40.34	2.55E-17
10	798	55	39.62	2.63E-17	798	55	39.62	2.63E-17
AVE	**514.5**	**54.5**	**39.97**	**2.59E-17**	**514.5**	**55**	**39.61**	**2.64E-17**
SD	**243.1059**	**3.02765**	**2.17222**	**2.65E-18**	**243.1059**	**2.5820**	**1.85646**	**2.28E-18**

Appendix E18:

Fowkes: WBC Infected

	(c) Fowkes: WBC Treated With IFN				**(d) Fowkes: WBC Treated With RBV**			
SN	$CD4^+$ count ($cells/mm^3$)	$\theta(^0C)$	γ_{sv} (mJ/m^2)	A_{132} (mJ/m^2)	CD4+ count ($cells/mm^3$)	$\theta(^0C)$	γ_{sv} (mJ/m^2)	A_{132} (mJ/m^2)
1	428	58	37.45	2.90E-17	428	56	38.90	2.72E-17
2	600	50	43.18	2.21E-17	600	46	45.95	1.89E-17
3	625	52	41.77	2.37E-17	625	55	39.62	2.63E-17
4	312	60	36.00	3.09E-17	312	60	36.00	3.09E17
5	464	61	35.28	3.18E-17	464	58	37.45	2.90E-17
6	247	57	38.18	2.81E-17	247	61	35.28	3.18E-17
7	852	53	41.05	2.46E-17	852	57	38.18	2.81E-17
8	115	64	33.10	3.47E-17	115	58	37.45	2.90E-17
9	704	55	39.62	2.63E-17	704	59	36.73	3.00E-17
10	798	59	36.73	3.00E-17	798	53	41.05	2.46E-17
AVE	**514.5**	**56.9**	**38.24**	**2.81E-17**	**514.5**	**56.3**	**38.66**	**2.76E-17**
SD	**243.1059**	**4.3830**	**3.1583**	**3.95E-18**	**243.1059**	**4.32178**	**3.07714**	**3.73E-18**

Appendix E19:

Fowkes: RBC Infected

	(c) **Fowkes: RBC Treated With IFN**				(d) **Fowkes: RBC Treated With RBV**			
SN	$CD4^+$ count ($cells/mm^3$)	$\theta(^0C)$	γ_{sv} (mJ/m^2)	A_{132} (mJ/m^2)	CD4+ count ($cells/mm^3$)	$\theta(^0C)$	γ_{sv} (mJ/m^2)	A_{132} (mJ/m^2)
1	428	55	39.62	2.63E-17	428	52	41.77	2.37E-17
2	600	54	40.34	2.55E-17	600	53	41.05	2.46E-17
3	625	58	37.45	2.90E-17	625	50	43.18	2.21E-17
4	312	59	36.73	3.00E-17	312	59	36.73	3.00E-17
5	464	57	38.18	2.81E-17	464	58	37.45	2.90E-17
6	247	60	36.00	3.09E-17	247	57	38.18	2.81E-17
7	852	61	35.28	3.18E-17	852	54	40.34	2.55E-17
8	115	63	33.83	3.37E-17	115	60	36.00	3.09E-17
9	704	56	38.90	2.72E-17	704	62	34.55	3.28E-17
10	798	62	34.55	3.28E-17	798	56	38.90	2.72E-17
AVE	**514.5**	**58.5**	**37.09**	**2.95E-17**	**514.5**	**56.1**	**38.82**	**2.72E-17**
SD	**243.1059**	**3.02765**	**2.19166**	**2.78E-18**	**243.1059**	**3.81371**	**2.745531**	**3.41E-18**

Appendix E20:

Fowkes: Serum Infected

	(c) **Fowkes: Serum Treated With IFN**				(d) **Fowkes: Serum Treated With RBV**			
SN	$CD4^+$ count ($cells/mm^3$)	$\theta(^0C)$	γ_{sv} (mJ/m^2)	A_{132} (mJ/m^2)	CD4+ count ($cells/mm^3$)	$\theta(^0C)$	γ_{sv} (mJ/m^2)	A_{132} (mJ/m^2)
1	428	50	43.18	2.21E-17	428	55	39.62	2.63E-17
2	600	61	35.28	3.18E-17	600	50	43.18	2.21E-17
3	625	53	41.05	2.46E-17	625	54	40.34	2.55E-17
4	312	60	36.00	3.09E-17	312	60	36.00	3.09E-17
5	464	59	36.73	3.00E-17	464	56	38.90	2.72E-17
6	247	63	33.83	3.37E-17	247	58	37.45	2.90E-17
7	852	55	39.62	2.63E-17	852	53	41.05	2.46E-17
8	115	65	32.38	3.57E-17	115	59	36.73	3.00E-17
9	704	57	38.18	2.81E-17	704	57	38.18	2.81E-17
10	798	54	40.34	2,55E-17	798	61	35.28	3.18E-17
AVE	**514.5**	**57.7**	**37.67**	**2.89E-17**	**514.5**	**56.3**	**38.67**	**2.76E-17**
SD	**243.1059**	**4.73873**	**3.41710**	**4.30E-18**	**243.1059**	**3.4010**	**2.44635**	**3.02E-18**

WU MODEL ANALYSIS

Appendix E21:

Wu: Whole Blood Infected

	(c) **Wu: Whole Blood Treated With IFN**				(d) **Wu: Whole Blood Treated With RBV**			
SN	$CD4^+$ count (cells/mm^3)	$\theta(^0C)$	γ_{sv} (mJ/m^2)	A_{132} (mJ/m^2)	CD4+ count (cells/mm^3)	$\theta(^0C)$	γ_{sv} (mJ/m^2)	A_{132} (mJ/m^2)
1	428	51	42.48	7.77E-17	428	51	42.48	7.77E-17
2	600	52	41.77	7.61E-17	600	52	41.77	7.61E-17
3	625	57	38.18	6.73E-17	625	53	41.05	7.43E-17
4	312	59	36.73	6.36E-17	312	58	37.45	6.55E-17
5	464	56	38.90	6.91E-17	464	59	36.73	6.36E-17
6	247	58	37.45	6.55E-17	247	57	38.17	6.73E-17
7	852	50	43.18	7.94E-17	852	55	39.62	7.09E-17
8	115	54	40.34	7.26E-17	115	56	38.90	6.91E-17
9	704	53	41.05	7.43E-17	704	54	40.34	7.26E-17
10	798	55	39.62	7.09E-17	798	55	39.62	7.09E-17
AVE	**514.5**	**54.5**	**39.97**	**7.17E-17**	**514.5**	**55**	**39.61**	**7.08E-17**
SD	**243.1059**	**3.02765**	**2.17222**	**5.3E-18**	**243.1059**	**2.58199**	**1.85732**	**4.55E-18**

Appendix E22:

Wu: WBC Infected

	Wu: WBC Treated With IFN				(c) **Wu: WBC Treated With RBV**			
SN	$CD4^+$ count (cells/mm^3)	$\theta(^0C)$	γ_{sv} (mJ/m^2)	A_{132} (mJ/m^2)	CD4+ count (cells/mm^3)	$\theta(^0C)$	γ_{sv} (mJ/m^2)	A_{132} (mJ/m^2)
1	428	58	37.45	6.55E-17	428	56	38.90	6.91E-17
2	600	50	43.18	5.94E-17	600	46	45.95	8.58E-17
3	625	52	41.77	7.61E-17	625	55	39.62	7.09E-17
4	312	60	36.00	6.18E-17	312	60	36.00	6.18E-17
5	464	61	35.28	5.99E-17	464	58	37.45	6.55E-17
6	247	57	38.18	6.73E-17	247	61	35.28	5.99E-17
7	852	53	41.05	7.43E-17	852	57	38.18	6.73E-17
8	115	64	33.10	5.42E-17	115	58	37.45	6.55E-17
9	704	55	39.62	7.09E-17	704	59	36.73	6.36E-17
10	798	59	36.73	6.36E-17	798	53	41.05	7.43E-17
AVE	**514.5**	**56.9**	**38.24**	**6.53E-17**	**514.5**	**56.3**	**38.66**	**6.84E-17**
SD	**243.1059**	**4.38305**	**3.15826**	**6.96E-18**	**243.1059**	**4.32178**	**3.07714**	**7.46E-18**

Appendix E23:

Wu: RBC Infected

	(c) **Wu: RBC Treated With IFN**				(d) **Wu: RBC Treated With RBV**			
SN	$CD4^+$ count ($cells/mm^3$)	$\theta(^0C)$	γ_{sv} (mJ/m^2)	A_{132} (mJ/m^2)	CD4+ count ($cells/mm^3$)	$\theta(^0C)$	γ_{sv} (mJ/m^2)	A_{132} (mJ/m^2)
1	428	55	39.62	7.09E-17	428	52	41.77	7.61E-17
2	600	54	40.34	7.26E-17	600	53	41.05	7.43E-17
3	625	58	37.45	6.55E-17	625	50	43.18	7.94E-17
4	312	59	36.73	6.36E-17	312	59	36.73	6.36E-17
5	464	57	38.18	6.73E-17	464	58	37.45	6.55E-17
6	247	60	36.00	6.18E-17	247	57	38.18	6.73E-17
7	852	61	35.28	5.99E-19	852	54	40.34	7.26E-17
8	115	63	33.83	5.61E-19	115	60	36.00	6.18E-17
9	704	56	38.90	6.91E-17	704	62	34.55	5.80E-17
10	798	62	34.55	5.80E-17	798	56	38.90	6.91E-17
AVE	**514.5**	**58.5**	**37.09**	**6.45E-17**	**514.5**	**56.1**	**38.82**	**6.88E-17**
SD	**243.1059**	**3.02765**	**2.19166**	**5.56E-18**	**243.1059**	**3.81372**	**2.74553**	**6.80E-18**

Appendix E24:

Wu: Serum Infected

	(c) **Wu: Serum Treated With IFN**				(d) **Wu: Serum Treated With RBV**			
SN	$CD4^+$ count ($cells/mm^3$)	$\theta(^0C)$	γ_{sv} (mJ/m^2)	A_{132} (mJ/m^2)	CD4+ count ($cells/mm^3$)	$\theta(^0C)$	γ_{sv} (mJ/m^2)	A_{132} (mJ/m^2)
1	428	50	43.18	7.94E-17	428	55	39.62	7.09E-17
2	600	61	35.28	5.99E-17	600	50	43.18	7.94E-17
3	625	53	41.05	7.43E-17	625	54	40.34	7.26E-17
4	312	60	36.00	6.18E-17	312	60	36.00	6.18E-17
5	464	59	36.73	6.36E-17	464	56	38.90	6.91E-17
6	247	63	33.83	5.61E-17	247	58	37.45	6.55E-17
7	852	55	39.62	7.09E-17	852	53	41.05	7.43E-17
8	115	65	32.38	5.22E-17	115	59	36.73	6.36E-17
9	704	57	38.18	6.73E-17	704	57	38.18	6.73E-17
10	798	54	40.34	7.26E-17	798	61	35.28	5.99E-17
AVE	**514.5**	**57.7**	**37.66**	**6.58E-17**	**514.5**	**56.3**	**38.67**	**6.84E-17**
SD	**243.1059**	**4.73873**	**3.41710**	**8.60E-18**	**243.1059**	**3.40098**	**2.44635**	**6.04E-18**

INFECTED SAMPLES WITH ATR AND ELT TREATMENT

NEUMANN MODEL ANALYSIS

Appendix E25:

Neumann: Whole Blood Infected

	Neumann: Whole Blood Treated With ATR				**Neumann: Whole BloodTreated With ELT**			
SN	$CD4^+$ count (cells/mm^3)	$\theta(^0C)$	γ_{sv} (mJ/m^2)	A_{132} (mJ/m^2)	CD4+ count (cells/mm^3)	$\theta(^0C)$	γ_{sv} (mJ/m^2)	A_{132} (mJ/m^2)
1	428	53	41.05	1.55E-17	428	52	41.77	1.49E-17
2	600	55	39.62	1.68 E-17	600	50	43.18	1.36 E-17
3	625	56	38.90	1.75 E-17	625	53	41.05	1.55 E-17
4	312	59	36.73	1.95 E-17	312	59	36.73	1.95 E-17
5	464	57	38.18	1.81 E-17	464	58	37.45	1.88 E-17
6	247	54	40.34	1.62 E-17	247	56	38.90	1.75 E-17
7	852	60	36.00	2.01 E-17	852	55	39.62	1.68 E-17
8	115	58	37.45	1.88 E-17	115	57	38.18	1.81 E-17
9	704	52	41.77	1.49 E-17	704	54	40.34	1.62 E-17
10	798	51	42.48	1.42 E-17	798	51	42.48	1.42 E-17
AVE	**514.5**	**55.5**	**39.25**	**1.72E-17**	**514.5**	**54.5**	**39.97**	**1.65E-17**
SD	**243.1059**	**3.02765**	**2.17992**	**1.99E-18**	**243.1059**	**3.02765**	**2.17222**	**1.98E-18**

Appendix E26:

Neumann: WBC Infected

	(g) Neumann: WBC Treated With ATR				(h) **Neumann: WBC Treated With ELT**			
SN	$CD4^+$ count (cells/mm^3)	$\theta(^0C)$	γ_{sv} (mJ/m^2)	A_{132} (mJ/m^2)	CD4+ count (cells/mm^3)	$\theta(^0C)$	γ_{sv} (mJ/m^2)	A_{132} (mJ/m^2)
1	428	54	40.34	1.62E-17	428	57	38.18	1.81E-17
2	600	49	43.88	1.29 E-17	600	55	39.62	1.68 E-17
3	625	50	43.18	1.36 E-17	625	54	40.34	1.62 E-17
4	312	60	36.00	2.01 E-17	312	60	36.00	2.01 E-17
5	464	58	37.45	1.88 E-17	464	58	37.45	1.88 E-17
6	247	62	34.55	2.15 E-17	247	62	34.55	2.15 E-17
7	852	57	38.18	1.81 E-17	852	51	42.48	1.42 E-17
8	115	65	32.38	2.35 E-17	115	59	36.73	1.95 E-17
9	704	52	41.77	1.49 E-17	704	53	41.05	1.55 E-17
10	798	59	36.73	1.95 E-17	798	56	38.90	1.75 E-17
AVE	**514.5**	**56.6**	**38.45**	**1.79E-17**	**514.5**	**56.5**	**38.53**	**1.81E-17**
SD	**243.1059**	**5.253**	**3.779195**	**3.46E-18**	**243.1059**	**3.374743**	**2.434114**	**2.23E-18**

Appendix E27:

Neumann: RBC Infected

	(q) **Neumann: RBC Treated With ATR**				(r) **Neumann: RBC Treated With ELT**			
SN	$CD4^+$ count ($cells/mm^3$)	$\theta(^0C)$	γ_{sv} (mJ/m^2)	A_{132} (mJ/m^2)	CD4+ count ($cells/mm^3$)	$\theta(^0C)$	γ_{sv} (mJ/m^2)	A_{132} (mJ/m^2)
1	428	57	38.18	1.81 E-17	428	58	37.45	1.88 E-17
2	600	55	39.62	1.68 E-17	600	60	36.00	2.01 E-17
3	625	56	38.90	1.75 E-17	625	54	40.34	1.62 E-17
4	312	59	36.73	1.95 E-17	312	59	36.73	1.95 E-17
5	464	58	37.45	1.88 E-17	464	57	38.18	1.81 E-17
6	247	60	36.00	2.01 E-17	247	63	33.83	2.21 E-17
7	852	63	33.83	2.21 E-17	852	53	41.05	1.55 E-17
8	115	61	35.28	2.08 E-17	115	61	35.28	2.08 E-17
9	704	62	34.55	2.15 E-17	704	65	32.38	2.35 E-17
10	798	54	40.34	1.62 E-17	798	58	37.45	1.88 E-17
AVE	**514.5**	**58.5**	**37.088**	**1.885E-17**	**514.5**	**58.8**	**36.869**	**2.115E-17**
SD	**243.1059**	**3.02765**	**2.191655**	**3.75E-18**	**243.1059**	**3.705851**	**2.679314**	**3.32E-18**

Appendix E28:

Neumann: Serum Infected

	Neumann: Serum Treated With ATR				**Neumann: SerumTreated With ELT**			
SN	$CD4^+$ count ($cells/mm^3$)	$\theta(^0C)$	γ_{sv} (mJ/m^2)	A_{132} (mJ/m^2)	CD4+ count ($cells/mm^3$)	$\theta(^0C)$	γ_{sv} (mJ/m^2)	A_{132} (mJ/m^2)
1	428	53	41.05	1.55E-17	428	53	41.05	1.55E-17
2	600	57	38.17	1.81 E-17	600	57	31.18	1.81 E-17
3	625	55	39.62	1.68 E-17	625	55	39.62	1.68 E-17
4	312	56	38.90	1.75 E-17	312	56	38.90	1.75 E-17
5	464	59	36.73	1.95 E-17	464	59	36.73	1.95 E-17
6	247	51	42.48	1.42 E-17	247	58	37.45	1.88 E-17
7	852	58	37.45	1.88 E-17	852	54	40.34	1.62 E-17
8	115	60	36.00	2.01 E-17	115	60	36.00	2.01 E-17
9	704	62	34.55	2.15 E-17	704	62	34.55	2.15 E-17
10	798	54	40.34	1.62 E-17	798	52	41.77	1.49 E-17
AVE	**514.5**	**56.5**	**38.529**	**1.78E-17**	**514.5**	**56.6**	**37.759**	**1.79 E-17**
SD	**243.1059**	**3.374743**	**2.4376**	**2.23E-18**	**243.1059**	**3.204164**	**3.26896**	**2.11E-18**

Appendix E29:

Fowkes: Whole Blood Infected

	Fowkes: Whole Blood Treated With ATR				**Fowkes: Whole BloodTreated With ELT**			
SN	$CD4^+$ count ($cells/mm^3$)	$\theta(^0C)$	γ_{sv} (mJ/m^2)	A_{132} (mJ/m^2)	CD4+ count ($cells/mm^3$)	$\theta(^0C)$	γ_{sv} (mJ/m^2)	A_{132} (mJ/m^2)
1	428	53	41.05	2.46E-17	428	52	41.77	2.37 E-17
2	600	55	39.62	2.63 E-17	600	50	43.18	2.21 E-17
3	625	56	38.90	2.72 E-17	625	53	41.05	2.46 E-17
4	312	59	36.73	3.00 E-17	312	59	36.73	3.00 E-17
5	464	57	38.18	2.81 E-17	464	58	37.45	2.90 E-17
6	247	54	40.34	2.55 E-17	247	56	38.90	2.72 E-17
7	852	60	36.00	3.09 E-17	852	55	39.62	2.63 E-17
8	115	58	37.45	2.90 E-17	115	57	38.18	2.81 E-17
9	704	52	41.77	2.37 E-17	704	54	40.34	2.55 E-17
10	798	51	42.48	2.29 E-17	798	51	42.18	2.29 E-17
AVE	**514.5**	**55.5**	**39.252**	**2.68E-17**	**514.5**	**54.5**	**39.94**	**2.59E-17**
SD	**243.1059**	**3.02765**	**2.179923**	**2.69E-18**	**243.1059**	**3.02765**	**2.135468**	**2.65E-18**

Appendix E30:

Fowkes: WBC Infected

	Fowkes: WBC Treated With ATR				**Fowkes: WBC TreatedWith ELT**			
SN	$CD4^+$ count ($cells/mm^3$)	$\theta(^0C)$	γ_{sv} (mJ/m^2)	A_{132} (mJ/m^2)	CD4+ count ($cells/mm^3$)	$\theta(^0C)$	γ_{sv} (mJ/m^2)	A_{132} (mJ/m^2)
1	428	54	40.34	2.55 E-17	428	57	38.18	2.81 E-17
2	600	49	43.88	2.12 E-17	600	55	39.62	2.63 E-17
3	625	50	43.18	2.21 E-17	625	54	40.34	2.55 E-17
4	312	60	36.00	3.09 E-17	312	60	36.00	3.09 E-17
5	464	58	37.45	2.90 E-17	464	58	37.45	2.90 E-17
6	247	62	34.55	3.28 E-17	247	62	34.55	3.28 E-17
7	852	57	38.18	2.81 E-17	852	51	42.48	2.29 E-17
8	115	65	32.38	3.57 E-17	115	59	36.73	3.00 E-17
9	704	52	41.77	2.37 E-17	704	53	41.05	2.46 E-17
10	798	59	36.73	3.00 E-17	798	56	38.90	2.72 E-17
AVE	**514.5**	**56.6**	**38.446**	**2.79E-17**	**514.5**	**56.5**	**38.53**	**2.78E-17**
SD	**243.1059**	**5.25357**	**3.779195**	**4.73E-18**	**243.1059**	**3.374743**	**2.434114**	**3.22E-18**

Appendix E31:

Fowkes: RBC Infected

	(s) Fowkes: RBC Treated With ATR				(t) Fowkes: RBC Treated With ELT			
SN	$CD4^+$ count (cells/mm^3)	$\theta(^0C)$	γ_{sv} (mJ/m^2)	A_{132} (mJ/m^2)	CD4+ count (cells/mm^3)	$\theta(^0C)$	γ_{sv} (mJ/m^2)	A_{132} (mJ/m^2)
1	428	57	38.18	2.83E-17	428	58	37.45	2.90 E-17
2	600	55	39.62	2.63 E-17	600	56	38.90	2.72 E-17
3	625	56	38.90	2.72 E-17	625	54	40.34	2.55 E-17
4	312	59	36.73	3.00 E-17	312	59	36.73	3.00 E-17
5	464	58	37.45	2.90 E-17	464	55	39.62	2.63 E-17
6	247	60	36.00	3.09 E-17	247	60	36.00	3.09 E-17
7	852	61	35.27	3.18 E-17	852	57	38.17	2.81 E-17
8	115	54	40.34	2.55 E-17	115	61	35.27	3.18 E-17
9	704	63	33.83	3.37 E-17	704	53	41.05	2.46 E-17
10	798	52	41.77	2.37 E-17	798	51	42.48	2.29 E-17
AVE	**514.5**	**57.5**	**37.809**	**2.86E-17**	**514.5**	**56.4**	**38.601**	**2.76E-17**
SD	**243.1059**	**3.374743**	**2.43921**	**3.07E-18**	**243.1059**	**3.204164**	**2.311038**	**2.86E-18**

Appendix E32:

Fowkes: Serum Infected

	(m) Fowkes: Serum Treated With ATR				(n) Fowkes: Serum Treated With ELT			
SN	$CD4^+$ count (cells/mm^3)	$\theta(^0C)$	γ_{sv} (mJ/m^2)	A_{132} (mJ/m^2)	CD4+ count (cells/mm^3)	$\theta(^0C)$	γ_{sv} (mJ/m^2)	A_{132} (mJ/m^2)
1	428	53	41.05	2.46 E-17	428	58	37.45	2.90 E-17
2	600	57	38.17	2.81 E-17	600	53	41.05	2.46 E-17
3	625	55	39.62	2.63 E-17	625	51	42.48	2.29 E-17
4	312	56	38.90	2.72 E-17	312	55	39.62	2.63 E-17
5	464	59	36.73	3.00 E-17	464	59	36.73	3.00 E-17
6	247	61	35.27	3.18 E-17	247	57	38.18	2.81 E-17
7	852	52	41.77	2.37 E-17	852	56	38.90	2.72 E-17
8	115	60	36.00	3.09 E-17	115	60	36.00	3.09 E-17
9	704	54	40.34	2.55 E-17	704	54	40.34	2.55 E-17
10	798	51	42.48	2.29 E-17	798	52	41.77	2.37 E-17
AVE	**514.5**	**55.8**	**39.033**	**2.71E-17**	**514.5**	**55.5**	**39.252**	**2.68E-17**
SD	**243.1059**	**3.425395**	**2.470259**	**3.07E-18**	**243.1059**	**3.02765**	**2.179923**	**2.69E-18**

Appendix E33:

Wu: Whole Blood Infected

	(c) Wu: Whole Blood Treated With ATR				Wu: Whole BloodTreated With ELT			
SN	$CD4^+$ count ($cells/mm^3$)	$\theta(^0C)$	γ_{sv} (mJ/m^2)	A_{132} (mJ/m^2)	CD4+ count ($cells/mm^3$)	$\theta(^0C)$	γ_{sv} (mJ/m^2)	A_{132} (mJ/m^2)
1	428	53	41.05	7.44E-17	428	52	41.77	7.61 E-17
2	600	55	39.62	7.09 E-17	600	50	43.18	7.94 E-17
3	625	56	38.90	6.93 E-17	625	53	41.05	7.43 E-17
4	312	59	36.73	6.36 E-17	312	59	36.73	6.36 E-17
5	464	57	38.18	6.73 E-17	464	58	37.45	6.55 E-17
6	247	54	40.34	7.26 E-17	247	56	38.90	6.91 E-17
7	852	60	36.00	6.18 E-17	852	55	39.62	7.09 E-17
8	115	58	37.45	6.55 E-17	115	57	38.18	6.73 E-17
9	704	52	41.77	7.61 E-17	704	54	40.34	7.26 E-17
10	798	51	42.48	7.77 E-17	798	51	42.48	7.77 E-17
AVE	**514.5**	**55.5**	**39.252**	**6.99E-17**	**514.5**	**54.5**	**39.97**	**7.12E-17**
SD	**243.1059**	**3.02765**	**2.179923**	**5.37E-18**	**243.1059**	**3.02765**	**2.172224**	**5.37E-18**

Appendix E34:

Wu: WBC Infected

	(i) Wu: WBC Treated With ATR				(j) Wu: WBC Treated With ELT			
SN	$CD4^+$ count ($cells/mm^3$)	$\theta(^0C)$	γ_{sv} (mJ/m^2)	A_{132} (mJ/m^2)	CD4+ count ($cells/mm^3$)	$\theta(^0C)$	γ_{sv} (mJ/m^2)	A_{132} (mJ/m^2)
1	428	54	40.34	7.26E-17	428	57	38.18	6.73 E-17
2	600	49	43.88	8.10 E-17	600	55	39.62	7.09 E-17
3	625	50	43.18	7.94 E-17	625	54	40.34	7.26 E-17
4	312	60	36.00	6.18 E-17	312	60	36.00	6.18 E-17
5	464	58	37.45	6.55 E-17	464	58	37.45	6.55 E-17
6	247	62	34.55	5.80 E-17	247	62	34.55	5.80 E-17
7	852	57	38.18	6.73 E-17	852	51	42.48	7.77 E-17
8	115	65	32.38	5.22 E-17	115	59	36.73	6.36 E-17
9	704	52	41.77	7.61 E-17	704	53	41.05	7.43 E-17
10	798	59	36.73	6.36 E-17	798	56	38.90	6.91 E-17
AVE	**514.5**	**56.6**	**38.446**	**6.80E-17**	**514.5**	**56.5**	**38.53**	**6.81E-17**
SD	**243.1059**	**5.25357**	**3.779195**	**9.96E-18**	**243.1059**	**3.3747**	**2.434114**	**6.05E-18**

Appendix E35:

Wu: RBC Infected

	(u) **Wu: RBC Treated With ATR**				(v) **Wu: RBC Treated With ELT**			
SN	$CD4^+$ count ($cells/mm^3$)	$\theta(^0C)$	γ_{sv} (mJ/m^2)	A_{132} (mJ/m^2)	CD4+ count ($cells/mm^3$)	$\theta(^0C)$	γ_{sv} (mJ/m^2)	A_{132} (mJ/m^2)
1	428	57	38.18	6.73E-17	428	58	37.45	6.55 E-17
2	600	55	39.62	7.09 E-17	600	56	38.90	6.91 E-17
3	625	56	38.90	6.91 E-17	625	54	40.34	7.26 E-17
4	312	59	36.73	6.36 E-17	312	59	36.73	6.36 E-17
5	464	58	37.45	6.55 E-17	464	55	39.62	7.09 E-17
6	247	60	36.00	6.18 E-17	247	60	36.00	6.18 E-17
7	852	61	35.28	5.99 E-17	852	57	38.18	6.73 E-17
8	115	54	40.34	7.26 E-17	115	61	35.28	5.99 E-17
9	704	63	33.83	5.61 E-17	704	53	41.05	7.43 E-17
10	798	52	41.77	7.61 E-17	798	51	42.48	7.77 E-17
AVE	**514.5**	**57.5**	**37.81**	**6.63E-17**	**514.5**	**56.4**	**38.60**	**6.83E-17**
SD	**243.1059**	**3.374743**	**2.438055**	**6.14E-18**	**243.1059**	**3.204164**	**2.309233**	**5.71E-18**

Appendix E36:

Wu: Serum Infected

	(o) **Wu: Serum Treated With ATR**				(p) **Wu: Serum Treated With ELT**			
SN	$CD4^+$ count ($cells/mm^3$)	$\theta(^0C)$	γ_{sv} (mJ/m^2)	A_{132} (mJ/m^2)	CD4+ count ($cells/mm^3$)	$\theta(^0C)$	γ_{sv} (mJ/m^2)	A_{132} (mJ/m^2)
1	428	53	41.05	7.43E-17	428	58	37.45	6.55E-17
2	600	57	38.18	6.72 E-17	600	53	41.05	7.43 E-17
3	625	55	39.62	7.09 E-17	625	51	42.48	7.77 E-17
4	312	56	38.90	6.91 E-17	312	55	39.62	7.09 E-17
5	464	59	36.73	6.36 E-17	464	59	36.73	6.36 E-17
6	247	61	35.28	5.99 E-17	247	57	38.18	6.73 E-17
7	852	52	41.77	7.61 E-17	852	56	38.90	6.91 E-17
8	115	60	36.00	6.18 E-17	115	60	36.00	6.18 E-17
9	704	54	40.34	7.26 E-17	704	54	40.34	7.26 E-17
10	798	51	42.48	7.77 E-17	798	52	41.77	7.61 E-17
AVE	**514.5**	**55.8**	**39.035**	**6.93E-17**	**514.5**	**55.5**	**39.252**	**6.99E-17**
SD	**243.1059**	**3.425395**	**2.468181**	**6.12E-18**	**243.1059**	**3.02765**	**2.179923**	**5.36E-18**

INFECTED SAMPLES WITH AM TREATMENT AND VA TREATMENT

NEUMANN MODEL ANALYSIS

Appendix E37:

Neumann: Whole Blood Infected

	Neumann: Whole Blood Treated With AM				**Neumann: Whole BloodTreated With VA**			
SN	$CD4^+$ count (cells/mm^3)	$\theta(^0C)$	γ_{sv} (mJ/m^2)	A_{132} (mJ/m^2)	CD4+ count (cells/mm^3)	$\theta(^0C)$	γ_{sv} (mJ/m^2)	A_{132} (mJ/m^2)
1	428	50	43.18	1.36E-17	428	53	41.05	1.55 E-17
2	600	56	38.90	1.75 E-17	600	52	41.77	1.49 E-17
3	625	51	42.48	1.42 E-17	625	57	38.18	1.81 E-17
4	312	59	36.73	1.95 E-17	312	58	37.45	1.88 E-17
5	464	57	38.18	1.81 E-17	464	56	38.90	1.75 E-17
6	247	53	41.05	1.55 E-17	247	55	39.62	1.68 E-17
7	852	54	40.34	1.62 E-17	852	50	43.18	1.36 E-17
8	115	58	37.45	1.88 E-17	115	59	36.73	1.95 E-17
9	704	52	41.77	1.49 E-17	704	54	40.34	1.62 E-17
10	798	55	39.62	1.68 E-17	798	51	42.48	1.42 E-17
AVE	**514.5**	**54.5**	**39.97**	**1.65E-17**	**514.5**	**54.5**	**39.97**	**1.65E-17**
SD	**243.1059**	**3.02765**	**2.172224**	**1.98E-18**	**243.1059**	**3.02765**	**2.172224**	**1.98E-18**

Appendix E38:

Neumann: WBC Infected

	(l) Neumann: WBC Treated With AM				(m) **Neumann: WBC Treated With VA**			
SN	$CD4^+$ count (cells/mm^3)	$\theta(^0C)$	γ_{sv} (mJ/m^2)	A_{132} (mJ/m^2)	CD4+ count (cells/mm^3)	$\theta(^0C)$	γ_{sv} (mJ/m^2)	A_{132} (mJ/m^2)
1	428	55	39.62	1.68E-17	428	51	42.48	1.42E-17
2	600	56	38.90	1.75 E-17	600	57	38.18	1.81E-17
3	625	50	43.18	1.36 E-17	625	56	38.90	1.75E-17
4	312	59	36.73	1.95 E-17	312	58	37.45	1.88E-17
5	464	60	36.00	2.01 E-17	464	55	39.62	1.68 E-17
6	247	57	38.18	1.81 E-17	247	60	36.00	2.01 E-17
7	852	58	37.45	1.88 E-17	852	54	40.34	1.62 E-17
8	115	66	31.66	2.42 E-17	115	53	41.05	1.55 E-17
9	704	61	35.28	2.08 E-17	704	59	36.73	1.95 E-17
10	798	63	33.83	2.21 E-17	798	52	41.77	1.49 E-17
AVE	**514.5**	**58.5**	**37.083**	**1.92E-17**	**514.5**	**55.5**	**39.252**	**1.72E-17**
SD	**243.1059**	**4.453463**	**3.210895**	**2.95E-18**	**243.1059**	**3.02765**	**2.179923**	**1.99E-18**

Appendix E39:

Neumann: RBC Infected

	(w) Neumann: RBC Treated With AM				(x) **Neumann: RBC Treated With VA**			
SN	$CD4^+$ count ($cells/mm^3$)	$\theta(^0C)$	γ_{sv} (mJ/m^2)	A_{132} (mJ/m^2)	CD4+ count ($cells/mm^3$)	$\theta(^0C)$	γ_{sv} (mJ/m^2)	A_{132} (mJ/m^2)
1	428	57	38.18	1.81E-17	428	59	36.73	1.95 E-17
2	600	56	38.90	1.75 E-17	600	56	38.90	1.75 E-17
3	625	58	37.45	1.88 E-17	625	54	40.34	1.62 E-17
4	312	59	36.73	1.95 E-17	312	57	38.18	1.81 E-17
5	464	55	39.62	1.68 E-17	464	58	37.45	1.88 E-17
6	247	60	36.00	2.01 E-17	247	64	33.10	2.28 E-17
7	852	61	35.28	2.08 E-17	852	60	36.00	2.01 E-17
8	115	54	40.34	1.62 E-17	115	61	35.28	2.08 E-17
9	704	63	33.83	2.21 E-17	704	58	37.45	1.88 E-17
10	798	53	41.05	1.55 E-17	798	55	39.62	1.68 E-17
AVE	**514.5**	**57.6**	**37.74**	**1.85E-17**	**514.5**	**58.2**	**37.31**	**1.90E-17**
SD	**243.1059**	**3.204164**	**2.315675**	**2.11E-18**	**243.1059**	**2.973961**	**2.15351**	**2.09E-18**

Appendix E40:

Neumann: Serum Infected

	(e) Neumann: Serum Treated With AM				(f) **Neumann: Serum Treated With VA**			
SN	$CD4^+$ count ($cells/mm^3$)	$\theta(^0C)$	γ_{sv} (mJ/m^2)	A_{132} (mJ/m^2)	CD4+ count ($cells/mm^3$)	$\theta(^0C)$	γ_{sv} (mJ/m^2)	A_{132} (mJ/m^2)
1	428	56	38.90	1.75E-17	428	58	37.45	1.88 E-17
2	600	55	39.62	1.68 E-17	600	55	39.62	1.68 E-17
3	625	58	37.45	1.88 E-17	625	52	41.77	1.49 E-17
4	312	60	36.00	2.01 E-17	312	60	36.00	2.01 E-17
5	464	63	33.83	2.21 E-17	464	50	43.18	1.36 E-17
6	247	59	36.73	1.95 E-17	247	59	36.73	1.95 E-17
7	852	57	38.18	1.81 E-17	852	54	40.34	1.62 E-17
8	115	61	35.28	2.08 E-17	115	51	42.48	1.42 E-17
9	704	65	32.38	2.35 E-17	704	57	38.18	1.80 E-17
10	798	67	30.95	2.48 E-17	798	56	38.90	1.75 E-17
AVE	**514.5**	**60.1**	**35.93**	**2.02E-17**	**514.5**	**55.2**	**39.47**	**1.71E-17**
SD	**243.1059**	**3.928528**	**2.841951**	**2.62E-18**	**243.1059**	**3.425395**	**2.461058**	**2.01E-18**

Appendix E41:

Fowkes: Whole Blood Infected

	Fowkes: Whole Blood Treated With AM				**Fowkes: Whole Blood Treated With VA**			
SN	$CD4^+$ count ($cells/mm^3$)	$\theta(^0C)$	γ_{sv} (mJ/m^2)	A_{132} (mJ/m^2)	CD4+ count ($cells/mm^3$)	$\theta(^0C)$	γ_{sv} (mJ/m^2)	A_{132} (mJ/m^2)
1	428	50	43.18	2.21E-17	428	53	41.053	2.46 E-17
2	600	56	38.90	2.72 E-17	600	52	41.7658	2.37 E-17
3	625	51	42.48	2.29 E-17	625	57	38.1746	2.81 E-17
4	312	59	36.73	2.10 E-17	312	58	37.4504	2.90 E-17
5	464	57	38.18	2.81 E-17	464	56	38.8973	2.72 E-17
6	247	53	41.05	2.46 E-17	247	55	39.6183	2.63 E-17
7	852	54	40.34	2.55 E-17	852	50	43.18	2.21 E-17
8	115	58	37.45	2.90 E-17	115	59	36.7254	2.99 E-17
9	704	52	41.77	2.37 E-17	704	54	40.337	2.55 E-17
10	798	55	39.62	2.63 E-17	798	51	42.475	2.29 E-17
AVE	**514.5**	**54.5**	**39.97**	**2.50E-17**	**514.5**	**54.5**	**39.96768**	**2.59E-17**
SD	**243.1059**	**3.02765**	**2.172224**	**2.64E-18**	**243.1059**	**3.02765**	**2.172689**	**2.63E-18**

Appendix E42:

Fowkes: WBC Infected

	(n) Fowkes: WBC Treated With AM				(o) **Fowkes: WBC Treated With VA**			
SN	$CD4^+$ count ($cells/mm^3$)	$\theta(^0C)$	γ_{sv} (mJ/m^2)	A_{132} (mJ/m^2)	CD4+ count ($cells/mm^3$)	$\theta(^0C)$	γ_{sv} (mJ/m^2)	A_{132} (mJ/m^2)
1	428	55	39.62	2.63E-17	428	51	42.475	2.29 E-17
2	600	56	38.90	2.72 E-17	600	57	38.1746	2.81 E-17
3	625	50	43.18	2.21 E-17	625	56	38.8973	2.72 E-17
4	312	59	36.73	3.00 E-17	312	58	37.4504	2.90 E-17
5	464	60	36.00	3.09 E-17	464	55	39.6183	2.63 E-17
6	247	57	38.18	2.81 E-17	247	60	36.00	3.09 E-17
7	852	58	37.45	2.90 E-17	852	54	40.337	2.55 E-17
8	115	66	31.66	3.66 E-17	115	53	41.053	2.46 E-17
9	704	61	35.28	3.18 E-17	704	59	36.7254	3.00 E-17
10	798	63	33.83	3.37 E-17	798	52	41.7658	2.37 E-17
AVE	**514.5**	**58.5**	**37.08**	**2.96E-17**	**514.5**	**55.5**	**39.25**	**2.68E-17**
SD	**243.1059**	**4.453463**	**3.210895**	**4.06E-18**	**243.1059**	**3.02765**	**2.179537**	**2.69E-18**

Appendix E43:

Fowkes: RBC Infected

	(y) **Fowkes: RBC Treated With AM**				(z) **Fowkes: RBC Treated With VA**			
SN	$CD4^+$ count ($cells/mm^3$)	$\theta(^0C)$	γ_{sv} (mJ/m^2)	A_{132} (mJ/m^2)	CD4+ count ($cells/mm^3$)	$\theta(^0C)$	γ_{sv} (mJ/m^2)	A_{132} (mJ/m^2)
1	428	57	38.18	2.81E-17	428	59	36.73	3.00 E-17
2	600	56	38.90	2.72 E-17	600	56	38.90	2.72 E-17
3	625	58	37.45	2.90 E-17	625	54	40.34	2.55 E-17
4	312	59	36.73	3.00 E-17	312	57	38.18	2.81 E-17
5	464	55	39.62	2.63 E-17	464	58	37.45	2.90 E-17
6	247	60	36.00	3.09 E-17	247	64	33.10	3.47 E-17
7	852	61	35.28	3.18 E-17	852	60	36.00	3.09 E-17
8	115	54	40.34	2.55 E-17	115	61	35.28	3.18 E-17
9	704	63	33.83	3.37 E-17	704	58	37.45	2.90 E-17
10	798	53	41.05	2.46 E-17	798	55	39.62	2.63 E-17
AVE	**514.5**	**57.6**	**37.74**	**2.87E-17**	**514.5**	**58.2**	**37.31**	**2.93E-17**
SD	**243.1059**	**3.204164**	**2.315675**	**2.92E-18**	**243.1059**	**2.973961**	**2.15351**	**2.75E-18**

Appendix E44:

Fowkes: Serum Infected

	(q) **Fowkes: Serum Treated With AM**				(r) **Fowkes: Serum Treated With VA**			
SN	$CD4^+$ count ($cells/mm^3$)	$\theta(^0C)$	γ_{sv} (mJ/m^2)	A_{132} (mJ/m^2)	CD4+ count ($cells/mm^3$)	$\theta(^0C)$	γ_{sv} (mJ/m^2)	A_{132} (mJ/m^2)
1	428	56	38.90	2.72E-17	428	58	37.45	2.90 E-17
2	600	55	39.62	2.63 E-17	600	55	39.62	2.63 E-17
3	625	58	37.45	2.90 E-17	625	52	41.77	2.37 E-17
4	312	60	36.00	3.08 E-17	312	60	36.00	3.09 E-17
5	464	63	33.83	3.37 E-17	464	50	43.18	2.21 E-17
6	247	59	36.73	3.00 E-17	247	59	36.73	3.00 E-17
7	852	57	38.18	2.81 E-17	852	54	40.34	2.55 E-17
8	115	61	35.28	3.18 E-17	115	51	42.48	2.29 E-17
9	704	65	32.38	3.57 E-17	704	57	38.18	2.81 E-17
10	798	67	30.95	3.76 E-17	798	56	38.90	2.72 E-17
AVE	**514.5**	**60.1**	**35.93**	**3.12E-17**	**514.5**	**55.2**	**39.47**	**2.66E-17**
SD	**243.1059**	**3.928528**	**2.84195**	**3.86E-18**	**243.1059**	**3.425395**	**2.461058**	**3.02E-18**

Appendix E45:

Wu: Whole Blood Infected

	(g) Wu: Whole Blood Treated With AM				(h) **Wu: Whole Blood Treated With VA**			
SN	$CD4^+$ count ($cells/mm^3$)	$\theta(^0C)$	γ_{sv} (mJ/m^2)	A_{132} (mJ/m^2)	CD4+ count ($cells/mm^3$)	$\theta(^0C)$	γ_{sv} (mJ/m^2)	A_{132} (mJ/m^2)
1	428	50	43.18	7.94E-17	428	53	41.05	7.43 E-17
2	600	56	38.90	6.91 E-17	600	52	41.77	7.61 E-17
3	625	51	42.48	7.77 E-17	625	57	38.18	6.73 E-17
4	312	59	36.73	6.36 E-17	312	58	37.45	6.55 E-17
5	464	57	38.18	6.73 E-17	464	56	38.90	6.91 E-17
6	247	53	41.05	7.43 E-17	247	55	39.62	7.09 E-17
7	852	54	40.34	7.26 E-17	852	50	43.18	7.94 E-17
8	115	58	37.45	6.55 E-17	115	59	36.73	6.36 E-17
9	704	52	41.77	7.61 E-17	704	54	40.34	7.26 E-17
10	798	55	39.62	7.09 E-17	798	51	42.48	7.77 E-17
AVE	**514.5**	**54.5**	**39.97**	**7.17E-17**	**514.5**	**54.5**	**39.97**	**7.17E-17**
SD	**243.1059**	**3.02765**	**2.172224**	**5.3E-18**	**243.1059**	**3.02765**	**2.172224**	**5.30E-18**

Appendix E46:

Wu: WBC Infected

	(p) Wu: WBC Treated With AM				(q) **Wu: WBC Treated With VA**			
SN	$CD4^+$ count ($cells/mm^3$)	$\theta(^0C)$	γ_{sv} (mJ/m^2)	A_{132} (mJ/m^2)	CD4+ count ($cells/mm^3$)	$\theta(^0C)$	γ_{sv} (mJ/m^2)	A_{132} (mJ/m^2)
1	428	55	39.62	6.18 E-17	428	51	42.48	7.09E-17
2	600	56	38.90	6.73E-17	600	57	38.18	6.91 E-17
3	625	50	43.18	6.91E-17	625	56	38.90	7.94 E-17
4	312	59	36.73	6.55E-17	312	58	37.45	7.26E-17
5	464	60	36.00	7.09E-17	464	55	39.62	6.18 E-17
6	247	57	38.18	6.91 E-17	247	60	36.00	7.09E-17
7	852	58	37.45	7.26E-17	852	54	40.34	6.55 E-17
8	115	66	31.66	7.43E-17	115	53	41.05	5.03 E-17
9	704	61	35.28	6.36E-17	704	59	36.73	5.99 E-17
10	798	63	33.83	7.61E-17	798	52	41.77	5.61 E-17
AVE	**514.5**	**58.5**	**37.083**	**6.99E-17**	**514.5**	**55.5**	**39.252**	**6.24E-17**
SD	**243.1059**	**4.453463**	**3.210895**	**5.36E-18**	**243.1059**	**3.02765**	**2.179923**	**5.96E-18**

Appendix E47:

Wu: RBC Infected

	(aa) Wu: RBC Infected With AM				(bb) **Wu: RBC Infected With VA**			
SN	$CD4^+$ count ($cells/mm^3$)	$\theta(^0C)$	γ_{sv} (mJ/m^2)	A_{132} (mJ/m^2)	CD4+ count ($cells/mm^3$)	$\theta(^0C)$	γ_{sv} (mJ/m^2)	A_{132} (mJ/m^2)
1	428	57	38.18	6.73E-17	428	59	36.73	6.36E-17
2	600	56	38.90	6.91 E-17	600	56	38.90	6.91 E-17
3	625	58	37.45	6.55 E-17	625	54	40.34	7.26 E-17
4	312	59	36.73	6.36 E-17	312	57	38.18	6.73 E-17
5	464	55	39.62	7.09 E-17	464	58	37.45	6.55 E-17
6	247	60	36.00	6.18 E-17	247	64	33.10	5.42 E-17
7	852	61	35.28	5.99 E-17	852	60	36.00	6.18 E-17
8	115	54	40.34	7.26 E-17	115	61	35.28	5.99 E-17
9	704	63	33.83	5.61 E-17	704	58	37.45	6.55 E-17
10	798	53	41.05	7.43 E-17	798	55	39.62	7.09 E-17
AVE	**514.5**	**57.6**	**37.74**	**6.61E-17**	**514.5**	**58.2**	**37.31**	**6.50E-17**
SD	**243.1059**	**3.204164**	**2.315675**	**5.84E-18**	**243.1059**	**2.973961**	**2.15351**	**5.58E-18**

Appendix E48:

Wu: Serum Infected

	(s) Wu: Serum Treated With AM				(t) **Wu: Serum Treated With VA**			
SN	$CD4^+$ count ($cells/mm^3$)	$\theta(^0C)$	γ_{sv} (mJ/m^2)	A_{132} (mJ/m^2)	CD4+ count ($cells/mm^3$)	$\theta(^0C)$	γ_{sv} (mJ/m^2)	A_{132} (mJ/m^2)
1	428	56	38.90	6.91E-17	428	58	37.45	6.55 E-17
2	600	55	39.62	7.09 E-17	600	55	39.62	7.09 E-17
3	625	58	37.45	6.55 E-17	625	52	41.77	7.61 E-17
4	312	60	36.00	6.18 E-17	312	60	36.00	6.18 E-17
5	464	63	33.83	5.61 E-17	464	50	43.18	7.94 E-17
6	247	59	36.73	6.36 E-17	247	59	36.73	6.36 E-17
7	852	57	38.18	6.73 E-17	852	54	40.34	7.26 E-17
8	115	61	35.28	5.99 E-17	115	51	42.48	7.77 E-17
9	704	65	32.38	5.22 E-17	704	57	38.18	6.73 E-17
10	798	67	30.95	4.83 E-17	798	56	38.90	6.91 E-17
AVE	**514.5**	**60.1**	**35.932**	**6.15E-17**	**514.5**	**55.2**	**39.465**	**7.04E-17**
SD	**243.1059**	**3.928528**	**2.841951**	**7.40E-18**	**243.1059**	**3.425395**	**2.461058**	**6.03E-18**

INFECTED SAMPLES WITH BP TREATMENT AND DH TREATMENT

NEUMANN MODEL ANALYSIS

Appendix E49:

Neumann: Whole Blood Infected

	Neumann: Whole Blood Treated With BP				**Neumann: Whole Blood Treated With DH**			
SN	$CD4^+$ count (cells/mm^3)	$\theta(^0C)$	γ_{sv} (mJ/m^2)	A_{132} (mJ/m^2)	CD4+ count (cells/mm^3)	$\theta(^0C)$	γ_{sv} (mJ/m^2)	A_{132} (mJ/m^2)
1	428	60	36.00	2.01E-17	428	50	43.18	1.36 E-17
2	600	50	43.18	1.36 E-17	600	55	39.62	1.68 E-17
3	625	52	41.77	1.49 E-17	625	58	37.45	1.88 E-17
4	312	56	38.90	1.75 E-17	312	59	36.73	1.95 E-17
5	464	59	36.73	1.95 E-17	464	49	43.89	1.29 E-17
6	247	51	42.48	1.42 E-17	247	56	38.90	1.75 E-17
7	852	55	39.62	1.68 E-17	852	54	40.34	1.62 E-17
8	115	58	37.45	1.88 E-17	115	57	38.18	1.81 E-17
9	704	53	41.05	1.55 E-17	704	48	44.58	1.23 E-17
10	798	54	40.34	1.62 E-17	798	51	42.48	1.42 E-17
AVE	**514.5**	**54.8**	**39.75**	**1.67E-17**	**514.5**	**53.7**	**40.535**	**1.60E-17**
SD	**243.1059**	**3.425395**	**2.4619**	**2.24E-18**	**243.1059**	**3.945462**	**2.81833**	**2.58E-18**

Appendix E50:

Neumann: WBC Infected

	(r) Neumann: WBC Treated With BP				(s) **Neumann: WBC Treated With DH**			
SN	$CD4^+$ count (cells/mm^3)	$\theta(^0C)$	γ_{sv} (mJ/m^2)	A_{132} (mJ/m^2)	CD4+ count (cells/mm^3)	$\theta(^0C)$	γ_{sv} (mJ/m^2)	A_{132} (mJ/m^2)
1	428	58	37.45	1.88E-17	428	56	38.90	1.75 E-17
2	600	50	43.18	1.36 E-17	600	58	37.45	1.88 E-17
3	625	55	39.62	1.68 E-17	625	57	38.18	1.81 E-17
4	312	57	38.18	1.81 E-17	312	60	36.00	2.01 E-17
5	464	60	36.00	2.01 E-17	464	62	34.55	2.15 E-17
6	247	59	36.73	1.95 E-17	247	59	36.73	1.95 E-17
7	852	53	41.05	1.55 E-17	852	61	35.28	2.08 E-17
8	115	62	34.55	2.15 E-17	115	65	32.38	2.35 E-17
9	704	56	38.90	1.75 E-17	704	63	33.83	2.21 E-17
10	798	54	40.34	1.62 E-17	798	55	39.62	1.68 E-17
AVE	**514.5**	**56.4**	**38.6**	**1.78E-17**	**514.5**	**59.6**	**36.29**	**1.99E-17**
SD	**243.1059**	**3.565265**	**2.566779**	**2.35E-18**	**243.1059**	**3.204164**	**2.321009**	**2.14E-18**

Appendix E51:

Neumann: RBC Infected

	Neumann: RBC Treated With BP				**Neumann: RBC Treated With DH**			
SN	$CD4^+$ count ($cells/mm^3$)	$\theta(^0C)$	γ_{sv} (mJ/m^2)	A_{132} (mJ/m^2)	CD4+ count ($cells/mm^3$)	$\theta(^0C)$	γ_{sv} (mJ/m^2)	A_{132} (mJ/m^2)
1	428	58	37.45	1.88E-17	428	55	39.62	1.68 E-17
2	600	57	38.18	1.81 E-17	600	53	41.05	1.55 E-17
3	625	56	38.90	1.75 E-17	625	56	38.90	1.75 E-17
4	312	59	36.73	1.95 E-17	312	49	43.88	1.29 E-17
5	464	62	34.55	2.15 E-17	464	58	37.45	1.88 E-17
6	247	60	36.00	2.01 E-17	247	57	38.18	1.81 E-17
7	852	55	39.62	1.68 E-17	852	51	42.48	1.42 E-17
8	115	61	35.28	2.08 E-17	115	54	40.34	1.62 E-17
9	704	65	32.38	2.35 E-17	704	52	41.77	1.49 E-17
10	798	63	33.83	2.21 E-17	798	48	44.58	1.23 E-17
AVE	**514.5**	**59.6**	**36.29**	**1.99E-17**	**514.5**	**53.3**	**40.83**	**1.57E-17**
SD	**243.1059**	**3.204164**	**2.321009**	**2.14E-18**	**243.1059**	**3.335**	**2.37803**	**2.17E-18**

Appendix E52:

Neumann: Serum Infected

	(g) Neumann: Serum Treated With BP				(h) **Neumann: Serum Treated With DH**			
SN	$CD4^+$ count ($cells/mm^3$)	$\theta(^0C)$	γ_{sv} (mJ/m^2)	A_{132} (mJ/m^2)	CD4+ count ($cells/mm^3$)	$\theta(^0C)$	γ_{sv} (mJ/m^2)	A_{132} (mJ/m^2)
1	428	58	37.45	1.88E-17	428	55	39.62	1.68 E-17
2	600	55	39.62	1.68 E-17	600	56	38.90	1.75 E-17
3	625	56	38.90	1.75 E-17	625	57	38.18	1.81 E-17
4	312	59	36.73	1.95 E-17	312	59	36.73	1.95 E-17
5	464	57	38.18	1.81 E-17	464	46	45.95	1.11 E-17
6	247	54	40.34	1.62 E-17	247	58	37.45	1.88 E-17
7	852	50	43.18	1.36 E-17	852	48	44.58	1.23 E-17
8	115	49	43.88	1.29 E-17	115	53	41.05	1.55 E-17
9	704	60	36.00	2.01 E-17	704	51	42.48	1.42 E-17
10	798	52	41.77	1.49 E-17	798	49	43.88	1.29 E-17
AVE	**514.5**	**55**	**39.61**	**1.68E-17**	**514.5**	**53.2**	**40.88**	**1.57E-17**
SD	**243.1059**	**3.741657**	**2.681568**	**2.44E-18**	**243.1059**	**4.516636**	**3.210558**	**2.93E-18**

Appendix E53:

Fowkes: Whole Blood Infected

	Fowkes: Whole Blood Treated With BP				**Fowkes: Whole BloodTreated With DH**			
SN	$CD4^+$ count ($cells/mm^3$)	$\theta(^0C)$	γ_{sv} (mJ/m^2)	A_{132} (mJ/m^2)	CD4+ count ($cells/mm^3$)	θowkes(^{0} C)	γ_{sv} (mJ/m^2)	A_{132} (mJ/m^2)
1	428	60	36.00	3.09E-17	428	50	43.18	2.21 E-17
2	600	50	43.18	2.21 E-17	600	55	39.62	2.63 E-17
3	625	52	41.77	2.37 E-17	625	58	37.45	2.90 E-17
4	312	56	38.90	2.72 E-17	312	59	36.73	3.00 E-17
5	464	59	36.73	3.00 E-17	464	49	43.88	2.12 E-17
6	247	51	42.48	2.29 E-17	247	56	38.90	2.72 E-17
7	852	55	39.62	2.63 E-17	852	54	40.34	2.55 E-17
8	115	58	37.45	2.90 E-17	115	57	38.18	2.81 E-17
9	704	53	41.05	2.46 E-17	704	48	44.58	2.04 E-17
10	798	54	40.34	2.55 E-17	798	51	42.48	2.29 E-17
AVE	**514.5**	**54.8**	**39.75**	**2.62E-17**	**514.5**	**53.7**	**40.53**	**2.53E-17**
SD	**243.1059**	**3.425395**	**2.4619**	**3.03E-18**	**243.1059**	**3.945462**	**2.817009**	**3.42E-18**

Appendix E54:

Fowkes: WBC Infected

	(t) Fowkes: WBC Treated With BP				(u) **Fowkes: WBC Treated With DH**			
SN	$CD4^+$ count ($cells/mm^3$)	$\theta(^0C)$	γ_{sv} (mJ/m^2)	A_{132} (mJ/m^2)	CD4+ count ($cells/mm^3$)	$\theta(^0C)$	γ_{sv} (mJ/m^2)	A_{132} (mJ/m^2)
1	428	58	37.45	2.90E-17	428	56	38.90	2.72 E-17
2	600	50	43.18	2.2 E-17	600	58	37.45	2.90 E-17
3	625	55	39.62	2.63 E-17	625	57	38.18	2.81 E-17
4	312	57	38.18	2.81 E-17	312	60	36.00	3.09 E-17
5	464	60	36.00	3.09 E-17	464	62	34.55	3.28 E-17
6	247	59	36.73	3.00 E-17	247	59	36.73	3.00 E-17
7	852	53	41.05	2.46 E-17	852	61	35.28	3.18 E-17
8	115	62	34.55	3.28 E-17	115	65	32.38	3.57 E-17
9	704	56	38.90	2.72 E-17	704	63	33.83	3.37 E-17
10	798	54	40.34	2.55 E-17	798	55	39.62	2.63 E-17
AVE	**514.5**	**56.4**	**38.6**	**2.76E-17**	**514.5**	**59.6**	**36.29**	**3.06E-17**
SD	**243.1059**	**3.565265**	**2.566779**	**3.21E-18**	**243.1059**	**3.204164**	**2.321009**	**3.00E-18**

Appendix E55:

Fowkes: RBC Infected

	(cc) **Fowkes: RBC Treated With BP**				(dd) **Fowkes: RBC Treated With DH**			
SN	$CD4^+$ count ($cells/mm^3$)	$\theta(^0C)$	γ_{sv} (mJ/m^2)	A_{132} (mJ/m^2)	CD4+ count ($cells/mm^3$)	$\theta(^0C)$	γ_{sv} (mJ/m^2)	A_{132} (mJ/m^2)
1	428	58	37.45	2.90E-17	428	55	39.62	2.63E-17
2	600	57	38.18	2.81E-17	600	53	41.05	2.46E-17
3	625	56	38.90	2.72E-17	625	56	38.90	2.72E-17
4	312	59	36.73	3.00E-17	312	49	43.88	2.12E-17
5	464	62	34.55	3.28E-17	464	58	37.45	2.90E-17
6	247	60	36.00	3.09E-17	247	57	38.18	2.81E-17
7	852	55	39.62	2.63E-17	852	51	42.48	2.29E-17
8	115	61	35.28	3.18E-17	115	54	40.34	2.55E-17
9	704	65	32.38	3.57E-17	704	52	41.77	2.37E-17
10	798	63	33.83	3.37E-17	798	48	44.58	2.04E-17
AVE	**514.5**	**59.6**	**36.29**	**3.06E-17**	**514.5**	**53.3**	**40.83**	**2.49E-17**
SD	**243.1059**	**3.204164**	**2.321009**	**3E-18**	**243.1059**	**3.335**	**2.37803**	**2.87E-18**

Appendix E56:

Fowkes: Serum Infected

	(u) **Fowkes: Serum Treated With BP**				(v) **Fowkes: Serum Treated With DH**			
SN	$CD4^+$ count ($cells/mm^3$)	$\theta(^0C)$	γ_{sv} (mJ/m^2)	A_{132} (mJ/m^2)	CD4+ count ($cells/mm^3$)	$\theta(^0C)$	γ_{sv} (mJ/m^2)	A_{132} (mJ/m^2)
1	428	58	37.45	2.90E-17	428	55	39.62	2.63E-17
2	600	55	39.62	2.63E-17	600	56	38.90	2.72E-17
3	625	56	38.90	2.72E-17	625	57	38.18	2.81E-17
4	312	59	36.73	3.00E-17	312	59	36.73	3.00E-17
5	464	57	38.18	2.81E-17	464	46	45.95	1.89E-17
6	247	54	40.34	2.55E-17	247	58	37.45	2.90E-17
7	852	50	43.18	2.21E-17	852	48	44.58	2.04E-17
8	115	49	43.88	2.12E-17	115	53	41.05	2.46E-17
9	704	60	36.00	3.09E-17	704	51	42.48	2.29E-17
10	798	52	41.77	2.37E-17	798	49	43.88	2.12E-17
AVE	**514.5**	**55**	**39.61**	**2.64E-17**	**514.5**	**53.2**	**40.88**	**2.49E-17**
SD	**243.1059**	**3.741657**	**2.681568**	**3.29E-18**	**243.1059**	**4.5166**	**3.2106**	**3.86E-18**

Appendix E57:

Wu: Whole Blood Infected

	(i) Wu: Whole Blood Treated With BP				(j) Wu: Whole Blood Treated With DH			
SN	$CD4^+$ count ($cells/mm^3$)	$\theta(^0C)$	γ_{sv} (mJ/m^2)	A_{132} (mJ/m^2)	CD4+ count ($cells/mm^3$)	$\theta(^0C)$	γ_{sv} (mJ/m^2)	A_{132} (mJ/m^2)
1	428	60	36.00	6.18E-17	428	50	43.18	7.94E-17
2	600	50	43.18	7.94E-17	600	55	39.62	7.09E-17
3	625	52	41.77	7.61E-17	625	58	37.45	6.55E-17
4	312	56	38.90	6.91E-17	312	59	36.73	6.36E-17
5	464	59	36.73	6.36E-17	464	49	43.88	8.10E-17
6	247	51	42.48	7.77E-17	247	56	38.90	6.90E-17
7	852	55	39.62	7.09E-17	852	54	40.34	7.26E-17
8	115	58	37.45	6.55E-17	115	57	38.18	6.73E-17
9	704	53	41.05	7.43E-17	704	48	44.58	8.27E-17
10	798	54	40.34	7.26E-17	798	51	42.48	7.77E-17
AVE	**514.5**	**54.8**	**39.75**	**7.11E-17**	**514.5**	**53.7**	**40.534**	**7.30E-17**
SD	**243.1059**	**3.425395**	**2.4619**	**6.04E-18**	**243.1059**	**3.945462**	**2.81701**	**6.82E-18**

Appendix E58:

Wu: WBC Infected

	(v) Wu: WBC Treated With BP				(w) Wu: WBC Treated With DH			
SN	$CD4^+$ count ($cells/mm^3$)	$\theta(^0C)$	γ_{sv} (mJ/m^2)	A_{132} (mJ/m^2)	CD4+ count ($cells/mm^3$)	$\theta(^0C)$	γ_{sv} (mJ/m^2)	A_{132} (mJ/m^2)
1	428	58	37.45	6.55E-17	428	56	38.90	6.91E-17
2	600	50	43.18	7.94E-17	600	58	37.45	6.55E-17
3	625	55	39.62	7.09E-17	625	57	38.18	6.73E-17
4	312	57	38.18	6.73E-17	312	60	36.00	6.18E-17
5	464	60	36.00	6.18E-17	464	62	34.55	5.80E-17
6	247	59	36.73	6.36E-17	247	59	36.73	6.36E-17
7	852	53	41.05	7.43E-17	852	61	35.28	5.99E-17
8	115	62	34.55	5.80E-17	115	65	32.38	5.22E-17
9	704	56	38.90	6.91E-17	704	63	33.83	5.61E-17
10	798	54	40.34	7.26E-17	798	55	39.62	7.09E-17
AVE	**514.5**	**56.4**	**38.6**	**6.83E-17**	**514.5**	**59.6**	**36.29**	**6.44E-17**
SD	**243.1059**	**3.565265**	**2.566779**	**6.36E-18**	**243.1059**	**3.204164**	**2.32101**	**6.98E-18**

Appendix E59:

Wu: RBC Infected

	(ee) **Wu: RBC Treated With BP**				(ff) **Wu: RBC Treated With DH**			
SN	$CD4^+$ count (cells/mm^3)	$\theta(^0C)$	γ_{sv} (mJ/m^2)	A_{132} (mJ/m^2)	CD4+ count (cells/mm^3)	$\theta(^0C)$	γ_{sv} (mJ/m^2)	A_{132} (mJ/m^2)
1	428	58	37.45	6.55E-17	428	55	39.62	7.09E-17
2	600	57	38.18	6.73E-17	600	53	41.05	7.43E-17
3	625	56	38.90	6.91E-17	625	56	38.90	6.91E-17
4	312	59	36.73	6.36E-17	312	49	43.88	8.10E-17
5	464	62	34.55	5.80E-17	464	58	37.45	6.55E-17
6	247	60	36.00	6.18E-17	247	57	38.18	6.73E-17
7	852	55	39.62	7.09E-17	852	51	42.48	7.77E-17
8	115	61	35.28	5.99E-17	115	54	40.34	7.26E-17
9	704	65	32.38	5.22E-17	704	52	41.77	7.61E-17
10	798	63	33.83	5.61E-17	798	48	44.58	8.27E-17
AVE	**514.5**	**59.6**	**36.29**	**6.24E-17**	**514.5**	**53.3**	**40.83**	**7.37E-17**
SD	**243.1059**	**3.204164**	**2.321009**	**5.98E-18**	**243.1059**	**3.335**	**2.37803**	**5.72E-18**

Appendix E60:

Wu: Serum Infected

	(w) **Wu: Serum Treated With BP**				(x) **Wu: Serum Treated With DH**			
SN	$CD4^+$ count (cells/mm^3)	$\theta(^0C)$	γ_{sv} (mJ/m^2)	A_{132} (mJ/m^2)	CD4+ count (cells/mm^3)	$\theta(^0C)$	γ_{sv} (mJ/m^2)	A_{132} (mJ/m^2)
1	428	58	37.45	6.55E-17	428	55	39.62	7.09E-17
2	600	55	39.62	7.09E-17	600	56	38.90	6.91E-17
3	625	56	38.90	6.91E-17	625	57	38.18	6.72E-17
4	312	59	36.73	6.36E-17	312	59	36.73	6.36E-17
5	464	57	38.18	6.73E-17	464	46	45.95	8.58E-17
6	247	54	40.34	7.26E-17	247	58	37.45	6.55E-17
7	852	50	43.18	7.94E-17	852	48	44.58	8.27E-17
8	115	49	43.88	8.10E-17	115	53	41.05	7.43E-17
9	704	60	36.00	6.18E-17	704	51	42.48	7.77E-17
10	798	52	41.77	7.61E-17	798	49	43.88	8.10E-17
AVE	**514.5**	**55**	**39.61**	**7.07E-17**	**514.5**	**53.2**	**40.88**	**7.38E-17**
SD	**243.1059**	**3.741657**	**2.681568**	**6.54E-18**	**243.1059**	**4.516636**	**3.210558**	**7.73E-18**

Appendix F1:

Neumann Model: Average Hamaker Coefficient (A_{132}) in (mJ/m^2)

Note: SD=± $\varkappa 10^{-18}$

			Treated A_{132} $\varkappa 10^{-17}$							
Blood Cells	**Infected A_{132} $\varkappa 10^{-17}$**	**Uninfected A_{132} $\varkappa 10^{-17}$**	**IFN**	**RBV**	**ATR**	**ELT**	**AM**	**VA**	**BP**	**DH**
Whole. Blood	1.82± 1.56	1.34± 3.31	1.65± 1.98	1.69± 1.72	1.72± 1.99	1.65± 1.98	1.65± 1.98	1.65± 1.98	1.67± 2.24	1.60± 2.58
WBC	2.24± 2.15	1.25± 1.71	1.81± 2.88	1.77± 2.80	1.62± 3.16	1.81± 2.23	1.92± 2.11	1.72± 1.98	1.78± 2.35	1.99± 2.14
RBC	2.04± 1.91	1.40± 2.27	1.91± 2.08	1.76± 2.50	1.89± 3.75	2.12± 3.32	1.85± 2.11	1.90± 2.09	1.99± 2.14	1.57± 2.17
Serum	2.11± 2.04	1.60± 2.48	1.86± 3.13	1.76± 2.23	1.78± 2.23	1.79± 2.11	2.02± 2.62	1.71± 2.01	1.68± 2.44	1.57± 2.93

Appendix F2:

Fowkes Model: Average Hamaker Coefficient (A_{132}) in (mJ/m^2)

Note: SD=± $\varkappa 10^{-18}$

			Treated A_{132} $\varkappa 10^{-17}$							
Blood Cells	**Infected A_{132} $\varkappa 10^{-17}$**	**Uninfected A_{132} $\varkappa 10^{-17}$**	**IFN**	**RBV**	**ATR**	**ELT**	**AM**	**VA**	**BP**	**DH**
Whole. Blood	2.82± 2.14	2.29± 2.77	2.59± 2.65	2.64± 2.28	2.68± 2.69	2.59± 2.65	2.50± 2.64	2.59± 2.63	2.62± 3.03	2.53± 3.42
WBC	3.41± 3.07	2.07± 2.20	2.81± 3.95	2.76± 3.73	2.79± 4.73	2.78± 3.22	2.96± 4.06	2.68± 2.69	2.76± 3.21	3.06± 3.00
RBC	3.13± 2.70	2.26± 2.99	2.95± 2.78	2.72± 3.41	2.86± 3.07	2.76± 2.86	2.87± 2.92	2.93± 2.75	3.06± 3.00	2.49± 2.87
Serum	3.23± 2.87	2.48± 3.23	2.89± 3.30	2.76± 3.02	2.71± 3.07	2.68± 2.69	3.12± 3.86	2.66± 3.02	2.64± 3.29	2.49± 3.86

Appendix F3:

Wu Model: Average Hamaker Coefficient (A_{132}) in (mJ/m^2)

Note: SD=± $\varkappa 10^{-18}$

			Treated **(A_{132})$\varkappa 10^{-17}$**							
Blood Cells	**Infected(A_{132}) $\varkappa 10^{-17}$**	**Uninfected.A_{132} $\varkappa 10^{-17}$**	**IFN**	**RBV**	**ATR**	**ELT**	**AM**	**VA**	**BP**	**DH**
Whole. Blood	7.99± 8.60	6.71± 4.31	7.17± 5.30	7.08± 4.55	6.99± 5.37	7.12± 5.37	7.17± 5.30	7.17± 5.30	7.11± 6.04	7.30± 6.82
WBC	8.21± 4.43	5.53± 6.16	6.53± 6.96	6.84± 7.46	6.80± 9.96	6.81± 6.05	6.99± 5.36.	6.44± 8.13	6.83± 6.36	6.24± 5.98
RBC	7.83± 5.98	6.10± 5.37	6.45± 5.56	6.88± 6.80	6.63± 6.14	6.83± 5.71	6.61± 5.84	6.50± 5.58	6.24± 5.98	7.37± 5.72
Serum	7.40± 6.49	5.89± 5.73	6.58± 8.60	6.84± 6.04	6.93± 6.12	6.99± 5.36	6.15± 7.40	7.04± 6.03	7.07± 6.54	7.38± 7.73

Appendix G1:

Functional group of Bryophillum extract

Wavenumber	**Functional group**	**Stretching band**
688.0813	Aromatic rings	C-H bend
874.8352	“	“
1124.367	Carboxylic acid	0-H
1326.764	“	“
1398.606	Alkanes	CH2 stretch
1633.724	Amides	N-H stretch
1722.596	Ester	C-0 band
1839.382	“	“
2011.799	Nitrile	C-N stretch
2158.657	“	“
2286.907	“	“
2458.73	“	“
2539.262	“	“
2677.982	Aldehydes	C-H stretch
2794.011	“	“
3029.446	Alkanes	CH2 bend
3181.108	Quinine	0-H bend
3387.628	“	“
3509.214	“	“
3611.87	Amides	C=0 stretch
3701.362	“	“
3825.945	“	“

Appendix G2:

Functional group of phyllantus amarus extract

Wavenumber	Functional group	Stretching
763.4623	Aromatic rings	C-H band
864.5204	“	“
1152.667	Carboxylic acid	0-H stretch
1337.996	Alkanes	CH2 stretch
1387.733	“	“
1637.321	Amides	N-H stretch
1944.39	Nitriles	C-N stretch
2130.77	“	“
2473.6	“	“
2639.376	Aldehydes	C-H stretch
2785.845	“	“
3009.718	Alkanes	CH2 bend
3260.097	Quinines	0-H bend
3453.763	“	“
3686.697	“	“
3817.148	Amides	C-0 stretch

Appendix G3

Functional group of annona muricata extract

Wavenumber	Functional group	Stretching band
740.4257	Aromatic rings	C-H stretching
856.2297	“	“
1397.944	Carboxylic acid	0-H stretch
1624.269	Amides	N-H bend
1864.144	Nitriles	C-N bend
2070.071	“	“
2192.384	“	“
2457.403	“	“
2618.574	Aldehydes	C-H bend
2739.436	“	“`
2825.428	“	“
2950.03	“	“
3164.685	Quinines	0-H bend
3342.726	“	“
3700.357	“	“
3828.939	Amides	C-0 stretch

Appendix G4

Functional group of vernonia amygdalina extract

Wavenumber	Functional group	Stretching band
725.2185	Aromatic rings	C-H stretching
833.7648	“	“
1308.469	Alkanes	CH2
1419.332	“	“
1618.531	Amides	N-H stretch
1921.28	Nitriles	C-N stretch
2004.281	“	“
2102.924	“	“
2477.44	“	“
2658.926	Aldehydes	C-H stretch
2839.67	“	“
2944.359	Alkanes	CH2 stretch
3098.275	“	“
3239.337	Quinines	0-H stretch
3401.031	“	“
3516.505	“	“
3579.099	“	“